From:	Dyer, Linda
To:	Singal, Balwant
Subject:	FW: Documents for NRC Public Meeting on Corrosion Head Loss Experiments Program (CHLE) - Part 1
Date:	Tuesday, August 21, 2012 9:23:48 AM
Attachments:	Abbreviated CHLE test plan rev 1.4.pdf CHLE-004 Equipment Design Rev 1.pdf CHLE-005 Chemical Constituents Rev 1.pdf CHLE-006 STP Material Calculation, Rev 1.pdf

---

Balwant, the document file sizes are too big to transmit to you in one email. I will send in parts. There will be six documents total.

Thanks,
Linda Dyer
Special Projects
South Texas Project
361-972-4783

From: Dyer, Linda
Sent: Tuesday, August 21, 2012 8:16 AM
To: 'Singal, Balwant'
Cc: Blossom, Steven; Kee, Ernie; Paul, Jamie; 'Kerry Howe'
Subject: Documents for NRC Public Meeting on Corrosion Head Loss Experiments Program (CHLE)

Balwant,
Please find attached the documents for the upcoming NRC/STP GSI-191 public meeting on Corrosion Head Loss Experiments (CHLE) Program.
Thank you for your help in arranging this meeting.

Thanks,
Linda Dyer
Special Projects
South Texas Project
361-972-4783

From:	Dyer, Linda
To:	Singal, Balwant
Subject:	FW: Documents for NRC Public Meeting on Corrosion Head Loss Experiments Program (CHLE) - Part 2
Date:	Tuesday, August 21, 2012 9:30:22 AM
Attachments:	CHLE-010_Test_Results_Rev_2.pdf CHLE-007 Debris Addition-Rev 3.pdf

---

Balwant, this email and attachments is part two of the transmittal of documents and completes the total of six documents transmitted to you. Please call if you have questions.

Thanks,
Linda Dyer
Special Projects
South Texas Project
361-972-4783

From: Dyer, Linda
Sent: Tuesday, August 21, 2012 8:16 AM
To: 'Singal, Balwant'
Cc: Blossom, Steven; Kee, Ernie; Paul, Jamie; 'Kerry Howe'
Subject: Documents for NRC Public Meeting on Corrosion Head Loss Experiments Program (CHLE)

Balwant,
Please find attached the documents for the upcoming NRC/STP GSI-191 public meeting on Corrosion Head Loss Experiments (CHLE) Program.
Thank you for your help in arranging this meeting.

Thanks,
Linda Dyer
Special Projects
South Texas Project
361-972-4783

WORKING DRAFT

STP CORROSION HEAD LOSS EXPERIMENTS (CHLE) TEST PLAN

REVISION 1.4

August 15, 2012

PROJECT DOCUMENTATION COVER PAGE

Document No: CHLE-003	Revision: 1.4	Page 2 of 22
Title: STP Corrosion/Head Loss Experiments Test Plan		
Project: Corrosion/Head Loss Experiment (CHLE) Program		Date: 15 August 2012
Client: South Texas Project Nuclear Operating Company		

Summary/Purpose of Analysis or Calculation:

The CHLE program is being conducted to support the risk-informed resolution of GSI-191 at the South Texas Project Nuclear Operating Company (STP). The tests consist of a series of 30-day tests in which materials will be added to a corrosion tank and fiberglass debris will be added to head loss columns. The solution from the corrosion tank will be circulated to the head loss columns to determine if the corrosion of materials in containment can contribute to head loss across the emergency core cooling system sump screens. This document describes the test plan for the experimental program.

Signatures:	Name:	Signature:	Date:
Prepared by:	Janet Leavitt	< signed electronically >	5/23/2012
UNM review:	Kerry Howe	< signed electronically >	6/5/2012
STP review:			
Soteria review:	Zahra Mohaghegh	< signed electronically >	6/4/2012 8/18/2012

Revision	Date	Description
1.3	6/5/2012	Draft document for preliminary NRC review
1.4	8/15/2012	Updated with test revisions

TABLE OF CONTENTS

NOTE: This test plan is a draft and describes the current status of the Corrosion / Head Loss Experiments to be conducted in support of South Texas Project's resolution of GSI-191. Development of details and values for parameters are currently in progress.

1. BACKGROUND

Most pressurized water reactors (PWRs) have attempted to resolve GSI-191 by following a deterministic approach as described in NEI 04-07 [1, 2]. In deterministic evaluations, uncertainty is addressed using conservatisms to ensure that a bounding evaluation has been performed. Numerous tests and analyses (with varying levels of success) have been performed in each subject area to better understand the physical phenomenon and reduce the level of conservatism in plant specific evaluations.

South Texas Project (STP) has decided to resolve GSI-191open issues through risk informed approach. The deterministic and risk informed approaches both attempt to address the physical phenomenon as realistically as possible. However, the primary difference is that the deterministic approach analyzes bounding scenarios and addresses uncertainty with conservatisms, whereas the risk informed approach analyzes best estimate conditions for the full spectrum of scenarios by considering probability and quantifying uncertainty as part of the evaluation.

The chemical effects testing and evaluations that have been performed over the last six or seven years have focused on analyzing bounding scenarios. Nevertheless, the knowledge base that has been developed is extensive and can be used to evaluate a wide variety of potential conditions.

2. OBJECTIVES

The overall objectives of these corrosion/head loss experiment (CHLE) tests are as follows:

1. Determine the significance of chemical effects on the resolution of GSI-191 at the STP nuclear power plants.
2. Generate data that can be used to develop a model or algorithm to provide input for the Containment Accident Stochastic Analysis (CASA) analysis to determine the impact of chemical effects on debris bed head loss through the use of the following modules/calculators:

    - **Precipitation** module used to predict precipitate solubility, type, quantity, and form as a function of STP related chemistry and material concentrations using the corrosion/dissolution and solubility components described below.
        - **Corrosion/dissolution** component used to predict material concentrations from corrosion/dissolution of materials in the containment pool as a function of STP related water volume, pool chemistry, material quantities, pool pH, pool temperature, and time.
        - **Solubility** component used to determine solubility limits of corrosion/dissolution materials as a function of STP related pH, temperature, precipitate type, and precipitate form.

    - **Head loss** module used to predict the increase in head loss across the emergency containment sump strainers due to the formation of chemical precipitates under STP related conditions.

3. GENERAL EXPERIMENTAL APPROACH

The CHLE analysis integrates three different types of tests to accomplish the objectives stated in section 2 and illustrated by Figure 1. The three different types of tests within the analysis are as follows: (1) 30-day integrated tank tests, (2) bench-scale laboratory tests, and (3) short-term integrated tank tests. Thermodynamic modeling will also be a part of the CHLE analysis by assisting in experimental design and/or result interpretation and is not intended not provide direct thermodynamic simulation results to be used by CASA.

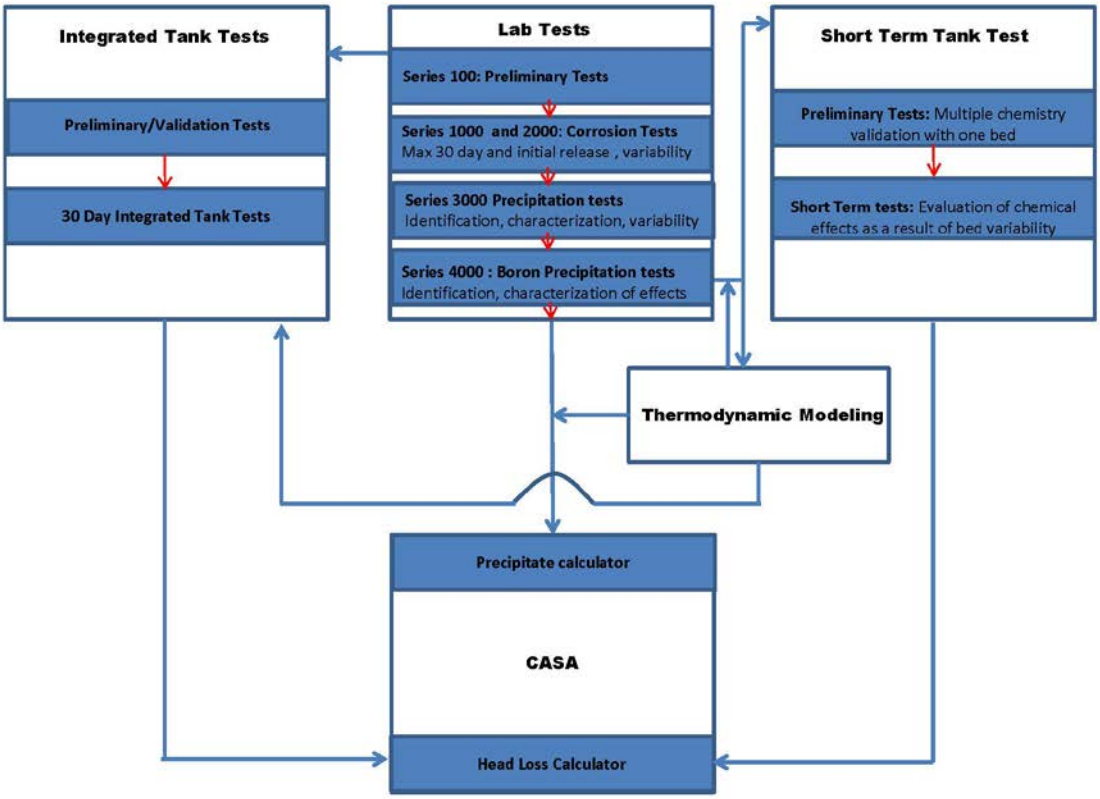

Figure 1: Schematic of the CHLE analysis

To effectively utilize the CHLE analyses in an efficient manner that captures all probable chemical effects for the development of CASA modules, hypothetical loss of coolant accident (LOCA) scenarios were fit into three categories determined by break sizes; Small Break LOCA (SBLOCA), Medium Break LOCA (MBLOCA) and Large Break LOCA (LBLOCA), Table 1. Categorizing LOCA scenarios by break size simplifies the multitudes of possible breaks into three manageable categories, defines the parameters that affect chemical corrosion/precipitation and facilitates consistency with the plant specific probabilistic risk assessment (PRA).

Table 1: LOCA Scenario defined by break type

LOCA Category	Pipe Break Size (in.)	Temperature Profile (°F)	Total Water Volume (ft^3)[1]	Time to Fill Pool (min)[2]
SBLOCA	< 2	Awaiting info	Awaiting info	Awaiting info
MBLOCA	2 – 6	193 – 94	71,778	80 [3]
LBLOCA	> 6	Awaiting info	71,778	Awaiting info

[1]Volume determined at 21 °C [4]
[2] The time to fill pool will be used to determine the rate at which TSP will be added to tank test

3.1 Integrated Tank Tests

The objective of this test series is to integrate corrosion and leaching of source materials (aluminum, Nukon fiber, etc.) with head loss through a debris bed using chemical parameters and simulated temperature conditions representative of STP LOCA scenarios (Table 1) over a 30-day duration. This section uses median chemical concentrations and Relap5-3d/MELCOR simulated temperatures derived from STP parameters. The 30-Day integrated tank tests will determine whether corrosion products form in a manner that will contribute to head loss in a debris bed, and when in the 30-day period they might form. Corrosion data obtained from this test series will be used in CASA, but quantitative head loss data will not because the fiber bed used in testing was designed to be an indicator bed used to detect chemical effects head loss and is not reflective of a fiber bed formed under plant conditions.

3.2 Bench-Scale Laboratory Tests

This tests series consists of a mixture of batch and flow-through loop experiments to accomplish the objectives listed below.

- Investigate variability related to corrosion and material release to the containment pool as a function of STP related conditions
- Investigate variability and identify threshold parameters related to solubility limits
- Characterize precipitate behavior as a function of thermal cycling
- Investigate in-core boron precipitation effects

This series of testing examines and captures the bounds determined by the statistical minimum and maximum STP values to determine variability related to parameters in the corrosion and solubility component of the precipitation module for use in CASA.

3.3 Short-Term Integrated Tank Tests

The objective of this test series is to quantify head loss under varying debris bed conditions using precipitate generated in-situ as determined from the bench-scale test investigations. The short-term tests will be used to develop variability related to parameters associated with the head loss modules for use in CASA.

4. METHODS AND MATERIALS FOR THE INTEGRATED TANK TESTS

The basic features of the tests are as follows:

1. The tests will take place in an integrated system that will allow corrosion of materials to take place in conditions representative of LOCA scenarios (Table 1), with simultaneous circulation of solution through three parallel head loss modules that consists of a simulated fibrous debris bed formed on a sump strainer screen.
2. The materials used in testing are representative of those identified at STP that are expected to participate in pool chemistry development. These identified materials will be in the same ratio of material area to sump pool volume in the CHLE tests as found at STP [5]. The tank is designed to maintains a well-mixed pool [6].
3. The test system will operate with a time-temperature profile [7] and chemistry make-up [3] representative of the defined LOCA scenarios (Table 1), with the exception that temperatures above 185 °F (85 °C) will not be tested. Additional source materials will be added to the tank so that the appropriate amount of corrosion products are formed at the end of the prolonged high temperature (>185 °F) phase [8].
4. A separate loop with a cooling element, filter, and heating element will aid in investigating if thermal cycling will cause precipitation of soluble aluminum concentrations dictated by experimental design or if it will affect the behavior of precipitation that may form at the higher temperature.

4.1 Integrated Tank Test Summary

Two types of tests will be run within the matrix of testing for the integrated CHLE tank series; Preliminary/Validation tests and 30 Day tests for the different LOCA scenarios defined in Table 1. The first series of tests will be used to ensure that the test equipment operates as intended and assist in final experimental design by providing detailed information related to specific areas of interest. Once the equipment and experimental design are validated, 30-Day integrated tests to evaluate chemical effects on head loss as a function of LOCA scenario will be performed. This testing series is not intended to determine the quantitative increase of head loss due to the corrosion products for use in CASA. Only corrosion and solubility information obtained from this test is intended for direct use in CASA. But it should be mentioned that quantitative increase of head loss due to corrosion products for use in CASA will be explored in the short term tank experiments using the bench test obtained information.

4.1.1 Preliminary/Validation Tests

Preliminary/Validation tests will be performed to (1) ensure the equipment and experimental design parameter set points result in the desired conditions as specified by the experimental plan and (2) provide information on specific areas or time of interest within the LOCA event. Identified tests are as follows:

- PT1- Validation of material release during the simulated high temperature periods. Due to the equipment temperature limitation (Max T =185 °F), it is necessary to simulate periods above the equipment temperature limitation using extra material for a specified time interval to artificially produce the in-situ corrosion and material release for these

periods. Therefore material release from the excess material will be measured and compared against the target release determined from bench scale tests.

- PT2- Validation of head loss across debris bed. A debris bed, developed in a manner where reproducibility is the main objective, will be tested using pre-formed WCAP-16530 precipitate to compare the functionality of the bed to register due to head loss due to chemical effects.

- PT3- Determination of spray phase unsubmerged coupon contribution to the containment pool. Allows for flexibility in experimental design by providing more knowledge of parameters

- PT4- Validation of temperature profile settings. This test series documents the experimentally derived test profile as a function of equipment limitations. It also allows for comparison of the experimentally derived profile to the Relap 5-3d/MELCOR simulated temperature profile for documentation purposes prior to test initiation.

- PT5- Documentation of experimentally derived pH profile. While the experimental pH upon test initiation will not be adjusted, this test series allows for comparison of the experimentally derived pH profile against the computer simulated pH profile for documentation purposes prior to test initiation.

- PT6- Determine bed to be used in testing using past debris preparation and currently added NEI preparation process.

4.1.2 30-Day Tests

Following the Preliminary/Validation tests, four 30-Day tests will be performed to evaluate chemical effects on head loss as a function of the identified LOCA scenarios (Table 1). Identified tests are as follows:

- T0- Determination of head loss due to the fiberglass bed dissolution or reactions with LOCA pool chemistry without corrosion product contributions. This will be done under MBLOCA conditions and allows for better characterization of chemical effects by providing a characterization of head loss over time due to bed interaction with solution alone. This will be used as a baseline to compare to head loss results from the integrated 30-Day MBLOCA test to detect head loss attributed to chemical effects (precipitate formation).

- T1- Determination of head loss due chemical effects as a result of MBLOCA conditions. Parameters taken from within the range dictated by the LOCA categorization (Table 1) will be used to create the experiment.

- T2- Determination of head loss due chemical effects as a result of LBLOCA conditions. Parameters taken from within the range dictated by the LOCA categorization (Table 1) will be used to create the experiment.

- T3- Determination of head loss due chemical effects as a result of SBLOCA conditions. Parameters taken from within the range dictated by the LOCA categorization (Table 1) will be used to create the experiment.

4.1.3 Summary Table of Tests

As previously stated, two types of tests will be run within the matrix of testing for the integrated CHLE tank series; Preliminary/Validation tests and 30-Day integrated tank tests. A summary of the earlier described integrated tank test is listed in Table 2.

Table 2: Summary of 30 Day tank test experiments

Test[1]	Objective	Materials[2]	Status	Comment
PT1	Validate material release of simulated high temperature period determined form batch tests	1-5	To be done	Test to begin after T1 completion.
PT2 (1-3)	Validate head loss across debris bed due to chemicals is outside of the noise of fiber only head loss	WCAP 16530 salts	Completed	Results available in report # CHLE-010
PT3	Determine the spray phase unsubmerged metal coupons contribution to the pool	1-5	Under review	The value of running this test scenario is currently being re-evaluated by the team
PT4-(1-3)	Validate that temperature profile results in target profile for each LOCA scenario	N/A	Complete	Results available in report # CHLE-010
PT5- (1,2)	Documentation of experimentally derived pH profile for comparison against computer simulated profile	N/A	Complete	Results available in report # CHLE-010
PT6	Determine fiber bed to use in test using past fiber preparation procedures and NEI fiber preparation procedures.	2, WCAP 16530 salts	Complete	Results available in report # CHLE-008
T0	Determine head loss due to the fiberglass bed dissolution or reactions with initial LOCA pool chemistry	2	Complete	Results available in report # CHLE-010
T1	Determine chemical effects on head loss as effects of MBLOCA	1,2	Ongoing	This test series is currently underway.
T2	Determine chemical effects on head loss as effects of LBLOCA	1-5	To be done	Test to begin after PTI completion
T3	Determine chemical effects on head loss as effects of SBLOCA	1-5	Under review	The value of running this test scenario is currently being re-evaluated by the team

[1]Chemistry reflective of final solution pH of 7.2, with TSP and boric acid addition[3]
[2]Materials [5]: (1) Aluminum (2), Nukon, (3) Inorganic coated zinc, (4) galvanized steel, (5) concrete

4.2 Integrated Tank Test Equipment

The test apparatus for the integrated tank tests has three main sections, as follows:

1. Material corrosion tank where materials present in containment can be placed to simulate the environment inside the containment structure during a LOCA.
2. Three vertical head loss assemblies to simulate the flow conditions through debris beds that forms on a sump screens.
3. Heat exchanger loop with capabilities to simulate plant conditions with an inline filter for evaluation of thermo-cycling effects on precipitate formation.

A simplified schematic of the test loop is shown in Figure 2. A photograph of the corrosion tank is shown in Figure 3. Additional test equipment details are presented in supporting documentation [6].

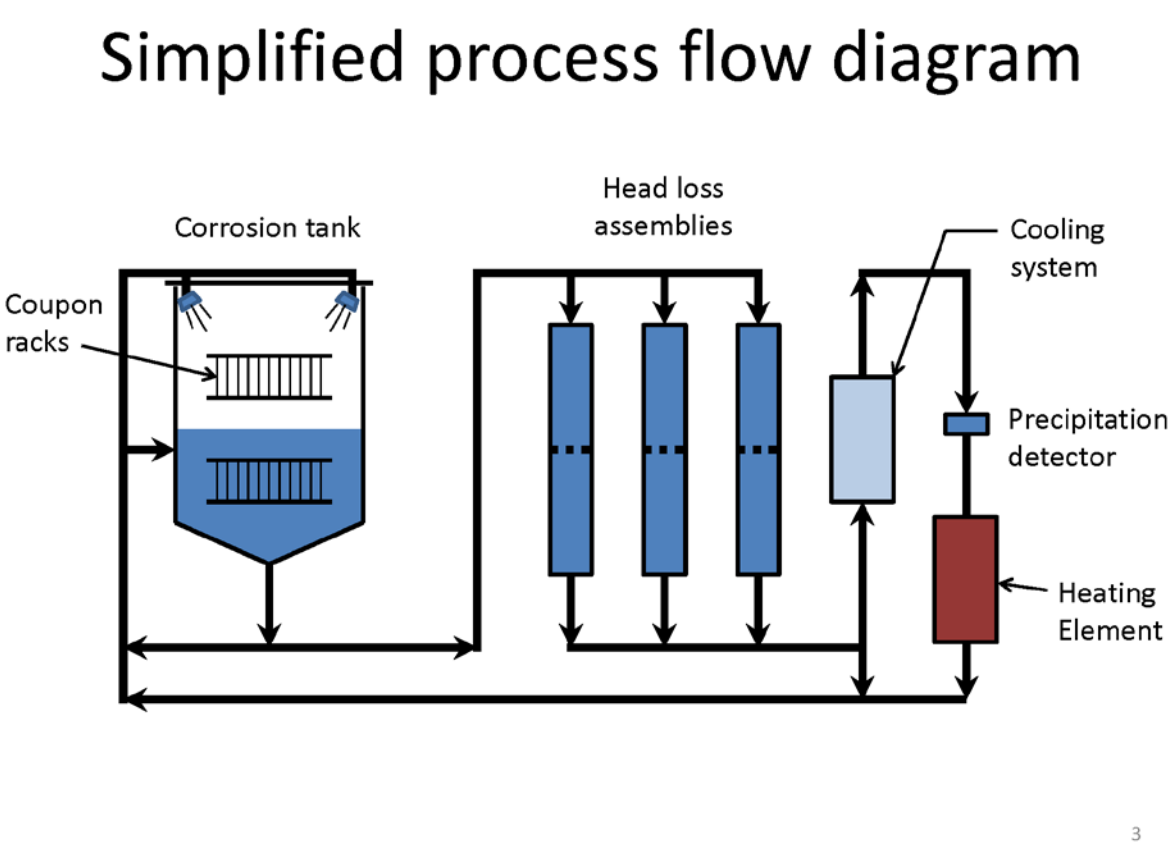

Figure 2: Simplified Process Flow Diagram of 30-Day Integrated Tank Test System

Figure 3: Corrosion tank and head loss modules for CHLE tests

4.3 Preliminary/Validation Tests

4.3.1 High Temperature Material Release Validation (PT1)

4.3.1.1 Objective

This test series is designed to provide validation of material release during the simulated high temperature periods, which only apply to LBLOCA. Due to the equipment temperature limitation (Max T =185 °F), it is necessary to simulate corrosion and material release for periods above the equipment temperature limitation. This will be done using extra material for a specified time interval to artificially produce the in-situ corrosion and material release for these periods[5].

4.3.1.2 Experimental Deign

Summaries of the experimental parameters are presented below. The target values for each of these parameters were chosen from a range of parameters generated from review of STP records[3, 5], Relap5-3D/MELCOR results [7], and CASA results[9].
Tank Flow rate: 25 gpm
Head loss module flow rate: N/A

Heat exchanger loop flow rate: N/A
TSP addition rate: TBD
Materials: Table 3
Chemicals: Table 4
Temperature Profile: Table 5
pH profile determined by procedure outlined in the Chemical addition documentation [5].

Table 3: Materials (All submerged) for testing

Materials	Surface area ft^2
Aluminum	0.47
Galvanized steel	Awaiting information
Zinc coated steel	
Fiberglass	
Concrete	

Table 4: Chemicals for testing

Chemical	Concentration (mg/L)
Boric acid	15,488
TSP	3,370

Table 5: Temperature profile for testing

Time (min)	Temperature (°C)	Time (min)	Temperature (°C)
0	Awaiting info	300	
20		500	
40		720	
60		900	
120		1100	
180		1300	
240		1440	

4.3.1.3 Experimental Results

Water samples will be taken for metal and phosphate analysis. If necessary, the coupons will be analyzed for corrosion rates. Results will be compared to bench test to verify experimental target of material release to solution is within 20% of the expected concentration determined by the bench (bench test series 200).

4.3.2 Head Loss Validation (PT2 (1-3))

See CHLE-010 for detailed experimental design.

4.3.3 Spray Phase Contribution (PT3)

4.3.3.1 Objective

This series of tests are designed to determine the contribution of spray phase unsubmerged coupons to the chemic composition in the containment pool. This series of test allows for

flexibility in experimental design by providing more knowledge of parameters. Non-spray phase contribution from unsubmerged coupons to the pool will be investigated in bench tests (600 test series).

4.3.3.2 Experimental Deign

Summaries of the experimental parameters are presented below. The target values for each of these parameters were chosen from a range of parameters generated from review of STP records[3, 5], MELCOR results [7], and CASA results[9].

Tank Flow rate: 25 gpm
Head loss module flow rate: N/A
Heat exchanger loop flow rate: N/A
TSP addition rate: N/A
Materials: Table 6
Chemicals: Table 7

Table 6: Materials (All non-submerged) for testing

Materials	Surface area (ft^2)
Aluminum	2.64
Galvanized steel	Awaiting information
Zinc coated steel	
Fiberglass	
Concrete	

Table 7: Chemicals for testing

Chemical	Concentration (mg/L)
Boric acid	15,488
TSP	3,370

4.3.3.3 Experimental Results

Multiple water samples will be taken before spray starts, while sprays are on and after sprays have been turned off to determine contribution of the spray materials to the containment pool. Samples times will be time zero, every hour after the sprays are in operation, when sprays are turned off, 12 hours after sprays are turned off and 24 hours after sprays are turned off. This may provide some flexibility in experimental design by allowing the unsubmerged coupons to be eliminated from the corrosion tank and providing the contribution from these coupons by salts or by extra surface area to be submerged for a predetermined amount of time. These results will be combined with the bench test 600 series before final decision is made.

4.3.4 Temperature Profile Validation (PT4 (1-3))

See CHLE-010 for detailed experimental design and associated results [10].

4.3.5 Solution pH Profile Documentation (PT5 (1,2))

See CHLE-010 for detailed experimental design and associated results [10].

4.3.6 Determination of 30 Day test Fiber Bed (PT 6)

See CHLE-008 for detailed experimental design and associated results [11].

4.4 30-Day Integrated Tests

4.4.1 Experimental Parameters

Summaries of the experimental parameters for each test within this test series are presented below. The target values for each of these parameters were chosen from a range of parameters generated from review of STP records[3, 5], MELCOR results [7], and CASA results[9].

The tank solution will be demineralized water with addition of the chemicals shown in Table 8. The anticipated pH for the duration of the test will be 7.2 ± 0.2 for the SBLOCA and 7.1 ± 0.2 for the MBLOCA and LBLOCA based on these chemical additions. The quantities of source materials for the corrosion and dissolution reactions are summarized in Table 9. For the LBLOCA and MBLOCA tests, some material will be located in the tank pool and the remainder of the material will be located in the tank vapor space. The division of materials between the two locations is shown in Table 10. The SBLOCA will have no material in the vapor space since containment sprays would not be initiated for a small break [6].

Table 8 : Chemical concentrations in each of the integrated 30-day CHLE tests

Chemical	T0-T2 (mg/L)	T3 (mg/L)
Boric acid (as B)	2708	TBD
Trisodium phosphate	3370	TBD
Lithium hydroxide (as Li)	0.42	TBD

Table 9: Source materials for corrosion in each of the integrated 30-day CHLE tests

Material	Ratio of materials for SBLOCA	Ratio of materials for MBLOCA/LBLOCA
Aluminum		0.078 ft^2/ft^3
Concrete		
Fiberglass		
Galvanized Steel		
Zinc Coated Steel		
Latent Debris (fiber only)		

Table 10: Surface area above and below containment flood level. This division is applicable for the MBLOCA and LBLOCA.

Material Type	Submerged (ft^2)	Unsubmerged (ft^2)
Aluminum	0.47	2.64
Concrete		
Fiberglass		
Galvanized Steel		
Zinc Coated Steel		
Latent Debris (Fiber only)		

The temperature in the system will decline over the 30-day test. The temperature will be controlled by changing the setpoint for the temperature controller at defined times to approximate the temperature profile anticipated for each size of break. An example of the temperature profile from MELCOR is shown in Figure 3. The temperature profiles for the remaining tests are shown in supporting documentation [7].

[NOTE: The temperature profiles will be determined by running MELCOR for each break size.]

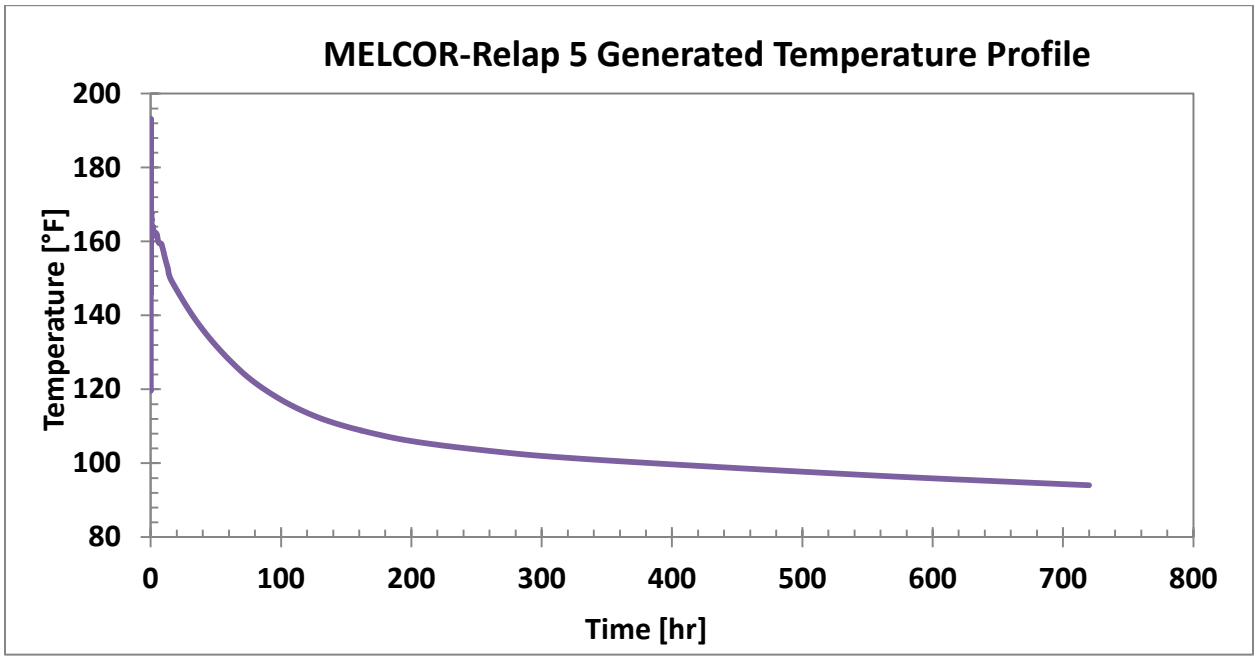

Figure 3: Temperature Profile predicted for a MBLOCA.

The tank sprays will be operated for the first 6.5 hours of the 30-day test for the MBLOCA and LBLOCA tests. The sprays will not be operated for the SBLOCA. The spray flowrate will be 4.7 gpm [6].

Nitric and hydrochloric acid generation is expected to occur as a function of radiolysis of water and cabling within the containment structure. Therefore, the acid generation will be accounted for by the addition of an acidic solution to be added over the thirty day test period [3].

4.4.2 Process Control and Analytical Measurements

Several parameters will be monitored continuously using on-line instrumentation and a data acquisition system. These parameters include flow, temperature, pH, and differential pressure. Additional parameters will be measured by collecting samples from the solution during test operation or by analyzing materials withdrawn from the tank after each test is complete. The analyses are summarized in Table 11.

Table 11: Process Control and Analytical measurements

Parameter	Location	Frequency
Continuous measurements		
Flow	Recirculation pipe, before debris bed	Continuously
pH	Recirculation pipe	Continuously
Temperature	Multiple locations	Continuously
Differential pressure	Across each debris bed, heat exchanger filter	Continuously
Grab samples of solution		
pH	Sample port	Daily
Metals: test dependent	Sample port	Daily
Metals (filtered): test dependent	Filter on sample port	Daily
Turbidity	Sample port	Daily
Total suspended solids	Filter on sample port	Daily
Measurements after 30-day test		
Weight of coupons	Metal coupons	Before and at End of test
Visual inspection of materials with SEM	Corrosion coupons, fiberglass surfaces in material corrosion tank, fiberglass in debris bed	End of test for specified test
Elemental composition of materials with EDS	Corrosion coupons, fiberglass surfaces in material corrosion tank, fiberglass in debris bed	End of test for specified test

4.4.3 Experimental Results

The testing described in this section is expected to produce the following results:

1. Temperature and pH as a function of time over a 30-day period.
2. Concentration of dissolved and total metals (Al, Fe, Cu, Zn, and Pb) in solution as a function of time over a 30-day period.
3. Turbidity and total suspended solids in solution as a function of time over a 30-day period.

4. Head loss through a fibrous debris bed as a function of time over a 30-day period.
5. Corrosion rate determined using defined procedure.

4.4.4 Input into the CASA Model

Corrosion and solubility information obtained from this test series will be used in the precipitation module of CASA. Any quantitative head loss information obtained from this testing will not be directly used by CASA. The short term tests (discussed later) are designed to provide quantitative head loss data for use in head loss module of CASA.

5. METHODS AND MATERIALS FOR THE BENCH SCALE LABORATORY TESTS

5.1 Bench Test Summary

The bench-scale tests are designed to fulfill a number of objectives. The tests will take place in three types of experimental equipment (1) sealed quiescent batch containers inside an autoclave or oven at temperatures up to 265 °F (129 °C), (2) sealed batch containers in a water bath (with integrated shaker table) at temperatures up to 185 °F (85 °C) and (3) a small-scale flow-through loop at temperatures up to 185 °F. The bench tests are divided into series based on the objectives and test equipment. The tests are summarized as follows:

5.1.1 Batch Test (Corrosion/Leaching)

The general objectives of this category of testing are to investigate variability related to corrosion and material release to the containment pool as a function of STP related conditions, investigate variability and identify threshold parameters related to solubility limits and characterize precipitate behavior as a function of thermal cycling. This series of testing examines and captures the bounds and variability related to parameters in the corrosion and solubility for use in CASA. The specific objectives for the identified tests within this category of testing are as follows:

- Series 100 – Tests for leaching of metals from materials will determine whether specific materials need to be included in the integrated 30-day tests and/or the quantity of those materials to be included.
- Series 200 – Investigate the rate of material corrosion/dissolution (Table 3) at temperatures above 185 °F (85 °C) for quantification of additional material to be inserted in the integrated 30-day tests to mimic the additional corrosion that would occur at temperatures above the maximum integrated test temperature.
- Series 300 – Investigates the volume of the batch test solution to be used for all corrosion test.to ensure experimental design does not produced biased results
- Series 400 – Investigate contribution of non-spray phase unsubmerged coupons to the containment pool.
- Series 500 – Investigate the effects of soluble aluminum on the dissolution of fiberglass

- Series 1000 – These tests will determine the maximum concentration of aluminum in solution at the end of 30 days as a function of variability in pH, boron concentration, temperature and combination of materials.
- Series 2000 – These tests will quantify the corrosion rate as a function of corrosion inhibition and the variability in corrosion rates for variable conditions of pH, boron concentration, temperature and combination of materials for CASA input for T < 185 °F (85 °C).

Further experimental details associated with each series are to follow.

5.1.2 Flow-Through Corrosion/Precipitation Tests

- Series 3000 – Precipitation tests will investigate precipitation as function of corrosion of materials under a given range of STP conditions. Temperatures will trace the full temperature profile of a LOCA. Evaluation of data will be used to determine: (1) best possible chemical formula for the precipitate, (2) if precipitate is amorphous Series 3000 – Precipitation tests or crystalline and (3) generate instructions to produce precipitate for short term tank tests.
- Series 4000 – In-core boron precipitation tests to investigate blockage related chemical effects in the core and any effects of post-core solution on the overall system efficiency.

5.1.3 Summary Table of Bench Scale Experiments.

As stated earlier two different types of test will be performed as part of the CHLE analyses bench scale test; Bench batch tests and Flow through loop test. A summary of the earlier described integrated tank test can be found in Table 12.

Table 12: Summary of laboratory tests

Series[1]	Objective	Materials and Chemicals	Status	Comment
100	Test metal leaching	STP soil and concrete boric acid and TSP	On going	Results under review
200	High temperature corrosion rate	Aluminum, galvanized steel, zinc coated steel, concrete, fiber glass boric acid and TSP	On going	Results under review. Maximum temperature reached 250F.
300	Corrosion Test shake down to ensure non-biased design	Aluminum and fiberglass boric acid and TSP	On going	Results under review
400	Determine contribution from unsubmerged coupon due to condensation	Aluminum, galvanized steel, zinc coated steel, concrete, fiber glass boric acid and TSP	Under review	The value of running this test scenario is currently being re-evaluated by the team
500	Determine effects of soluble aluminum on the dissolution of fiberglass	Fiberglass and aluminum salt (Aluminum chloride) boric acid and TSP	To be done	N/A
1000	Determine max 30 day aluminum release concentration	Aluminum only, and aluminum and nukon boric acid and TSP or boric acid and NaTB	To be done	N/A
2100	Determine variations in aluminum corrosion rate due to changes in boron, TSP concentrations and temperature	Aluminum and nukon boric acid and TSP	To be done	N/A
2200	Determine effects of Nukon variations in aluminum corrosion rate due to changes in the ratio of aluminum to Nukon quantities	Nukon and aluminum boric acid and TSP	To be done	N/A
2300	Determine increase in aluminum corrosion rate due to absence of silicon	Aluminum boric acid and TSP	To be done	N/A
2400	Determine increase in aluminum corrosion rate due to absence of phosphate	Aluminum and nukon boric acid and NaTB	To be done	N/A
2500	Determine increase in aluminum corrosion rate due to absence of silicon and phosphate	Aluminum boric acid and TSP	To be done	N/A
2600	Determine variation in aluminum corrosion rate resulting from a substitution of microtherm for Nukon.	Aluminum and microtherm boric acid and TSP	To be done	N/A
2700	Determine variation in aluminum corrosion rate resulting from presence of other metals	Aluminum, copper, iron, zinc, concrete, fiberglass boric acid and TSP	To be done	N/A
3000	Provide solubility limits	TBD from 2000 Series boric acid and TSP	Under review	May be accomplished through short term tank tests with lower max temperature.

3100	Determine variability of precipitate behavior	TBD from 2000 Series boric acid and TSP	Under review	May be accomplished through short term tank tests with lower max temperature.
3200	Determine heat exchanger influences	TBD from 2000 Series boric acid and TSP	Under review	May be accomplished through short term tank tests with lower max temperature.
4000	Evaluate in core and exiting solution chemical effect due to blockage	TBD from 2000 Series boric acid and TSP	Under review	The value of running this test scenario is currently being re-evaluated by the team

[1] Solution pH ±0.1 for all series, except 1000 and 2100 is 7.2. Solution pH for the other two series is 6.0, 7.2,and 7.7. Temperature ranges up to 260 °F.

5.2 Bench Scale Laboratory Test Equipment

5.2.1 Batch Corrosion/Leaching Tests

Batch tests will take place in sealed half full containers in temperatures < 185 °F (85 ° C). For temperatures above the boiling point of water, the containers will be placed in an autoclave. No agitation of samples will take place. For temperatures below the boiling point of water, the samples will be placed in a temperature-controlled water bath. The water bath will have a shaking platform to provide agitation to the samples.

5.2.2 Flow-Through Loop Test

A schematic of the flow-through loop is presented in the CHLE equipment calculation [6] and will operate at temperatures as high as 260 °F.

Details associated with each of laboratory tests are currently under revision, therefore are not included in this draft

6. METHODS AND MATERIALS FOR SHORT TERM TANK TESTS

6.1 Short Term Tank Test Summary

The short-term integrated tank tests will use the same experimental conditions as the 30-day integrated tank tests. The debris bed conditions will correlate to the debris beds prepared in the High Temperature Vertical Loop Testing conducted by Alion. This testing will be done using four different bed types and three different solution chemistries.

Further details associated with this section of testing will not be included until Alion's High Temperature Vertical Loop test plans are finalized.

7. References

1. NEI, *Pressurized Water Reactor Sump Performance Evaluation Methodology. Revision 0*, 2004, NEI.
2. NEI, *Safety Evaluation by the Office of Nuclear Reactor Regulation Related to NRC Generic Letter 2004-02, Nuclear Energy Institute Guidance Report "Pressurized Water Reactor Sump Performance Evaluation Methodology*, 2004.
3. UNM, *Chemical Addition Calculation*, 2012, University of New Mexico: Albuquerque, NM.
4. Alion, *STP Post-LOCA Water Volume Analysis*, 2012, Alion Science and Technology: Albuquerque, NM.
5. UNM, *CHLE Test Materials* 2012, University of New Mexico: Albuquerque, NM.
6. UNM, *Equipment Design* 2012, University of New Mexico.
7. TAMU, *Relap5 3d-MELCOR temperature Report*, 2012, University of Texas, Austin: Texas.
8. UNM, *Calculation for material area needed for high temperature corrosion*, 2012, University of New Mexico: Albuqueruqe, NM.
9. LANL, *CASA report for STP conditions*, 2012.
10. UNM, *CHLE Tank Test Results for Blended and NEI Fiber Beds with Aluminum Addition*, 2012.
11. UNM, *Debris Bed Preparation and Formation Test Results*, 2012.

PROJECT DOCUMENTATION COVER PAGE

Document No: CHLE-004	Revision: 1	Page 1 of 11
Title: CHLE Equipment Description and Specifications		
Project: Corrosion/Head Loss Experiment (CHLE) Program		Date: 16 August 2012
Client: South Texas Project Nuclear Operating Company		

Summary/Purpose of Analysis or Calculation:

The Chemical Head Loss Experiment (CHLE) tank tests equipment is designed to simulate probable South Texas Project (STP) LOCA conditions. The CHLE tank test equipment consists of three primary sections: (1) the material corrosion tank, (2) the vertical head loss modules, and (3) the heat exchanger loop. The purpose of this document is to provide detailed information and describe associated parameters that scale each section of equipment to simulate probable STP LOCA conditions.

Signatures:	Name:	Signature:	Date:
Prepared by:	Janet Leavitt/Kyle Hammond	< signed electronically >	3/12/2012
UNM review:	Kerry Howe	< signed electronically >	8/16/2012
STP review:			
Soteria review:	Zahra Mohaghegh	< signed electronically >	5/11/2012 8/18/2012

Revision	Date	Description
0	3/12/2012	Original document
1	8/16/2012	Revised with heat exchanger system

Table of Contents

List of Figures

List of Tables

Definitions and Acronyms

RCB	Reactor Containment Building
RCS	Reactant Cooling System
RWST	Refueling Water Storage Tank
SI	Safety Injection
LOCA	Loss of Coolant Accident
STP	South Texas Project

1.0 Purpose

The Chemical Head Loss Experiment (CHLE) tank tests equipment is designed to simulate probable South Texas Project (STP) LOCA conditions. The CHLE tank test equipment consists of three primary sections: (1) the material corrosion tank, (2) the vertical head loss modules, and (3) the heat exchanger loop. The purpose of this document is to provide detailed information and describe associated parameters that allow each section of the CHLE equipment to simulate probable STP LOCA conditions to evaluate key chemical effects.

2.0 Material Corrosion Tank

The material corrosion tank is an existing piece of equipment used in the previous Integrated Chemical Effects Testing. Tank mixing and spray related conditions were the factors used to scale CHLE conditions to simulate probable STP LOCA Conditions.

2.1 Equipment Description

The 304 stainless steel tank, Figure 1, is nominally 4 ft x 4 ft x 6.6 ft in size and has a bottom that slopes to a centrally-located discharge port. For testing purposes, the tank can be theoretically divided into upper and lower sections. The upper section of the tank is designed to accommodate all vapor space materials in containment that contribute to chemical effects through exposure to containment sprays. The lower section of the tank is designed to accommodate solution and materials that may be submerged in containment. A removable cover and gantry crane allow for placing and removing samples into the desired areas of the tank. The tank is insulated and contains two titanium-jacketed 3.5-kW rod-type heaters in the tank pool to maintain the temperature of the solution at a maximum of 185 °F (85 °C) ± 5 °F. The heaters are fully redundant to provide the required heating capacity which allows experiments to continue uninterrupted in the event of failure of a single heater.

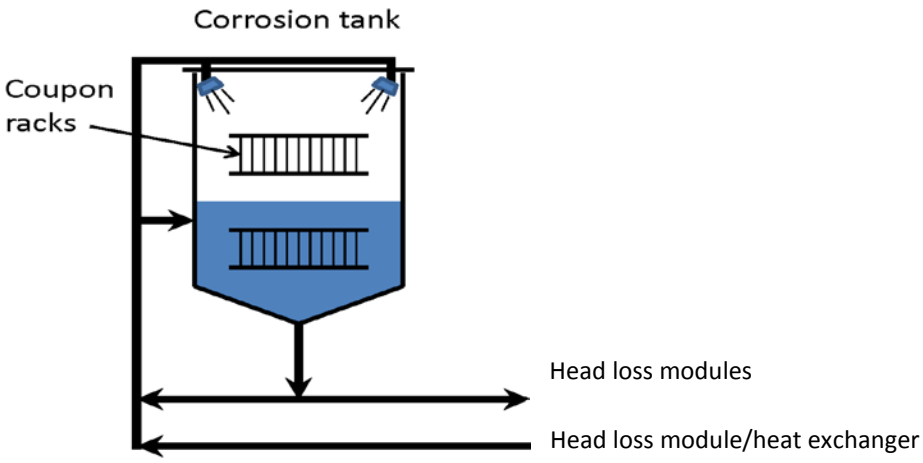

Figure 1: Simplified process flow diagram showing corrosion tank integration within CHLE

Solution can enter the tank through injection headers in the lower portion of the tank (submerged area) and/or through spray nozzles in the upper portion of the tank (non-submerged area). Flow to the tank is controlled manually with a variable speed drive pump and a throttle valve. The injection headers used to provide turbulence in the tank pool are in the lower portion of the tank, below the water line on the north and south walls. These headers are 1-in.-diameter pipes with a symmetric pattern of holes to distribute the solution discharge. In the upper section of the tank, the spray nozzles are located in the four corners near the top of the vapor space. Throttle valves and flow meters allow the flow to be apportioned to the spray nozzles and flow injection headers at the desired rates [1]. The piping to the spray section of the tank is 3/4-in Chlorinated Polyvinyl Chloride (CPVC) and contains a rotometer and ball valve for flow control. Proper arrangement of valves directs solution from the tank to the upper spray nozzles.

The corrosion tank is monitored for temperature, pH, and flow rate. Tank temperature is monitored in four locations within the tank, three in the pool and one in the vapor space. The tank solution pH and flow are monitored outside the tank in an instrumentation pipe loop. Detailed information associated with equipment instrumentation is presented elsewhere [1].

2.2 Scaled Parameters

Pool mixing in the CHLE corrosion tank equipment section was used to help simulate STP post-LOCA conditions. A Computational Fluid Dynamics (CFD) model of both the STP post-LOCA pool and the CHLE corrosion tank pool were created to determine the pool velocities. The pool velocities were not required to be equivalent, but were desired to result in similar mixing. The CFD model was developed under isothermal conditions. The CFD modeling resulted in a range of fluid velocity of 1 ft/s to 0.009 ft/s for the STP post-LOCA pool and a range of fluid velocities of 0 – 0.250 ft/s for the CHLE corrosion tank [2]. The CHLE pool provides a well-mixed pool that is reasonably representative of the range of velocities in the STP post-LOCA pool. The CFD modeling of the CHLE corrosion tank pool also allows for placement of materials into well mixed areas for optimal corrosion exposure.

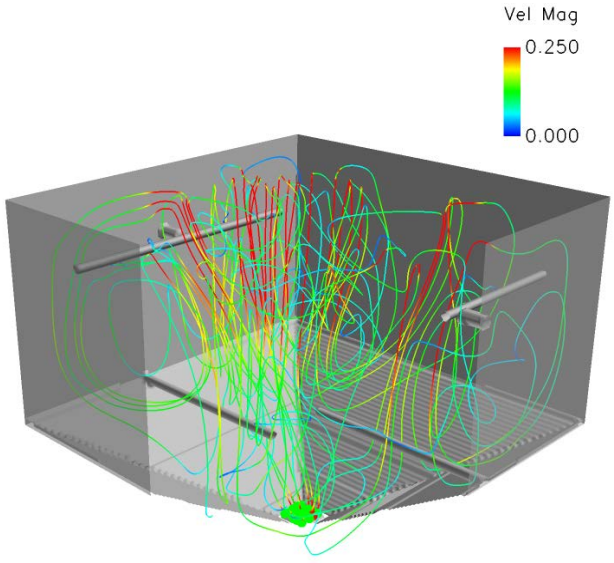

Figure 2: CHLE CFD Model

The spray flow rate and time are parameters used within the CHLE corrosion tank section to help simulate STP post-LOCA pool conditions. The CHLE corrosion tank spray flow rate was calculated from the ratio of STP spray flow rate and cross-sectional area of STP to the CHLE spray flow rate and cross-sectional area of the material corrosion tank, Equation 1. Using this approach, the volumetric flow rate of liquid through the sprays in the material corrosion tank was determined to be 4.7 gpm [3].

$$\frac{\dot{V}_{stp}}{A_{stp}} = \frac{\dot{V}_{CHLE}}{A_{CHLE}} \quad (1)$$

The 6.5 hour spray time for the CHLE tank tests is dictated by STP operating instructions [4]. While operating instructions present varying spray times, the longest time that the sprays are expect to remain on was chosen to be the CHLE test spray time which allows for maximum chemical exposure to the unsubmerged materials in efforts to capture possible chemical effects due to the spray phase.

3.0 Vertical Head loss Module

The CHLE tank system has three identical vertical head loss modules, independently pumped, that are designed to run in parallel or individually; isolated from the corrosion tank. The flow rate to the columns and screen area were used to determine the CHLE approach velocity which helps simulate probable STP LOCA conditions.

3.1 Equipment Description

The upper portions of the 6-in diameter vertical head loss modules are 30 inches long, lower portion is 12 inches long, constructed of stainless steel and are sealed at the top with a blind flange. The blind flanges can be removed to introduce debris into the head loss assembly (Figure 2 and 3). The upper section of piping also has an air vent to allow gas to be vented from the head loss assembly, if necessary. The middle section of the assembly is constructed of 1/4-in thick polycarbonate to allow view of the debris bed (6 inches below and 12 inches above) with a perforated plate supported by a ring located 6-in from the bottom. There are vents above and below this area to assist in post-test activities. A differential pressure (DP) transducer is also piped to ports above and below the bed in the middle section of this assembly to measure the pressure loss through the debris bed. Each module has a dedicated flow meter to monitor flow to the column. Detailed information associated with equipment instrumentation is found elsewhere [1].

The middle part of the assembly is 23-in long with flanges to allow for fully intact bed removal. This middle section is connected to a CPVC flange with O-rings to avoid use of chemical solvents that may fail due to thermal expansion.

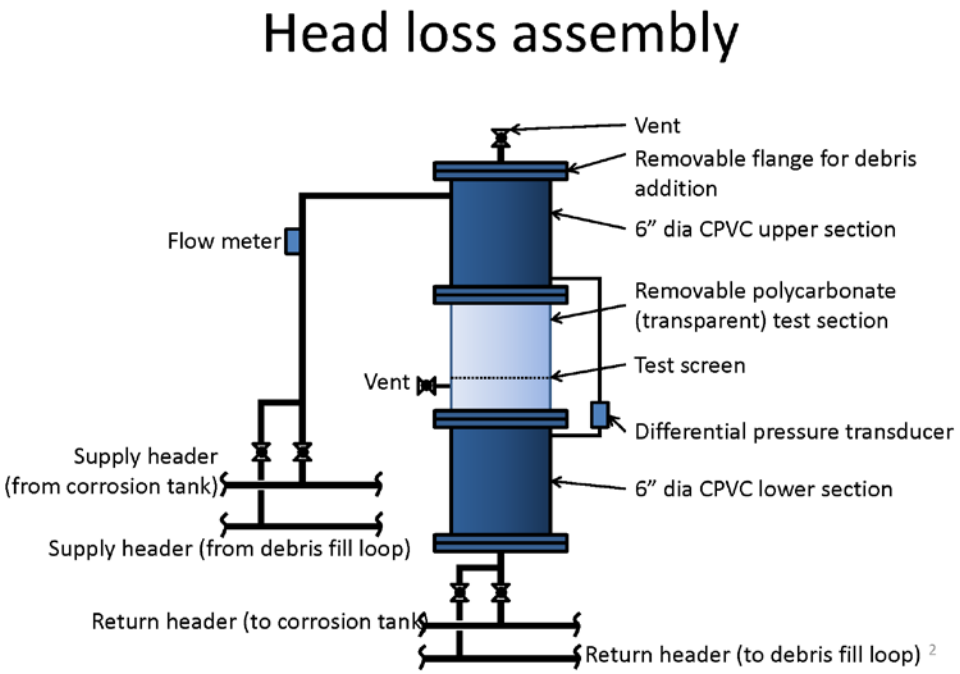

Figure 3: Head loss Design assembly

Figure 4: Head loss assembly

The supply and discharge piping to each head loss assembly is 1/2-in 316 stainless steel pipe, with threaded fittings. Each assembly has a pump with the necessary piping and valve configuration to carry a constant flow of solution from and to the material corrosion tank or within the bed formation recirculation loop which allows for isolation and independent circulation of a single column. The leg of piping to the material corrosion tank has a globe valve for flow control and the leg to the bed formation recirculation has a ball valve for isolation. The globe valve provides back pressure to prevent or minimize degassing below the debris bed due to negative pressure in the head loss assembly.

3.2 Scaled Parameters

The CHLE column approach velocity in the head loss model section was used to help simulate STP post-LOCA conditions. The column flow rate was controlled to produce a velocity across the 6 inch strainer (same material as used at STP) to produce the equivalent approach velocity, 0.010 ft/s, expect to occur in an STP post-LOCA scenario [1].

4.0 Heat Exchanger Loop

The CHLE heat exchanger loop is designed to cool a slip stream of the test solution to capture chemical effects due to thermal-cycling during a post-LOCA scenario. It will not be run constantly during the 30 Day test, but for a predetermined time period during specified sections of the test. The target temperature drop will be determined using MELCOR/RELAP 5 simulations [4] for specific LOCA conditions.

4.1 Equipment Description

This loop consists of ½ inch chemically inert rigid tubing, a stainless steel shell and tube heat exchanger, two inline filters, a gear pump, two temperature probes and a differential pressure indicator, as shown in Figures 5 and 6. Detailed information associated with equipment instrumentation is found elsewhere [1]. The heat exchanger (Exergy model 00268-3) is 12.88” long with 1/8” inlet and outlet for both shell and tube flow path. Two inline filter holders with a 47-mm diameter membrane filter (0.1 μm) are located slightly before the inlet of the exchanger and slightly after the discharge of the exchanger. A differential pressure (DP) transducer with a range of 0 to 5 psi (0 to 11.5 ft of water) is used to monitor head loss of the cooled solution passing through the filter down stream of the heat exchanger. The pressure drop will be used as an indicator of precipitate formation. After passing the cooled solution through the filter holder, the water will not be independently reheated but reheated by mixing with a larger stream of and returned to the material corrosion tank.

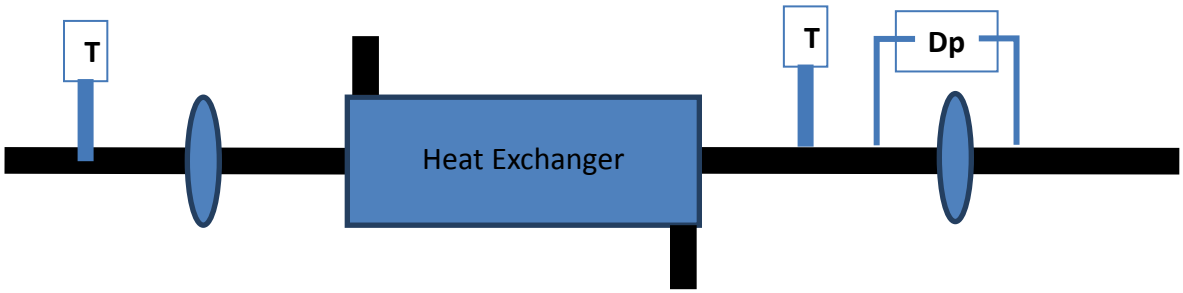

Figure 5: Heat exchanger design

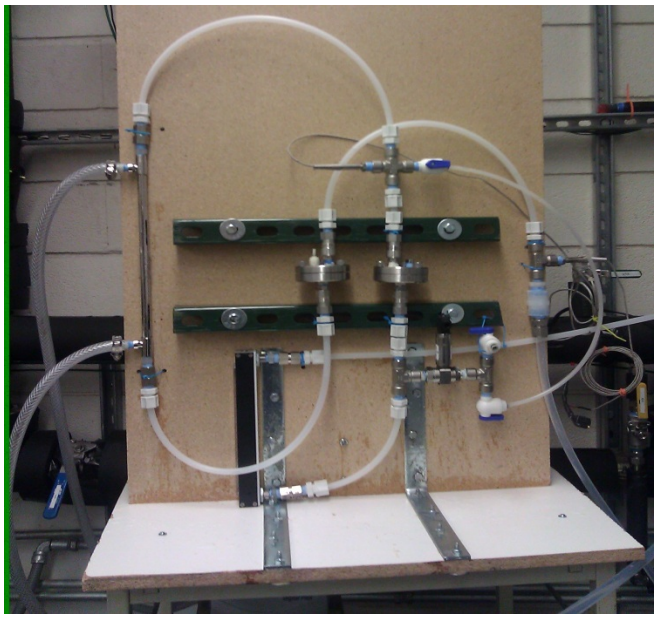

Figure 6: Heat exchanger section of CHLE tank equipment

4.2 Scaled Parameters

The heat exchanger was chosen so that it could achieve a temperature decrease of 50 °C, which is greater than the maximum temperature decrease during a LOCA at STP [4]. The operating conditions of the heat exchanger to achieve this temperature drop are described in Table 1. The slip stream exposed to the heat exchanger is not scaled to that at STP. The purpose of the slip stream was to capture thermal-cycling effects through monitoring filters and head loss indications.

Table 1: Heat exchanger design specifications

Metric Units		
Heat Exchanger Model		00268-3
	Tube Side	Shell Side
Fluid	Water	Water
Temperature In(°C)	85	15
Temperature Out(°C)	34.58	15.87
Mass Flow (g/sec)	3.26	188.82
Volumetric Flow (lpm)	0.2	11.36
Pressure Drop (kPa)	0.25	822.16
Heat Transfer (W)	687	

5.0 Equipment Summary

A summary of key design parameters is presented in Table 2. All results were gathered from current STP data or calculations performed on STP plant specifications. It was important to properly scale STP plant

conditions to the CHLE equipment to allow for experimental conditions to simulate probable STP LOCA conditions. Based on the results gathered above, the CHLE tank equipment should properly model probable STP LOCA conditions to evaluate key chemical effects.

Table 2: Summary of CHLE tank equipment parameters used to scale to STP conditions

Description	Value
STP Pool pool velocities (STP/CHLE) (ft/s)	1 - 0.009 /0 - 0.25
Spray Flow/Time (STP/CHLE) (hrs)	6.5
Strainer Velocity (STP/CHLE) (ft/s)	0.009/0.010
Heat exchanger temperature drop (^{o}C)	TBD

6.0 References

1. UNM, *Instrument Calibrations*, 2012, UNM: Albquerque NM.
2. Alion, *CDF Modeling of STP and CHLE pools*, 2012, ALION Science and Technology.
3. Alion, *GSI-191 Containment Recirculation Sump Evaluation: CFD Transport Analysis*, 2007.
4. TAMU, *Relap5 3d-MELCOR temperature Report*, 2012, University of Texas, Austin: Texas.

PROJECT DOCUMENTATION COVER PAGE

Document No: CHLE-005	Revision: 1	Page 1 of 47
Title: Determination of the initial pool chemistry for the CHLE test		
Project: Corrosion/Head Loss Experiment (CHLE) Program		Date: 13 August 2012
Client: South Texas Project Nuclear Operating Company		

Summary/Purpose of Analysis or Calculation:

The purpose of this calculation is to determine the chemical constituents and associated concentrations in the Corrosion/Head Loss Experiment (CHLE) bulk solution before the addition of corrosion or dissolution products. A review of 2 years of historical analyte data obtained from STP was performed to identify chemical constituents that may be included in the CHLE tests. Upon identification of the chemical constituents to be included, a maximum, minimum, and average concentrations were determined for each constituent in the three sources of solution: the refueling water storage tank, the reactant cooling system, and the safety injection accumulators. The chemical constituent concentrations and solution volume of these three sources were used to determine the final mass of the chemical constituents. The final mass of the chemical constituents and the total volume of solution as a result of a Loss-of-Coolant Accident (LOCA) were used to calculate minimum, maximum, and average chemical constituent concentrations which will be used in the CHLE test matrix. The average concentrations of the chemical constituents will be used for the 30 day tank tests bulk solution. The minimum and maximum chemical constituent concentrations will be included within the bounds of the laboratory tests.

Signatures:	Name:	Signature:	Date:
Prepared by:	Janet Leavitt	< signed electronically >	8/13/2012
UNM review:	Kerry Howe	< signed electronically >	8/13/2012
STP review:			
Soteria review:	Zahra Mohaghegh	< signed electronically >	5/11/2012 8/18/2012

Revision	Date	Description
0	3/12/2012	Draft document for internal review
1	8/13/2012	Includes revisions from internal review

Table of Contents

List of Figures

List of Tables

Definitions and Acronyms

RCB	Reactor Containment Building
RCS	Reactant Cooling System
RWST	Refueling Water Storage Tank
SI	Safety Injection
SFP	Spent Fuel Pool
RMWST	Reactor Makeup Water Storage Tank
BAT	Boric Acid Tank
BARS	Boric Acid Recovery System

1 Purpose

The purpose of this calculation is to determine the chemical constituents and associated concentrations in the Chemical Head Loss Experiment (CHLE) bulk solution before the addition of corrosion or dissolution products. These values are important in conducting a risk informed approach in evaluation of potential safety issues as a result of a Loss of Coolant Accident (LOCA). The chemical constituent and associated concentrations of the post-LOCA reactor containment building (RCB) pool solution are necessary to determine the initial pool chemistry to predict the subsequent solution chemistry resulting from dissolution and corrosion of materials. A potential exists for the interaction of the pool chemistry and materials in containment to produce chemical precipitates that may negatively influence head loss across the sump strainer; possibly resulting in failure of the Emergency Core Cooling System (ECCS). An accurate value of total chemical constituent masses and containment pool volume determined from the various sources of solution will allow the CHLE analyses to investigate the most probable pool chemistry of a LOCA. This approach will determining a more realistic consequence of chemical reaction due to LOCA conditions on head loss across the sump strainer of the ECCS as compared to that determined using the deterministic approach.

To accomplish the task, two years of historical analyte data obtained from STP was reviewed to identify chemical constituents and associated concentrations that will be included in the CHLE tests. A maximum, minimum, and average concentration for the identified constituents were determined for each of the three sources of solution: the refueling water storage tank (RWST), the reactant cooling system (RCS), and the safety injection accumulators (accumulators). The chemical constituent concentrations and solution volume of each of these three sources [1] were used to determine the final mass of the chemical constituents for a post-LOCA pool solution. The average concentrations of the chemical constituents determined the 30 day CHLE tank tests bulk solution makeup. The minimum and maximum chemical constituent concentrations will be included within the bounds of the CHLE laboratory tests.

2 Methodology

The chemical constituents of the initial containment pool solution following a LOCA are variable because the final pool volume and chemical constituent concentrations are determined from three possible sources of solution. Each source of solution has a range of chemical constituents with associated concentrations and different solution volumes. For LBLOCA and MBLOCA, the final pool volume and chemistry is a combination of three sources of solution as follows: RWST (~80 % water mass), RCS (~ 16% water mass), and accumulators (~4% water mass) [1]. For a SBLOCA, the final pool volume is only a combination of two solution sources, the RWST (~ 85 % water mass) and the RCS (~ 15% water mass)[1].

Each source of solution is monitored for specific chemical constituents or analytes of interest and the sampling frequency for each analyte is variable. The type of analyte monitored and the frequency of mointoring is determined by the operational uses of the solution sources. The RCS and RWST are monitored for multiple chemical constituents, while the accumulators are only monitored for boron concentration. The solution in the accumulators are not monitored as closely as the other sources

because they are filled using the RWST solution. While the accumulators are charged from the RWST, they only have the same chemical make up at the point of recharge. The RWST solution is used during outages resulting in a hydraulic connection to the spent fuel pool (SFP). This connection results in other chemical constituents such as silicon to become part of the RWST chemistry.

Two years of historical data for aqueous chemical constituent concentrations in the various sources of solution at STP were collected and reviewed. Before the historical data was analyzed, data reflective of shut down operations was removed. The analyses of data obtained from normal operating conditions was used to identify which monitored chemical constituents would be eliminated and which would be included in the CHLE analyses. For the chemical constituents to be included in the CHLE analyses, the respective minimum, maximum, and average concentrations from each source of solution were determined using one of the three methods described below.

2.1 Statistics

The procedure used to determine a valid mathematical representation of a random variable given its sample of observed values. In statistics this procedure is known as a fitting procedure and typically consists of three steps:

1. Choose families of distributions to fit
2. Estimate distribution parameters for each family from step 1
3. Test the quality of the fit using quality of the fit statistics

It was decided to limit attention to the following three families of distributions - Normal, Lognormal and Johnson. The use of the Normal and Lognormal distributions is a standard practice. The Johnson distribution is known for its ability to model a wide variety of skewness and kurtosis combinations, so it was also used in the analyses to allow for greater flexibility of the fitting results.

Parameter estimation for the Normal and Lognormal distributions was done using Maximum Likelihood Estimation (MLE) procedure. If $x_1, x_2, \ldots, x_n$ is a sample then MLE for the Normal and Lognormal distributions are given by

- Normal: $\hat{\mu} = \sum_{i=1}^{n} x_i / n, \ \hat{\sigma}^2 = \sum_{i=1}^{n} [x_i - \hat{\mu}]^2 / n$
- Lognormal: $\hat{\mu} = \sum_{i=1}^{n} \ln(x_i) / n, \ \hat{\sigma}^2 = \sum_{i=1}^{n} [\ln(x_i) - \hat{\mu}]^2 / n$

For the Johnson distribution, numerical algorithms have to be used to estimate its parameters. The algorithm used in this analyses was proposed by Wheeler [2] and uses fifth order statistics to perform the fit.

The quality of fit was done using the two-sample Kolmogorov-Smirnov statistics (KS-statistics), where the first sample is the data used for the fitting and the second sample is data generated from the fitted distribution[3]. KS-statistic computes a distance between the empirical cumulative distribution functions of two samples, which is then used to compute the p-value of the test. We conclude that the two samples come from different distributions if the p-value is less than 0.05.

The entire procedure was coded in R language. The estimation of the Normal and Lognormal distributions was done using MASS package. The SuppDists library was used in the fit of the Johnson distributions. Finally, the two-sample KS test was done using STATS package.

For some of the data which could not be successfully fit using the above fitting techniques, cumulative probability graphs that result in an "S" type curve were produced to assist with interpretation of the data. This type of distribution has the advantage of providing an overall picture which shows the sum of deviation to any particular point [4].

Upon reviewing the statistically obtained data, it was decided that the median which is the middle value of the set of data is to be used as the average for the data analyzed as opposed to the mean value which is the arithmetic average, computed by adding up a collection of numbers and dividing by their count [4]. The median was chosen because it is not as sensitive to minimum and maximum values within the range of data analyzed. For data successfully fit with a distribution, the median and mean are equivalent. The minimum and maximum is represented by the range of data.

2.2 pH Profile as a Function of TSP Dissolution and Break Type

The pH profile was calculating using the rate of pool fill and the rate of TSP dissolution[5]. The TSP baskets are 2 feet tall with the bottom of the baskets positioned 6 inches above the floor. The baskets have TSP in them to a nominal depth 20 inches. For purposes of TSP submergence, the water volume calculation assumed the top of the TSP is at an elevation of 26 inches (2.17 feet). The containment building has a floor area of 12,300.9 ft^2 [1], thus, the pool reaches the top of the TSP when the pool volume is 26,642 ft^3. Break flows for a MBLOCA have been estimated at 1200 lbm/s [6], which corresponds to a flow rate of 1150 ft^3/min. The containment spray flow rate with two trains in operation is 5800 gpm (775 ft^3/min). Thus, the total fill rate for the containment pool can be estimated at 1,925 ft^3/min and the time to fill to a depth of 26 inches is 14 minutes. Since this time is relatively short and other uncertainties exist that affect the rate of TSP dissolution, the time to start TSP injection for the CHLE tests will be 15 minutes.

2.3 Acid Generation Due to Irradiation

The acid generation due to irradiation was previously calculated by STP using the Polestar QA software STARpH 1.05 code with the purposes of (1) determining the pH of the STP containment pool solution as a function of time following a LOCA using the alternative source term and (2) determining the maximum DF for the removal of elemental iodine form the containment atmosphere [7].

3 Design Input and Analyses

For each chemical constituent monitored by STP, the constituent concentration was reviewed. If the concentration of a chemical constituent was at trace levels (ppb or µg/L), it was eliminated from the list. If the concentration was significant (ppm or mg/L), the associated minimum, maximum and average concentrations based on the historical data was determined using one of the methods previously outlined.

3.1 Containment Pool Volume

The containment pool solution is the sum of three possible sources of solution; the RCS, the RWST, and accumulators. Each source of solution injects into the pool as dictated by operational constraints resulting in a range of the final post-LOCA pool volume and mass. The range of pool solution mass used in the minimum and maximum pH calculation for STP [8] are referred to as design basis in this document, and are listed in Table 1. The average operational solution volumes and masses which were determined from statistical review of operating conditions and operational constraints [1] and are listed in Table 2. The analysis of the operational solution mass for each source results in a "best estimate" which has a smaller final pool solution mass range (4.2-4.5 million lb) than the design basis range (3.7 – 5.4 million lb). The "best estimate" of the operation solution mass as listed in Table 2 was used in calculations of chemical constituents masses predicted to exist in the final pool volume.

Table 1: Design basis containment pool volume as a function of LOCA type [8].

Source	Min (lb)	Pool Contribution	Max (lb)	Pool Contribution
RWST	2,988,450	80%	4,505,980	84%
Accumulators	218,182	6%	228,015	4%
RCS	534,400	14%	631,700	12%
Total Mass	3,741,032	100%	5,365,695	100%

Table 2: "Best Estimate" Operating containment pool volume as a function of LOCA type [1].

Source	SBLOCA (lb)	Volume[1] (ft^3)	Pool Contribution	MBLOCA and LBLOCA (lb)	Volume[1] (ft^3)	Pool Contribution
RWST	3,630,265	58,238	86%	3,630,265	58,238	81%
Accumulators	0	0	0%	231,334	9,828	5%
RCS	612,644	3,711	14%	612,644	3,711	14%
Total Mass	4,242,909	68,066	100%	4,474,243	71,778	100%

[1] at 21 °C

3.2 **Trisodium Phosphate**

Trisodium phosphate dodecahydrate (TSP) is a buffer that exists in containment to maintain the pool pH greater or equal to pH 7 [9]. It is not present in any of the three sources of solution which contribute to the final pool volume. Instead, there are six baskets filled with a total of 11,500 to 15,100 lb of granular TSP [5] strategically located within the post-LOCA flood region of containment [9] which dissolves into solution in response to a LOCA. The range of TSP mass listed is a result of the density range associated with TSP (57 ± 3 lb/ft^3) and loading procedures [10]. Simply, the TSP in containment was not measured by weight, but calculated from volume. Each basket has two standardized marks that are two inches apart and is filled with granular TSP to any point between these marks [11]. A review of the basket levels [12] provide basis that the mass of TSP in containment is closer to the maximum cited range; therefore the TSP mass of 15,100 lb will be used as a scaling factor in the CHLE tests.

TSP dissolution has been calculated to occur within 80 minutes in the pool [9]. This was done using an experimentally obtained dissolution rate of 0.7 lb/ft^2 which was determined from dissolution of a solid block of TSP in 160 ^oF water with no agitation [13]. The total dissolution time is based on the assumptions that the baskets are completely submerged in approximately 15 minutes and that only the top and bottom surfaces of the basket are included in the surface area calculation; this allows for determination of an easily-calculated uniform rate of TSP dissolution. In an actual post-LOCA situation (LBLOCA and MBLOCA), all TSP surfaces would be exposed to the sump solution at initial temperatures exceeding 200 ^oF with significant agitation and the baskets would be submerged within 15 minutes [8, 9] which suggest that the dissolution rate is conservative.

For SBLOCA, it may take longer than 15 minutes for the baskets to become submerged, the maximum initial temperature may be less than 160 ^oF, agitation may not be as significant when compared to the larger LOCA scenarios and the final pool volume may be less than that of the larger LOCA scenarios. The mass of TSP in containment exposed the smaller final pool volume is not near the saturation limit for TSP; therefore the dissolution of TSP within solution may have a similar dissolution rate.The dissolution rate and the longer time required to fill the pool will result in a higher TSP concentration due to the volume dictated by the fill rate and possibly result in a characteristically different pH profile.

Since the review of STP records [12] indicate that the mass of TSP in the basket is reflective of the maximum range defined, the maximum mass (15,100 lb) and the median total pool volume (71,778 ft^3) for a LBLOCA/MBLOCA will be used to determine the TSP concentration (3.37 g/L) to be used in the CHLE tests. It has been determined that a SBLOCA will not be modeled in the CHLE tests, therefore this concentration was not calculated.

3.3 **Boron**

Boron in the form of boric acid is a neutron absorber that exists in the pool solution during any LOCA scenario. The three sources of solution (accumulators, RCS, and RWST) that contribute to the final pool volume as a result of a LOCA are maintained independently of each other possibly resulting in different

boron concentrations. The ranges of boron concentration for each source of solution used in the minimum and maximum pH design basis calculation are listed in Table 3 [5]. This range of boron concentrations with the range in solution volumes results in a wide range of boron mass within the containment pool.

Table 3: Design basis Boron concentration ranges for contributing sources.

Water Source	Minimum Concentration (mg/L)	Maximum Concentration (mg/L)
Accumulators	2700	3000
RWST	2800	3000
RCS	0	3500

Review of historical data showed that the sources of solution that contribute to the final pool volume as a result of a LOCA are maintained within a narrower band of concentrations (Table 4) as compared to the design basis. The last seven years of historical accumulator data was processed to provide a thorough analysis, since they are monitored less frequently. Since the RCS and RWST are monitored frequently, only the last two years of historical data was processed. The following sections explain the review of this data.

Table 4: Operating Boron concentration ranges for contributing sources.

Water Source	Minimum Concentration (mg/L)	Maximum Concentration (mg/L)
Accumulators	2767	2952
RWST	2895	2962
RCS	3.7	3105

3.3.1 RCS Boron

3.3.1.1 RCS Boron Analyses

The historical review of operation data for boron concentration observed in the RCS sources of both units is presented by Figure 1. A histogram for each RCS (Figures 2 and 4) was created for the statistical analysis to identify a minimum, maximum, and average boron concentration. As shown by Figure 2 and 4, the boron concentration as a function of time does not fit a normal Gaussian distribution; the concentration is not random but instead is controlled to vary the power output of the reactor. Thus, relative cumulative frequency graphs (Figures 3 and 5) were prepared to examine the distribution of the data. On the basis of these graphs, the median was determined to be a suitable value to use in the 30-day CHLE tests.

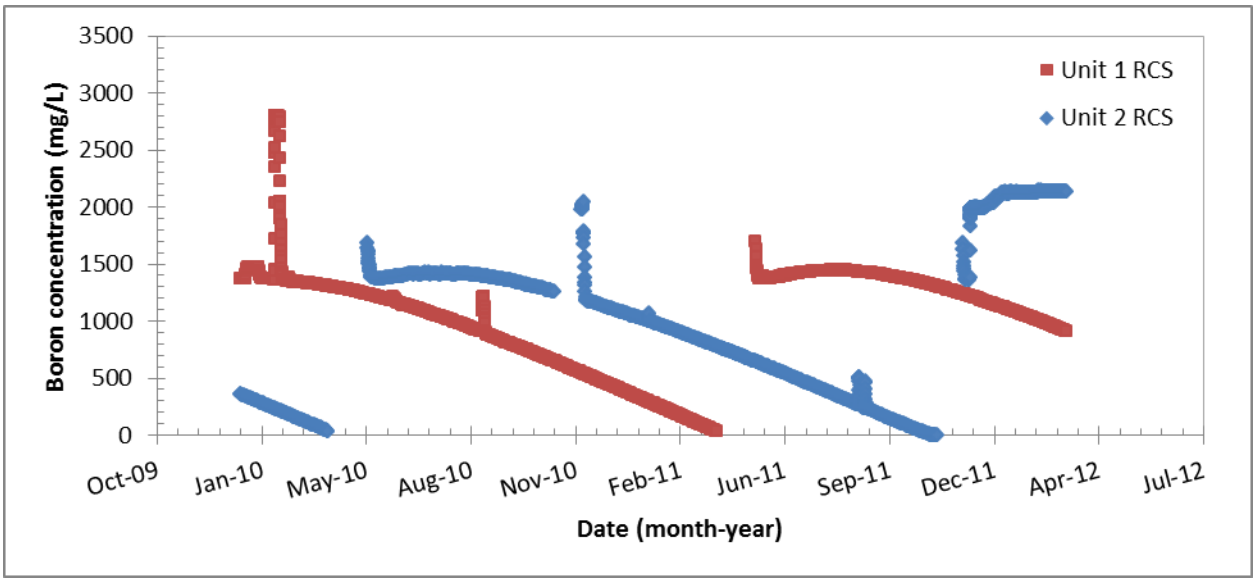

Figure 1: Boron concentration for Unit 1 and 2 RCS as a function of time.

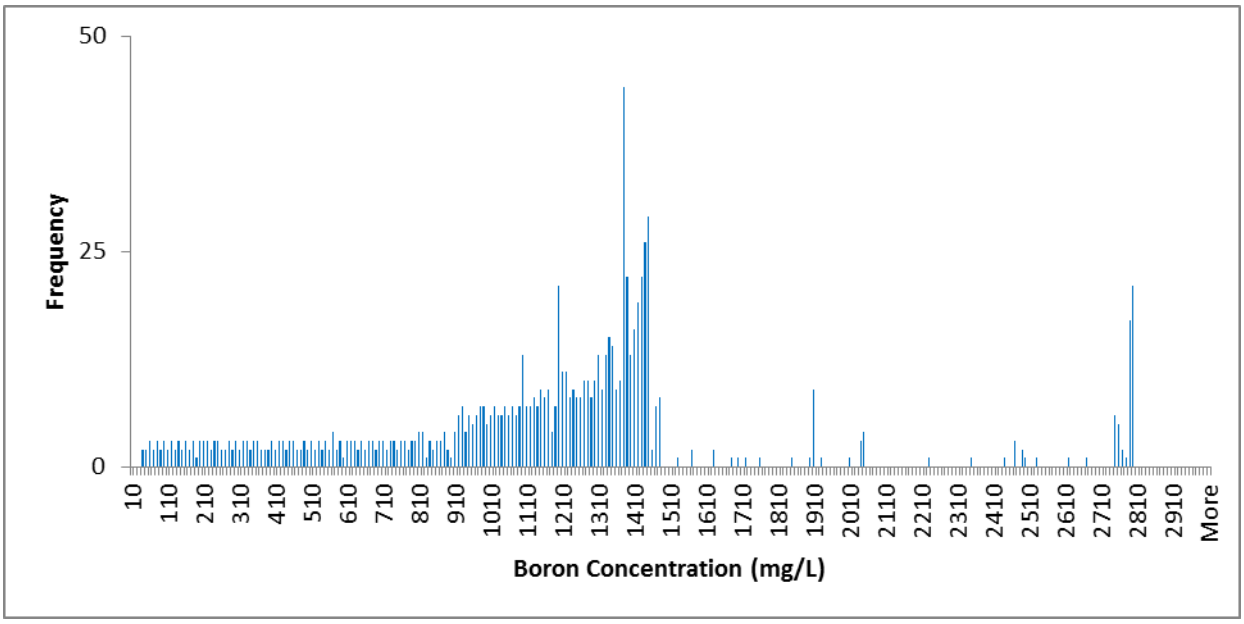

Figure 2: RCS 1 Boron histogram.

Table 5: Statistical RCS 1 data (Figure 2).

RCS 1	
Mean (mg/L)	1185
Standard Error (mg/L)	19
Median (mg/L)	1218
Mode (mg/L)	1374
Standard Deviation (mg/L)	584
Kurtosis	2
Skewness	1
Minimum (mg/L)	35
Maximum (mg/L)	2797
Count	915

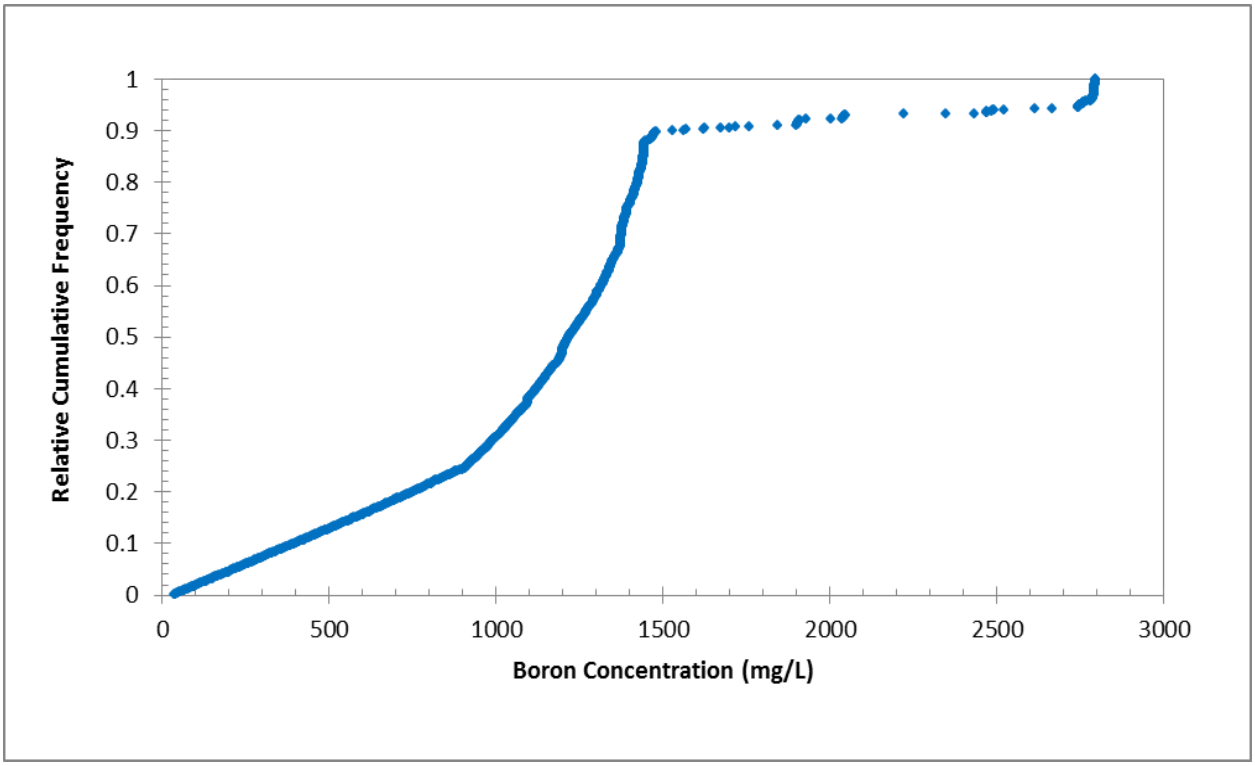

Figure 3: RCS 1 Boron relative cumulative frequency graph.

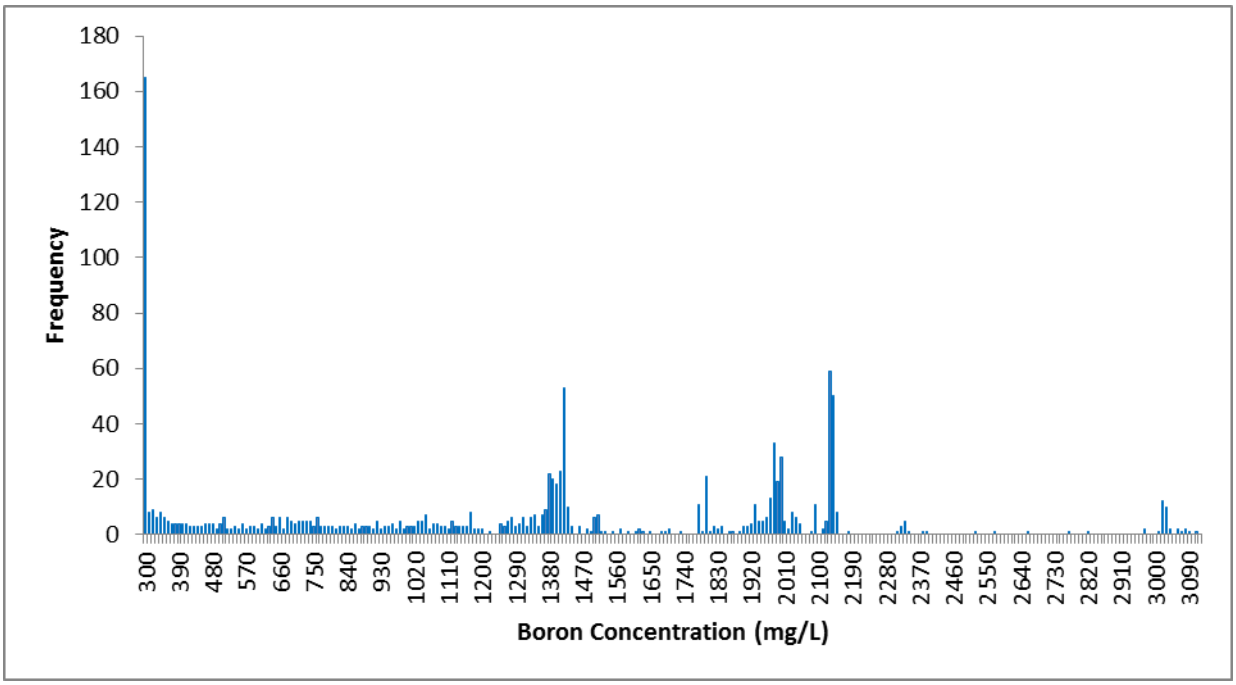

Figure 4: RCS 2 Boron histogram.

Table 6: Statistical RCS 2 data (Figure 4).

RCS 2 B	
Mean (mg/L)	1265.6
Standard Error (mg/L)	22.5
Median (mg/L)	1372.0
Mode (mg/L)	1416.0
Standard Deviation (mg/L)	760.3
Kurtosis	-0.8
Skewness	0.1
Minimum (mg/L)	3.7
Maximum (mg/L)	3105.0
Count	1138.0

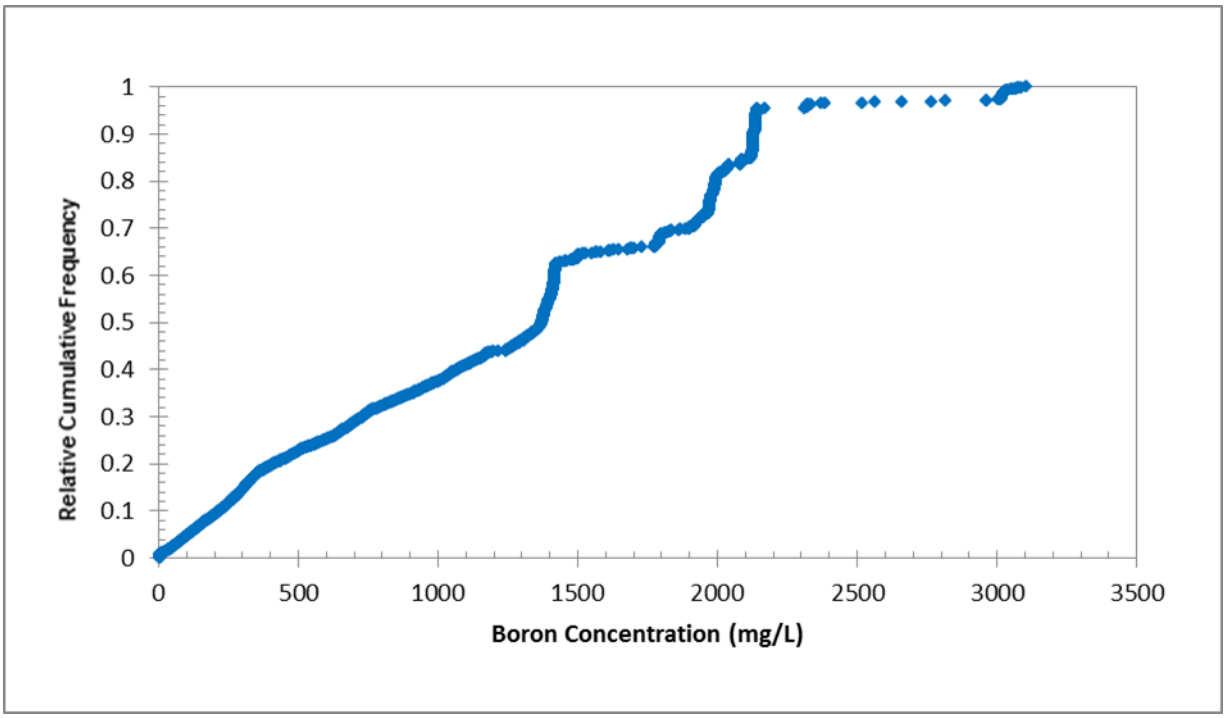

Figure 5: RCS 2 Boron relative cumulative frequency graph.

3.3.1.2 RCS Boron Concentration Results

Summary of results from the RCS boron analysis is presented in Table 7. The median value will be used as the average value for the RCS boron concentration. It should also be noted that the difference in pH using the range of boron concentrations (minimum, maximum, and median values) for the RCS in combination with the median boron concentrations determined for the RWST and accumulator with the TSP concentration determined for the 30 Day test, only resulted in a pH ranging between 7.09 and 7.24 (Appendix A). This is within experimental accuracy of ±0.2 pH units.

Table 7: Summary of Boron concentrations.

Source	Minimum (mg/L)	Maximum (mg/L)	Median (mg/L)
RCS 1	35	2797	1218
RCS 2	3.7	3105	1372

3.3.2 RWST Boron Concentration

3.3.2.1 RWST Boron Concentration Analyses

The historical data (Figure 6) was successfully statistically fit (Figures 7 and 8) resulting in a statistically valid median (Tables 8 and 9) for both sets of data reflective of the RWST of units 1 and 2.

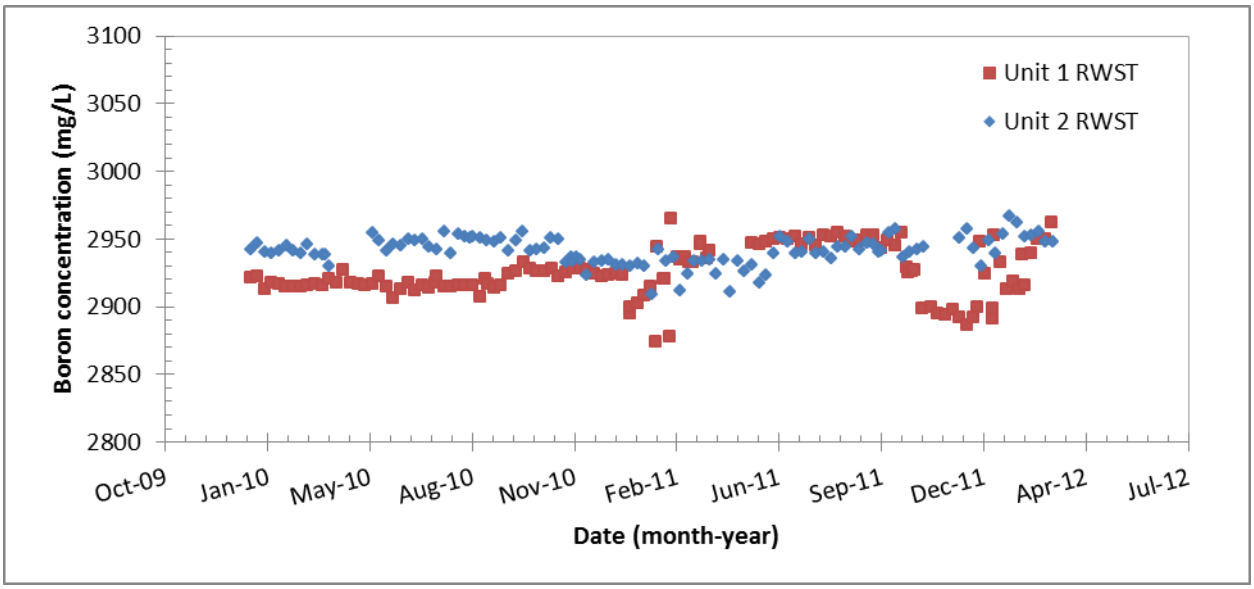

Figure 6: Boron concentration in Unit 1 and Unit 2 RWST as a function of time.

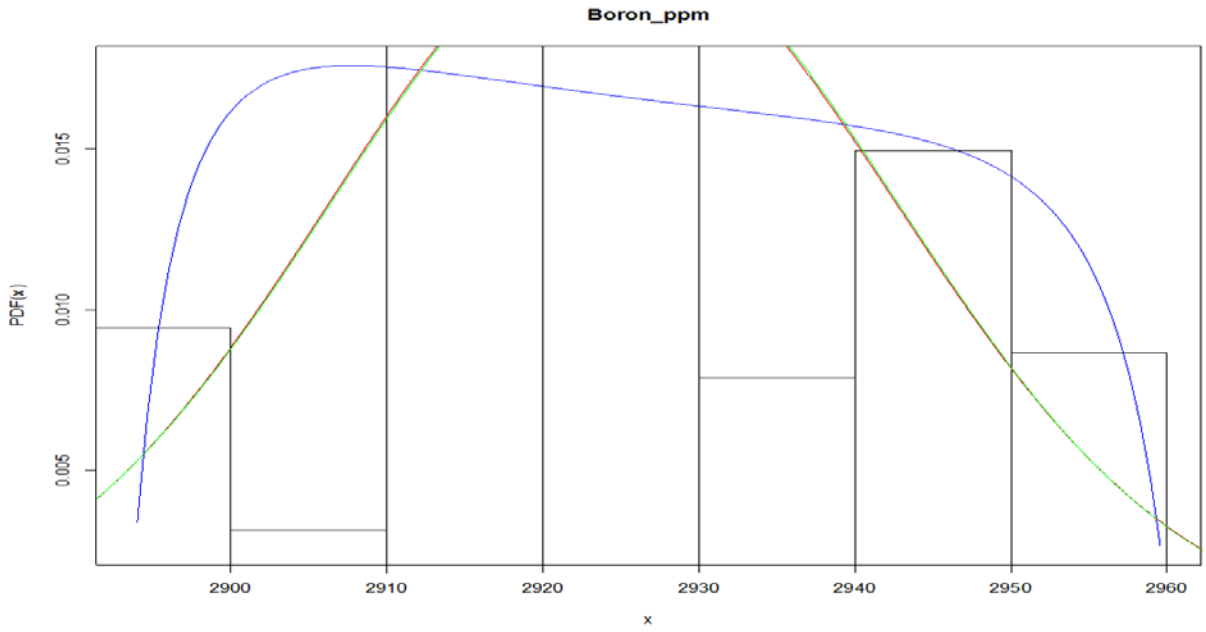

Figure 7: Probability distribution function of RWST 1 Boron concentration. The blue line is the Johnson fit and the green line is the normal fit.

Table 8: Probability distribution statistics for RWST 1 Boron concentrations.

Parameters	Normal	Lognormal	Johnson
Min (mg/L)	2895		
Max (mg/L)	2958		
Mean (mg/L)	2925	2925	2920
Median (mg/L)	2925	2925	2925
Variance (mg/L)^2	328	328	344

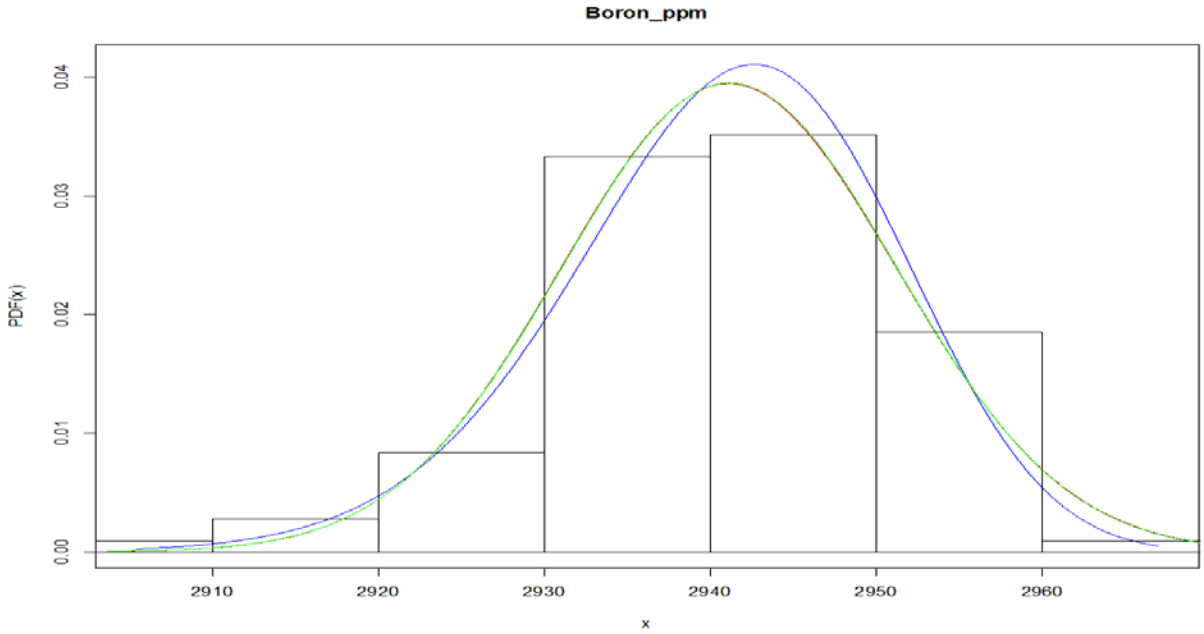

Figure 8: Probability distribution function of RWST 2 Boron concentration. The blue line is the Johnson fit and the green line is the normal fit.

Table 9: Probability distribution statistics for RWST 2 Boron concentrations.

Parameters	Normal	Lognormal	Johnson
Min (mg/L)	2916		
Max (mg/L)	2962		
Mean (mg/L)	2941[1]	N/A	N/A
Median (mg/L)	2941[1]	N/A	N/A
Variance (mg/L)^2	108[1]	N/A	N/A

[1] The raw data associated with Figure 8 was not available at the time of report. The associated information was calculated using excel.

3.3.2.2 RWST Boron Concentration Results

Both RWST sources fit a Gaussian distribution using the different fitting procedures. Since all the fits result in a very similar median, the normal distribution fit median is the median to be used. A summary of boron concentrations observed in the RWST sources of both units, Table 10.

Table 10: Statistical results from the Boron concentration analyses of the RWST.

Source	Minimum (mg/L)	Maximum (mg/L)	Median (mg/L)
RWST 1	2895	2958	2925
RWST 2	2916	2962	2941

3.3.3 Accumulator Boron Concentration

3.3.3.1 Accumulator Boron Concentration Analyses

Historical data (Figure 9) for accumulator 1A could not be fit resulting in a normal Gaussian distribution (Figure 10) because the declining concentration from February 2008 to April 2012 did not follow a random pattern. Thus, a relative cumulative frequency graph (Figure 11) was prepared to examine the distribution of the data. On the basis of the relative cumulative frequency, the median was determined to be a suitable value to use in the 30-day CHLE tests. Parameters from the statistical analysis are shown in Table 11. All other accumulators were successfully fit with a normal, log normal, and Johnson distributions (Figures 12-16) resulting in mean and median values that were nearly identical for the various distributions (Tables 12-16).

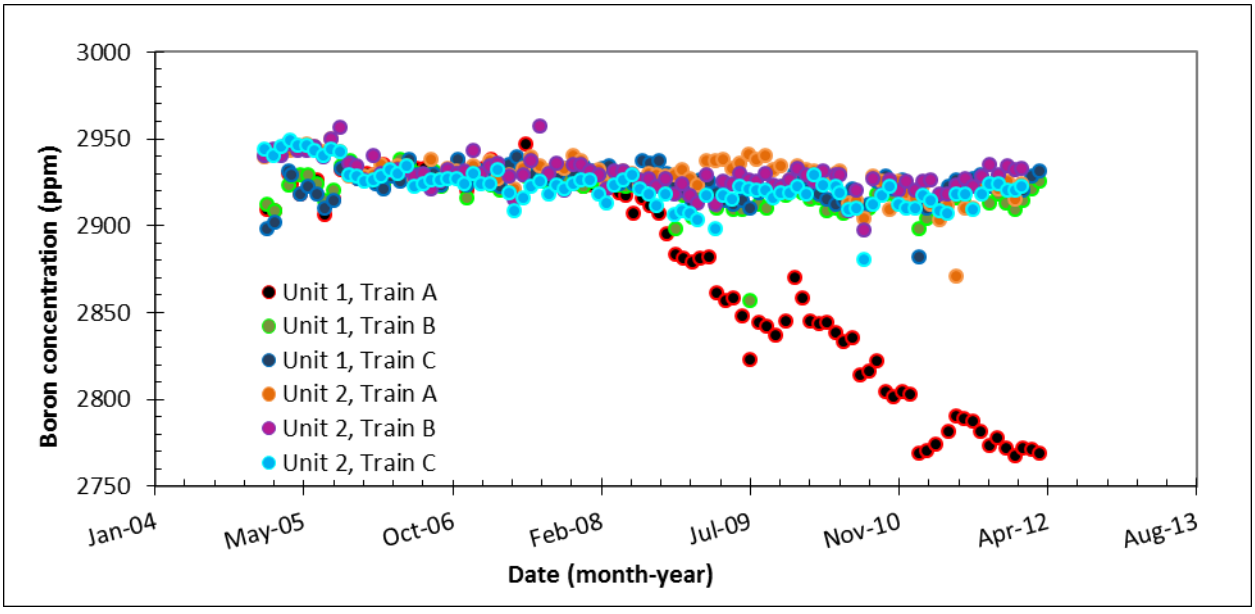

Figure 9: Boron concentration of Accumulators as a function of time.

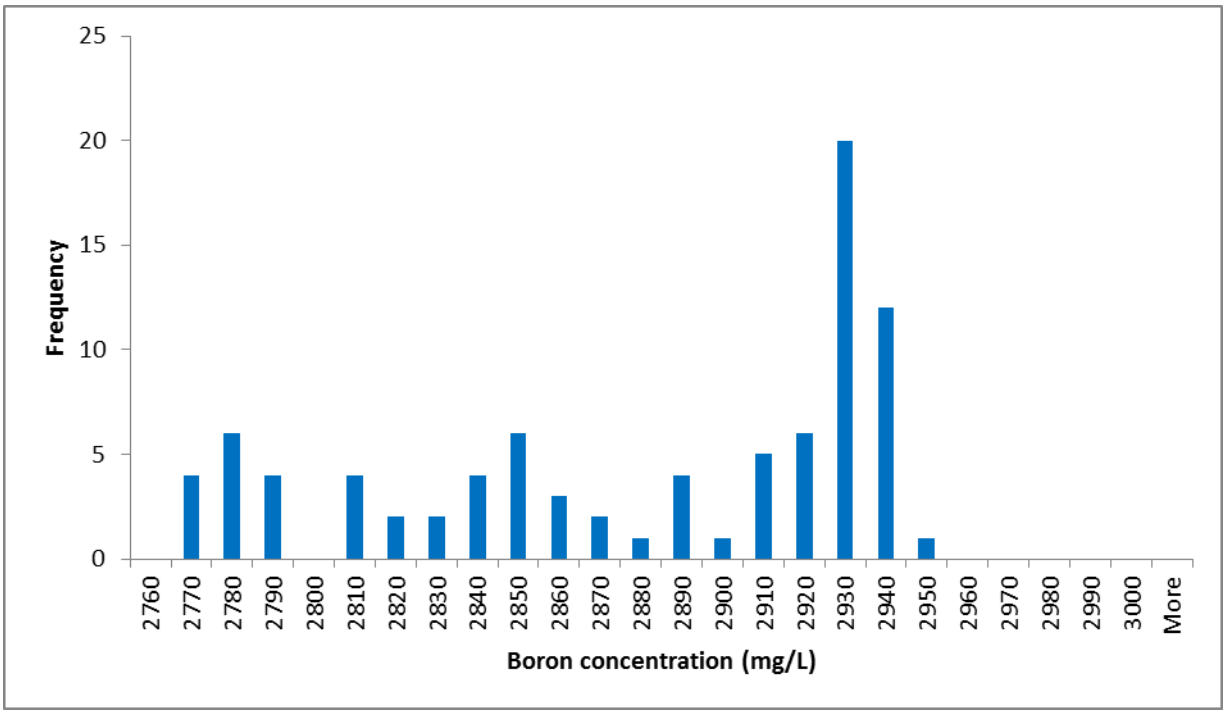

Figure 10: Accumulator 1A Boron histogram.

Table 11: Statistics for Accumulator 1A (Figure 10).

ACC 1A	
Mean (mg/L)	2874.4
Standard Error (mg/L)	6.3
Median (mg/L)	2906.0
Mode (mg/L)	2927.0
Standard Deviation (mg/L)	59.0
Kurtosis	3485.2
Skewness	-1.2
Minimum (mg/L)	-0.6
Maximum (mg/L)	2767.0
Count	2947.0
Mean (mg/L)	87.0

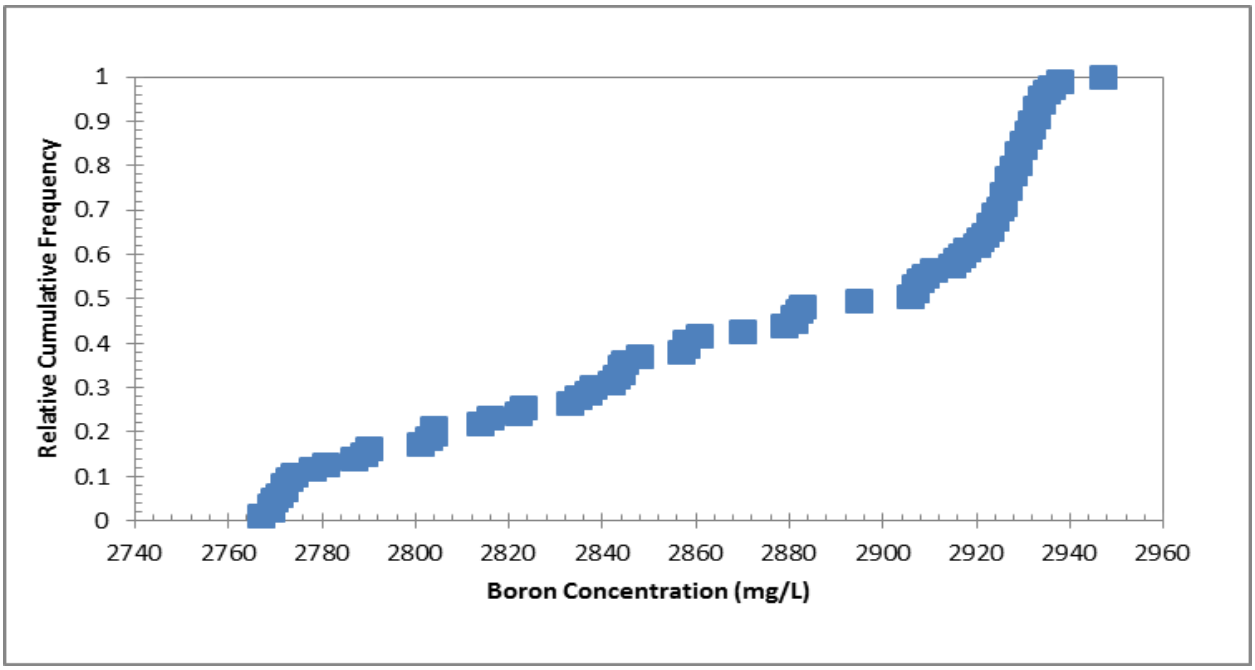

Figure 11: Accumulator 1A Boron relative cumulative frequency graph.

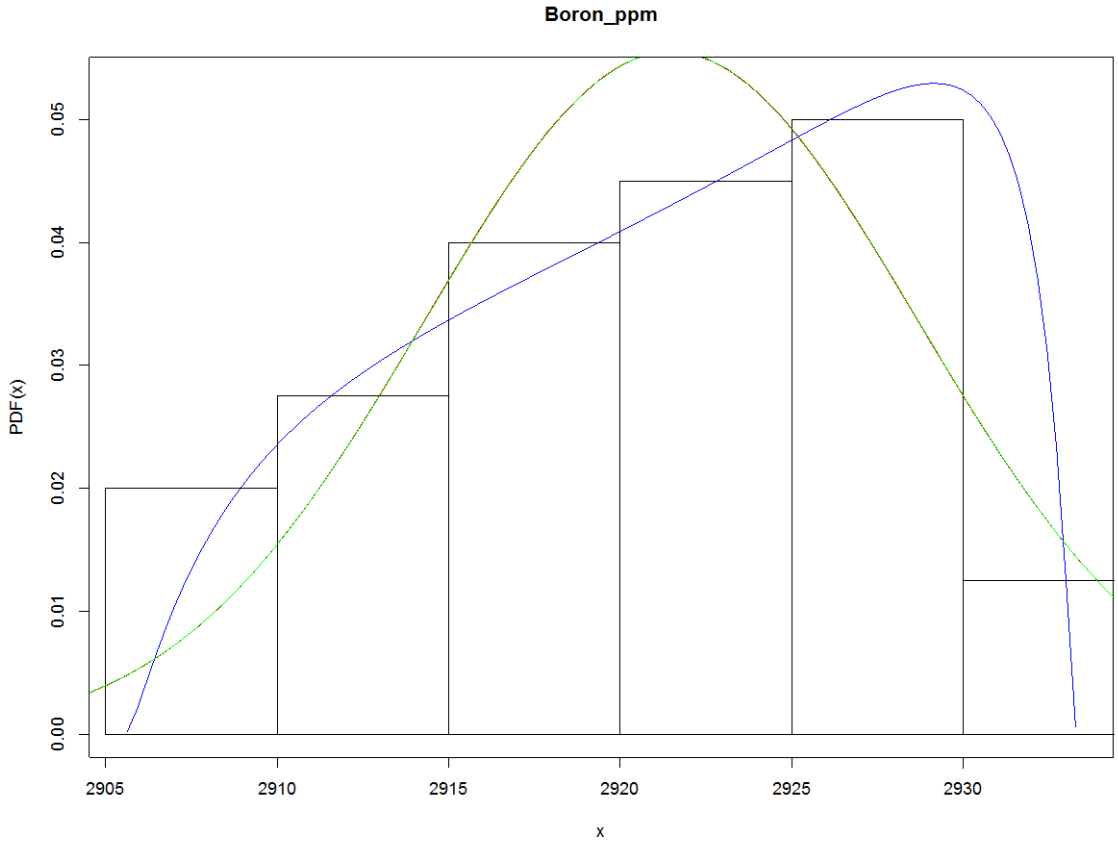

Figure 12: Probability distribution function of Accumulator 1B Boron concentration. The blue line is the Johnson fit and the green line is the normal fit.

Table 12: Probability distribution function for Accumulator 1B Boron concentrations.

Parameters	Normal	Lognormal	Johnson
Min (mg/L)	2906		
Max (mg/L)	2933		
Mean (mg/L)	2922	2922	2916
Median (mg/L)	2922	2922	2923
Variance $(mg/L)^2$	52	52	81

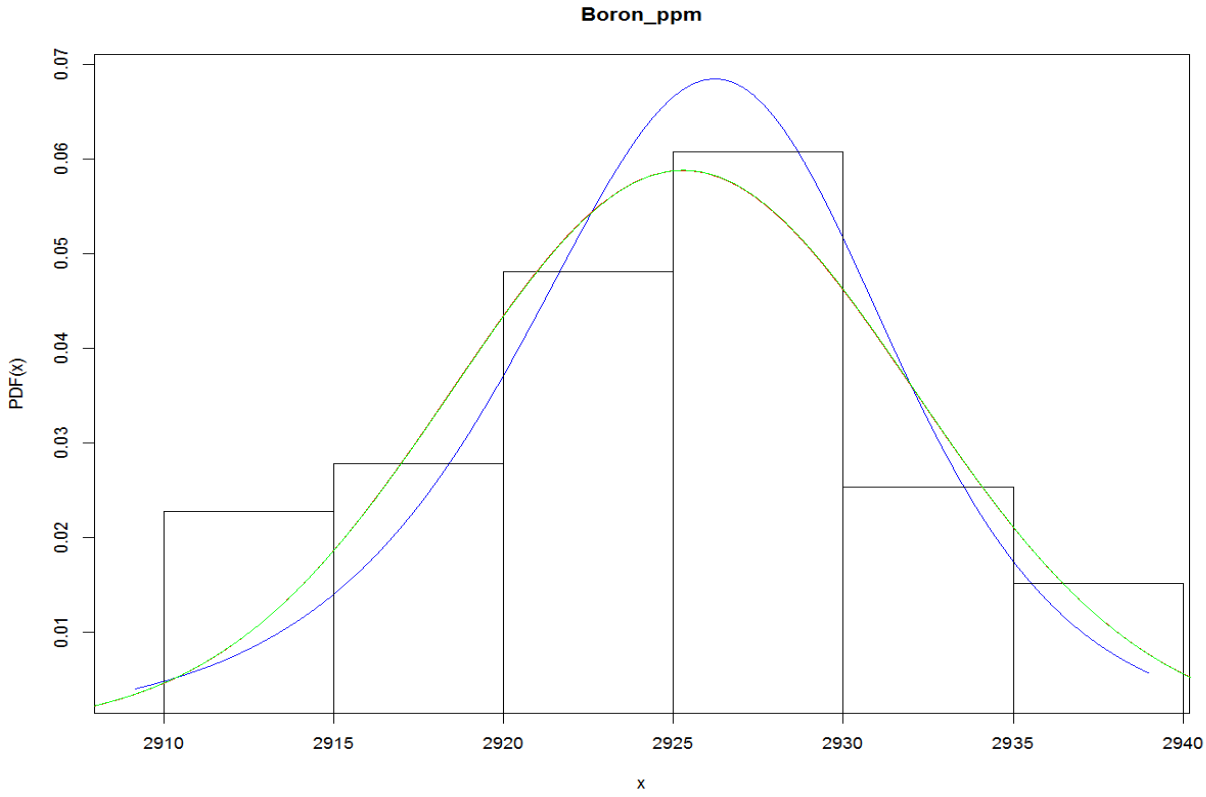

Figure 13: Probability distribution function of Accumulator 1C Boron concentration. The blue line is the Johnson fit and the green line is the normal fit.

Table 13: Probability distribution function for Accumulator 1C Boron concentrations.

Parameters	Normal	Lognormal	Johnson
Min (mg/L)	2906		
Max (mg/L)	2942		
Mean (mg/L)	2925	2925	2925
Median (mg/L)	2925	2925	2926
Variance $(mg/L)^2$	46	46	48

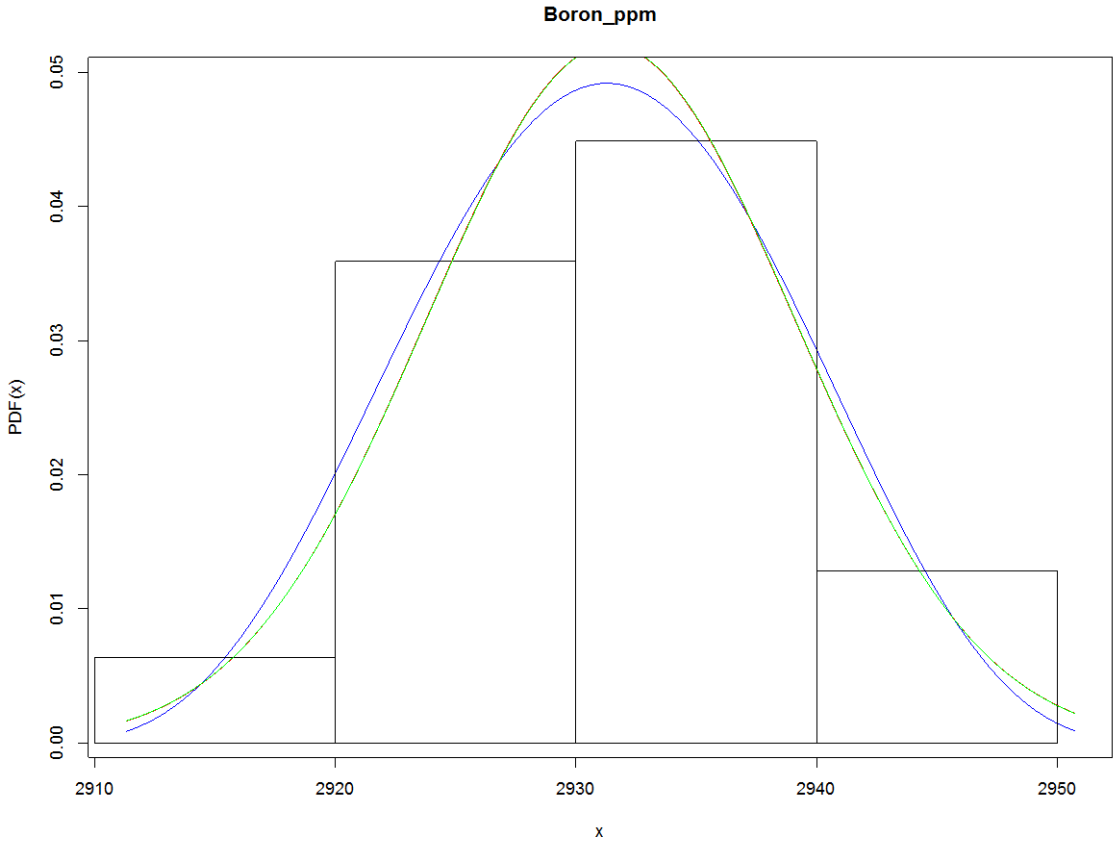

Figure 14: Probability distribution function of Accumulator 2A Boron concentration. The blue line is the Johnson fit and the green line is the normal fit.

Table 14: Probability distribution statistics for Accumulator 2A Boron concentrations.

Parameters	Normal	Lognormal	Johnson
Min (mg/L)	2914		
Max (mg/L)	2951		
Mean (mg/L)	2931	2931	2925
Median (mg/L)	2931	2931	2931
Variance $(mg/L)^2$	59	59	90

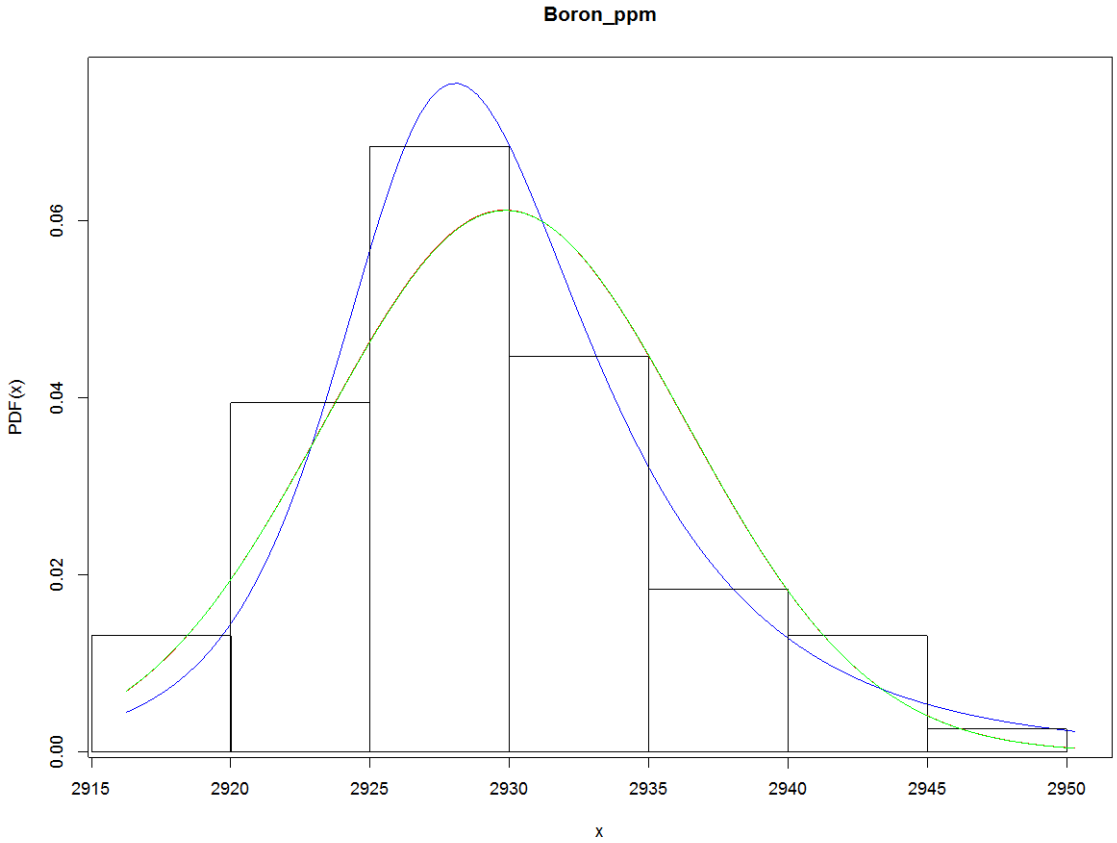

Figure 15: Probability distribution function of Accumulator 2B Boron concentration. The blue line is the Johnson fit and the green line is the normal fit.

Table 15: Probability distribution statistics for Accumulator 2B Boron concentrations.

Parameters	Normal	Lognormal	Johnson
Min (mg/L)	2917		
Max (mg/L)	2950		
Mean (mg/L)	2930	2930	2930
Median (mg/L)	2930	2930	2929
Variance $(mg/L)^2$	43	42	59

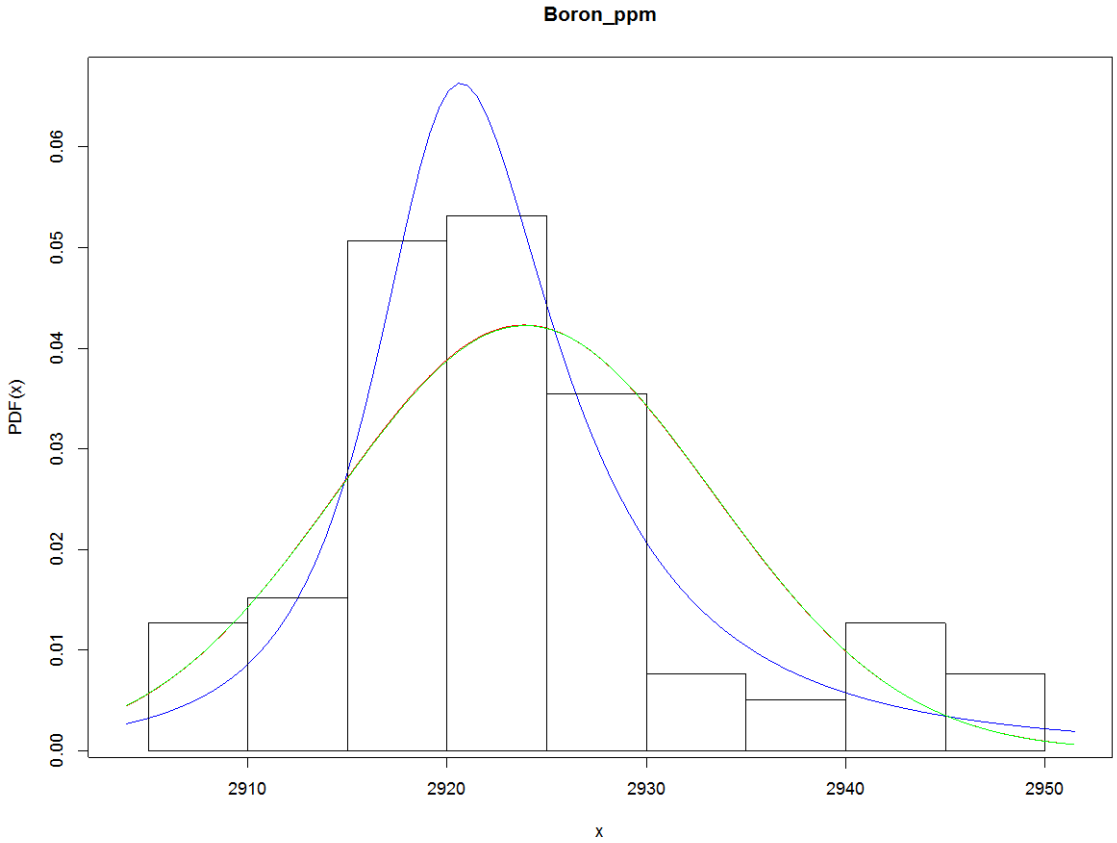

Figure 16: Probability distribution function of Accumulator 2C Boron concentration. The blue line is the Johnson fit and the green line is the normal fit.

Table 16: Probability distribution statistics for Accumulator 2C Boron concentrations.

Parameters	Normal	Lognormal	Johnson
Min (mg/L)	2904		
Max (mg/L)	2952		
Mean (mg/L)	2924	2924	2924
Median (mg/L)	2924	2924	2922
Variance $(mg/L)^2$	89	89	184

3.3.3.2 Accumulator Boron Concentration Results

All accumulators except accumulator 1A were fit well with a normal distribution; thus, the median determined from the normal distribution will be used as the accumulator boron concentration in the 30-day CHLE tests. For accumulator 1A, the median from the raw data will be used in the 30-day CHLE tests. The accumulator boron concentrations used in the CHLE tests are summarized in Table 17.

Table 17: Summary of accumulator concentration ranges.

Source	Median (mg/L)	Minimum (mg/L)	Maximum (mg/L)
Accum 1A	2906	2767	2947
Accum 1B	2922	2906	2933
Accum 1C	2925	2906	2942
Accum 2A	2931	2914	2951
Accum 2B	2930	2917	2950
Accum 2C	2924	2904	2952

3.3.4 Final Boron Concentration Results

The 30 Day CHLE test will use the average of the values resulting from the complete analysis values listed in Table 18 for boron concentrations. The values listed in Table 19 will be covered within the bounds of the lab test.

Table 18: Boron concentration used to determine the concentration in the 30-day CHLE tests.

	Unit 1 (mg/L)	Unit 2 (mg/L)
Source	Median	Median
RCS	1218	1372
Accum A	2906	2931
Accum B	2922	2930
Accum C	2925	2924
RWST	2925	2941

Table 19: Boron concentrations to be investigated in the CHLE tests.

	Unit 1 (mg/L)		Unit 2 (mg/L)	
Source	Minimum	Maximum	Minimum	Maximum
RCS	35	2797	3.7	3105
Accum A	2767	2947	2914	2951
Accum B	2906	2933	2917	2950
Accum C	2906	2942	2904	2952
RWST	2895	2958	2916	2962

3.4 Silicon

The SFP contains Boraflex panels that contain significant amounts of silicon in the form of silicon dioxide (silica). As the panels degrade over time, silica is released to the SFP resulting in a long term increasing trend for SFP silica concentration. During refueling outages, the refueling cavity is flooded from the RWST and hydraulic contact between the SFP and reactor cavity is established to facilitate fuel movement between the reactor and SFP. The hydraulic contact and fuel movement allows silica to migrate to the reactor cavity and increase the silica concentration of the cavity water.

Following core reload, the reactor cavity is drained back to the RWST resulting in increased RWST silica concentrations compared to pre-outage levels. The RWST is not used as a RCS makeup source during normal power operations. RCS dilution and makeup is performed using the Reactor Makeup Water Storage Tank (RMWST) which contains demineralized water along with the Boric Acid Tanks (BATS) which provide a source of borated water for blended makeup.

The silica concentration in the RWST is managed by the use of a Boric Acid Recovery System (BARS) which is used periodically to lower silica concentration in the RWST. The BARS is efficient in removing silica although most of the boron is retained in solution. The only approved method to lower SFP silica is by small drain and refill evolutions. The RWST and/or SFP cleanup evolutions are performed as needed to prevent silica concentration from impacting the RCS chemistry. The RCS is maintained at < 1 ppm silica at 100% power, while the silica concentration in the RWST and accumulators can be higher. Therefore the concentration of the pool solution will be dependent on the concentration of silica and associated solution volume of each contributing source to the final pool volume.

3.4.1RCS Silicon Concentration

3.4.1.1 RCS Silicon Analyses

The historical review of operation data for silicon concentration as silica dioxide observed in the RCS sources of both units is presented by Figure 17. A histogram for each RCS (Figures 18 and 19) was created to be begin the statistical analysis to identify a minimum, maximum and average silicon concentration as silica dioxide (Table 20 and 21). The data did not fit a normal Gaussian distribution for either unit.

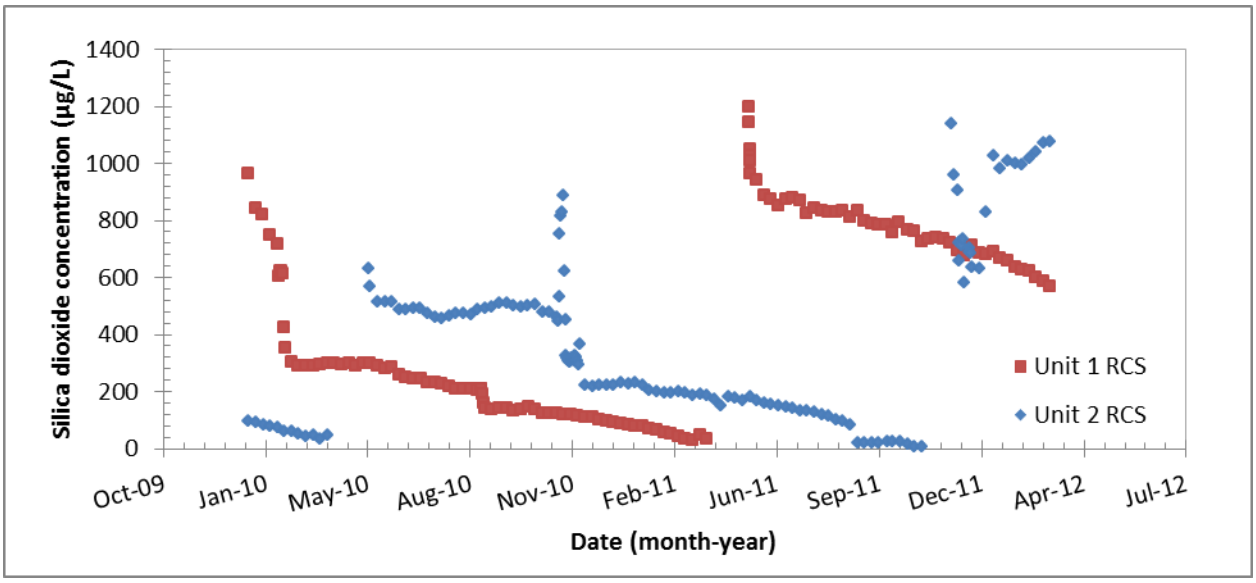

Figure 17: Silicon as silica dioxide concentration in Unit 1 and Unit 2 RCS as a function of time.

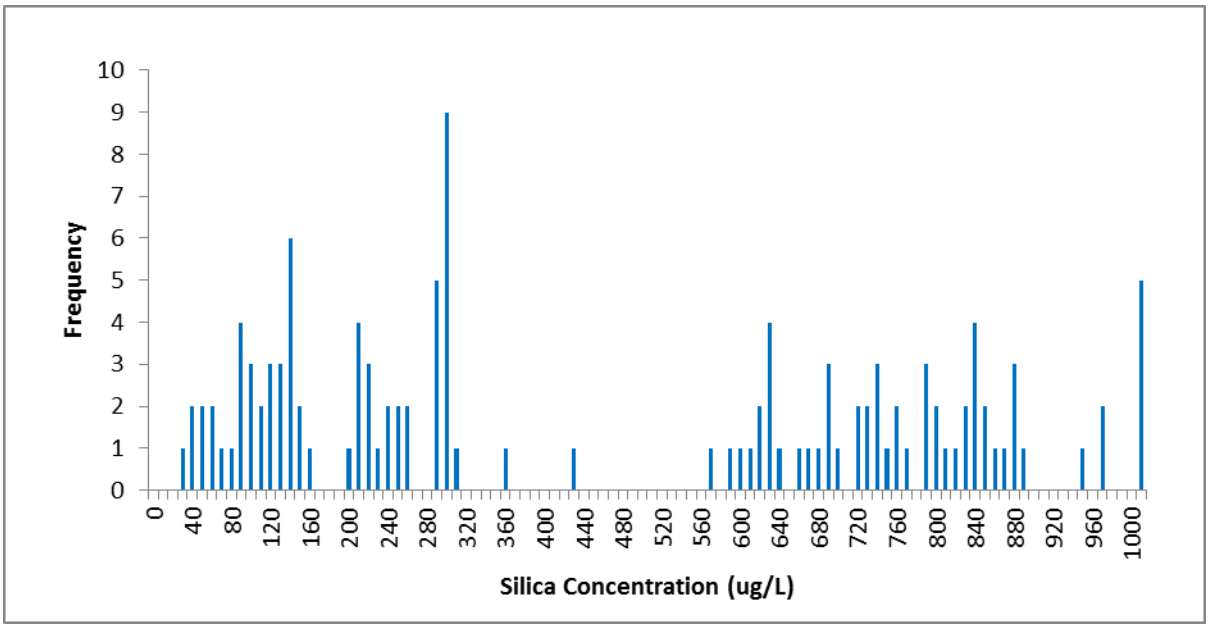

Figure 18: RCS 1 Silica histogram.

Table 20: Statistics for RCS 1 Silica (Figure 18).

RCS 1 Silica	
Mean (µg/L)	352.7
Standard Error (µg/L)	34.2
Median (µg/L)	234.0
Mode (µg/L)	962.0
Standard Deviation (µg/L)	318.7
Kurtosis	0.1
Skewness	1.2
Minimum (µg/L)	30.0
Maximum (µg/L)	1196.0
Count	87.0

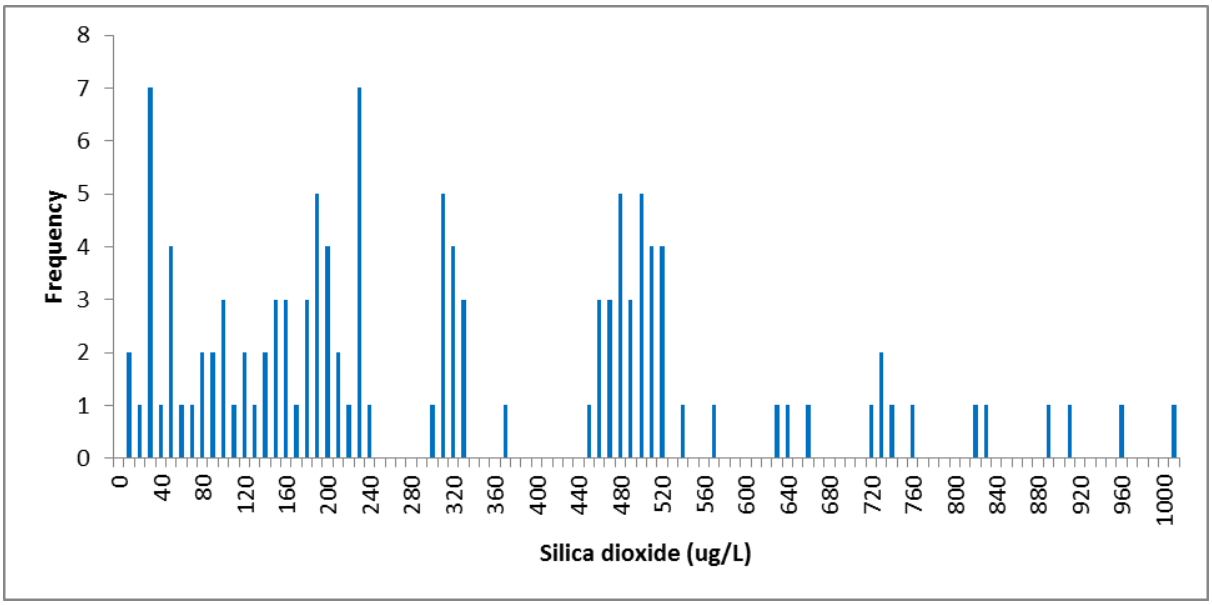

Figure 19: RCS 2 Silica histogram.

Table 21: Statistics for RCS 2 Silica (Figure 19).

RCS 2 Silica	
Mean (µg/L)	320.9
Standard Error (µg/L)	22.3
Median (µg/L)	230.5
Mode (µg/L)	317.0
Standard Deviation (µg/L)	242.0
Kurtosis	58544.4
Skewness	0.4
Minimum (µg/L)	0.9
Maximum (µg/L)	5.0
Count	1140.0
Mean (µg/L)	118.0

3.4.1.2 RCS Silicon results

Since silicon is known to passivate aluminum, it was determined silicon will not be added in the tank test. The maximum and minimum concentrations (Table 20 and 21) observed at STP will be captured in the bench tests.

3.4.2 RWST Silicon Concentration

3.4.2.1 RWST Silicon Analyses

The historical review of operation data for silicon concentration as silica dioxide observed in the RCS sources of both units is presented by Figure 20. A histogram for each RCS (Figures 21 and 22)was created to be begin the statistical analysis to identify a minimum, maximum and average silicon

concentration as silica dioxide (Table 22 and 23). The data did not fit a normal Gaussian distribution for either unit.

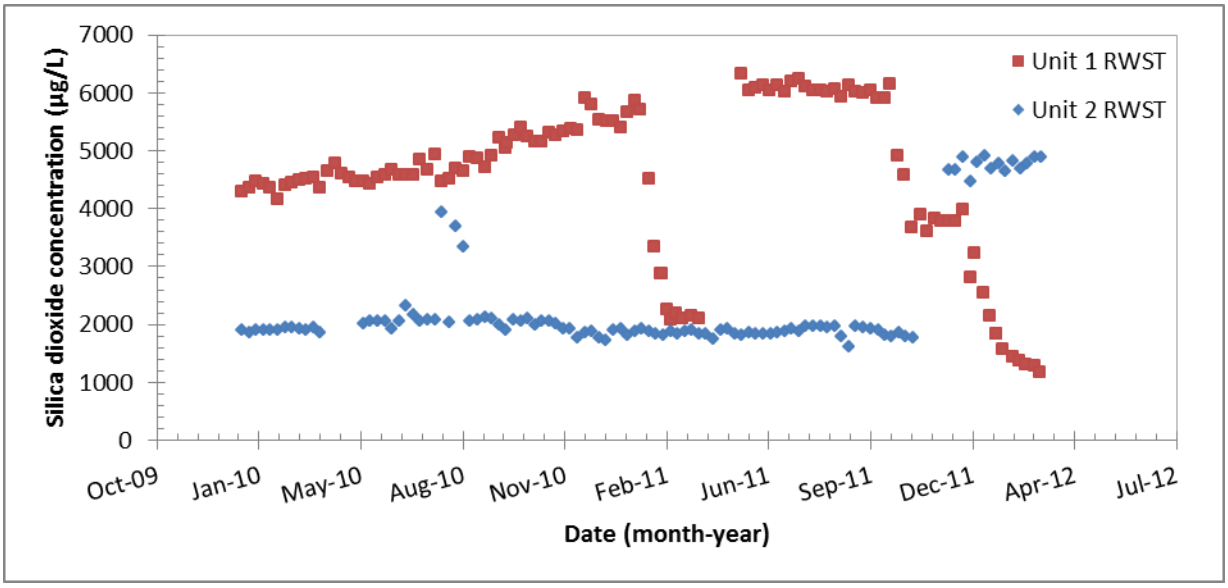

Figure 20: Silicon as silica dioxide concentration in Units 1 and 2 RWST as a function of time.

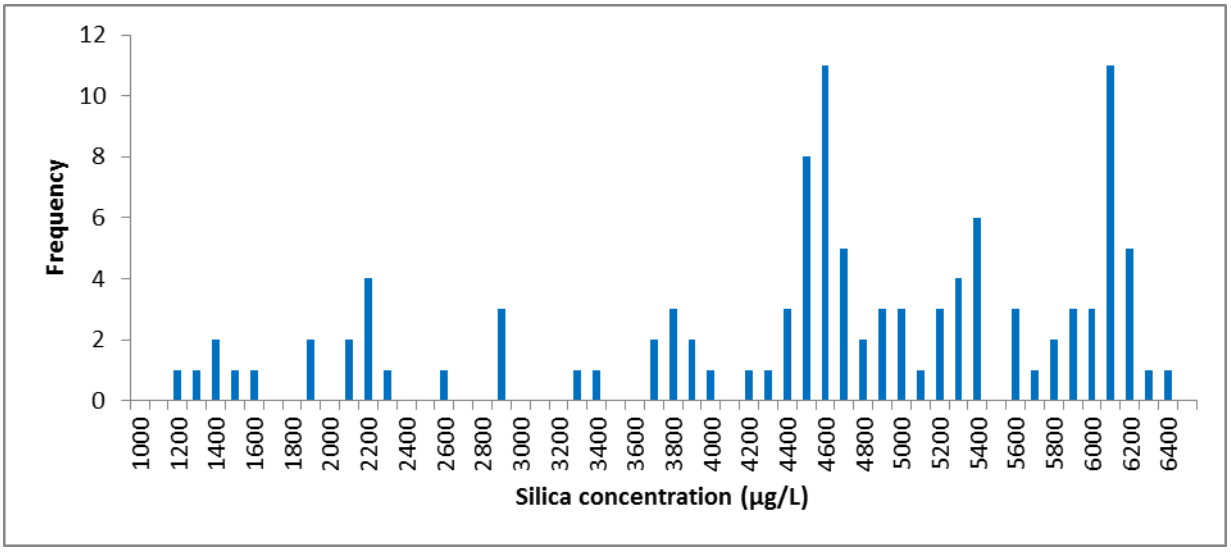

Figure 21: RWST 1 Silica histogram.

Table 22: Statistics for RWST 1 Silica (Figure 21).

RWST 1 Silica	
Mean (µg/L)	4518.8
Standard Error (µg/L)	131.4
Median (µg/L)	4665.0
Mode (µg/L)	4470.0
Standard Deviation (µg/L)	1378.6
Kurtosis	-0.1
Skewness	-0.9
Minimum (µg/L)	1175.0
Maximum (µg/L)	6330.0
Count	110.0

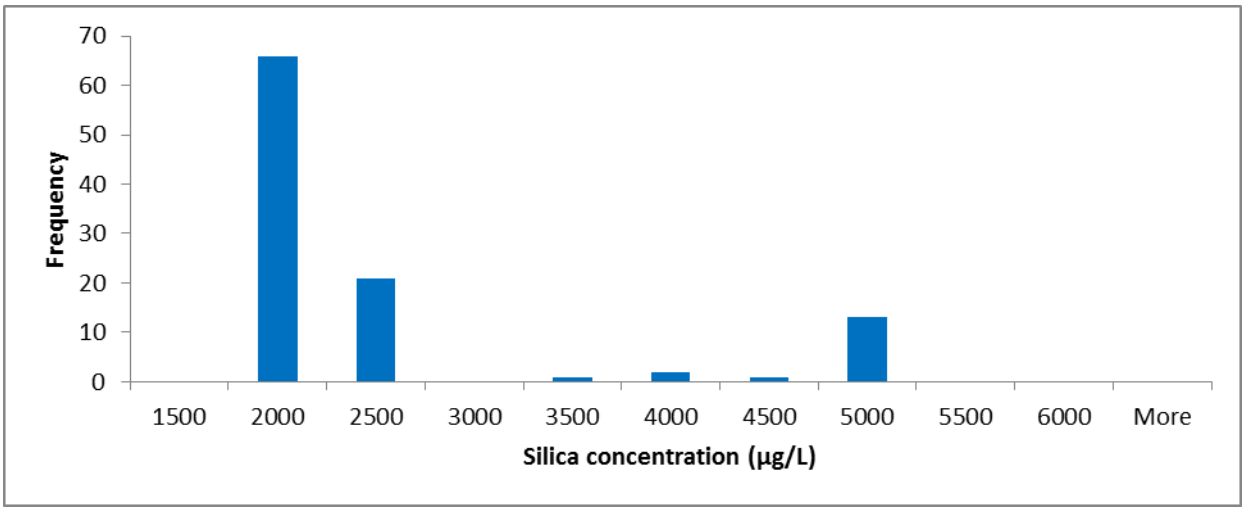

Figure 22: RWST 2 silica histogram.

Table 23: Statistics for RWST 2 (Figure 22).

RWST 2 Silica	
Mean (µg/L)	2358.0
Standard Error (µg/L)	98.3
Median (µg/L)	1930.0
Mode (µg/L)	2060.0
Standard Deviation (µg/L)	1002.6
Kurtosis	1.9
Skewness	1.9
Minimum (µg/L)	1620.0
Maximum (µg/L)	4910.0
Count	104.0

3.4.2.2 RWST Silicon Results

Again, since silicon is known to passivate aluminum, it was determined that silicon will not be added in the tank tests. The maximum and minimum concentrations observed at STP (Table 22 and 23) will be captured in the bench tests.

3.4.3 Silicon Results

Since silicon can passivate aluminum and lower the corrosion rate, it was decided not to add silicon in the tank test. The minimum and maximum concentration of silicon as silica dioxide for the analysis of historical data, Table 24, will be covered in the bench scale test.

Table 24: Results associated with Silica histogram.

Unit	Minimum Concentration (μg/L)	Maximum Concentration (μg/L)
RCS 1	30	1196
RCS 2	0.9	1140
RWST 1	1175	6330
RWST 2	1620	4910

3.5 Lithium

Lithium in the form of lithium hydroxide is present only in the RCS and is used to maintain the RCS solution pH = 7.2 at 592 ^{o}F. The concentration of lithium hydroxide is variable in the RCS solution and is determined by the concentration of boric acid in solution. The concentration of lithium in the pool solution will be less than in the RCS and will depend on the associated solution volume of each contributing source to the final pool volume.

3.5.1 RCS Lithium Concentration

3.5.1.1 Lithium RCS Analyses

The historical trend of the lithium concentration observed in the RCS for both Unit 1 and 2, Figure 23, was not processed statistically because the lithium concentration is determined by the boron concentration which has already been determined for the CHLE tests.

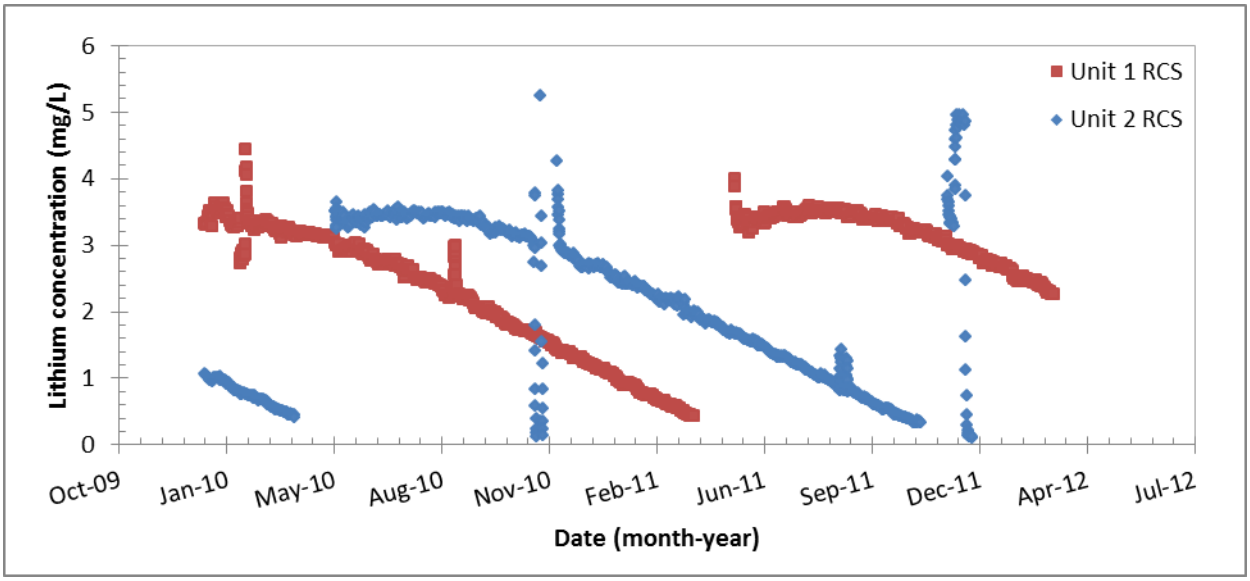

Figure 23: Lithium concentration in Unit 1 and Unit 2 RCS as a function of time.

3.5.1.2 Lithium RCS Results

While historical plant data was obtained for the lithium concentration, the lithium concentration is dictated by the boron concentration to maintain pH in the RCS. Therefore, the median boron concentration dictates lithium concentration and the only lithium contribution to the pool is from the RCS.

Table 25: LBLOCA and MBLOCA concentration of Boron and Lithium in RCS.

Unit	Median Boron Concentration (mg/L)	Lithium Concentration in RCS (mg/L)
RCS 1	1218	2.9
RCS 2	1372	3.3

3.6 Zinc

Zinc in the form of zinc acetate is added to the RCS as a dose rate mitigation control. The concentration of zinc varies between 5 to 10 ppb and depends on the time elapsed over the course of the fuel cycle. The concentration of zinc in of the pool solution will be less than that found in the RCS and will depend on the associated solution volume of each contributing source to the final pool volume.

3.6.1 RCS Zinc Concentration

3.6.1.1 RCS Zinc Analyses

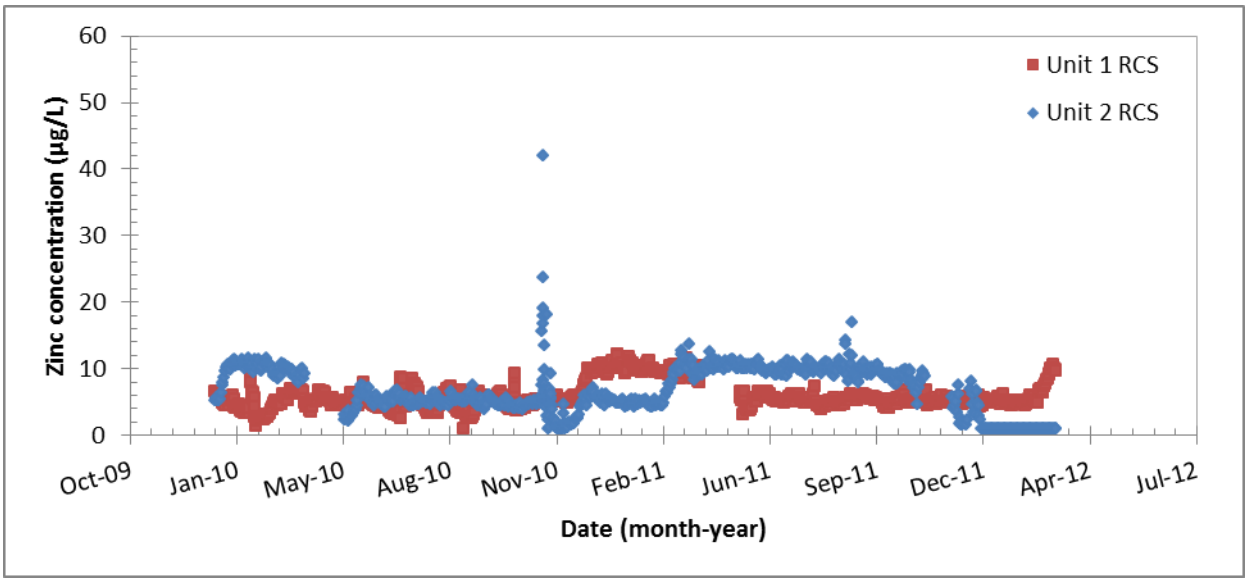

Figure 24: Zinc concentration in Unit 1 and 2 RCS as a function of time.

3.6.1.2 RCS Zinc Results

Zinc acetate is added only to the RCS, which is only approximately 15% of total pool volume. It is below 10 ppb at any given time. Therefore, the contribution of zinc from chemicals added at STP will not be included in the CHLE analyses.

3.7 Environmental Contribution (O_2 and CO_2)

Oxygen and carbonate in the form of carbon dioxide is present in containment because of its presence in the atmosphere.

3.7.1 Oxygen

3.7.1.1 Oxygen Analysis

While there may be trace amount of oxygen in the RWST or the accumulators (not monitored for), there is very little to no oxygen in the RCS (Figure 29). During a LOCA event, the atmosphere is the largest source of oxygen in containment which is in equilibrium with the pool solution. During outages, the air in containment exchanges with the ambient atmosphere, which contains 21 percent oxygen by volume. The containment building at STP contains 3,374,000 ft^3 of air[14]. Thus, the total quantity of oxygen in the air in the containment building prior to a LOCA is 57,900 lb.

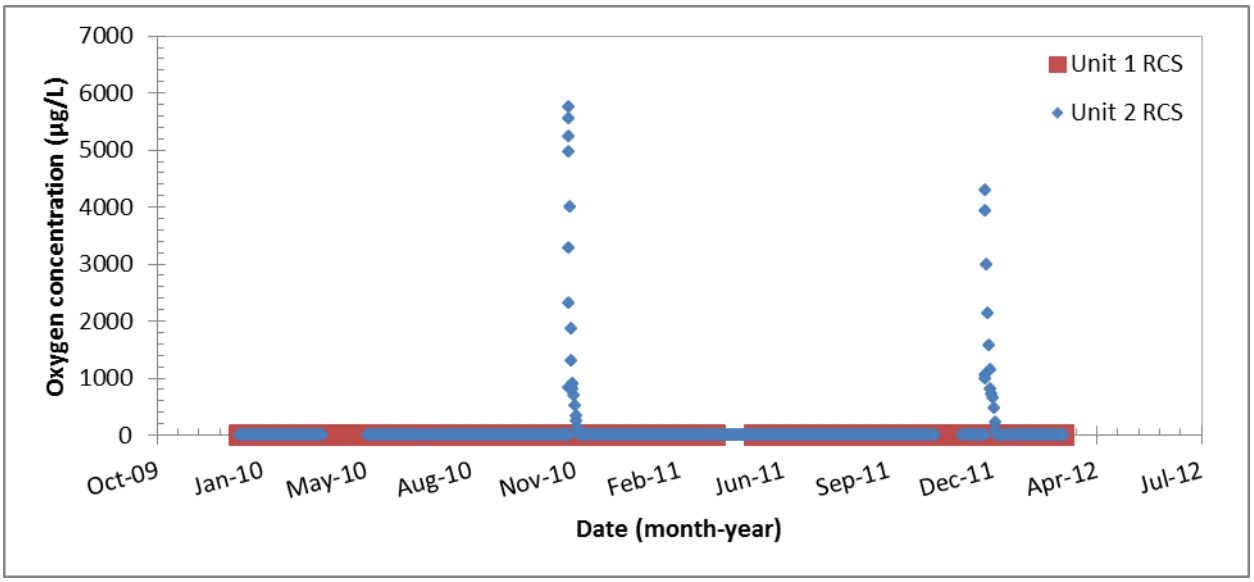

Figure 25: Oxygen concentration in Unit 1 and Unit 2 RCS as a function of time.

During a LOCA, water spills from RCS piping or is sprayed from the containment spray system and thus has opportunity for oxygen to transfer from the air to the water. Oxygen has relatively low solubility in water; the saturation concentration is 8.12 ppm at 25 °C. Oxygen partitions between the gas and liquid phases according to Henry's Law, which is dependent on temperature. Assuming that no oxygen is initially present in the RCS, RWST, or accumulator water, there is sufficient oxygen in the air to essentially reach the saturation concentration. The equilibrium concentration in the pool water as a function of temperature is shown in Figure 16. The total quantity of oxygen in the pool water at equilibrium will be 12.3 lb at 85 °C to 30.4 lb at 25 °C. Since this is less than 0.06 percent of the oxygen inside containment, the pool solution will not be limited with respect to oxygen.

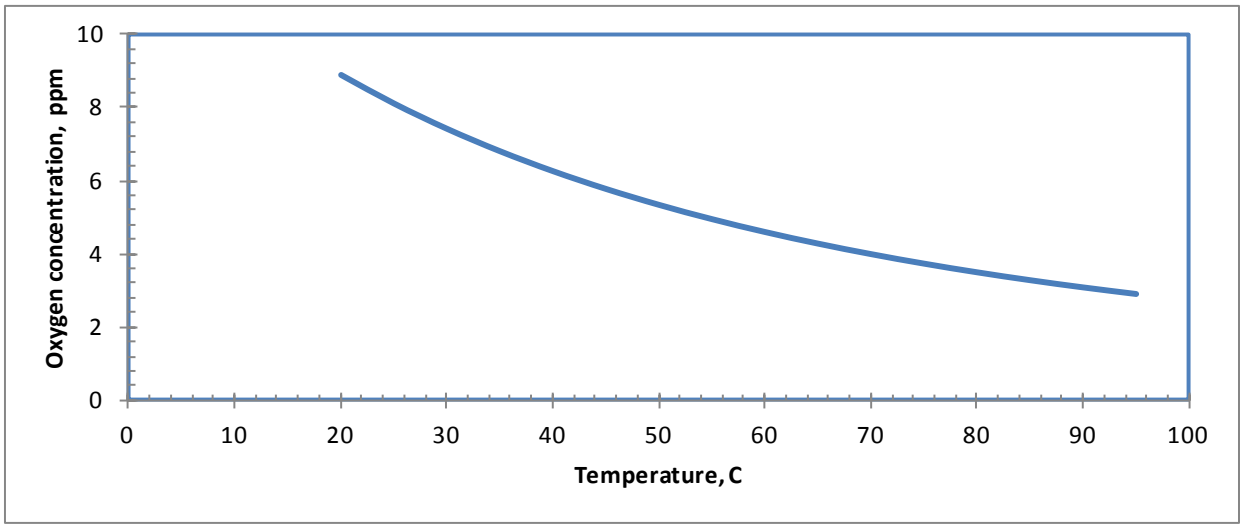

Figure 26: Decrease in oxygen concentration as a function of temperature.

3.7.1.2 Oxygen Results

The CHLE experiments will be conducted with oxygen present. The solution will initially be oxygenated when the tank is filled, the solution will be exposed to the atmosphere inside the tank, and the lid will occasionally be opened, so no special provisions are necessary to provide oxygen to the system.

3.7.2 Carbonate

3.7.2.1 Carbonate Analysis

A potential chemical interaction in a LOCA is reaction between calcium (from leaching of concrete or other materials) and carbonate to form calcium carbonate precipitate. Carbonate can enter the pool solution as carbon dioxide from the air. During a LOCA, water spills from RCS piping or is sprayed from the containment spray system and thus has opportunity for carbon dioxide to transfer from the air to the water. Carbon dioxide has relatively low solubility in water; the saturation concentration is 0.55 ppm at 25 °C. Carbon dioxide partitions between the gas and liquid phases according to Henry's Law, which is dependent on temperature. Furthermore, once carbon dioxide is present in the water, it transforms to bicarbonate and carbonate, with the relative concentration of each species being dependent on pH.

During outages, the air in containment exchanges with the ambient atmosphere, which contains 390 ppm carbon dioxide by volume. The containment building at STP contains 3,374,000 ft^3 of air [14]. Thus, the total quantity of carbon dioxide in the air in the containment building prior to a LOCA is 148 lb. Assuming that no carbonate is initially present in the RCS, RWST, or accumulator water, there is sufficient carbon dioxide in the air to essentially reach the saturation concentration at low pH. At higher pH, the fraction of carbon dioxide that transitions to carbonate increases and at high pH the total carbonate present in the containment pool during a LOCA would be lower than the total carbonate present in a completely open system. At pH 7.2 the total carbonate present in the containment pool at STP would be about 90 percent of the carbonate present in a completely open system. Thus, allowing the CHLE tank to be open to the atmosphere provides a slightly conservative (slightly higher) concentration of carbonate compared to the STP containment during a LOCA.

3.7.2.2 Carbonate Results

The CHLE experiments will be conducted with carbon dioxide present. The solution will initially be aerated when the tank is filled, the solution will be exposed to the atmosphere inside the tank, and the lid will occasionally be opened, so no special provisions are necessary to provide carbon dioxide to the system.

3.7.3 Summary of Environmental Contribution results

No special provisions are necessary to control the interaction between the atmosphere and pool solution in the CHLE tests.

3.8 Impurities

Magnesium, aluminum, calcium, copper, and sulfate are impurities that are monitored because they may influence disposition of scale on the fuel rods. Corrosion products such as fluoride, chloride and nickel are another form of impurities which are monitored to access corrosion concern. These impurities, if present in significant concentrations, may influence the overall pool chemistry of the CHLE analysis. Therefore the historical trends were reviewed to determine inclusion and concentration to be used in the analysis.

3.8.1 Impurities

3.8.1.1 Impurity Analyses

Historical trends of impurity data for the RWST and RCS are listed below. There is no surveillance data for these impurities for the accumulators; thus the accumulators are not included in this analysis.

RCS Related Graphs

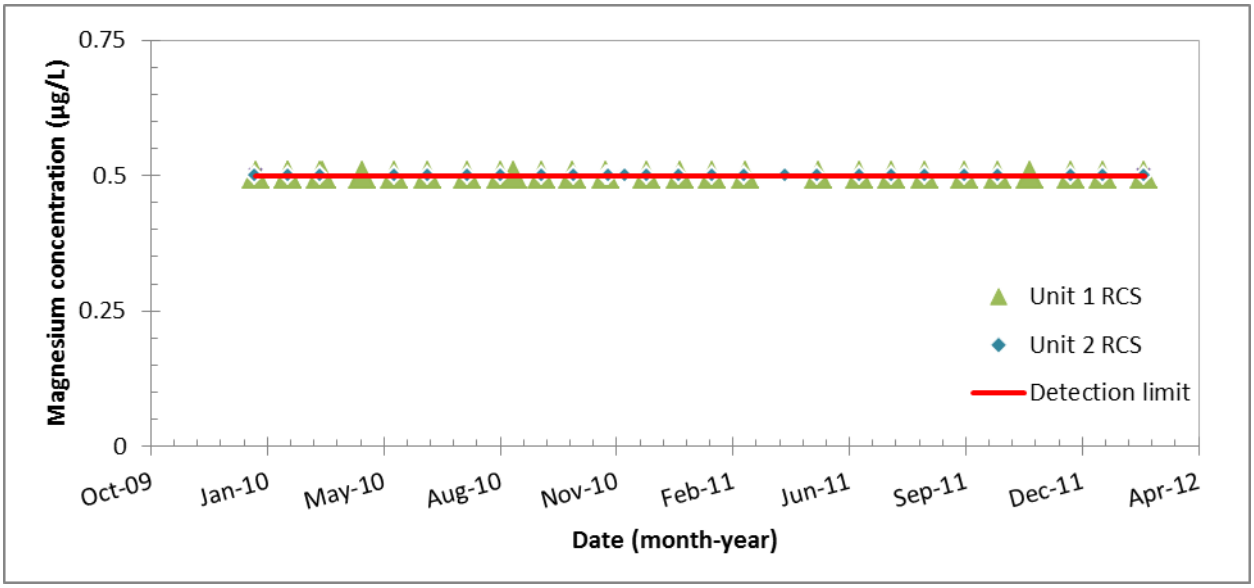

Figure 27: Magnesium concentration in Unit 1 and Unit 2 RCS as a function of time.

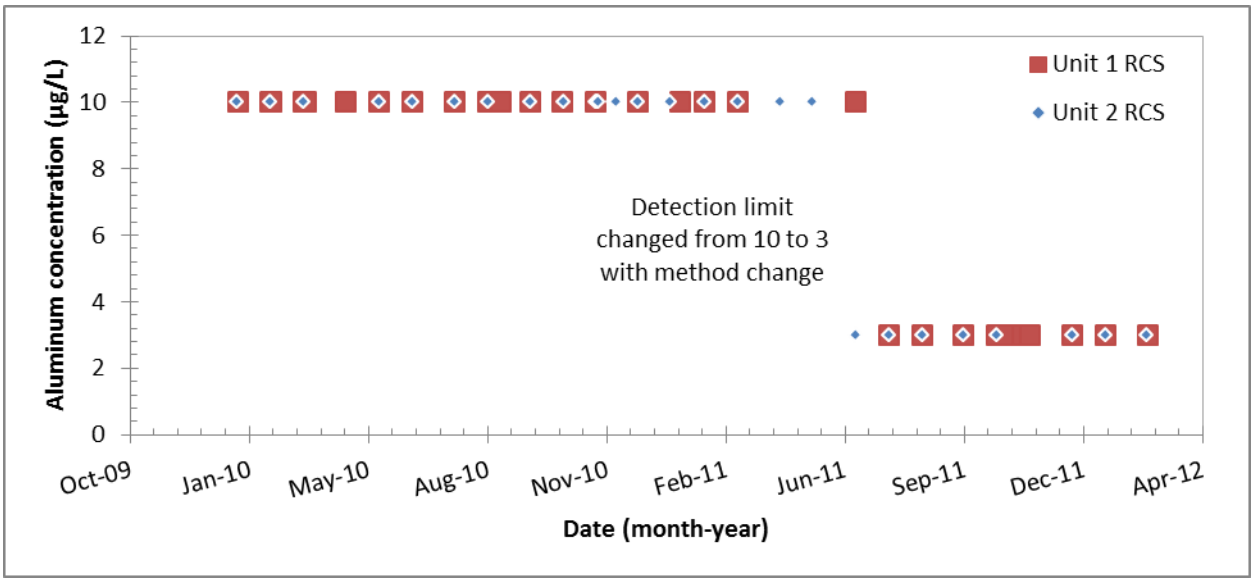

Figure 28: Aluminum concentration in Unit 1 and Unit 2 RCS as a function of time.

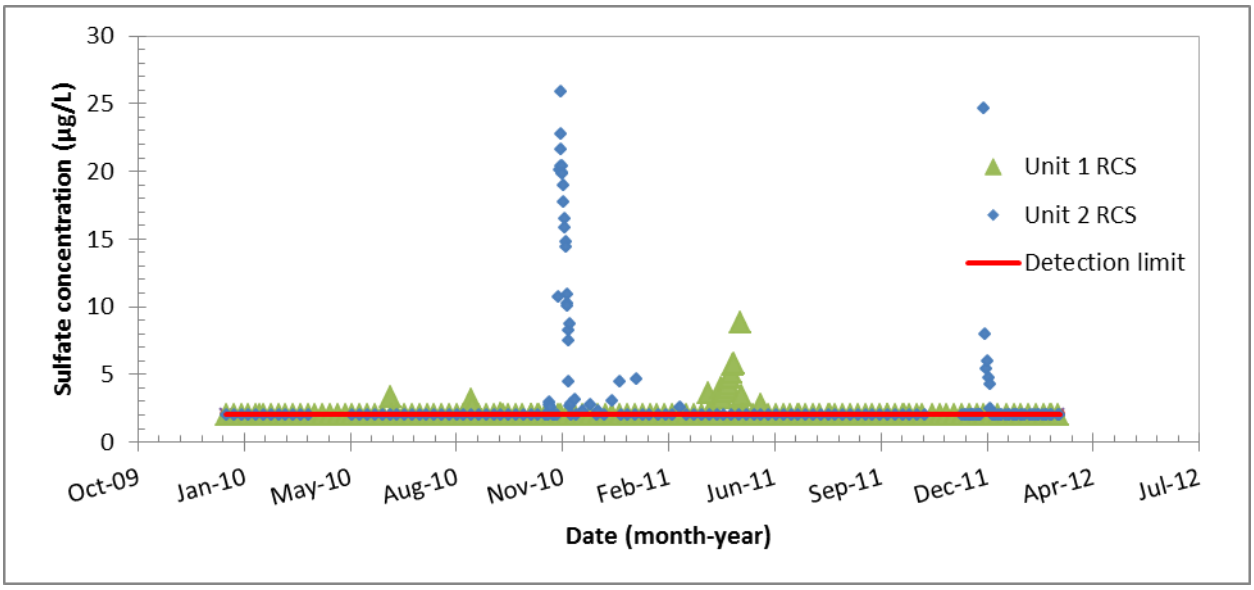

Figure 29: Sulfate concentration in Unit 1 and Unit 2 RCS as a function of time.

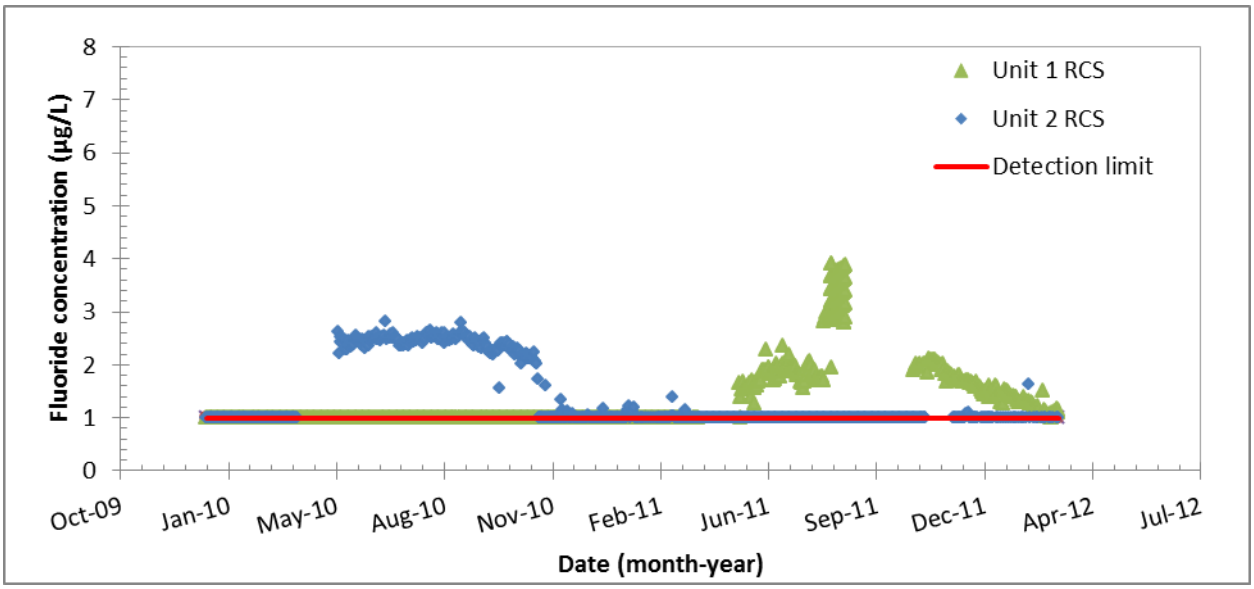

Figure 30: Fluoride concentration in Unit 1 and Unit 2 RCS as a function of time.

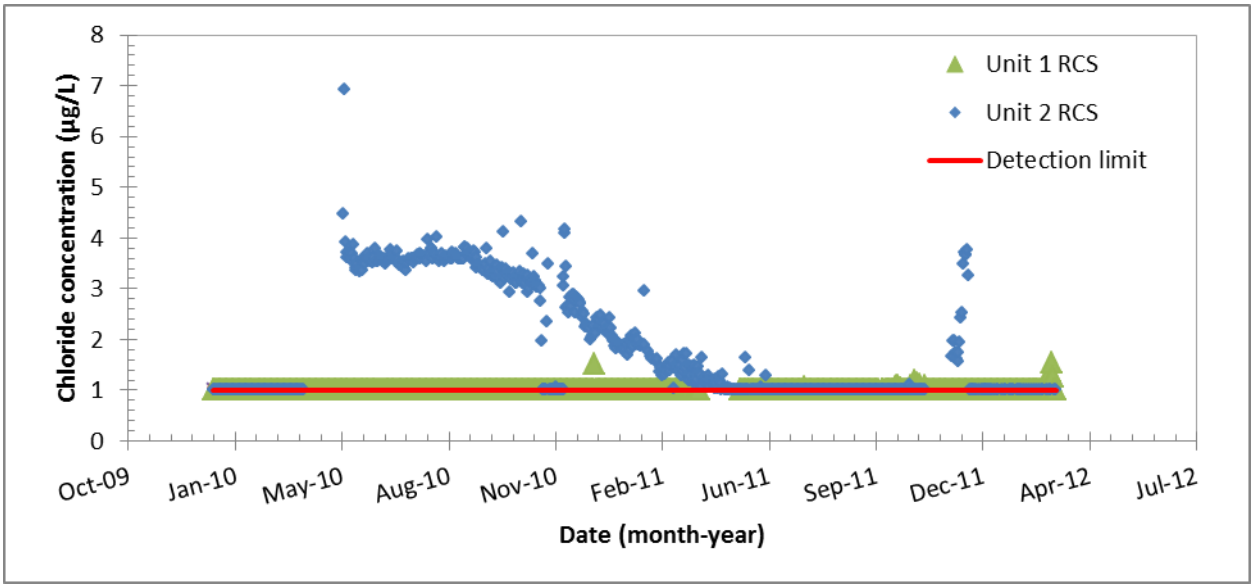

Figure 31: Chloride concentration in Unit 1 and Unit 2 RCS as a function of time.

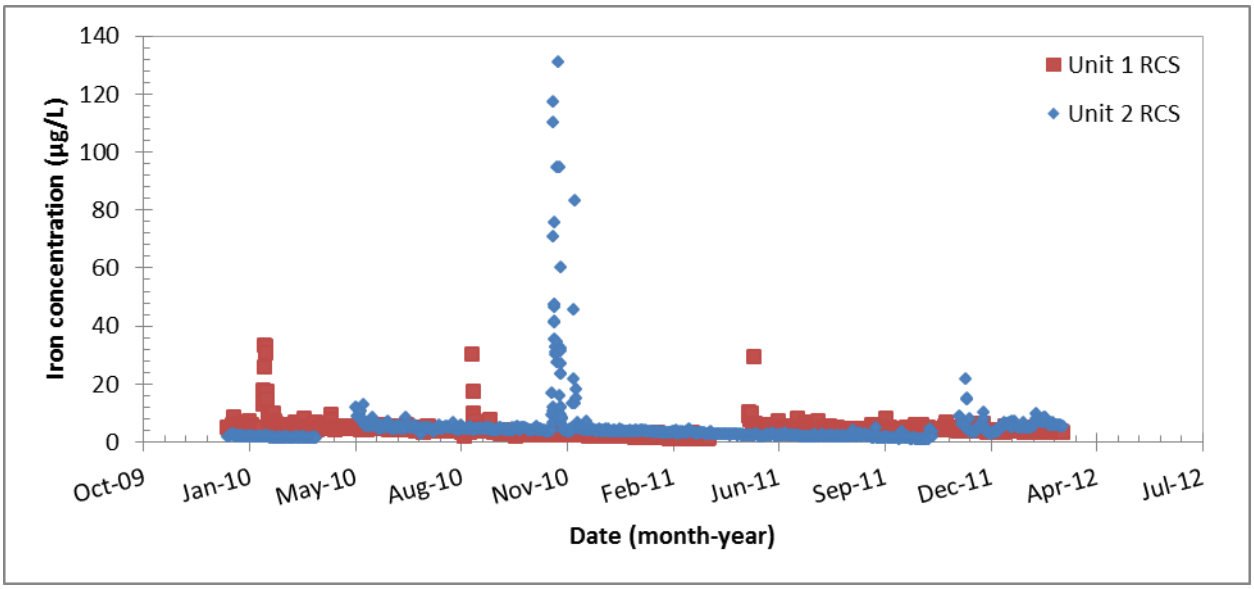

Figure 32: Iron concentration in Unit 1 and Unit 2 RCS as a function of time.

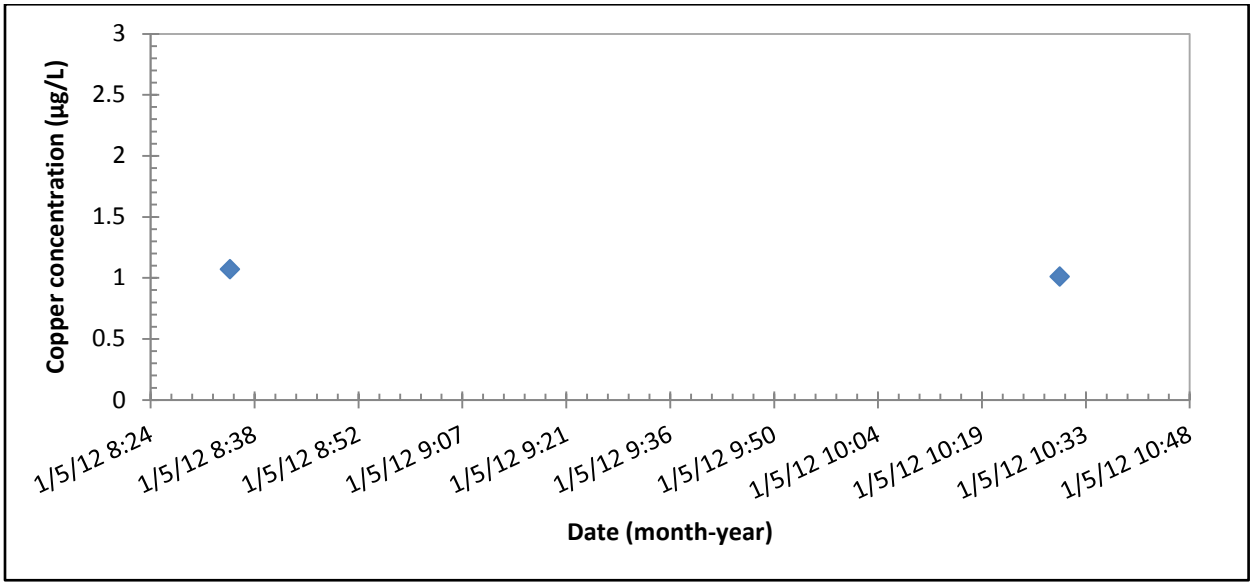

Figure 33: Copper concentration in Unit 1 RCS as a function of time.

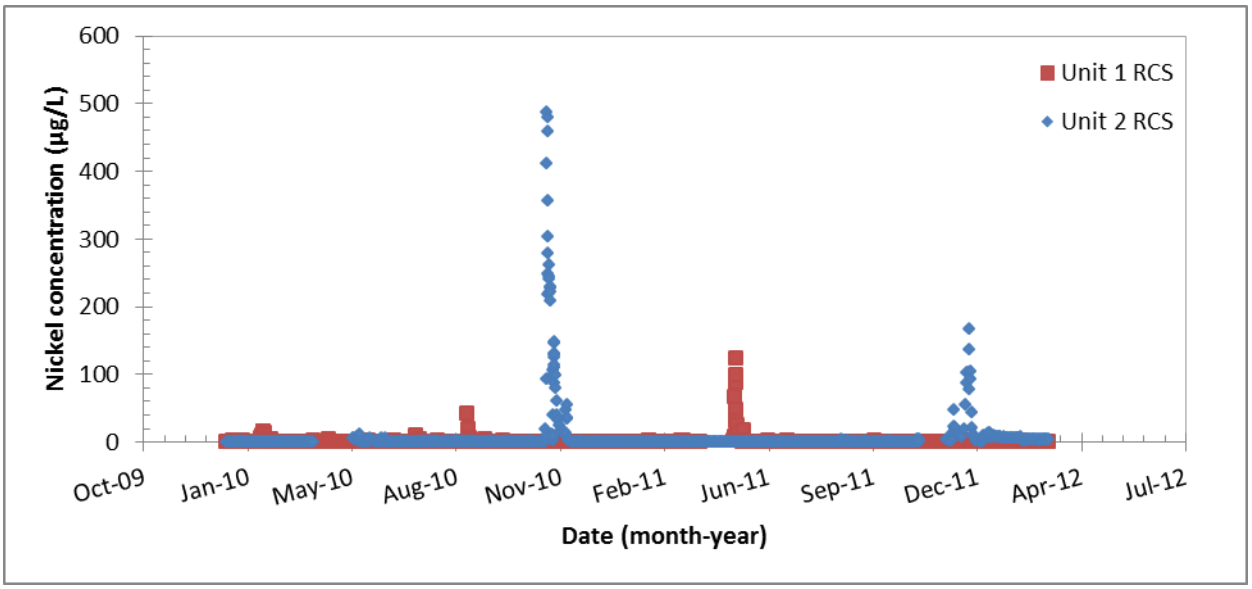

Figure 34: Nickel concentration in Unit 1 and Unit 2 RCS as a function of time.

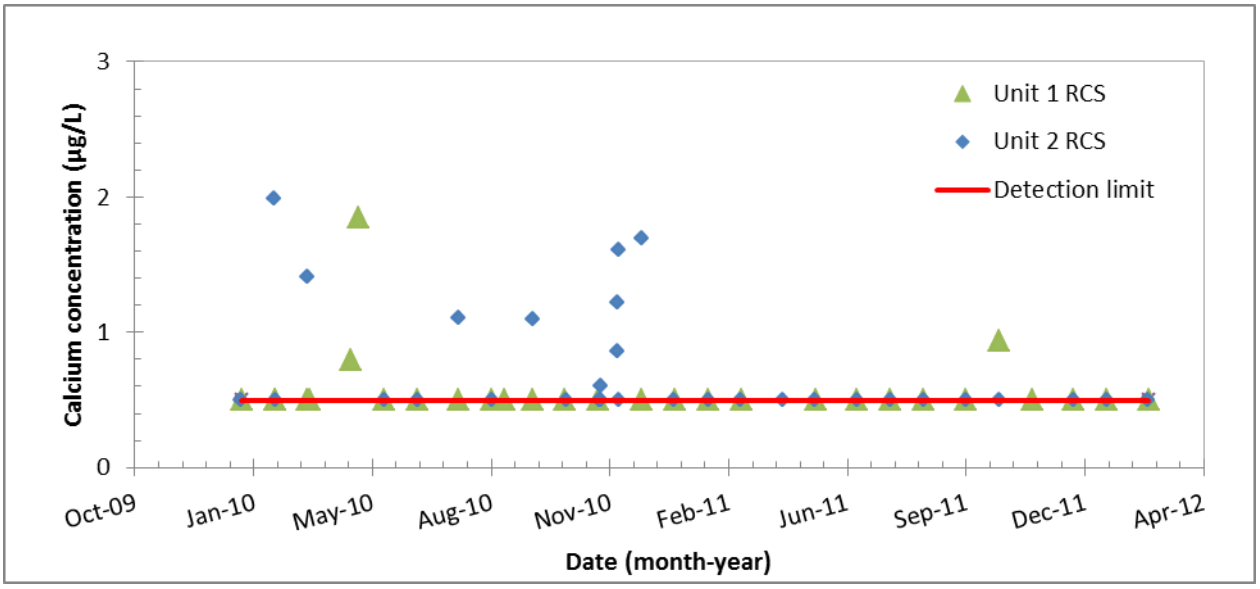

Figure 35: Calcium concentration in Unit 1 and Unit 2 RCS as a function of time.

RWST Related Graphs

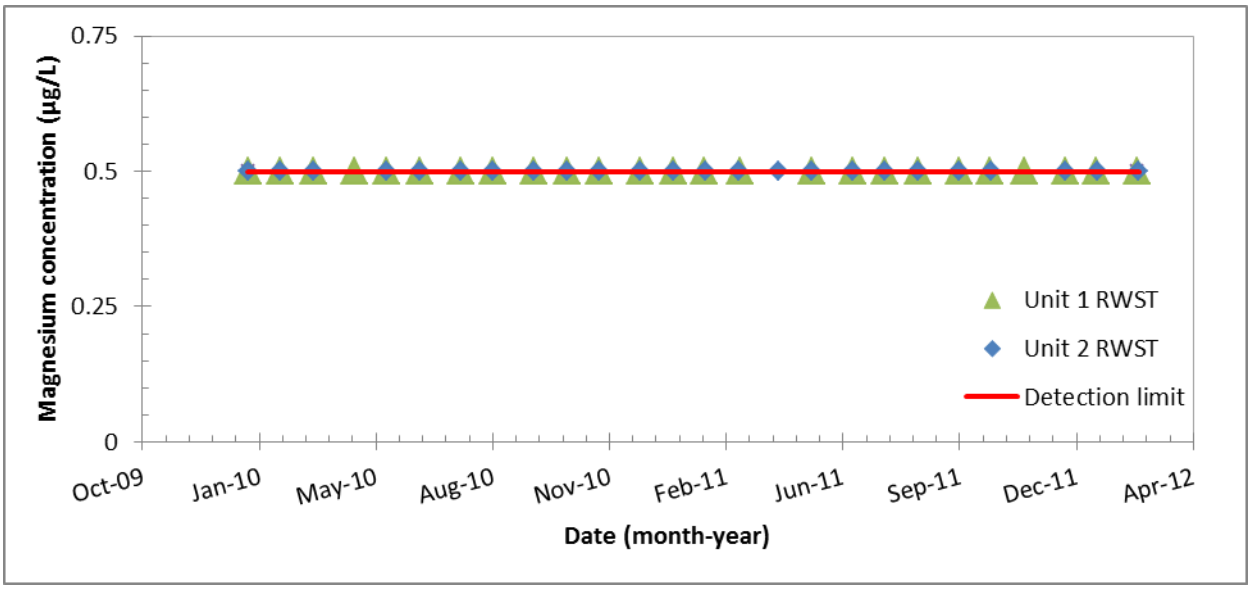

Figure 36: Magnesium concentration in Unit 1 and Unit 2 RWST as a function of time.

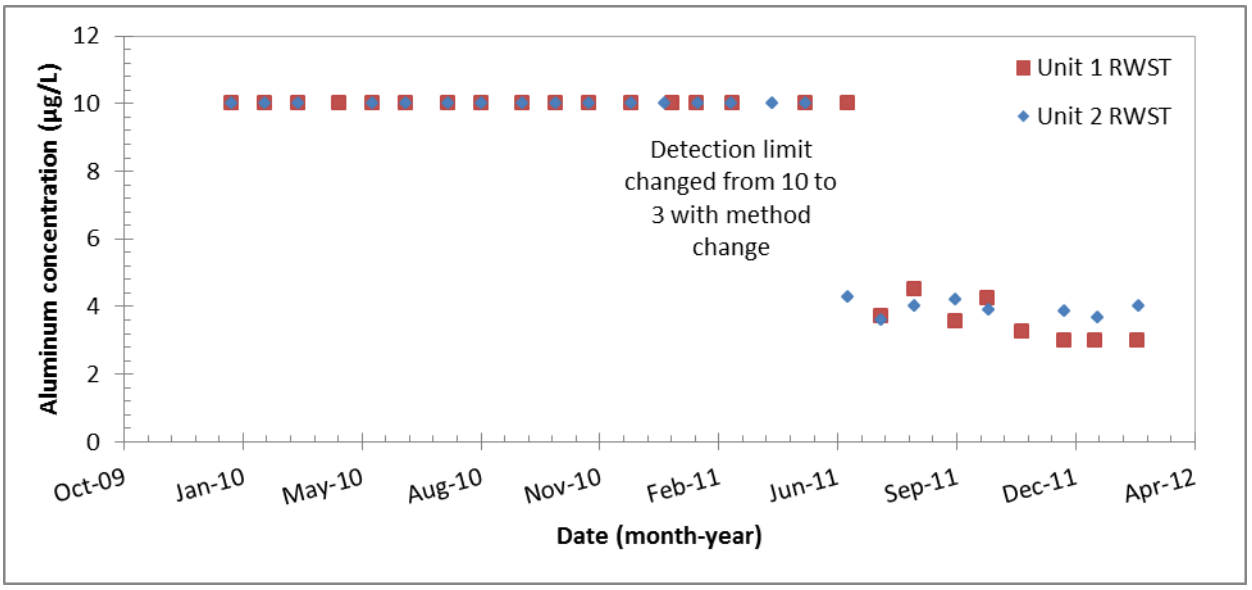

Figure 37: Aluminum concentration in Unit 1 and Unit 2 RWST as a function of time.

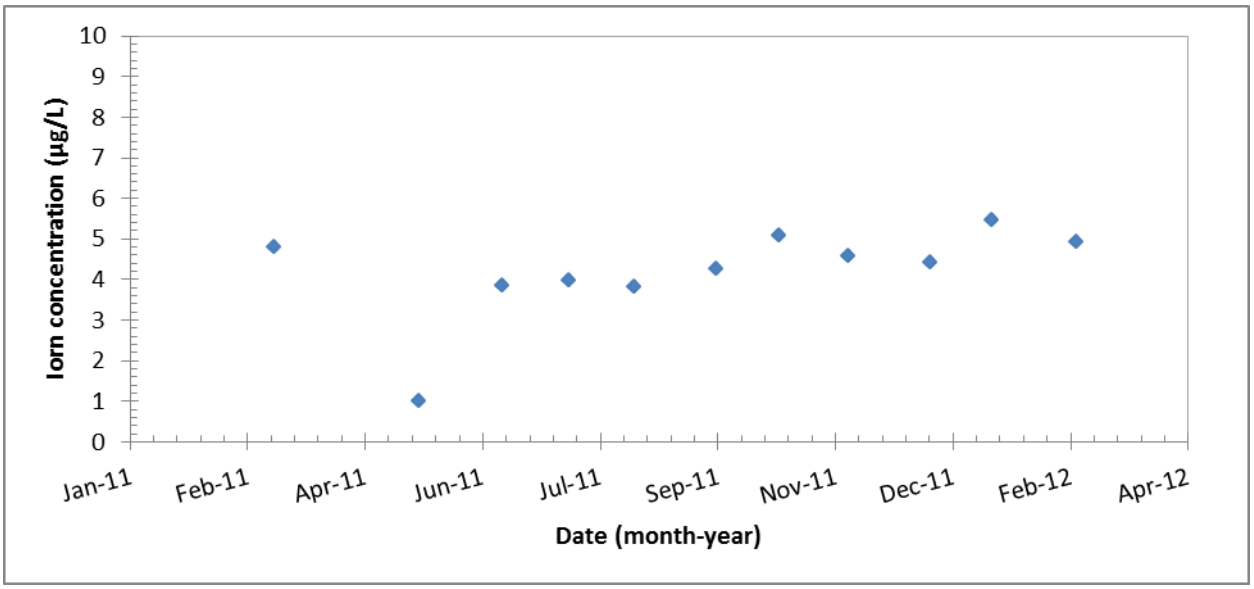

Figure 38: Iron concentration in Unit 1 RWST as a function of time.

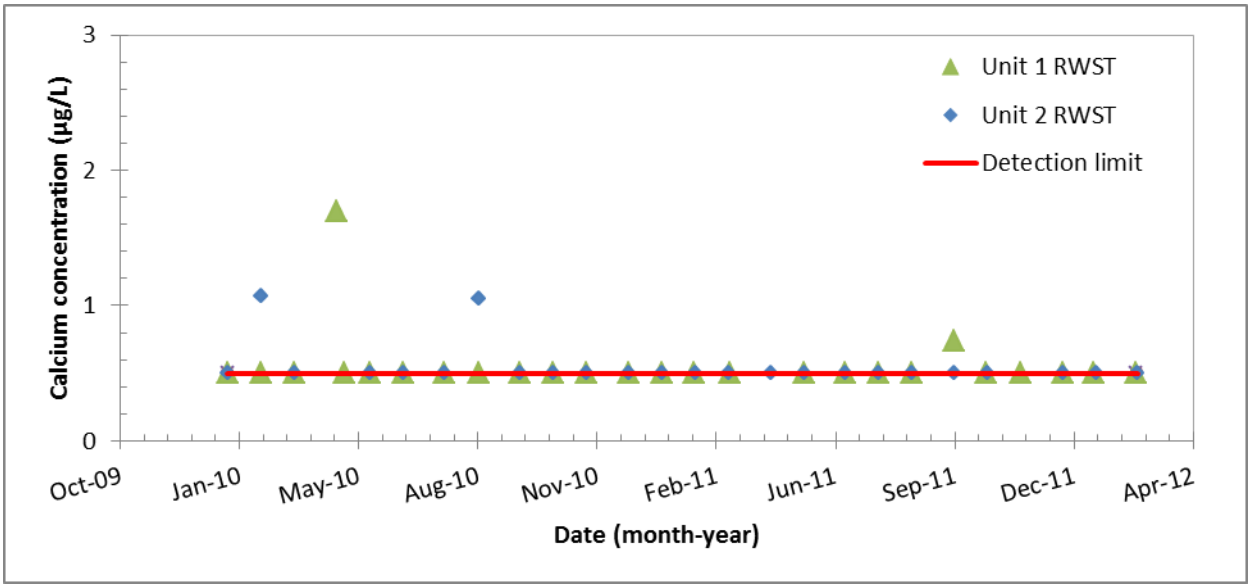

Figure 39: Calcium concentration in Unit 1 and Unit 2 RWST as a function of time.

3.8.1.1 **Impurity Results**

All impurities in both the RWST and RCS of both units were only detected in very small concentrations (µg/L or ppb levels), Figures 27-39; Therefore, they will be excluded from the chemical makeup of the initial pool concentration in the CHLE analyses.

3.9 Pool pH

The pool pH following a LOCA will vary due to the dissolution of TSP mass into the range boric acid concentrations in solution. For the STP design basis, using values (Table 3) for boric acid with the range

of TSP listed in Section 3.2 and solution volumes (Table 1), the pH during a LOCA will range 4.5 and will rise to a final pH of ~7.7 upon complete dissolution of TSP [5]. Using operational values for both solution volumes (Table 2) and boric acid concentrations (Table 18 and 19), with 15,100 lb of TSP, results in a smaller range of pH values as discussed below.

3.9.1 pH Analyses and Results

The pH range to be covered in the CHLE analyses was calculated from the operational values of the RCS, RWST, and accumulators for solution volumes (Table 2) and boric acid concentrations (Tables 18 and 19). These values listed , Table 26, are calculated at 21 °C (Appendix A). This range of pH values (Table 26) only reflects the expected variance of the final pool pH. This range does not reflect the full pH profile expected as a result of a LOCA event; i.e. before, during, and after TSP dissolution into the pool. Therefore the median values for the steady state pH will be used in the CHLE tank test. The pH profile from dissolution of TSP into solution will be mimicked by pumping in a concentrated solution of TSP starting at 15 minutes after test initiation over a 65 minute duration as explained by sections 2.2 and 3.2. Therefore the test will have the lower pH approximately 4.5 (250 mM boron) and increase to approximately 7.2 ± 0.1 over the first 80 minutes of testing.

Table 26: pH of the 30 Day test using the largest TSP concentration.

Statistical Parameter	pH
Median	7.17
Maximum	7.24
Minimum	7.09

Since TSP dissolution occurs within the first 1-2 hours of a 30 day test, it was decided to bound the minimum pH for bench tests through analysis of aluminum solubility characteristics as a function of pH as opposed to the initial pH of ~4.5, which rises quickly to the steady state pH during a LOCA. As seen in Figure 40, approximate minimum solubility of aluminum in borated buffered water ranges between 5.5 and 6.5 at the temperatures listed which encompasses the operational range of the tank test; therefore the average pH value of 6.0 will be the minimum pH in the bench test. The mid-point pH for the bench test will be the same as that used in the CHLE tank test, and the largest pH will be 7.7 as determined by conservative STP calculations [8].

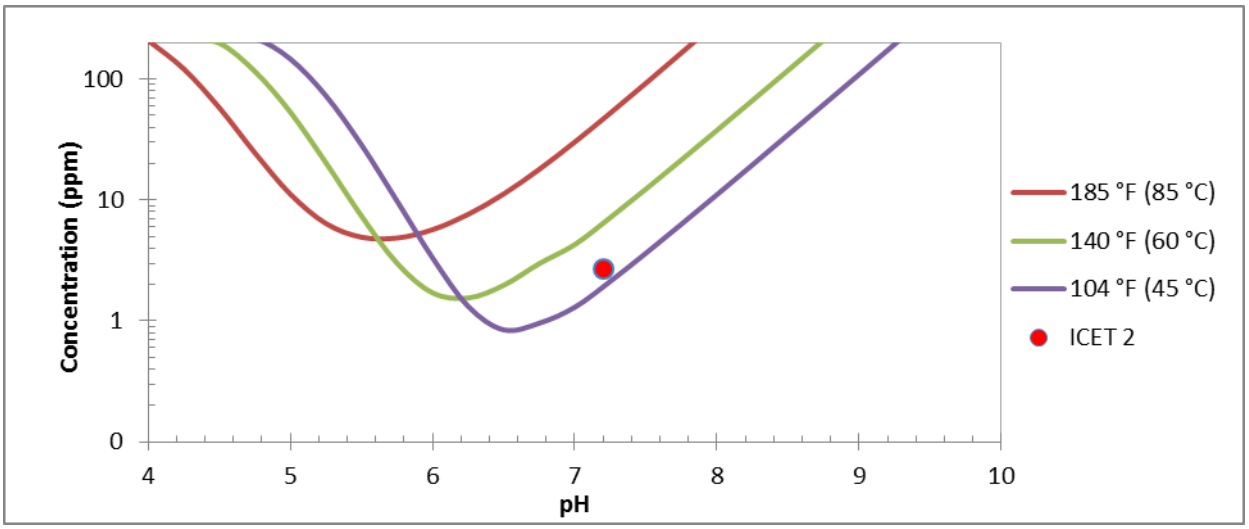

Figure 40: Aluminum solubility in borated buffered water.

3.10 Acid Generation Due to Irradiation

Strong acid is expected to form due to irradiation of containment following a LOCA. Nitric acid can form in response to irradiation of air and water. Hydrochloric acid may form due to irradiation or heating of electrical cable insulation [15]. The generation of these strong acids may result in a decrease of pool solution pH over time leading to the formation or increased formation of chemical precipitates of concern.

3.10.1 Acid Generation Results

Calculations to determine the concentrations of strong acids following a LOCA at STP were previously performed [7] . It was determined that 8.0E-4 M hydrochloric acid 2.5 E-4 M nitric acid would form over a thirty day period, Figure 41. The generation of both the hydrochloric and nitric acid is expected to decrease the pH by approximately 0.15 pH units over the same thirty day time period which can be seen in Figure 42.

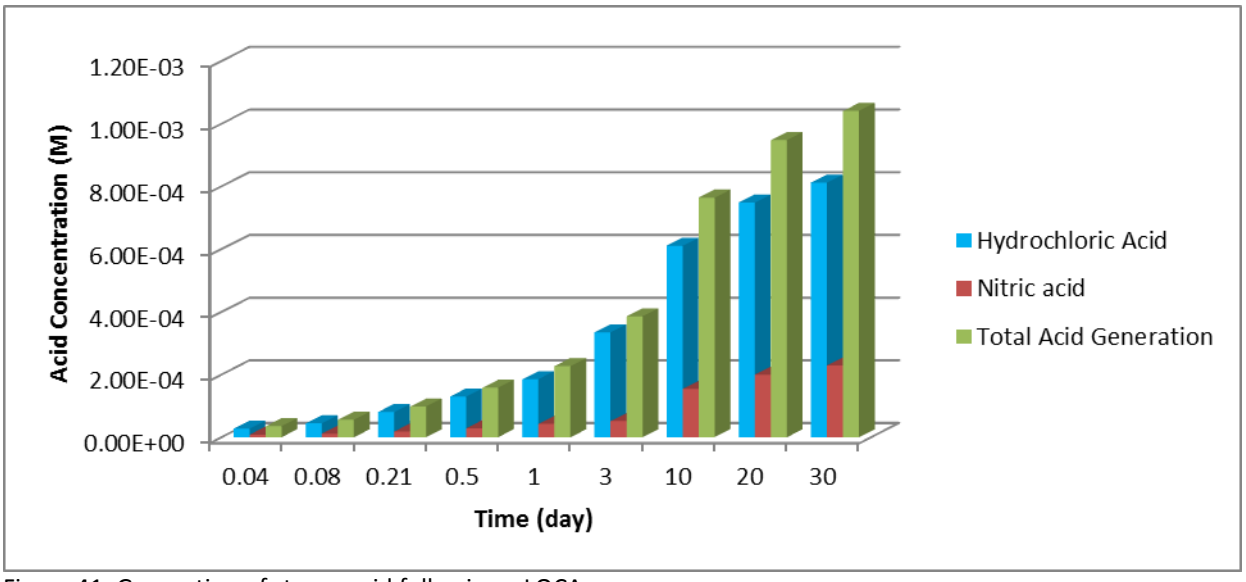

Figure 41: Generation of strong acid following a LOCA.

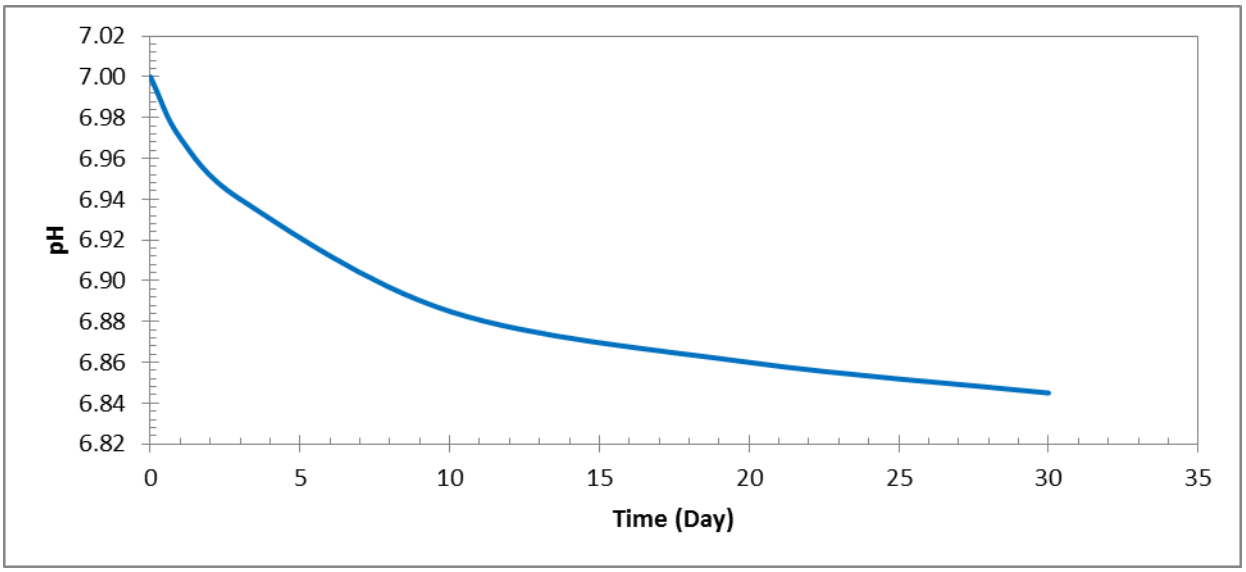

Figure 42: Decrease in pool solution pH as a result of acid generation, using an initial pH of 7 as a basis for comparison.

It is widely accepted that the solubility of the precipitates of concern, (i.e. aluminum hydroxide), is pH and temperature dependent. As shown by Figure 40, the post LOCA pool chemistry of ICET Test 2, which is similar to STP chemistry, results in solubility conditions near the minimum solubility concentration for the precipitates of concern. While a decrease of 0.15 pH units does not appear to be a significant change in solution pH, the temperature of the pool solution also decreases further reducing the solubility of possible precipitates.

3.10.2 Results

It was decided to add nitric and hydrochloric acid over time because the solution will be exposed to a chiller loop which may drop the temperature to or below the solubility limit of aluminum in solution. Therefore it is necessary to capture the possible effects of acid generation with temperature changes in the 30 Day test to fully evaluate the integrated chemical effects.

4 CHLE Pool Chemistry

The concentrations identified in Section 3 were multiplied by the 'best estimate' volume of corresponding solution to determine the pool chemistry of the CHLE test. A pH profile as detailed in sections 2.2 and 3.2 will be captured in the tank tests while a range of pH values will be captured in the the bench scale test. Table 27 contains a summary of chemical conditions to be captured by the CHLE tests. Table 28 list the acid to be added to the tank tests.

Table 27: Chemical conditions to be covered by the CHLE analyses.

Chemical	Bench Test Minimum (mg/L)	Bench Test Maximum (mg/L)	Tank Test (mg/L)
Boric Acid (Boron)	14,351 (2509)	16,918 (2958)	15,488 (2708)
Silicon	0.45	2.48	0
Lithium	N/A	N/A	0.42
TSP[1]	TBD	TBD	3,370
Final solution pH	6.0	7.7	7.2

[1] The concentration of TSP to be used in the bench test will be dictated by the boric acid concentrations and the target pH.

Table 28: Acid addition to CHLE test.

To be added	HNO_3[1] (ml)	HCL[2] (ml)
24 hours	2.04	12.15
Day 3	2.84	14.05
Day 10	5.23	25.93
Day 20	3.30	12.92
Day 28	2.13	5.99

[1] Molarity of nitric acid is 15.7

[2] Molarity of hydrochloric acid is 12.1

5 Conclusion

In conclusion, these results were derived using a risk-informed approach. This approach provides a more accurate estimate of the chemical concentration than previous evaluations. The mass calculated from volumes and concentrations listed within this document will be used as design parameters for the CHLE analyses.

6 References

1. Alion, *STP Post-LOCA Water Volume Analysis*, 2012, Alion Science and Technology: Albuquerque, NM.
2. Wheeler, R.E., *Quantile estimators of Johnson curve parameters.* Biometrika, 1980. **67**(3): p. 725-728.
3. Conover, W.J., *Practical Nonparametric Statistics*. 1971, New York: John Wiley & Sons.
4. DeCoursey, W.J., *Statistics and Probability for Engineering Applications with Microsoft Excel*. 2003, MA: Elsevier Science.
5. STP, *TGX - Required Mass of TSP for LOCA Sump Solution pH Adjustment*, 2001, South Texas Project Nuclear Operating Company.
6. TAMU, *6" Cold Leg Break Simulation Results Sump Temperature = 200 – 150 ºF*, 2012.
7. STP, *Post-LOCA Containment Sump pH and Maximum Iodine DF for AST Chapter 15 Analyses*, 2006, South Texas Project: Bay City, Texas.
8. STP, *MC-6480; MIN & MAX SUMP pH*, 1999, South Texas Project Nuclear Operating Company.
9. Rubin, K., J.L. Grover, and W.A. Henninger, *Spray Additive Elimination Analysis for the South Texas Project*, 1989: Pittsburgh, Pensylvania.
10. STP, *Containment Spray System*, 199?
11. STP, *Structural Reactor Containment Buidling TSP Baskets Fabrication and installation*, 2008, South Texas Project Nuclear Operating Company.
12. STP, *Condition Record 97-6223*, 1997, South Texas Project Nuclear Operating Company.
13. Wilkins, J.L., *TSP dissoluiton*, R.C. De Young, Editor 1973, Omaha Public Power.
14. Alion, *GSI-191 Containment Recirculation Sump Evaluation: CFD Transport Analysis, Revision 3*, October 21, 2008.
15. Beahm, E.C., R.A. Lorenz, and C.F. Weber, *Iodine Evoluiton and pH control*, 1992, Oak Ridge National Laboratory.

PROJECT DOCUMENTATION COVER PAGE

Document No: CHLE-006	Revision: 1	Page 1 of 14
Title: STP Material Calculations		
Project: Corrosion/Head Loss Experiment (CHLE) Program		Date: 15 August 2012
Client: South Texas Project Nuclear Operating Company		

Summary/Purpose of Analysis or Calculation:

A survey of materials within containment at South Texas Project Nuclear Operating Company (STP) was performed to identify material that may leach corrosion or dissolution constituents into the pool solution as a result of a Loss of Coolant Accident (LOCA). This survey was performed to identify materials to include in the Chemical Head loss Experiment (CHLE) analyses and to determine the ratio of material surface area to solution volume [1] for testing purposes.

Signatures:	Name:	Signature:	Date:
Prepared by:	Janet Leavitt/Kyle Hammond	< signed electronically >	3/12/2012
UNM review:	Kerry Howe	< signed electronically >	8/15/2012
STP review:			
Soteria review:	Zahra Mohaghegh	< signed electronically >	5/11/2012 8/18/2012

Revision	Date	Description
0	3/12/2012	Original document
1	8/14/2012	Revised to resolve internal comments

Table of Contents

List of Figures

List of Tables

Definitions and Acronyms

RCB	Reactor Containment Building
RCS	Reactant Cooling System
RWST	Refueling Water Storage Tank
SI	Safety Injection
ECCS	Emergency Core Cooling System
LOCA	Loss of Coolant Accident
STP	South Texas Project
CHLE	Chemical Head Loss Experiments
ICE	Integrated Chemical Effects

1 Purpose

A survey of materials within containment at South Texas Project Nuclear Operating Company (STP) was performed to identify materials that may leach corrosion or dissolution constituents into the containment pool solution as a result of a Loss of Coolant Accident (LOCA). This survey was performed to identify materials to include in the Chemical Head loss Experiment (CHLE) analyses and to determine the ratio of material surface area to solution volume [1] for testing purposes. These values are important in conducting a risk informed approach in evaluation of potential safety issues after a LOCA. The initial pool chemistry and the corrosion or dissolution constituents within the pool solution may react to form chemical precipitates that may negatively impact head loss across the sump strainer, resulting in failure of the Emergency Core Cooling System (ECCS). An accurate assessment of materials that will leach corrosion or dissolution constituents into the pool solution and the ratio of material surface area to volume within containment will allow the CHLE analyses to investigate the most probable pool chemistry of a LOCA; thus determining the most realistic consequence of chemical reactions on head loss across the sump strainer as a result of LOCA conditions

2 Methodology

A survey of materials in containment was conducted at STP. Surface areas or volumes of materials within containment were determined and reviewed for possible exposure to the containment pool solution. Materials with very low surface area or probability of exposure to the pool solution were eliminated from the list of materials to be included in the CHLE analyses. For materials to be included in the CHLE analyses, ratio of surface areas or volumes of materials to the pool volume [1] were determined using the following equation.

$$M_{chle} = \frac{V_{chle}}{V_{stp}} M_{stp}$$

Where M_{chle} is the material surface area or volume to be included in the CHLE analyses, V_{chle} is the volume of the solution in the tank for the CHLE analyses, V_{stp} is the steady-state volume of the pool within the STP containment, and M_{stp} is the material surface area or volume in containment.

3 Design Input and Analyses

The following data was obtained from a survey of material identified to be present in containment at STP. Materials within containment that can leach metals into the containment pool are divided between non-submerged and submerged surfaces. Non-submerged material surfaces are those exposed to the containment spray during a LOCA. Although some condensation may remain on equipment and material above the containment flood level, the amount of corrosion products contributed from this material is relatively small compared to the corrosion product generated by submerged materials. With the exception of fiberglass insulation, the division of submerged and non-submerged materials is not affected by break type. Materials found to exist within containment at STP are as listed below:

- Aluminum – from valve actuator components and scaffolding
- Fiberglass (Nukon and Microtherm) –used as insulation on pipes
- Concrete – represented exposed concrete surfaces
- Zinc – in galvanized steel and in zinc-based protective coatings
- Lead – permanent lead shielding blankets
- Copper – wiring, cables, and tubes of the fan coolers
- Latent debris – dirt and lint for air flowing into containment vents
- Carbon steel – component of structural steel, steam generators, piping, etc.

Aluminum and zinc, primarily in the form of galvanized steel or non-top coated inorganic zinc based primer, have been identified as the materials most susceptible to corrosion following a LOCA [2-4]. Lead [5] and carbon steel [4] may also corrode within the expected pH range of about 4.5 – 7.5 [6] following a LOCA, releasing metal ions into the pool solution. Fiberglass and concrete can leach constituents such as calcium and silicon into solution [4], which may produce chemical precipitates in the tri-sodium phosphate (TSP) buffered pool solution. Copper and iron (from steel) are relevant because they may affect the corrosion rates of other materials, such as aluminum [7]. Since all the above materials exist within STP containment and are expected to be present within the pool chemistry if exposed to the pool solution, all were evaluated to determine available surface area and probable exposure to the pool solution.

The pool volume at STP varies depending on the volume of water in the reactor cooling system (RCS), refueling water storage tanks (RWST), and safety injection accumulators. The RCS and RWST contribute to the pool volume in all LOCAs. The accumulators do not discharge in small break LOCAs (SBLOCAs), and therefore SBLOCAs technically have a smaller pool volume and therefore larger ratio of material to pool volume than other sizes of LOCAs. However, the accumulators only contribute about 4 percent of the pool volume so the effect is relatively minor. The pool volume for LBLOCA and MBLOCA were calculated to be 71,778 ft^3 at 21 ^oC [1]. The pool volume for a SBLOCA was calculated to be 61,949 ft^3 at 21 ^oC [1].

3.1 **Aluminum**

3.1.1 STP Survey

Sources of aluminum in containment include structures such as scaffolding and small components such as valves and aluminum coatings. Most of these materials are above the containment pool elevation, but may be exposed to containment sprays. Both integrated and separate effects tests have shown that the corrosion of aluminum can be significant and may cause precipitates [4, 8, 9]. There are 5,567 ft^2 (10% submerged and 90% non-submerged) of aluminum in containment at STP[10]. This corresponds to a ratio of aluminum surface area to pool volume of 0.078 ft^2/ft^3.

3.1.2 CHLE Test Parameter

Based on the information obtained from the STP survey for aluminum, the surface area of aluminum in the CHLE tests will be 2.64 ft^2 in the vapor space (unsubmerged, subjected to sprays) and 0.47 ft^2 submerged in the pool solution.

3.2 **Fiberglass insulation**

3.2.1 STP Survey

There are two type of fiberglass insulation in solution: (1) Nukon and (2) Microtherm. Nukon insulation is classified as E-glass which is an amorphous material containing silicon dioxide, calcium oxide, aluminum oxide and boric oxide[4]. Microtherm insulation is classified as amorphous silica material which contains materials made up of predominately amorphous silica with a small percentage of E-glass[4]. The amount of fiberglass insulation within containment is determined by break type and is listed in Table 2.

Table 1: Ranges of ratio values for volume of materials to pool solution as a function of break type

Break type	Nukon Ratio (ft^3/ ft^3)	Microtherm Ratio (ft^3/ ft^3)
SBLOCA	Awaiting information	
MBLOCA	8.36E-04	0
LBLOCA		

3.2.2 CHLE Test Parameter

The amount of insulation is a function of break type which results in a range of material volumes. This range is dictated by the break sizes that fall within the category of LOCA scenarios. The amount of insulation material to be used in each of the 30 Day tank test is determined by debris generation calculations by the CASA Grande program.

Table 2: Ratio of volume of materials to pool solution in the CHLE analyses

Fiberglass Type	**SBLOCA (ft^3)**	**MBLOCA (ft^3)**	**LBLOCA (ft^3)**
Nukon		60	
Microtherm		0	

3.3 **Concrete**

3.3.1 STP Survey

Most concrete surfaces in within containment are coated [11]. However, some uncoated surfaces could be exposed to the pool or spray water by direct jet impingement within the zone of influence (ZOI). Also, there are some concrete surfaces with unqualified or degraded qualified coatings which may fail.

Awaiting calculation from Alion

Also, bench test will be done to characterize metals leaching from concrete. As shown by the evaluation of Table 3 (Appendix A) very little calcium (<0.5 mg/L) in solution theoretically may be required to form a calcium phosphate precipitate in a TSP buffered system, but depends on temperature and pH. Therefore evaluating leaching rates of metals, specifically calcium, from the concrete is necessary.

Table 3: Calcium concentration required to form precipitation.

Test Case	TSP Concentration (mg/L)	Boron Concentration (mg/L)	pH[a]	Calcium Concentration (mg/L)
1	4032	2486	7.33	0.36
2	4032	2659	7.26	0.41
3	4032	2897	7.18	0.48
4	4435	2486	7.36	0.31

[a] Value reference to 21 C., value determined using STP operating median boron concentration and STP representative TSP concentration
[B] Log K = -28.92 [12]

3.3.2 CHLE Test Parameter

The concrete used for the CHLE tests will be made at the University of New Mexico (UNM)following the procedure provided by Westinghouse and used for the ICET tests [13]. The UNM concrete was be subjected to leaching bench test for comparison with a concrete core obtained from a nuclear power plant to evaluate leaching differences due to material preparation.

3.4 **Latent debris**

3.4.1 STP Survey

This material type accounts for dust and fibers that exist in containment as a result of environmental conditions. The maximum value of latent debris in STP containment has been determined to be 170 lb. dirt/dust and 30 lb. fiber [14]. This corresponds to a mass to volume ratio of 0.002 lb/ft^3 for dirt/dust and 0.0004 lb/ft^3 for fiber in containment. While it is known that the TSP buffered system may be sensitive to the addition of metals to solution, it is unknown if the soil leaches any attributable concentration of metals. Therefore, bench test will be done to evaluate metal leaching from the STP soil.

3.4.2 CHLE Test Parameter

Latent debris is defined as fiber and dust. The fiber used for Latent debris is Nukon insulation and will be taken into account within the total fiberglass added to tests. The dust used in the CHLE analyses is soil obtained from the STP site using the standard environmental sampling procedure [15]. The use of the material within the 30 Day CHLE test will be evaluated by bench test that investigate metal leaching. Any detectable metal leaching will be incorporated as a salt in the CHLE tank test.

3.5 Zinc (Galvanized Steel and Coating)

3.5.1 STP Survey

Galvanized steel and zinc based paints or coatings are sources of zinc within containment. There are 273,749 ft^2 (10% submerged and 90% non-submerged) of galvanized steel in STP containment [10]. This quantity corresponds to a surface area to volume ratio 3.81 ft^2/ft^3. There are 417,839 ft^2 (10% submerged and 90% non-submerged) of inorganic coated zinc steel within containment at STP [16]. This quantity corresponds to a surface area to volume ratio of 5.82ft^2/ft^3.

These numbers are the conservative quantities. They are currently under review by the team to determine nominal quantities.

3.5.2 CHLE Test Parameter

The inclusion of galvanized steel and zinc coated material in the LBLOCA 30-day test is currently under review by the project team. If they are included, the surface area of galvanized steel in the CHLE tests will be X ft^2 in the vapor space (unsubmerged, subjected to sprays) and X ft^2 submerged in the pool solution. The surface area of zinc coated material in the CHLE tests will be X ft^2 in the vapor space (unsubmerged, subjected to sprays) and X ft^2 submerged in the pool solution.

3.6 Copper

3.6.1 STP Survey

Various source of copper are found in containment at STP. These sources include wiring, cables, and tubes of the fan coolers [17].

3.6.2 CHLE Test Parameter

While copper is present in STP containment, none of it will be submerged during a LOCA. In addition, significant quantities of the unsubmerged copper will be protected from spray impingement. Copper cable and wiring will not be subjected to spray as long as some insulation is in place.
As a result of all these factors, copper is excluded from the long-term CHLE tests. However since it is known that copper ma y accelerate aluminum corrosion [7], the effects of copper on aluminum corrosion under STP conditions will be investigated in short-term bench-scale corrosion tests.

3.7 Lead

3.7.1 STP Survey

Lead exists in STP containment in two forms: (1) lead blankets and (2) lead pipe insulation. There are approximately 500 lead blankets (1 ft x 3 ft) in containment (45 % are submerged and 55% not submerged) [18]. The equivalent thickness for a lead sheet in the blanket is 3/16 [19]. These lead

blankets are stored in drums with holes to prevent them from floating away if containment floods, but the sources of lead are sealed within vinyl-laminated nylon covers which provide a protection barrier between the material and pool solution.

The lead pipe insulation is sparsely present in containment as illustrated by Figure 1. The volume/mass values associated with the locations as listed in Figure 1 are listed in Table 1. Give that only three locations within containment have lead pipe insulation, the probability that they will be in the zone of influence is relatively low [20]. Since the contribution of lead from the pipe insulation is not a likely occurrence in a LOCA , the probable contribution from this material to the pool solution is neglected.

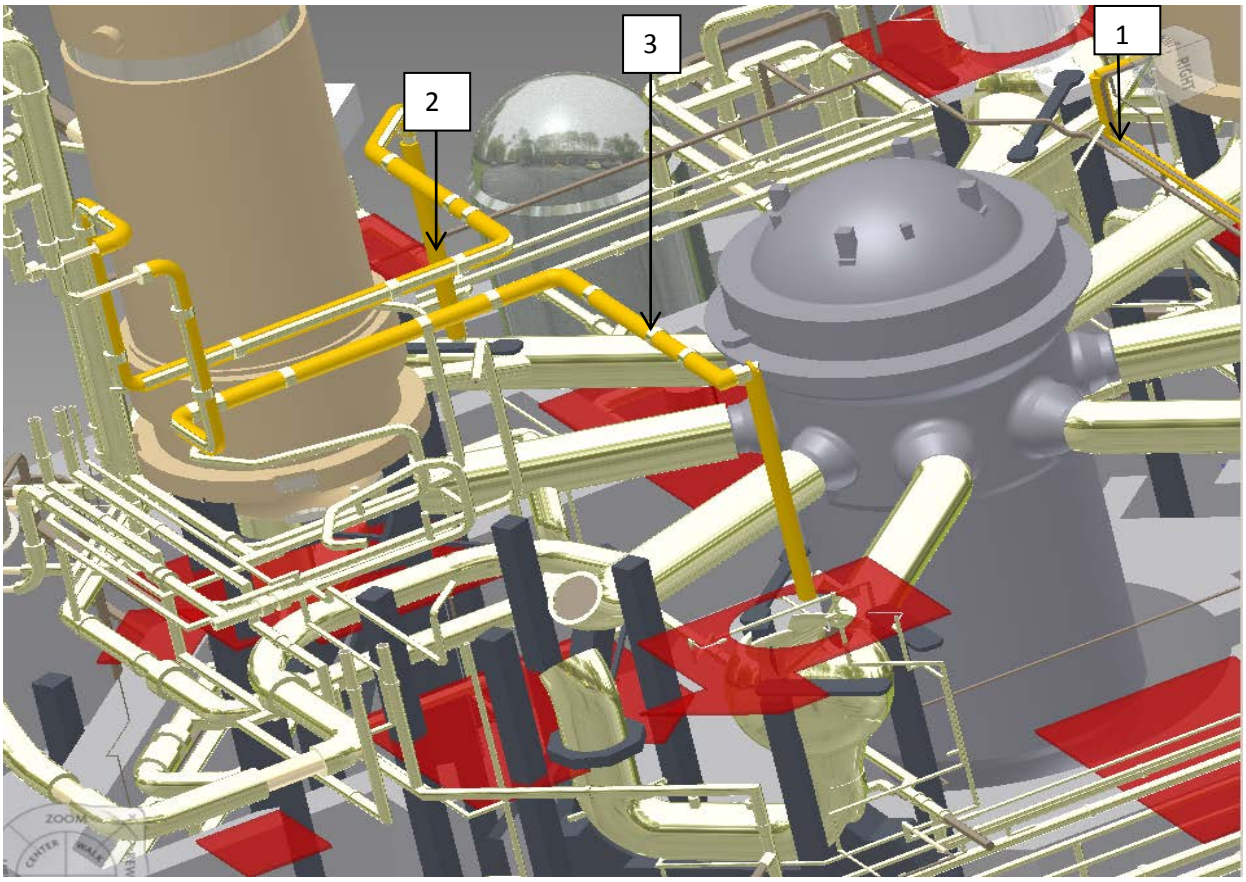

Figure 1: Simplified CAD image showing locations of lead insulated pipes are indicated in yellow.

Table 4: Volume and mass of lead insulation within STP containment

Number	Official Name	Mass (lb_m)	Volume (ft^3)
1	4CV-10010-BB1	930.7771	14.90962
2	4RC-1123-BB1	1437.241	23.02239
3	4RC-1422-BB1	1399.997	22.42536
Total	Lead Blanket Insulation	3768.015	60.35737

A literature search of lead precipitate using ions known to exist in solution as a guide (regardless of concentration) was done to identify possible precipitates and gather thermodynamic information associated with the solubility limits, Table 5. Since lead can form a variety of precipitate products in the pool with, some which theoretically require very little soluble lead (lead phosphates and lead chlorides) in solution (Table 6), it was determined that bench test will be performed to characterize lead corrosion in the CHLE pool chemistry and the formation of precipitates. It should also be noted, however, that phosphate is commonly used as a corrosion inhibitor for lead.

Table 5: Lead precipitate and associated thermodynamic data associated with solubility

Solids	Log K	Sources
$Pb(BO_2)_2(s)$	6.5192	NIST [12]
$Pb(OH)_2(s)$	8.15	MTQ3.11[21]
$Pb_2O(OH)_2(s)$	26.19	NIST [12]
$Pb_3(PO4)_2(s)$	-43.53	NIST[12]
$PbHPO_4(s)$	-23.805	NIST [12]
$PbO:0.3H_2O(s)$	12.98	MTQ3.11[21]
$PbCl_2$	-4.78	NIST [12]
$PbSO_4$	-7.79	NIST [12]
Solid	Solubility 1[A] (mg/L)	Solubility 2 [B] (mg/L)
$Pb(C_2H_3O_2)_2$[22]	551,006	2,185,084
$Pb(NO_3)_2$ [23]	565,000	1,270,000

[A] Solubility 1 for lead acetate is at 25 C and for Lead Nitrate it is at 20 C
[B] Solubility 2 for lead acetate is at 50 C and for Lead Nitrate is at 100 C

Table 6: Lead concentration to form lead phosphate precipitate using STP representative chemistry

Test Case	TSP Concentration (mg/L)	Boron Concentration (mg/L)	pH	lead Concentration (mg/L)
1	4032	2486	7.33	2.50E-05
2	4032	2659	7.26	2.87E-05
3	4032	2897	7.18	3.38E-05
4	4435	2486	7.36	2.14E-05

3.7.2 CHLE Test Parameter

While there is a significant surface area of lead and copper available in containment, lead will be excluded from the CHLE analyses since it is not directly exposed to spray or pool solution and the probability of material exposure due to destruction of protective outer layers is very low. However, since lead is highly insoluble, bench test will be performed to investigate lead corrosion under STP conditions.

3.8 **Uncoated Carbon Steel**

3.8.1 STP Survey

Uncoated carbon steel is generally present in containment as structural supports. 168,836 ft^2 (10% submerged and 90% non-submerged) is present in STP containment [16]. This quantity corresponds to a surface area to volume ratio of 2.35 ft^2/ft^3.

3.8.2 CHLE Test Parameter

While there is a significant amount of carbon steel in containment, previous research found that carbons steel corrosion occurred in insignificant amounts [9]. The ICET tests contained 0.15 ft^2/ft^3 of carbon steel, with 34 percent of the material submerged and 66 percent in the vapor space. The unsubmerged uncoated steel coupons had very little change in weight, with changes ranging from +1.3 to -0.4 g, compared to a mean pre-test weight of 1025 g. The submerged uncoated steel coupons in Test #1 (high pH) had a weight change of -23.3 g, but had very little weight change in the remainder of the tests (ranging from +1.4 to -1.1 g). In ICET Test #2, which corresponded most closely to the STP conditions, the unsubmerged coupons gained 1.3 g and the submerged coupons gained 1.4 g of weight. Iron concentrations remained nearly undetectable throughout the full duration of all the ICET tests. The highest concentrations of iron were less than 0.1 mg/L, during the first few days of ICET Test #3. Iron was undetectable during the entire ICET Test #2.

Based on the previously mentioned results, uncoated carbon steel will not be included in the CHLE tank tests.

4 Summary

A survey of material in containment at STP was performed. For materials that are expected to contribute to the containment pool chemistry, a ratio of surface area or volume of material to the volume of solution in containment at STP was determined. These ratios were used to determine the quantity of materials to include in the 30 Day CHLE tank test, Tables 4 and 5. This approach provides accurate materials and quantities to include in the integrated test as compared to previous evaluations. This approach allows for focus on materials of concern and probable chemical reactions associated with those materials.

Table 7: Surface area of materials in the CHLE analyses

Material	**Surface area(ft^2)**	
	Submerged	**Non-submerged**
Aluminum	0.47 ft^2	2.64 ft^2
Galvanized Steel		
Zinc coating		
Concrete	TBD	TBD
Latent debris		
Latent debris dirt contribution		

Table 8: Volume of materials in the CHLE analyses

Fiberglass Type	**SBLOCA (ft^3)**	**MBLOCA (ft^3)**	**LBLOCA (ft^3)**
Nukon		60	
Microtherm		0	

5 References

1. Alion, *STP Post-LOCA Water Volume Analysis*, 2012, Alion Science and Technology: Albuquerque, NM.
2. Burchell, R.C. and W.D. D., *Corrosion Study for Determining Hydrogen Generation from Aluminum and Zinc During Post Accident Conditions*, 1976: Pittsburgh, Pennsylvania.
3. Griess, J.C. and B.A. L., *Design Considerations of Reactor Containment Spray Systems – Part III. The Corrosion of Materials in Spray Solutions*, 1969: Oak Ridge, Tennessee.
4. Lane, A.E., et al., *Evaluation of Post-Accident Chemical Effects in Containment Sump Fluids to Support GSI-191*, 2006, Westinghouse Electric Company: Pittsburge, PA.
5. Revie, R. and W. C., *Corrosion and Corrosion Control : An Introduction to Corrosion Science and Engineering*. 2008, Hoboken, NJ: Wiley.
6. STP, *TGX - Required Mass of TSP for LOCA Sump Solution pH Adjustment*, 2001, South Texas Project Nuclear Operating Company.
7. Davis, J.R., ed. *Corrosion of Aluminum and Aluminum Alloys*. 1999, ASM International.
8. Reid, R.D., K.R. Crytzer, and A.E. Lane, *Evaluations of Additional Inputs to the WCAP-16530-NP Chemical Model*, 2007, Westinghouse Electric Company Pitssburge, PA.
9. Dallman, J., et al., *Integrated Chemical Effects Test Project: Consolidated Data Report*, 2006, Los Alamos National Laboratory: NM.
10. STP, *Added Commodities Inside The RCB*, 2003, South Texas Project.
11. Sande, T., K.H. Howe, and J.J. Leavitt, *Expected Impact of Chemical Effects on GSI-191 Risk-Informed Evaluation for South Texas Project*, 2011, Alion Science and Technology: Albuqueruqe, NM.
12. NIST, *NIST Critically Selected Stability Constants of Metal Complexes: Version 8.0*, 2008, National Institute of Standards and Technology: Gaithersburg, MD.
13. STP, *STPEGS UFSAR*, in *Concrete*.
14. Alion, *GSI 191 Containment Sump Evaluation: Debris Generation*, 2008.
15. STP, *REMP Sample Collection*, in *Soil Surface Sample*2009. p. 26.
16. Schulz, W., *Zinc and Galvanized Steel inside containment*, J. Leavitt, Editor 2012, G-Mail.
17. STP, *RCB HVAC Heat Sink Area Estimate*, South Texas Project.
18. Schulz, W., *Lead inside containment*, J. Leavitt, Editor 2012, G-Mail.
19. Industries, L. *Lead Blankets*. 2012; Product specifications]. Available from: http://www.lancsindustries.com/lead-wool-blankets/.
20. Mertens, A., *CAD Model Summary: Sourth Texas Reactor Building CAD Model for Use in GSI-191 Analyses*, 2011, Alion Science and Technology: Albuquerque, NM.
21. Allison, J.D., D.S. Brown, and K.J. Novo-Gradac, *MINTEQA2/PRODEFA2, A Geochemical Assessment Model for Environmental Systems: Version 3.0 User's Manual*, 1991, Environmental Protection Agency, Office of Research and Development: Washington, DC.
22. Dundon, M.L. and W.E. Henderson, *Measurement of Solubility by floating Equilibrium. The solubility of Lead Acetate.* Journal of the American Chemical Society, 1922. **44**(6): p. 1196-1203.
23. Lide, D.R., ed. *CRC Handbook of Chemistry and Physics 80th Edition*. 1999.

Max TSP Concentraiton	
10.61	mM
4031.8	mg/L
PO4	10.61
Na	31.83
PO4	11.67
Na	35.01

Ca3PO42	
Log K (beta)	-28.92
K	1.20226E-29

	mM	pH	[PO4]	[PO4]^2	k/[PO4]^2	[Ca] M	[Ca] mM	[Ca] mg/L
Min B	230	7.325	1.30E-07	1.68E-14	7.14E-16	8.94E-06	8.94E-03	3.58E-01
Median B	246	7.257	1.06E-07	1.11E-14	1.08E-15	1.03E-05	1.03E-02	4.10E-01
Max B	268	7.178	8.24E-08	6.79E-15	1.77E-15	1.21E-05	1.21E-02	4.84E-01
110% tsp	230	7.362	1.64E-07	2.69E-14	4.46E-16	7.64E-06	7.64E-03	3.06E-01

Test Case	TSP Concentration (mg/L)	Boron Concentration (mg/L)	pH	Calcium Concentration (mg/L)
1	4032	2486	7.33	0.36
2	4032	2659	7.26	0.41
3	4032	2897	7.18	0.48
4	4435	2486	7.36	0.31

Solubility of anhydrous Lead Acetate

Pb(C2H3O2)2

325.3 g/Mole

Pb	207.2	1	207.2
C	12.011	4	48.0
O	15.9994	4	64.0
H	1.00794	6	6.0
		MW	325.3

Temperature (^{o}C)	Solubility (g/ 100 g H20)	Mol Pb(C2H3O2)2	Density (g/L)	Vol of water (L)	Solubility (M)	Solubility (ppm)
25	55.2	0.16969513	998.2	0.10018	1.693897	5.51E+05
50	221.14	0.679825745	988.1	0.101204	6.717358	2.19E+06

Solids	Log K	Sources
Pb(BO2)2(s)	6.5192	NIST 13.1
Pb(OH)2(s)	8.15	MTQ3.11
Pb2O(OH)2(s)	26.19	NIST 46.7
Pb3(PO4)2(s)	-43.53	NIST46.4
PbHPO4(s)	-23.805	NIST 46.7
PbO:0.3H2O(s)	12.98	MTQ3.11
PbCl2	-4.78	NIST 46.8
PbSO4	-7.79	NIST 46.9

Solids	Log K	Sources
Pb(BO2)2(s)	6.5192	NIST 13.1
Pb(OH)2(s)	8.15	MTQ3.11
Pb2O(OH)2(s)	26.19	NIST 46.7
Pb3(PO4)2(s)	-43.53	NIST46.4
PbHPO4(s)	-23.805	NIST 46.7
PbO:0.3H2O(s)	12.98	MTQ3.11
PbCl2	-4.78	NIST 46.8
PbSO4	-7.79	NIST 46.9

Solid	Solubility 1 (mg/L)	Solubility 2 (mg/L)
Pb(C2H3O2)2	551,006	2,185,084
Pb(NO3)2	565,000	1,270,000

Lead Nitrate

Pb(NO3)2 (g/mol) 331.2

Solubility Pb(NO3)2	Solubility (g/100 ml H20)	Mol Pb(NO3)2	Solubility (M)	Solubility (ppm)
20	56.5	0.170591787	1.705918	5.65E+05
100	127	0.383454106	3.834541	1.27E+06

[HCL] (M)	8.00E-04	6.40E-07
Log K	-4.78	
[Pb] (M)	3.86E-02	
[Pb] (ppm)	0.19	
[PO4-3]	4.50E-08	
[H+]	6.98E-08	
Log K	-23.85	
[Pb] (M)	4.49E-10	
[Pb] (ppm)	2.17E-09	

$Pb_3(PO_4)_2(s)$	-43.53	NIST46.4
$PbHPO_4(s)$	-23.805	NIST 46.7
$PbCl_2$	-4.78	NIST 46.8

	mM	pH	$[PO_4]$	$[PO_4]^2$	$10^K/[PO_4]^2$	[Pb] M	[Pb] mg/L
Min B	230	7.325	1.30E-07	1.68E-14	1.75E-30	1.21E-10	2.50E-05
Median B	246	7.257	1.06E-07	1.11E-14	2.65E-30	1.38E-10	2.87E-05
Max B	268	7.178	8.24E-08	6.79E-15	4.34E-30	1.63E-10	3.38E-05
110% tsp	230	7.362	1.64E-07	2.69E-14	1.10E-30	1.03E-10	2.14E-05

Test Case	TSP Concentration (mg/L)	Boron Concentration (mg/L)	pH	lead Concentration (mg/L)
1	4032	2486	7.33	2.50E-05
2	4032	2659	7.26	2.87E-05
3	4032	2897	7.18	3.38E-05
4	4435	2486	7.36	2.14E-05

PROJECT DOCUMENTATION COVER PAGE

Document No: CHLE-007	Revision: 3	Page 1 of 9
Title: Debris Bed Requirements and Preparation Procedures		
Project: Corrosion/Head Loss Experiment (CHLE) Program		Date: 11 August 2012
Client: South Texas Project Nuclear Operating Company		

Summary/Purpose of Analysis or Calculation:

Corrosion/Head Loss Experiment (CHLE) tests are being performed to support the risk-informed resolution of GSI-191 at the South Texas Project Nuclear Operating Company (STP). Fiberglass debris will be added to the head loss modules in the CHLE tests to form a debris bed to investigate the interaction between the fiber and any corrosion products that may form. Capture of corrosion products may be manifested as an increase of head loss through the debris bed. This document describes the source, preparation, quantity, and procedures for addition of fiberglass and particulate matter to the head loss modules to form the debris beds.

Signatures:	Name:	Signature:	Date:
Prepared by:	Kerry Howe/Cody Williams		7/6/2012
UNM review:	Janet Leavitt		8/1/2012
STP review:			
Soteria review:	Zahra Mohaghegh		8/10/2012

Revision	Date	Description
0	5/1/2012	Draft document for internal review
1	7/6/2012	Includes updates for blended fiber preparation method
2	8/8/2012	Includes edits from internal review
3	8/11/2012	Includes edits from oversight review

Table of Contents

List of Figures

List of Appendices

Definitions and Acronyms

CHLE	Corrosion Head Loss Experiments
ECCS	Emergency Core Cooling System
NEI	Nuclear Energy Institute
NRC	Nuclear Regulatory Commission
PCI	Performance Contracting, Inc.
STP	South Texas Project Nuclear Operating Company

1 Purpose

A reproducible debris bed is an essential prerequisite to the Corrosion/Head Loss Experiments. Without a reproducible debris bed, it will be difficult to assess whether corrosion products cause an increase in head loss through the Emergency Core Cooling System (ECCS) strainers. This document describes the source of the materials that will be used to make the debris beds representative of STP conditions for the head loss experiments, the methods for preparing the materials and introducing them into the head loss modules, and experiments to determine the quantity of debris needed to make a suitable debris bed.

2 Methodology

The selection of debris and development of procedures is based partially on previous industry experience with head loss testing, as relayed to the project team by Alion Science and Technology. The debris preparation procedures are based on a guidance document developed by the Nuclear Energy Institute (NEI, 2012). The Nuclear Regulatory Commission (NRC) reviewed the NEI plan but declined to officially endorse it as the only way to produce acceptable debris because of the dependence on human actions (Ruland, 2012). The NEI document is included in Appendix A. The guidance from these sources forms the basis for the preliminary plan. The actual quantity of debris and procedures for forming the beds will be developed through experimental testing and validation as described in this document.

3 Design Input and Analyses

A schematic of the head loss modules is shown in Figure 1 and a photograph is shown in Figure 2. The modules have an inside diameter of 6.0 inches and cross-sectional area of 0.196 ft^2. With an approach velocity of 0.010 ft/s, the required flow rate is 0.88 gpm. The debris bed requirements, material sources, preparation, quantity, addition procedures, and acceptance criteria are described in the following sections.

3.1 Debris Bed Requirements

The debris beds are formed with only NUKON™ fiberglass insulation or a combination of NUKON™ and silicon carbide particles. Once the appropriate debris quantities have been established, all beds should be prepared with the same quantity of debris. A properly formed bed will be reproducible with head loss varying by no more than ± 25 percent from one bed to the next and be visually uniform with a top surface that appears horizontal with vertical variation of no more than 0.5 inches (1.27 cm) as relayed to the project team by Alion Science and Technology.

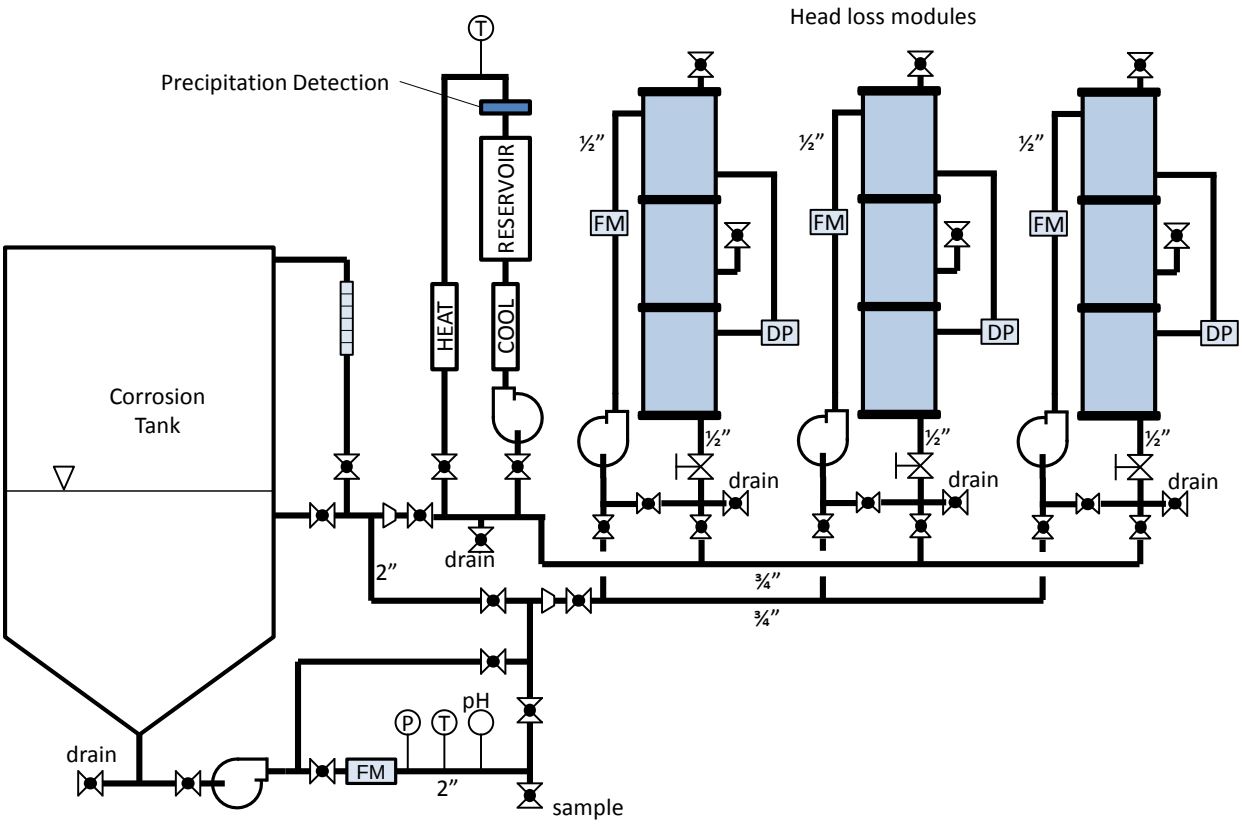

Figure 1 – Schematic of Head Loss Modules.

Figure 2 – Photograph of Head Loss Modules.

3.2 Material Source and Specifications

NUKON™ fiberglass insulation was purchased from Performance Contracting Inc., 16047 West 110th Street, Lenexa, KS 66219 (PCI). The blankets used are 2 feet x 4 feet x 2.5 inches thick and have a bulk specific weight of 2.4 lb/ft^3. The blankets are heat-treated on one side according to the procedure in NEI (2012) by PCI prior to being shipped to UNM.

The silicon carbide is Green Silicon Carbide, size F600, manufactured by Electro Abrasives, LLC., 701 Willet Road, Buffalo, NY 14218. Green Silicon Carbide is an extremely hard (Moh 9.4) manmade mineral. The F600 grit has a size distribution between about 5 and 30 µm. The nominal size distribution as reported on the Electro Abrasives website is shown in Figure 3. The size distribution was not independently validated for this project because the only purpose of the particles is to produce a reproducible debris bed. Typical composition, as reported on the Electro Abrasives website is shown in Table 1. The MSDS sheet is included in Appendix B.

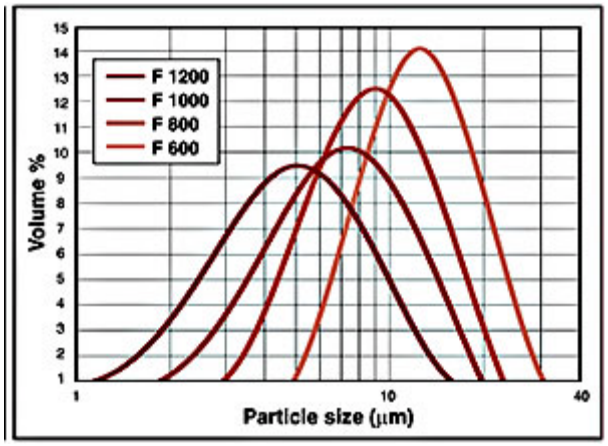

Figure 3 – Size Distribution for Green Silicon Carbide as reported by Electro Abrasives, LLC.

Table 1 – Typical Composition of Green Silicon Carbide as reported by Electro Abrasives, LLC.

Species	Composition (percent)
SiC	99.5
SiO_2	0.2
Si	0.03
Fe	0.04
C	0.1

3.3 Debris Bed Quantity

The thickness of debris bed required to achieve the desired head loss has not been identified in previous testing and is unknown. Testing that examined a range of conditions is summarized in Section 4 below. Nominally, the tested beds focused on 1-inch thick increments based on nominal bed density, which requires 0.016 ft^3 or 0.039 lb (17.8 g) of fiberglass. Debris quantities up to 140 g were tested.

3.4 Debris Preparation

Methods for aging fibrous debris preparation were developed in earlier experimental programs and are described in Section 6.3 of NEI (2012). Aging of the NUKON™ insulation for UNM CHLE test was performed by PCI (baked on one side). No further preparations of the raw materials (NUKON™ or the green silicon carbide) were performed at UNM.

Two fiber bed preparation methods were used in the UNM CHLE tests, described as the NEI fiber preparation method (Section 3.4.1) and the blended method (Section 3.4.2). Instruction for preparation of silicon carbide or how to make debris beds with this material was not found in the NEI or other debris preparation/ bed formation documents. The silicon carbide is weighed on a top-loading balance to a resolution of 0.01 g and added to the NUKON™ mixture as relayed to the project team by Alion Science and Technology.

3.4.1 NEI Fiber Preparation Method

Fine debris is generated with a pressure washer using the procedure described in Section 6.6 of NEI (2012). The procedure for creating various classes of debris from NUKON™ fiberglass is described in the NEI document. For the CHLE head loss tests, all fiberglass debris is categorized as fines according to the size classification scheme in Table 3-2 in NUREG/CR-6808 (2003). Table 3-2 is included in Appendix C. Water for the preparation of fiber was deionized water by reverse osmosis treatment to achieve a conductivity ≤ 50 µS/cm.

A section with equal portions of baked and unbaked NUKON™ fiber is taken from the fiber blanket shipped from PCI. The fiber weight is determined using a top-loading balance with a resolution of 0.01 g and recorded prior to the fiber being separated. Detailed step-wise direction of this preparation is included in Appendix D. Initial batches of NUKON™ fiberglass is separated by first splitting the fiber into four equal sheets, two unbaked sections and two baked sections. The four sections of the NUKON™ blanket are then cut with shears into approximately 1” X 1” sections followed by hand tearing the unbaked portions to produce approximately 0.5” X 0.5 “ sections. The prepared fiber is placed in a clean 5-gal pail with approximately 1 inch of RO water in the bottom of the pail. Fibers are separated using RO water run through a Cleanforce 1800-psi 1.5 gpm Axial Cam Heavy-Duty Electric pressure washer (Model # CF1800HD)with a 40 degree small diameter fan type tip, with the nozzle maintained slightly below the water surface. The fiber is subjected to the process until it passes a visual inspection. The degree of fiber separation is confirmed by visual inspection, by pouring the mixture into a glass dish, placing the

dish on a light table, and swirling the solution gently. The resulting fiber clumps are then compared to the pictures in Appendix C.

The required fiber-mass-to-water-volume ratio is less than or equal to 0.21 lb/gal (25 g/L). A batch with 18 g of fiber requires a minimum of 0.72 L which is less water than results due to the separation process. Therefore, the processed, separated fibers are collected in a stainless steel fine mesh kitchen colander. Buffered, borated solution is then added to the strained fiber prior to loop addition.

3.4.2 Blended Fiber Preparation Method

Blended debris is generated using a Black and Decker model number BS2100S. The fiber is weighed, separated, and cut in the same way as described above, see Appendix D for detailed information. To separate the fiber into fines, this method uses the blender instead of the pressure washer. The pieces of fiber are place in the blender and mixed with 0.8 L of buffered, borated solution. The blender is then switched to the chop setting and allowed to blend for 25 seconds. The mixture is poured into a beaker and the blender swished once to remove fiber that clung to the sides and blades. The fiber does not require any straining or addition of water.

3.5 **Debris Addition Procedures**

Experience with various methods of debris introduction in previous testing demonstrated that maintaining a low approach velocity and adding the debris mixture slowly produces the most uniform bed. The method used for adding NUKON^{TM} to the test system will be as follows. The test section will be filled with DI water at room temperature to one inch above the level of the inlet pipe. The inlet pipe is 6 inches below the top of the head loss modules. The distance between the top opening of the head loss modules and the debris support screen is about 50 inches. The recirculation pump will be turned on and the flow control valve set to the flow rate that corresponds to an approach velocity of 0.1 ft/s in the test section. Trisodium phosphate dodecahydrate and boric acid in quantities reflective of STP chemistry is then added to the loop and allowed to dissolve.

The debris mixture will be agitated thoroughly using a glass stir rod prior to addition to the test loop. The debris will then be added slowly over the course of two minutes while constantly being stirred to keep the fibers agitated. After the debris mixture has settled against the screen, the pump will be allowed to circulate until the head loss reaches an approximate zero slope on the graph of differential pressure versus time. Once this conditions has been met, the head loss is considered to be stabilized. Once the head loss is stabilized, the loop velocity is reduced to the test velocity of 0.01 ft/s. The head loss will be recorded over the circulation time.

3.6 **Debris Bed Validation and Acceptance**

The condition of the fiber fines will be validated by visual comparison to the table in Appendix C while the fiber solution is swirled gently in a glass dish placed on a light table.

The fiber bed will be acceptable when it meets the criteria described in Section 3.1.

4 Results

Detailed results of the experiments to develop reproducible debris beds are presented elsewhere (UNM, 2012). This section is intended to briefly summarize key results associated with bed characteristics as a result of different preparation approaches. The beds tested were not successful in retaining silicon carbide particles; therefore this material was not used in further testing. The original target for head loss for the debris beds was 0.50 ± 0.20 feet (0.22 ± 0.087 psi) of head loss when the approach velocity of water through the bed is 0.0090 ft/s and the temperature is 185 °F, after the head loss through the beds has been allowed to stabilize for 1 hour. Based on a linear ratio to water viscosity, the target head loss at room temperature (68 °F) is 1.50 ± 0.60 feet (0.65 ± 0.26 psi). Initial testing revealed that it was not possible to achieve this head loss with quantities of NUKON debris that are representative of realistic debris beds in the STP containment because of the low approach velocity and lack of particles in the debris beds.

With the blended bed methodology, a 20 gram mass of fiber resulted in a very uniform 0.5 to 0.625 inch (1.34-1.6 cm) bed with 6.22 to 6.37 inches of head loss at 0.1 ft/s and 0.55 to 0.68 inches of head loss at 0.01 ft/s with water at room temperature. With the NEI bed methodology, a 20 gram mass of NEI processed fiber produced beds with approximately 2 inch (5 cm) of height with a head loss of approximately 2.75 inches of water at 0.1 ft/s and 0.5 inches at 0.01 ft/s with water at room temperature. The initial head loss was lower than originally intended but the reproducibility was acceptable. Because the test apparatus instrumentation can detect small changes in head loss (0.1 inches of water), the lower than expect initial head loss was deemed acceptable. In later multi-day testing, the blender processed fiber beds increased in head loss without particulate in solution as time progressed whereas the NEI processed fiber beds maintained its initial head loss throughout the duration of testing. In both tests, the bed thickness did not change significantly during the tests. Upon draining the column and removal of beds, the blender process beds lost 33 percent of their initial height, while the NEI process beds lost 40 percent of their initial height.

5 References

Nuclear Energy Institute (NEI). "ZOI Fibrous Debris Preparation: Processing, Storage, and Handling, Revision 1", January 2012.

NUREG/CR-6808. "Knowledge Base for the Effect of Debris on Pressurized Water Reactor Core Cooling Sump Performance," February, 2003.

Ruland, W.H. Letter to John Butler of the Nuclear Energy Institute with the subject line "Fibrous Debris Preparation procedure for Emerengy Core Cooling System Recirculation Sump Strainer Testing, Revision 1" dated April 26, 2012.

University of New Mexico (UNM). "CHLE-008 Debris Bed Formation Results, Rev 2", June 2012

APPENDIX A

ZOI FIBROUS DEBRIS PREPARATION: PROCESSING, STORAGE, AND HANDLING

REVISION 1, JANUARY 2012

NUCLEAR ENERGY INSTITUTE

ZOI Fibrous Debris Preparation: Processing, Storage and Handling

Revision 1
January 2012

Nuclear Energy Institute

Generic Procedure

ZOI Fibrous Debris Preparation: Processing, Storage and Handling

TABLE OF CONTENTS

ZOI Fibrous Debris Preparation: Processing, Storage and Handling

1. SCOPE

This document covers the procedures for processing, storage and handling of the fiber that will be used in sump strainer testing. The resulting fibrous debris from this procedure is intended to represent fibrous material generated as a result of jet impingement within the appropriate zone of influence (ZOI). The overall test program is described in a test plan. This document is intended to outline the procedures to be used by the technical support team to process, store and handle fibrous debris that will be used as part of the test program. The material will be procured externally and processed to meet the requirements before it is used.

2. PURPOSE

The purpose of this document is to ensure that the requirements for processing, storage and handling of the fibrous debris that will be used for the XYZ Sump Strainer Test Program will be met, and that any additional requirements relating to processing, storage and handling are also identified.

3. DEFINITIONS

- Fines – readily suspendable in water (Classes 1 through 3 of Table 3-2 of NUREG/CR-6808)
- Small pieces – clumps of fibers ≤ 4 inches on a side (Classes 4 through 6 of Table 3-2 of NUREG/CR-6808)
- Large pieces – clumps of fibers > 4 inches on a side (Class 7 of Table 3-2 of NUREG/CR-6808)

4. GENERAL REQUIREMENTS

- The fiber required for the testing is specified in the test plan as to the type of material to be used for preparation per this document, e.g., Nukon, Mineral Wool, Temp-Mat, etc. The fibers will be processed as fines, small pieces, and large pieces, as dictated by the test plan.

- All weight measurements shall be performed using calibrated scales.
- The weighed debris must be stored and clearly labelled with weight, type, and date. This is done to prevent the possibility of incorrectly identifying the material at the time of its use. Documentation of the weighed debris shall be per the requirements of the test plan.
- The debris must be handled in a safe manner to ensure minimal hazard to personnel. Each relevant material safety data sheet (MSDS) must be read before handling debris and each worker must wear appropriate personal protective equipment (PPE).
- A data sheet, in a form similar to Attachment B, shall be used to document the completion of the applicable steps of this procedure.

5. RESPONSIBILITIES

The Scope of Work will be performed in accordance with this document and the test plan developed for the specific client.

6. PROCESS

This section identifies the procedures to be used to procure, store, process and handle fibrous debris. Fibrous debris will be heated on a hot plate to simulate the aged insulation in the plant before a loss of coolant accident (LOCA), and processed to achieve the required fiber size distribution.

6.1 Safety

Due to its potential negative effect on health and status as an irritant, the fiber material requires appropriate safety precautions when handling. These procedures are outlined in Appendix A. Due care must be used to ensure operator safety.

6.2 Initial Procurement and Storage

Fiber materials will be procured from specified manufacturers. The procured materials will be stored in a sheltered location prior to further processing. The fiber will normally be received as rolls or bundles.

6.3 Aging of Fiber

NOTE
Fiber material that had previously been heat treated, but may not have had full documentation as provided in the following steps may still be used for final debris size preparation provided a visual inspection of the acceptability of the heat treatment (as described below) is performed and documented within the test plan.

- The fiber shall be aged by heating one side of the insulation on a hot plate at 300°C, ± 38°C for 6 to 8 hours. (Previous testing has shown this temperature and time to be adequate to appropriately age the material.)

  The specific aging procedure is as follows:

  - A batch (sheet) of fiber is placed on the hot plate.
  - A method is provided to periodically monitor plate temperature.
  - The hot plate is energized with the time of starting recorded.
  - When plate temperature reaches the required temperature, the time is recorded (start of 6 to 8 hour heating).
  - After time at temperature, the hot plate is deenergized. This time is recorded.
  - When safe to do so, the insulation material is removed from the hot plate and allowed to cool to near ambient conditions.
  - The insulation is then inspected to ensure the heat treatment was effective. Inspection criteria for acceptance is a gradient of color in the fiberglass from the hot face to approximately half way through the thickness of the insulation sheet commensurate with the temperature gradient through the insulation sheet. (Reference 7.b)
  - The aged fiber is then weighed and placed into labelled bags that identifies the type of fiber, how processed, and the weight.

6.4 Storage of Fiber

The aged insulation is stored in a sheltered location approved by the testing engineer. Each bag is labelled to identify how the debris was processed, the type of debris, the batch number and the lot number, if available.

NOTE
Prior to performance of Step 6.5, if used, the mass of material specified by the test plan shall be obtained as specified in the first two bullets of Step 6.6. Post-soaking weights do not need to be obtained.

6.5 Soaking of Aged Debris (Optional)

As specified by the test plan, the aged debris may be soaked to remove the aging produced particulate matter such as unattached binders and combustion products. This is done by soaking the fibrous debris in a container of water for no less than two minutes and then draining the contents through a Tyler 65 mesh screen (or functional equivalent) to remove small particles and excess water. If used, this step should be accomplished just prior to subsequent steps to prepare the fibers for testing. Long term storage of wetted materials in closed containers should be avoided.

6.6 Preparation of Aged Debris Fines

NOTE
Wetted materials should not be stored for longer than approximately 24 hours prior to use due to the potential for changes to the properties of the material.

- The mass of fiber required by the test plan is identified and this quantity is removed from the bulk aged material through either mechanical means (shears, knife, or equivalent) or by hand separation.
- The removed aged fiber is then weighed and recorded.
- Smaller batches of fiber are then separated from the quantity separated from the bulk quantity by pulling material such that the final volume will result in a fiber to water ratio of ≤ 0.72 lbs/gal (86 gm/l) of water.
- The smaller batches of fiber are then placed in the bottom of a suitable container (typically a cut off section of a plastic barrel) that has been rinsed clean of other materials and contains the required amount of water necessary to maintain the specified fiber volume to water ratio.

NOTE
- Precautions should be taken during the following step to minimize direct impingement of the water jet on the fibers.
- The quantity of water required for the following step is not as important as the ability to verify that the fibers are separated and readily suspendable in the resulting solution.

- Fiber separation is then accomplished by using a high pressure water jet from a commercially available 1500 psi pressure washer with a small diameter fan type tip (recommended), with the nozzle maintained at slightly above or slightly below the water surface. The time necessary to separate the clumps into individual fibers varies, but is generally accomplished within about 2 to 4 minutes.
- The degree of fiber separation is confirmed, by visual inspection, to meet expectations and consistency with previous batches, including meeting the definition of fines provided previously.
- Several batches, prepared as described above for subsequent introduction and use in testing, are then mixed together to create the quantity needed for testing. The batches that are mixed should be combined such that the combined mixture results in a fiber mass to volume of water ratio less than or equal to approximately 0.21 lbs/gal (25 gm/l). The combined materials are then agitated through use of the pressure washer previously described or with other mechanical agitation (paddle or paint stirrer) prior to addition to the test loop. The test plan shall contain the necessary step to verify that minimal agglomeration of the fibers has occurred at the time of addition to the test loop.

6.7 Preparation of Aged Debris Small and Large Pieces

NOTE
Wetted materials should not be stored for longer than approximately 24 hours prior to use due to the potential for changes to the properties of the material.

- The mass of fiber (small or large pieces) for each specific addition is measured and soaked in a sufficient quantity of water in a suitable container, or as specified by the test plan.
- The mixture is then stirred with a hand paddle until the pieces are fully saturated and separated from one another (usually 30 seconds to one minute).
- The degree of fiber clumps separation is confirmed to meet expectations and consistency with previous batches, including meeting the definition of small or large pieces previously provided.

6.8 Photographs of Fibrous Debris

Prior to the fiber addition, photographs of prepared fiber may be taken to confirm that the desired size distribution is acceptable.

6.9 Records

The test plan shall specify the methods to be used for documenting the debris preparation information generated as a result of this document. For fibrous debris preparation, the Datasheet shown in Appendix B is an example of the type of documentation that can be used. The Datasheet records key information such as material processing date(s), reference purchase order number, mass, instruments used, etc.

7. REFERENCES

a. Revised Guidance for Review of Final Licensee Responses to Generic Letter 2004-02, “Potential Impact of Debris Blockage On Emergency Recirculation During Design Basis Accidents at Pressurized-Water Reactors”, March 28, 2008 (ML080230234)
b. NUREG/CR-6808, “Knowledge Base for the Effect of Debris on Pressurized Water Reactor Core Cooling Sump Performance,” February 2003

Appendix A

Safe Handling of Fibrous Materials

Fibrous materials can cause irritation due to contact (see MSDS before handling). In addition, some of the fibers or fiber products produced can be inhaled or ingested which represents a personnel risk unless necessary precautions are taken. Personnel handling this material should wear appropriate PPE, including an appropriate air filtration mask, safety glasses, gloves and long-sleeved clothing to prevent skin irritation. If necessary, a shower should be taken after handling to remove fibers. Care should be taken during processing and handling to minimize airborne fibers.

Appendix B

Example Datasheet for Fibrous Material Preparation

Test Number	Test Date	Mass of Nukon Required (g or lbs)	Mass of Mineral Wool Required (g or lbs)	Mass of Temp-Mat Required (g or lbs)	Mass of XXX Fiber Required (g or lbs)	Weigh Scale Instrument Number	Aged Fiber Batch #	Separation Method	Operator

APPENDIX B

MATERIAL SAFETY DATA SHEET (MSDS)

FOR GREEN SILICON CARBIDE

ELECTRO ABRASIVES CORPORATION
701 Willet Road
Buffalo, NY 14218
Telephone: 716-822-2500
Fax: 716-822-2858
e-mail: info@electroabrasives.com
web-site: www.electroabrasives.com

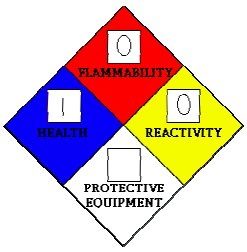

NFPA

HMIS

MATERIAL SAFETY DATA SHEET

Rev 5/12/08

To the purchaser: This MSDS contains important environmental safety and health information for your employees who will be using this product. Please be sure this information is given to them. If you resell this product, a copy of the MSDS should be given to the buyer.

MANUFACTURERS NAME: **Electro Abrasives Corp** PHONE NO: **716-822-2500**
ADDRESS: **701 Willet Road Buffalo New York 14218**

SECTION I

TRADE NAME: **Electrocarb** DOT CLASS ID NUMBER: **N/A**
CHEMICAL & COMMON NAME(S): **Green Silicon Carbide Grain**
FORMULA: **SiC**

SECTION II

OSHA POTENTIAL HAZARDOUS INGREDIENTS		%	EXPOSURE LIMITS		
COMPONENT	CAS #	(optional)	ACGIH-TLV	OSHA PEL	OTHER
SiC	**409-21-2**		**99+**	**10mg/m3**	**15mg/m3 Total Dust**

SECTION III. PHYSICAL DATA

BOILING POINT (deg F)	**N/A**	SPECIFIC GRAVITY (H2O = 1)	**3.2**
VAPOR PRESSURE (mm Hg)	**N/A**	ACIDITY (ph)	**6-7**
VAPOR DENSITY (AIR = 1)	**N/A**	EVAPORATION RATE (BUTL ACETATE = 1	**N/A**
SOLUBILITY IN WATER	**(Negligible)**	MELTING POINT	**SUBLIMES AT 4700 deg F**

VOLATILES BY VOLUME **N/A**

APPEARANCE & ODOR **Shiny, green, granular-odorless material**

SECTION IV. FIRE & EXPLOSION HAZARD DATA

FLASH POINT **N/A** FLAMMABLE LIMITS **:** LEL: **N/A**
DEL: **N/A**

EXTINGUISHING MEDIA: **Not flammable**

SPECIAL FIRE FIGHTING PROCEDURES: **None required**

UNUSUAL FIRE & EXPLOSION HAZARDS: (See Reactivity Section for other physical hazards) **None**

SECTION V. REACTIVITY DATA

STABILITY:	**STABLE**
CONDITIONS TO AVOID:	**NONE**
INCOMPATIBILITY (Materials to Avoid):	**NONE**
HAZARDOUS DECOMPOSITION PRODUCTS:	**NONE**
HAZARDOUS POLYMERSATION:	**WILL NOT OCCUR**

SECTION VI. HEALTH HAZARD DATA

PRIMARY ROUTES OF ENTRY: **NASAL**
LISTED AS CARCINOGEN: **NO**

SYMTOMS AND EFFECTS OF OVEREXPOSURE:
Lung irritation may be evidenced by shortness of breath. Prolonged exposure may lead to pulmonary problems. Avoid dust from Sic 240 mesh & finer.

EMERGENCY AND FIRST AID PROCEDURES:
Remove from dusty area.

SECTION VII. SPILL OR LEAK PROCEDURES

STEPS TO BE TAKEN IN CASE MATERIAL IS RELEASED OR SPILLED:

Uncontaminated material may be scooped up for use.
If Contaminated scoop or vacuum into a receptacle for disposal.

WASTE DISPOSAL METHOD:

Use a sanitary landfill in accordance with local, State, and Federal regulations.

SECTION VIII. RECOMMENDED CONTROL MEASURES

RESPIRATORY PROTECTION: **U.S. Bureau of Mines approved for dusts and pneumoconiosis**.
VENTILATION: LOCAL EXHUAST: **Normal dust collector**.
MECHANICAL (General) : **N/A**
SPECIAL: **N/A**
PROTECTIVE GLOVES: **N/A**. EYE PROTECTION: **Goggles**
OTHER PROTECTIVE EQUIPMENT**: N/A**
SPECIAL PROTECTIVE MEASURES FOR REPAIR AND MAINTENANCE OF CONTAMINATED EQUIPMENT: **N/A**

SECTION IX. SPECIAL PRECAUTIONS

PRECAUTIONS TO BE TAKEN IN HANDLING & STORING (Including appropriate hygienic practices)
Use with commonly accepted industrial safety procedures. Avoid ingestion, inhalation of dust, exposure to eyes or prolonged contact with skin.

APPENDIX C

NUREG/CR-6808, TABLE 3-2

SIZE CLASSIFICATION SCHEME FOR FIBROUS DEBRIS

Table 3-2 Size Classification Scheme for Fibrous Debris[3-2]		
No.	Description	
1		Very small pieces of fiberglass material; “microscopic” fines that appear to be cylinders of varying L/D.
2		Single, flexible strands of fiberglass; essentially acts as a suspending strand.
3		Multiple attached or interwoven strands that exhibit considerable flexibility and that, because of random orientations induced by turbulent drag, can exhibit low settling velocities.
4		Fiber clusters that have more rigidity than Class 3 debris and that react to drag forces as a semi-rigid body.
5		Clumps of fibrous debris that have been noted to sink when saturated with water. Generated by different methods by various researchers but easily created by manual shredding of fiber matting.
6		Larger clumps of fibers lying between Classes 5 and 7.
7	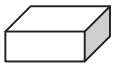	Fragments of fiber that retain some aspects of the original rectangular construction of the fiber matting. Typically precut pieces of a large blanket to simulate moderate-size segments of original blanket.

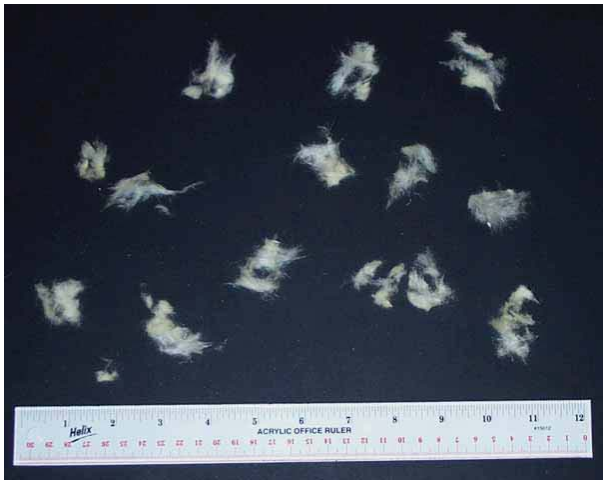

Fiberglass shreds in size Class 3

Fiberglass shreds in size Class 5

Figure 3-3. Fiberglass Insulation Debris of Two Example Size Classes

APPENDIX D

DETAILS AND PHOTOGRAPHS OF DEBRIS PREPARATION PROCEDURES

Appendix D

Images below are intenteded to provided clarification of the fiber debris preparation preparation.

A. Don appropriate PPE which included laboratory jacket, glasses, gloves, and a dust mask.
B. Cut a section of the large fiber blanket provided by PCI, weigh it using scale with 0.01 gram accuracy, and record mass.
C. The section should contain equal portions of the baked (tan) and unbaked (yellow) sections of fiber.
D. The weighed section should be visually separated into baked and unbaked sections.
E. The baked section should be separated again.
F. The unbaked section should be separated again.
G. The separation should result into four equivalent sections of fiber (two baked and two unbaked sections).
H. The fiber section should be cut length wise.
I. The length wise section should be cut to result in approximately 1” X 1” section of fiber.
J. All four sections should be cut as explained by steps H and I.
K. The unbaked 1” X 1” sections should be torn in half by hand again to produce 0.5” X 0.5” sections because it is more difficult to separate the unbaked sections with the pressure washer.
L. The fiber is now ready to be processed either by the blender or pressure washer.
M. Fiber after NEI method.
N. Fiber after blender method.


A

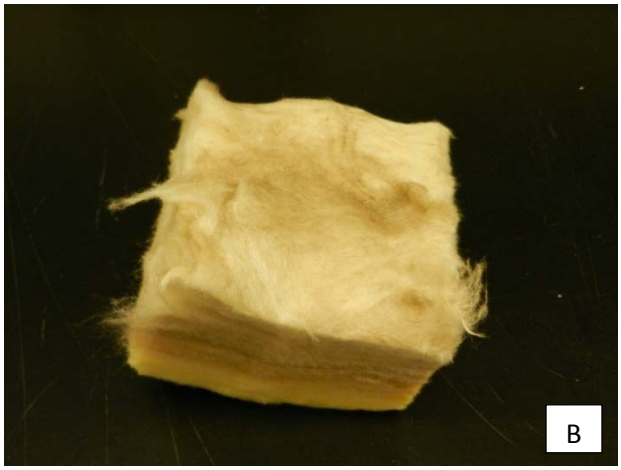
B


C


D

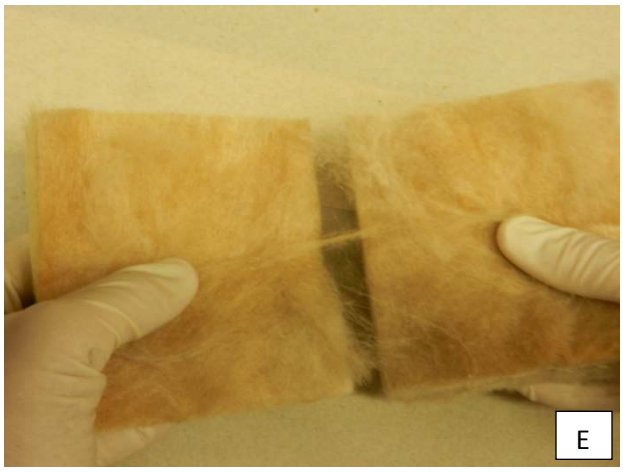
E


F


G


H


I


J


K


L

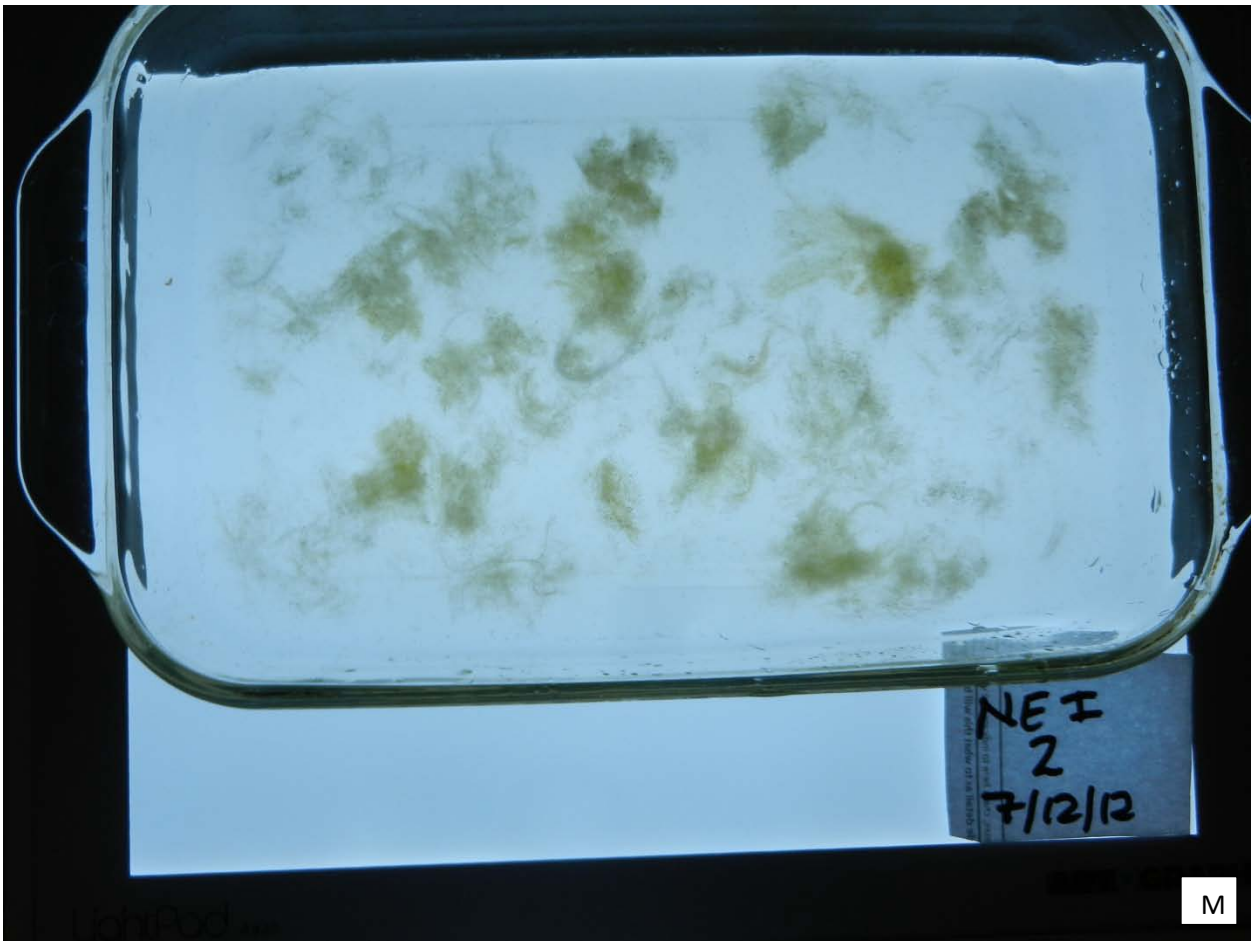
NEI
2
7/12/12
M


N

PROJECT DOCUMENTATION COVER PAGE

Document No: CHLE-010	Revision: 2	Page 1 of 31
Title: CHLE Tank Test Results for Blended and NEI Fiber Beds with Aluminum Addition		
Project: Corrosion/Head Loss Experiment (CHLE) Program		Date: 19 August 2012
Client: South Texas Project Nuclear Operating Company		

Summary/Purpose of Analysis or Calculation:

Corrosion/Head Loss Experiment (CHLE) tests are being performed to support the risk-informed resolution of GSI-191 at the South Texas Project Nuclear Operating Company (STP). This document presents the results of two multi-day tests performed in the CHLE test system (incorporating both the tank and the head loss assemblies) that evaluated methods for preparing the fiber beds for the 30-day tank tests. Two fiber preparation methods were tested: (1) fine chopping of fibers in a blender, and (2) separation of fibers using the NEI pressure-washing method.

To test the response of each fiber preparation method to the presence of chemical products, aluminum nitrate was added very slowly in successive batches over several days. The aluminum nitrate addition began after about 7 days of circulation under fiber only conditions.

Role:	Name:	Signature:	Date:
Prepared by:	Kerry Howe	< signed electronically >	7/23/2012
UNM review:	Janet Leavitt	< signed electronically >	
STP review:	Ernie Kee	< signed electronically >	8/17/2012
Soteria review:	Zahra Mohaghegh	< signed electronically >	8/18/2012

Revision	Date	Description
1	7/23/2012	Draft document for internal review
2	8/19/2012	Addressed internal review comments

Table of Contents

Introduction

The purpose of this report is to describe the results from experiments conducted as part of the Corrosion Head Loss Experimental (CHLE) program. The CHLE tests are being conducted at the University of New Mexico to investigate long-term chemical effects on Emergency Core Cooling System (ECCS) strainer debris beds under prototypical conditions for the South Texas Project in support of the NRC Generic Safety Issue (GSI) 191 risk-informed resolution. Two objectives within the CHLE program are to determine (1) whether or not chemical precipitates can form in the post loss-of-coolant accident (LOCA) environment, and (2) whether any observed products either nucleate directly on or accumulate within prototypical fiberglass debris beds.

An important consideration is that the fiber debris beds that are used in the chemical effect testing be suitable surrogates for debris that would be formed during a LOCA. Attributes that affect the suitability of a particular debris bed design include the stability of the debris bed, the reproducibility of the results, and the ability of the debris bed to participate in chemical interactions under a variety of conditions. Debris beds used in some previous GSI-191 work are not necessarily applicable to the current study for three reasons. First, the approach velocities historically used in head loss testing were more than an order of magnitude higher than the STP strainer design. Second, the historical observations were typically for short periods compared to the CHLE investigations. Third, the Nuclear Energy Institute (NEI) has recently developed a debris preparation method [2] that is believed to be prototypical of debris formed during a LOCA, and most previous head loss testing have used other debris preparation methods. The Nuclear Regulatory Commission (NRC) reviewed the NEI plan and noted it is generically an acceptable way of producing debris, but declined to officially endorse it as the only way to produce acceptable debris because of the dependence on human actions [3].

Two types of fiber bed preparation methods have been evaluated for possible use within the CHLE program. First, the most recent debris formulation advocated by NEI for strainer testing involves baking fiber blankets on one side at 300 °C for 6 to 8 hours, followed by disaggregation with a commercial pressure-washer; this method is referred to as the NEI pressure-washing method in this report. Second, fiber blankets were subjected to the same backing procedure, but were separated by fine chopping of fibers in a blender. A previous report, *CHLE-008: Debris Bed Preparation and Formation Test Results* [1] performed an initial investigation of these debris bed preparation methods with respect the attributes for suitability described above. The experiments described in that report found that the NEI pressure-washing method resulted in more stable and reproducible debris beds than the blended bed method in relatively short (several hour) head loss tests. However, the blended debris beds experienced greater head loss when precipitates prepared according to the WCAP protocol were introduced directly into the head loss assemblies or into the CHLE tank, leading to the perception that the blended fiber debris beds are more sensitive detectors for the presence of precipitates.

The current test results extend the knowledge about the suitability of these debris preparation methods, and provide additional information about the formation of precipitates in the prototypical chemical environment. The tests had two key components. First, the stability and reproducibility of the debris beds were investigated over a longer period (about 7 days) to

evaluate whether the debris beds would be suitable for the long-term CHLE tests, which may be up to 30 days long. This portion of the study was conducted with no corrosion materials in the tank or corrosion products added to the solution. Second, after 7 days of fiber-only operation, aluminum nitrate was slowly injected into the tank to simulate the slow release of aluminum that would occur as the result of corrosion. This aluminum addition method is believed to be a closer surrogate for corrosion product introduction than direct addition of the WCAP formulation.

The key objective for selection of bed morphology in the CHLE program is that the debris type be representative of nominal beds that are likely to accumulate within the spectrum of break sizes; i.e., the bed should not be artificially constructed. The tests described here explore the attributes of two alternative bed preparation methods; both of which might be considered realistic under different recirculation flow regimes, but neither which can alone fully inform the resolution of chemical induced head-loss affects. Therefore, practical considerations regarding test stability for the purpose of studying 30-day chemical behavior is a dominant concern for the selection of a debris preparation protocol. Head loss through debris beds involves a wide variety of physical phenomena. These phenomena include initial debris size, fiber separation, and fiber fracture, prototypical debris transport, and accumulation. None of these factors affects the chemical behavior of fiberglass in the system, but all of these factors affect the degree of head loss that can be experienced at the strainer. Issues like particulate to fiber ratio, maximum bed thickness, thin bed formation under quiescent flow conditions, etc. will be studied systematically in the vertical head-loss test series.

The testing program was conducted from 28 June 2012 to 24 July 2012. Throughout the tests, the chemical system in the tank was prototypical of the post-LOCA chemical environment at STP; the chemicals included boric acid, trisodium phosphate, lithium hydroxide, hydrochloric acid, and nitric acid. The support screen use was prototypical of the ECCS strainers at the STP plant. A temperature profile characteristic of a medium-break LOCA as predicted by MELCOR and RELAP-5 was used. The approach velocity to the debris beds was 0.01 ft/s to be consistent with the strainers at STP.

The results of this series of tests are summarized in the next section, and detailed results of the tests are presented after that.

Summary of Results

The following conclusions can be drawn from this test series:

- The fiber beds prepared with blending in a blender were not reproducible between columns. After 6 days of operation, the head loss varied from 1.2 inches of water to 61 inches of water through debris beds that were circulating the same water at the same rate (see Figure 1).
- The fiber beds prepared with the blended preparation method formed small, dense nodules of fiber at the base of the fiber bed, immediately adjacent to the perforated support plate. The nodules formed a dimple pattern that matched the pattern of holes in

the perforated plate, indicating that the smaller fibers formed by the blending process were able to form a more dense fiber mat in a localized area (see Figure 14).

- The difference in head loss among the three columns with the blended fiber preparation appears to be due to a trace amount of dirt or other material that collected in the small, dense fiber nodules at the base of the fiber bed. The debris bed with the highest head loss visually had the greatest amount of darker material present in the nodules. The fiber beds were visibly clean through the rest of the depth, suggesting that little or no head loss occurred through the bulk of the depth of the fiber bed and that nearly all of the head loss occurred in the fiber where it contacted the perforated plate, indicating significant nonhomogeneity to the head loss characteristics of the bed (see Figure 14).
- The fiber beds prepared with the NEI pressure-washing method were reproducible between columns. After 6 days of operation, the head loss varied from 0.36 inches of water to 0.48 inches of water through debris beds that were circulating the same water at the same rate (see Figure 2). Similar behavior continued until the test was terminated after 12 days.
- The fiber beds prepared with the NEI pressure-washing method did not form the dense nodules of fiber that were observed with the blended fiber beds (see Figure 15). The absence of these nodules and the reproducible behavior of the NEI beds lends further credibility to the conclusion that these nodules were responsible for the non-reproducible behavior of the blended fiber beds.
- The blended fiber preparation method resulted in shorter fibers (often called “shards” or “fragments”) than with the NEI pressure-washing method (see Figure 9 and Table 1), which may have led to the ability of the bed to form the dense nodules at the holes in the perforated plate. The shorter fibers led to a more compact debris bed (see Figure 10). Low porosity nodules are formed by local bed compaction, enabled by the mobility of short fiber shards formed during the chopping procedure. Local compaction in regions of flow acceleration near the strainer penetrations is further enabled by loosely aggregated beds formed under very low approach velocity.
- The debris beds did not change thickness significantly over the course of the test, which lasted over 8 days for the blended fiber debris bed and over 12 days for the NEI fiber debris bed (see Figures 11 and 12). Further, minimal differences in thickness were observed between beds despite the wide variation in measured pressure loss. The lack of change in bed thickness, coupled with the visually clean nature of the debris beds, lends credibility to the conclusion that the head loss associated with the blended fiber debris bed was due to localized conditions at the perforated plate.
- Turbidity was an excellent indicator of the precipitation of aluminum hydroxide precipitates in solution (see Figure 22, 23, and 24).
- Essentially all of the aluminum that was added to solution formed a precipitate, as indicated by turbidity measurement and supported by total and filtered aluminum analyses.
- The addition of 1 mg/L of aluminum in solution caused the formation of in-situ precipitates that caused head loss through the blended fiber debris beds. An additional 5 mg/L (6 mg/L total) caused sufficient head loss to terminate the test (see Figure 29).
- Aluminum in solution in the form of pre-formed WCAP precipitates also caused head loss sufficient to terminate a similar blended fiber debris bed test (see Figure 30).

- The addition of up to 40 mg/L of aluminum over a period of 6 days was not sufficient to cause head loss through the NEI fiber debris beds (see Figure 31). However, the same amount of aluminum in the form of pre-formed WCAP precipitates caused extensive head loss that terminated a similar test within 3 hours (see Figure 32). These results indicate that precipitates formed in-situ through the addition of aluminum nitrate at a slow rate have significantly different characteristics from those of the pre-formed WCAP precipitates.
- Particle size analyses indicate that the size of precipitates formed in-situ are up to 10 times smaller than the pre-formed WCAP precipitates with similar solution conditions (0.17 µm versus 1.6 µm in diameter, see Table 2). This significant difference in size appears to be sufficient to cause the pre-formed WCAP precipitates to be retained by the NEI fiber debris beds but allow the in-situ precipitates to pass through the NEI fiber debris beds. The results indicate that head loss may be less significant than indicated by the use of pre-formed WCAP precipitates, depending on the filtration characteristics of the debris bed.
- Zeta potential analyses indicate that solution chemistry affects the surface charge of pre-formed WCAP precipitates. When tests were conducted in deionized water, pre-formed WCAP precipitates had a positive zeta potential. When tests were conducted in Albuquerque tap water, the pre-formed WCAP precipitates were nearly neutral. When tests were conducted in water containing boric acid and TSP, the precipitates had a significant negative charge. The reversal of charge depending on solution chemistry suggests that head loss testing using pre-formed WCAP precipitates may not adequately predict the extent of head loss through a strainer under conditions in which debris beds are not reliant on physical sieving for the retention of particles.
- Despite the slow introduction of aluminum nitrate, corrosion conditions were not perfectly emulated. It is possible that conditions that minimize aluminum release, such as the passivation of aluminum surfaces or the formation of a low-solubility oxide layer, would result in an upper limit to the aluminum concentration measured in solution. In addition, saturation conditions relevant for direct nucleation of precipitation products within the fiber bed may have been artificially exceeded. If direct nucleation is a credible formation mechanism, then the tests reported here best describe the filtration behavior between the two preparation methods and not necessarily the in-situ head-loss sensitivity. Direct nucleation would avoid the complications of particle filtration, perhaps leading to different head loss response in the debris beds. As a result, additional tests that investigate precipitate formation under prototypical corrosion conditions are needed.

The following sections of this report provide detailed results from the experiments. Individual sections are presented on (1) head loss, (2) approach velocity, (3) temperature, (4) bed formation and morphology, (5) water chemistry, and (6) effect of aluminum addition. Following those sections, overall conclusions of this test series are presented.

Head Loss through Fiberglass Debris Beds

The primary diagnostic parameter monitored during these tests was the head loss through the fiberglass debris beds. The head loss through the two types of debris beds differed from each other as displayed in Figures 1 and 2. For the blender-chopped bed, the head losses through the

three beds were relatively similar to each other during the initial period of operation. The head losses through beds 1, 2, and 3 were 0.6, 0.6, and 0.9 inches of water column after 90 minutes of operation, respectively, and 0.6, 0.6, and 1.0 inches of water after 5 hours of operation, respectively. As time progressed, the head losses through the beds deviated more. After 1 day of operation, the head losses through beds 1, 2, and 3 were 0.7, 1.4, and 6.2 inches of water, respectively. After 6 days of operation, the head losses through beds 1, 2, and 3 had stabilized at 1.2, 21, and 61 inches of water, respectively, a 50-fold difference between beds 1 and 3.

Head loss depends on characteristics of the debris bed and the fluid passing through the bed. Changing water temperature causes changes in fluid viscosity and density that changes the measured head loss. To isolate changes in head loss due to changes in bed morphology independently of the changes in fluid viscosity and density, the head loss data can be corrected to a constant temperature. The head loss data was corrected for viscosity by applying the ratio of water viscosity at the measured and standard temperatures, and corrected for density by calculating the change in static head between pressure taps due to the decreasing fluid density at higher temperature. In Figures 1 and 2, the head loss data have been corrected to a temperature of 104 °F (40 °C), which is the approximate temperature at the end of each of the tests.

The debris beds prepared with the NEI pressure-washing protocol were more consistent with one another and more consistent over time. Column 3 started with less head loss than did the other columns, but after less than 1 day of operation, the head loss of column 3 had increased to be similar to that of the other columns. After 5 hours of operation, the head losses through beds 1, 2, and 3 were 0.64, 1.0, and 0.41 inches, respectively. After 6 days of operation, the head losses through beds 1, 2, and 3 were 0.42, 0.36, and 0.48 inches, respectively. The similar behavior between columns continued until the test was terminated after 12 days.

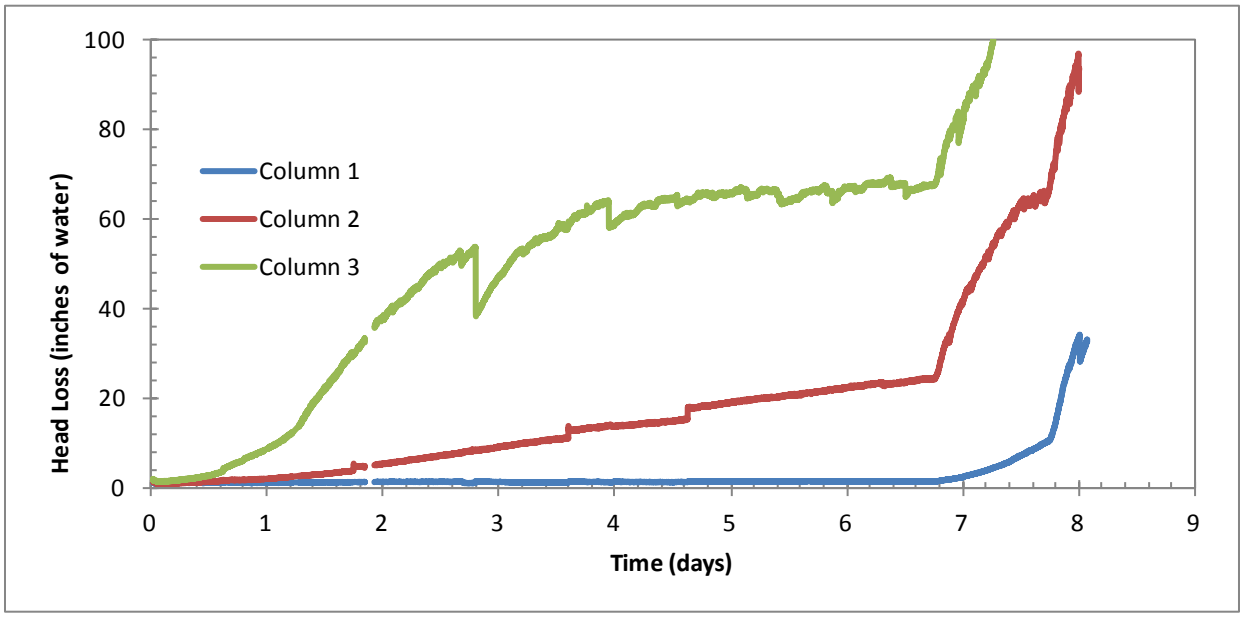

Figure 1: Temperature-corrected head loss through fiberglass debris beds prepared by chopping in a blender (corrected to 104 °F). Aluminum nitrate addition started at about 6.75 days.

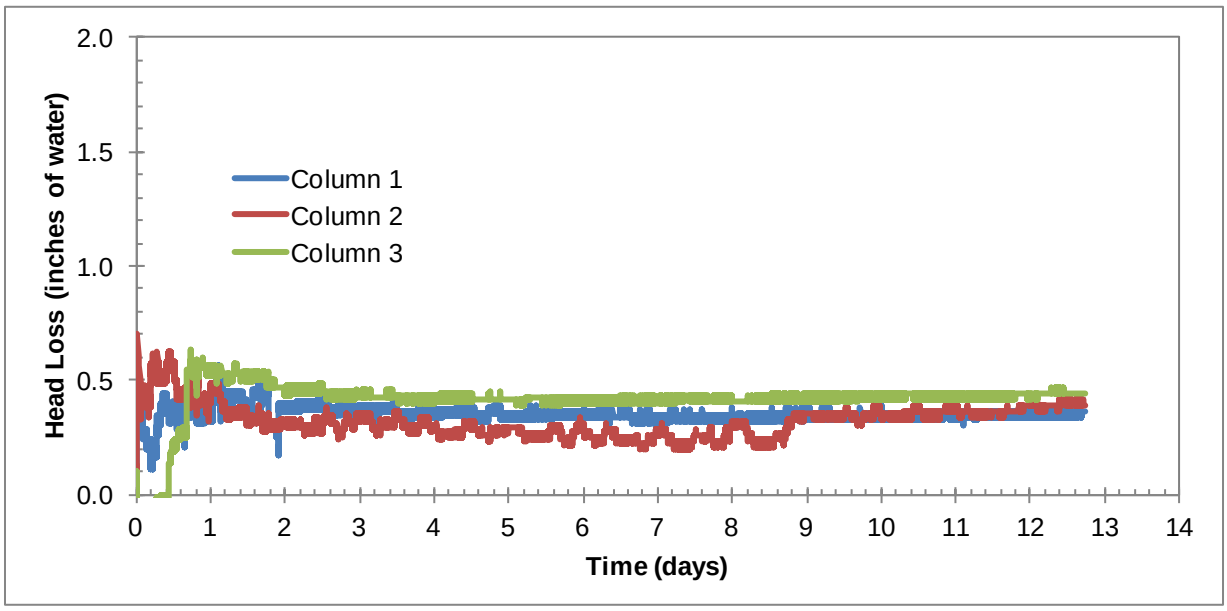

Figure 2: Temperature-corrected head loss through fiberglass debris beds prepared using the NEI pressure-washing method (corrected to 104 °F).

Approach Velocity through Fiberglass Debris Beds

The approach velocity was maintained near 0.01 ft/s in all three columns for both tests. Approach velocity was adjusted by throttling a valve on the discharge side of centrifugal pumps that fed each column independently of the others. The approach velocities are displayed in Figures 3 and 4. The throttle valves required occasional adjustment to maintain the desired 0.01 ft/s approach velocity during the first several days of each test, but little or no adjustment was required later in the tests. Overall, Figures 3 and 4 show that the velocity through the debris beds was maintained at acceptable velocities over the duration of each test.

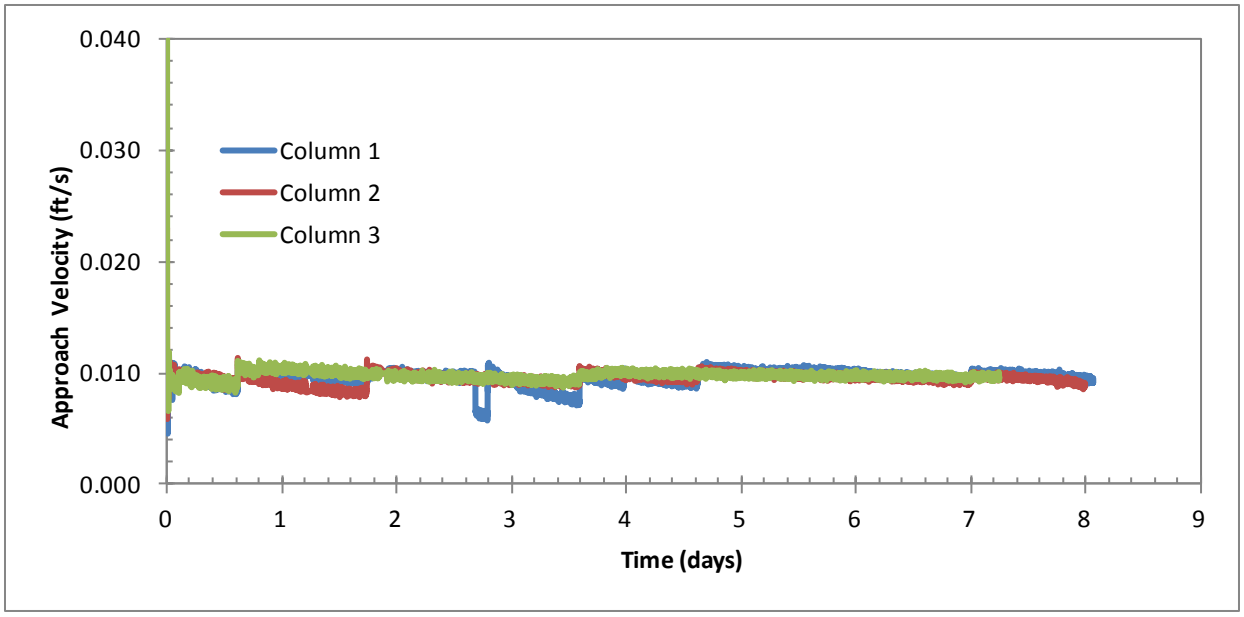

Figure 3: Superficial filtration velocity through fiberglass debris beds prepared using the blending method.

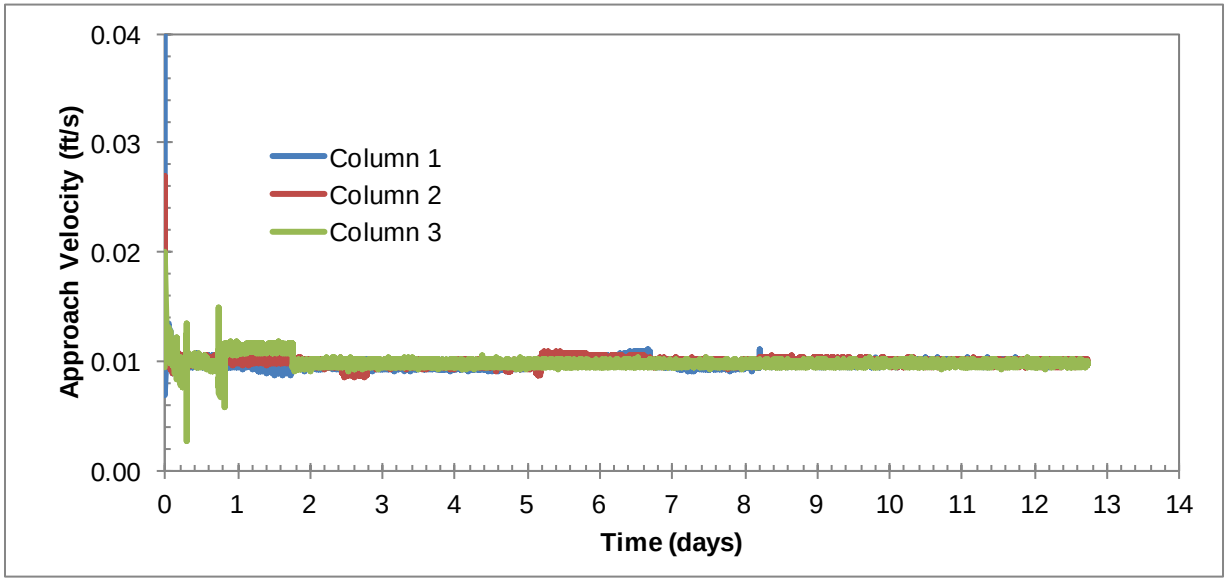

Figure 4: Superficial filtration velocity through fiberglass debris beds prepared using the NEI pressure-washing method.

Temperature

Temperature Profile over Time

The temperature during each test was designed to decline over time to reflect the temperature present in the containment building following a LOCA. The temperature in these tests was modeled to emulate a break of a 6-inch pipe in containment at STP (a medium break LOCA). The target temperature profile was generated by running the MELCOR/RELAP-5 computer simulations at Texas A&M University. The predicted temperature started at about 185 °F (85 °C) and declined rapidly in the first few minutes as the leaked water came in contact with concrete and other surfaces. The temperature then increased over several hours as materials within the containment building heated up, reaching a temperature of 162 °F (72 °C) about 4 hours into the event. The CHLE temperature control system was designed to provide a more gradual decline to this temperature after 4 hours, and then to track the temperature predicted by MELCOR/RELAP-5 for the remainder of the experiment. The temperature profiles are shown in Figures 5 and 6.

During the test with the fiber beds prepared by the blending method, the temperature dropped rapidly to 162 °F (72 °C) after 4 hours into the test, but was followed by a period of constant temperature because of the failure of a temperature controller to initialize overnight. The temperature was reduced to be in compliance with the desired temperature profile before the end of the first day, and remained within 5 °F (2.8 °C) of the desired temperature until the final day of the test. The measured temperature exhibited a sawtooth pattern because the temperature controller tended to overshoot the target temperature. The increase in temperature ranged from 1.3 to 1.6 °F (0.7 to 0.9 °C) between a low-temperature reading and the next high-temperature point. Toward the end of the test, an attempt was made to adjust the deadband on the temperature controller, but the amount of overshooting increased slightly.

The operation of the temperature controller was improved for the test with the NEI pressure-washed fiber, as presented in Figure 6. The measured temperature was consistently within about 1.8 °F (1 °C) of the target temperature throughout the duration of the test and without the overshooting of the controller that had been exhibited in the test with the blended fiber.

Temperature Variation in Tank

The temperature was measured at four locations within the CHLE tank: three in the pool and one in the vapor space. The three locations in the pool consisted of a point near the center and two points in corners of the tank. The average temperature in corners was within 0.2 °F (0.1 °C) of the temperature in the center of the tank, indicating that the thermal conditions within the tank were uniform. The comparison between the temperature in the vapor space and in the center of the pool is shown in Figure 7. In general, the temperature in the vapor space was 4 to 5 °F (2.2 to 2.8 °C) lower than the temperature in the center of the pool.

Temperature Differential in Head Loss Columns

The temperature was also measured continuously in each head loss column about 6 inches above the debris screen. Initially, the temperature in the columns was somewhat lower than the

temperature in the tank because of heat loss in the connecting piping and in the columns. The difference in temperature between the center of the tank and column 1 is shown in Figure 8. The other columns are not shown because their results are virtually identical to column 1. At the beginning of the test, the temperature in the columns was about 1.8 °F (1 °C) lower than in the tank. But as the tank temperature decreased, the temperature difference between the tank and columns decreased. After 6 days, when the temperature in the tank had dropped to about 113 °F (45 °C), the temperature in the columns had converged to that in the tank.

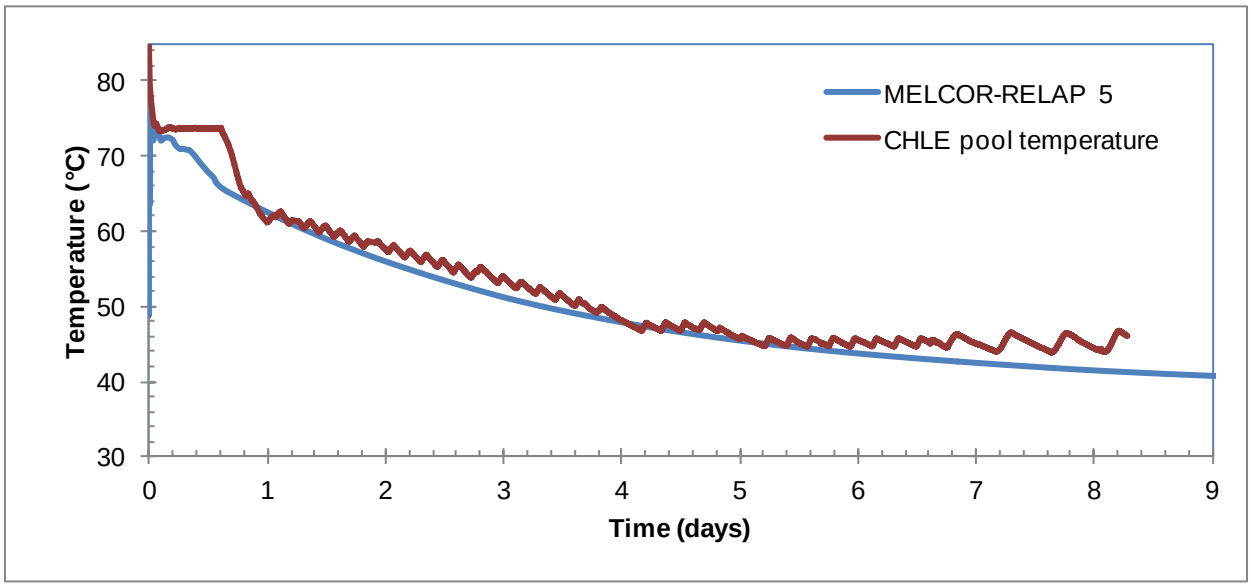

Figure 5: Tank temperature during the experiment using fiberglass debris beds prepared using the blending method.

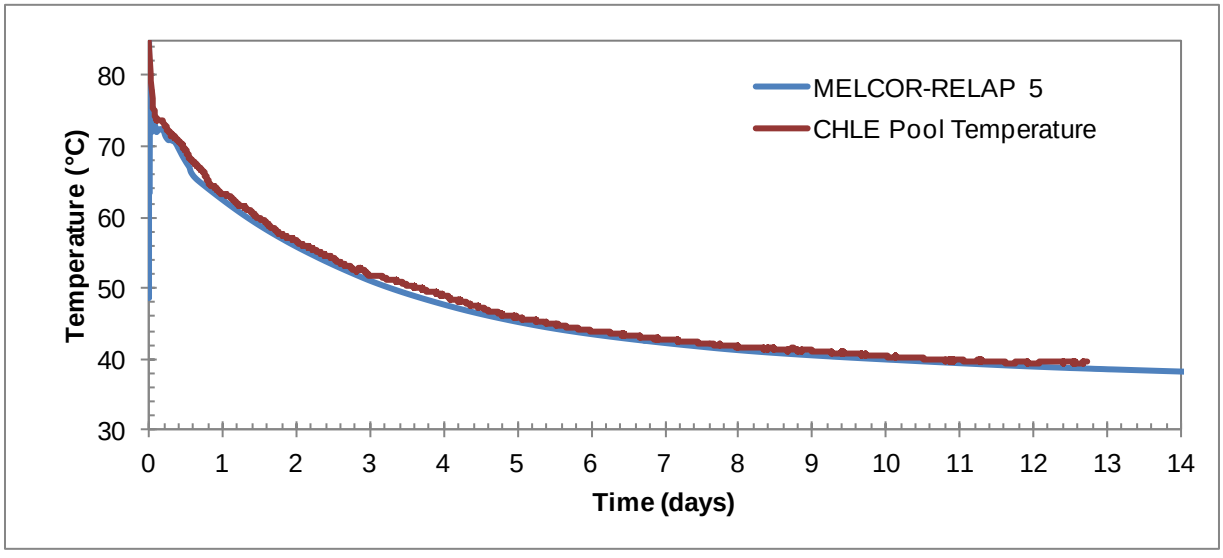

Figure 6: Tank temperature during the experiment using fiberglass debris beds prepared using the NEI pressure-washing method.

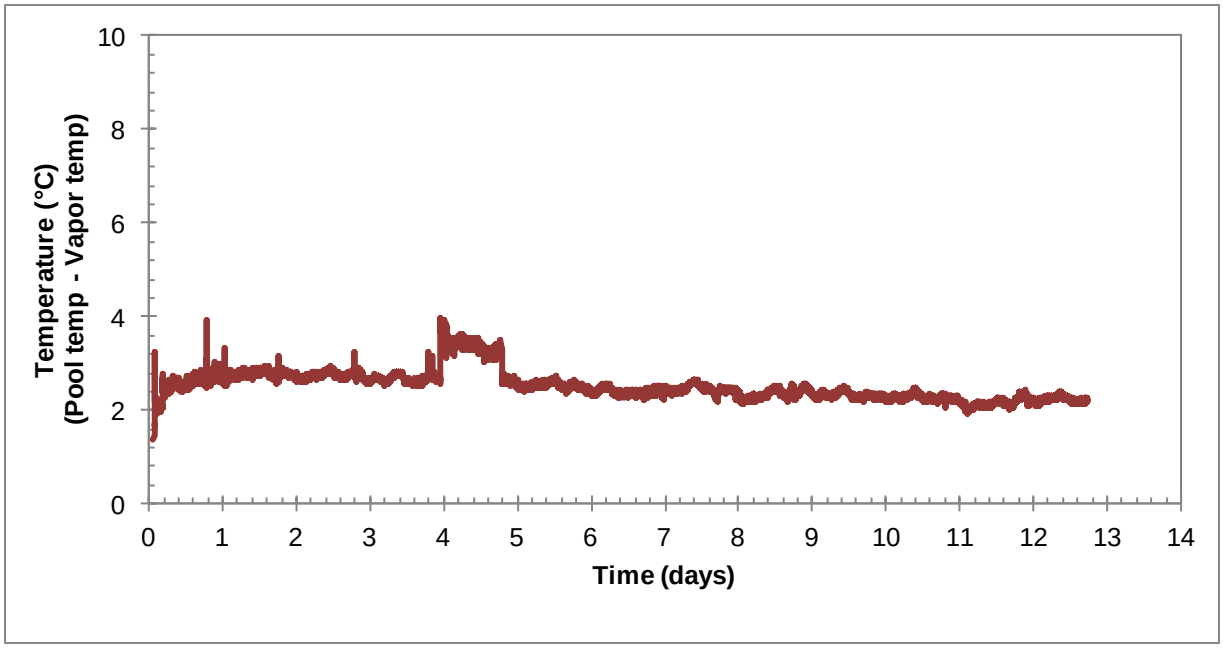

Figure 7: Difference between the pool temperature and the vapor-space temperature in the tank during the experiment using fiberglass debris beds prepared using the NEI pressure-washing method.

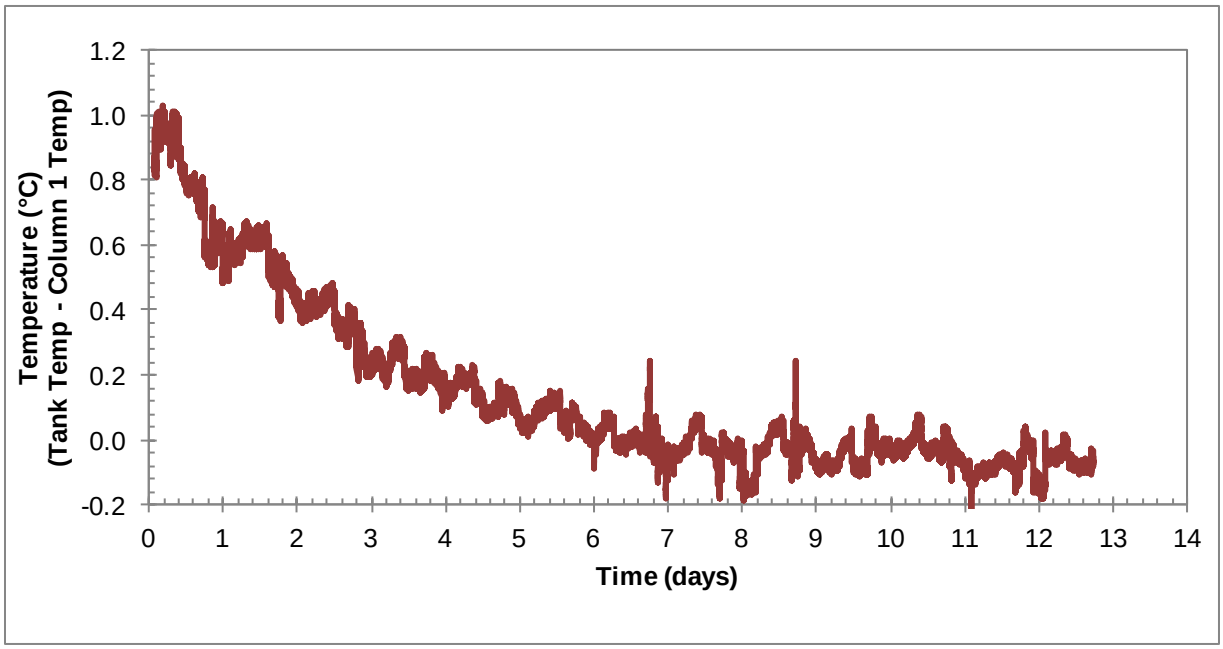

Figure 8: Difference between the pool temperature and the temperature in Column 1 just above the debris bed during the experiment using fiberglass debris beds prepared using the NEI pressure-washing method.

Bed Formation and Morphology

The difference in fiber preparation resulted in variability in the characteristics of the fibers and how they formed debris beds. The difference in fiber preparation was evident when the debris was examined on a light table, as shown in Figure 9. The photographs in Figure 9 show the contents of a 8 x 13 inch glass pan. The blended fiber preparation consisted almost entirely of individual fibers with few or no clumps. The NEI fiber preparation contained more loose clumps of fibers. In addition, the blended fiber method resulted in visually shorter fiber lengths. The visual difference in fiber length was corroborated with data on fiber length generated by IPS Testing Services, a company that measures fiber length for the paper industry [4]. IPS tested samples of fiber prepared by the two methods and reported the data in Table 1. Sixty-two percent of the blended fibers were less than 0.5 mm, but only 44% of the NEI fibers were. The measurement system could not detect the length of fibers that were less than 0.2 mm, which included 21 percent of the blended fibers and 13 percent of the fibers from the NEI preparation. IPS reported NEI fibers up to 7 mm in length, but only a maximum of 3 mm for the blended fibers.

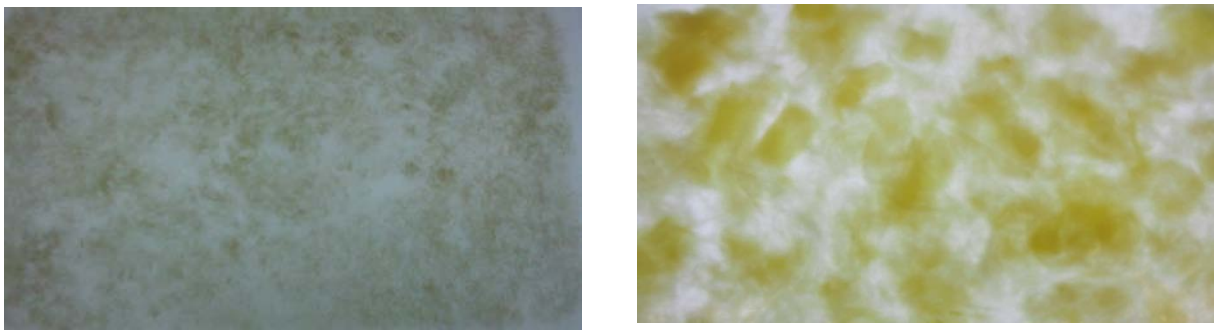

A **B**

Figure 9: Examination of debris on a light table from (A) blended fiber preparation, and (B) NEI pressure-washed fiber preparation.

Table 1: Fiber Length of the Debris Prepared by Blended and NEI Preparation Methods

	Blended preparation (% of fibers)	NEI pressure-washed preparation (% of fibers)
< 0.5 mm	62	44
0.51 to 1.0 mm	18	24
> 1.0 mm	13	32

The difference in fiber preparation was also evident when the debris was placed in the head loss columns, as shown in Figure 10. The beds were formed with the same approach velocity in both tests, 0.1 ft/s. The blended fiber preparation shown in Figure 10A had an initial bed thickness of about 0.6 inches (1.5 cm), but the NEI pressure-washed fiber preparation shown in Figure 10B had an initial overall bed thickness of about 2.6 inches (6.5 cm), even though both types of fiber beds contained the same amount of fiber on a mass basis (18 grams). These thicknesses

correspond to an in-place initial density of 4.0 lb/ft^3 for the blended fiber beds and 0.9 lb/ft^3 for the pressure-washed fiber beds.

For each type of fiber preparation, the beds in the three head loss columns were fairly consistent with each other. For the blended fiber preparation, the thickness of the bed in each column was slightly different, with Column 1 having the thickest bed and Column 3 having the thinnest bed. The trend in thickness is consistent with the trend in accumulated head loss at the end of the test (i.e., Column 3 had the thinnest bed and the highest head loss). However, the differences were minor, as shown in Figure 11. Furthermore, the thickness of the debris beds did not change significantly over the duration of the test, even though the head loss changed dramatically for Columns 2 and 3, as noted earlier. The change in head loss over the duration of the tests cannot be attributed to the change in bed thickness, given that head loss is expected to vary linearly with bed thickness for a perfectly homogeneous debris configuration.

Similarly, the debris beds formed of NEI pressure-washed debris in the three columns were similar in overall thickness, but Column 2 had the thickest bed, followed by Columns 1 and 3, as shown in Figure 12. The top surface of the NEI pressure-washed debris beds was less uniform than for the blended fiber beds. The NEI pressure-washed debris beds were thicker in the center of the column and somewhat thinner at the edges where the debris bed touched the column wall.

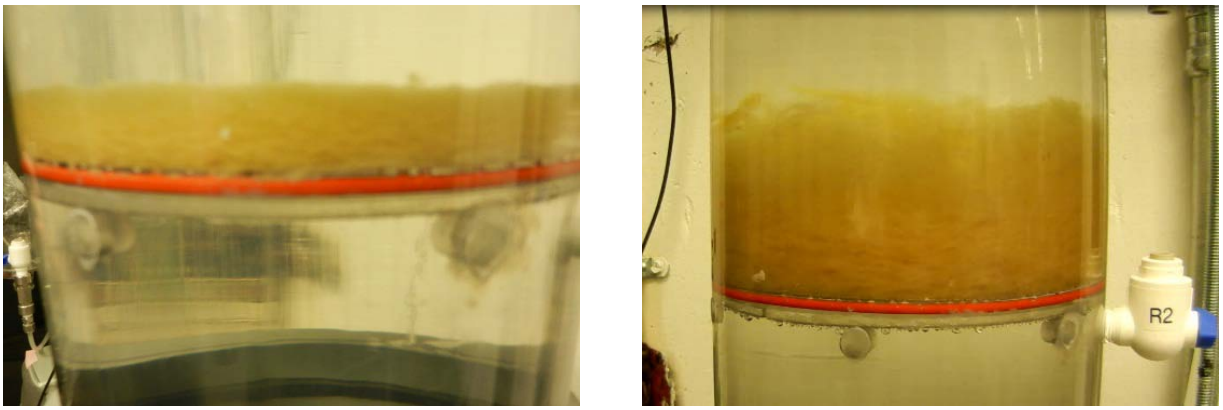

A **B**

Figure 10: Debris beds in head loss columns at the beginning of test operation. (A) Column 2 blended fiber debris bed and (B) Column 2 NEI pressure-washed fiber debris bed.

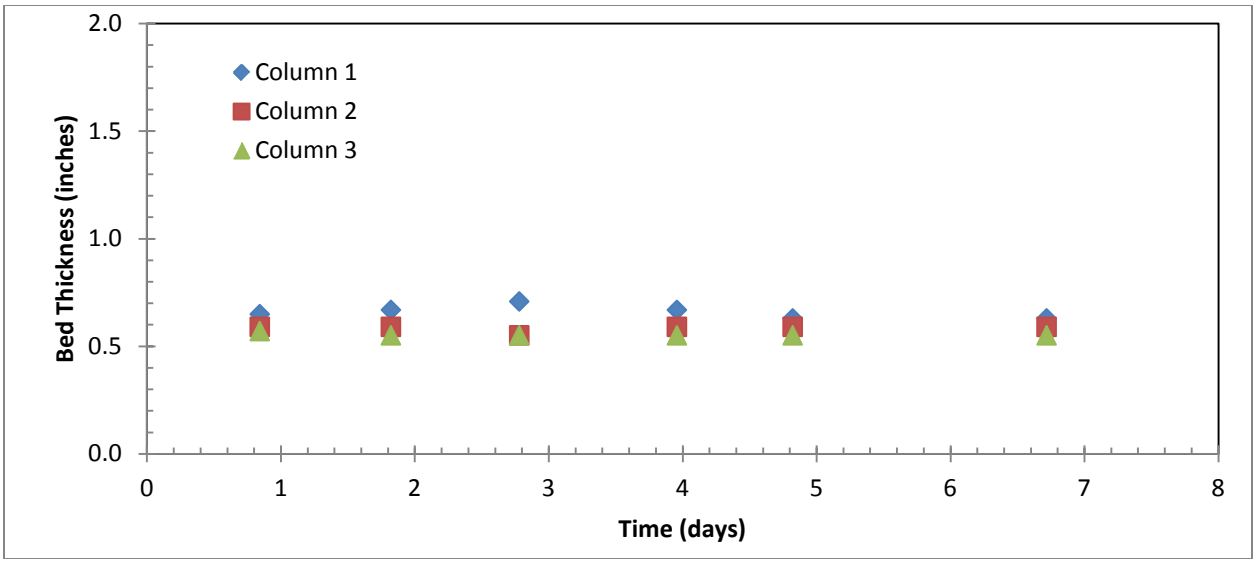

Figure 11: Thickness of blended fiber debris beds in head loss columns.

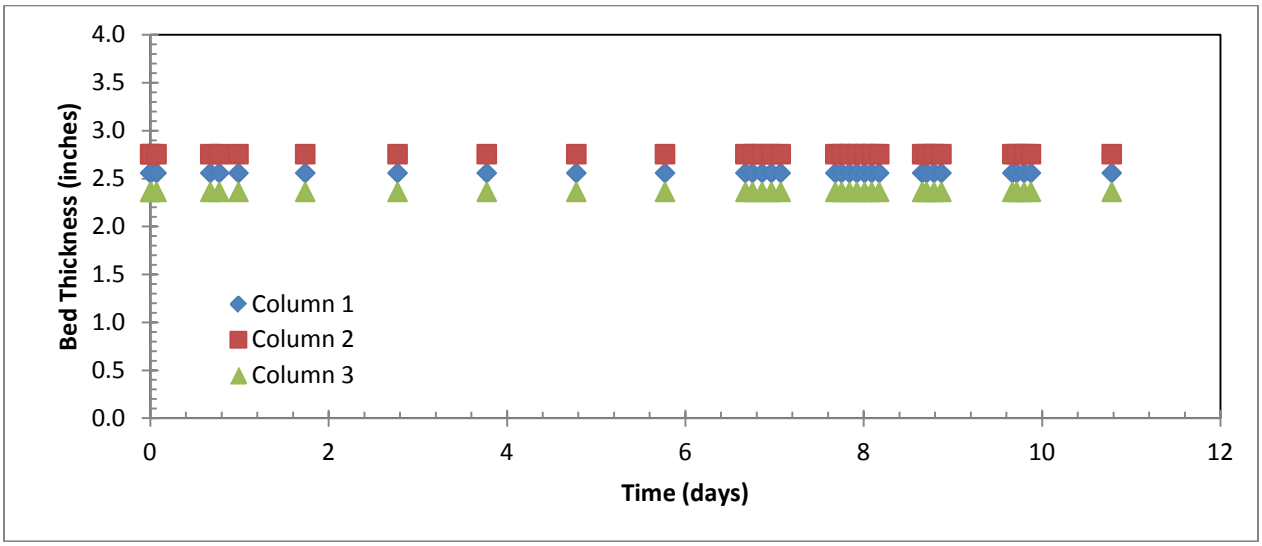

Figure 12: Thickness of NEI pressure-washed fiber debris beds in head loss columns.

Differences were also observed when the tests were complete and the debris beds were removed from the head loss columns. The blended fiber debris beds compressed slightly when water was removed from the column, from a thickness of about 0.6 inches (1.5 cm) to 0.4 inches (1 cm). After water was removed, water droplets falling from the inside of the column formed craters on the otherwise uniform surface of the blended fiber beds, as shown in Figure 13, indicating that the surface of the bed was soft and pliant.

As water was drained from the columns, the NEI pressure-washed debris beds collapsed more significantly, from about 2.6 inches (6.6 cm) to 0.8 inches (2 cm) in thickness. The surface of the NEI debris beds was much rougher and less uniform after being removed from the column, as shown in Figure 13C.

A **B** **C**

Figure 13: Photographs of the debris beds after the tests were complete. (A) Column 2 blended fiber debris bed in column after water was drained and clear section was removed from the test assembly (craters are from falling water droplets). (B) Column 2 blended fiber debris bed after being removed from column. (C) Column 1 NEI pressure-washed debris bed after being removed from column.

After being removed from the head loss columns, the debris beds were stored in a dark refrigerated room at 4 °C until they could be examined in detail. For the blended debris beds, visual examination indicated the blended fiber beds to have a uniform, flat top surface. The craters from the water droplets in the bed from Column 3 appeared to have filled in over time and were less prominent than they had been when the bed was removed from the column. In all beds, the fibers were tightly packed so that the surface of the bed appeared similar to a piece of felt material. Individual fibers were not readily visible. Examination with a 16x magnification lens (Loupe) did not provide a significantly different view of the bed surfaces.

When a portion of the bed was torn from the surface and rubbed between two fingers, it stayed as an intact mat of fibers. However, the debris beds were easily torn and exhibited very little resistance when pulled apart by hand. The debris beds were cut vertically with a scissors, and the cross-section of the bed appeared uniform from top to bottom, also visibly similar to a piece of felt.

The most significant feature of the blended debris beds appeared at the bottom of the bed, where the debris bed was in contact with the perforated support plate. When the debris beds were peeled from the support plate, they exhibited nodules of fiber in a dimple pattern identical to the holes in the support plate. The bottom of the bed of all three columns with blended fiber preparation are shown in Figure 14. The texture of the nodules was significantly different from that of the fiber at the top or center of the debris bed. When rubbed between two fingers, the nodules were hard, almost as if a rock were embedded in the debris bed. When a nodule was pulled apart by hand, however, it offered no physical resistance and separated easily into a small mass of fibers with no evident larger solid materials. Visually, the nodules in bed 3 were darker than in bed 2, which were subsequently darker than in bed 1. The color might indicate that another material such as dirt was retained in the localized area of the fiber immediately at the perforated screen holding the debris beds. The debris beds appeared clean throughout their depth, as evidenced in the cross-section of the beds shown in Figure 14. The difference in the retention of dirt in the fiber at the perforated plate may have been the cause of the difference in

head loss among the three columns, being that the trend in color is consistent with the trend in head loss (darker color corresponding to greater head loss).

The dimple pattern evident at the bottom of the blended beds was barely evident on the NEI pressure-washed beds, as shown in Figure 15. These images indicate that the longer fibers present in the pressure-washed beds spanned the holes of the perforated screen differently, leading to different hydraulic conditions in the immediate vicinity of the support screen. The difference in fiber bed characteristics at the support screens appears to be a significant cause of the difference in head loss among the three columns for the blended fiber beds and between the blended fiber and pressure-washed columns.

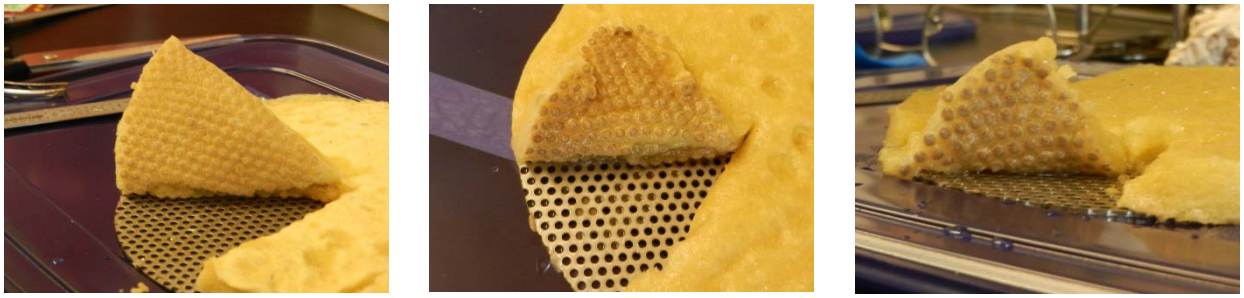

A **B** **C**

Figure 14: Dimple pattern from the support plate on the bottom side of the blended fiber debris beds in (A) Column 1, (B) Column 2, and (C) Column 3. The dimples in Column 3 are darker than in Column 1. Also, the cross section of the debris bed, most evident on Column 3, appears clean throughout the entire depth of the debris bed.

A **B** **C**

Figure 15: Bottom side of the NEI pressure-washed fiber debris beds in (A) Column 1, (B) Column 2, and (C) Column 3.

Water Chemistry

pH

The pH in the tank solution was measured using both an on-line pH probe and grab samples measured with a tabletop laboratory pH meter. The on-line probe was more difficult to calibrate than the laboratory pH meter and could not be calibrated while a test was in progress whereas the laboratory pH meter could be calibrated. The pH measurements by both the in-line probe and the laboratory pH meter are shown in Figure 16 for the blended fiber test and Figure 17 for the NEI fiber test. During the blended fiber test, the average pH was 7.35 using the on-line pH probe and 7.18 using the laboratory pH meter. The laboratory pH meter was calibrated each time it was used and was closer to the expected pH value of 7.2 based on calculations of the chemicals in the solution. The on-line probe was replaced with a new probe before the NEI test started. For the NEI fiber test, the average pH value was 7.13 using the on-line probe and 7.23 using the laboratory pH meter. Again, the laboratory pH meter was closer to the expected pH value of 7.2.

Calcium and Silica

Calcium and silica were measured in the pool solution, along with the aluminum. The calcium results are shown in Figure 18 for the blended fiber beds and Figure 19 for the NEI fiber beds. The calcium concentration was fairly constant with time in both tests. In the blended fiber test, the calcium concentration was about 1.5 mg/L but in the NEI fiber test was somewhat higher, about 2.0 to 2.2 mg/L.

The silica results are shown in Figure 20 for the blended fiber beds and Figure 21 for the NEI fiber beds. The results were similar in both tests, starting at about 2.5 mg/L (after the TSP had been added to the tank and the solution had been circulating through the head loss columns for about 90 minutes) and gradually rising over a period of several days to a concentration of about 4.0 mg/L, where it stayed for the remainder of the tests.

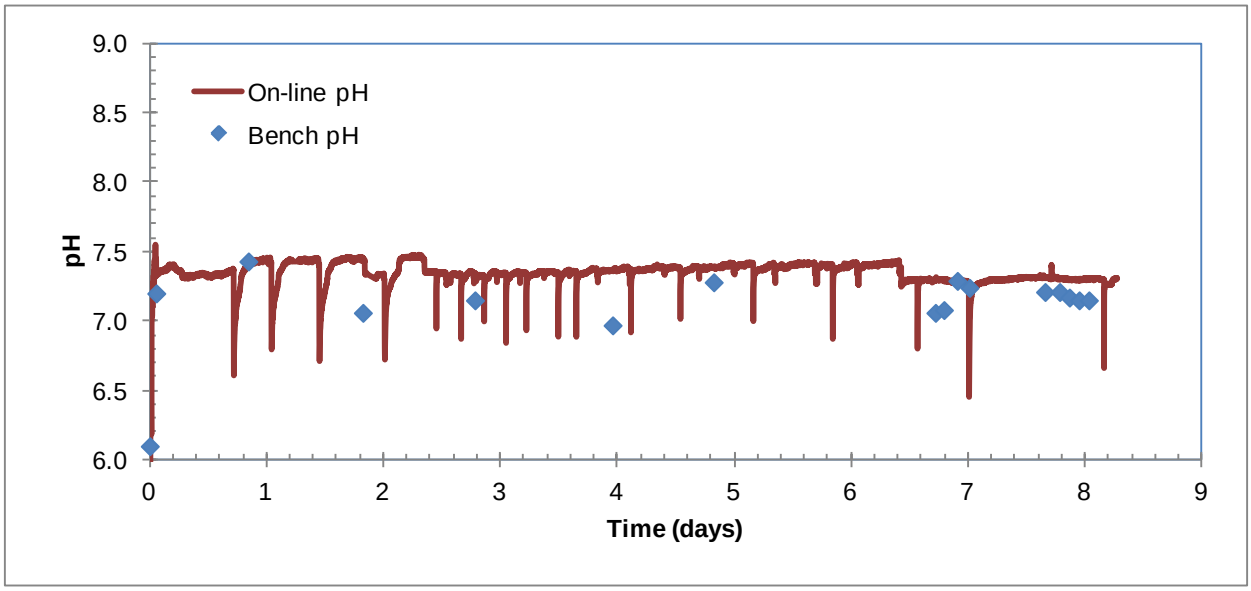

Figure 16: pH during the blended fiber test.

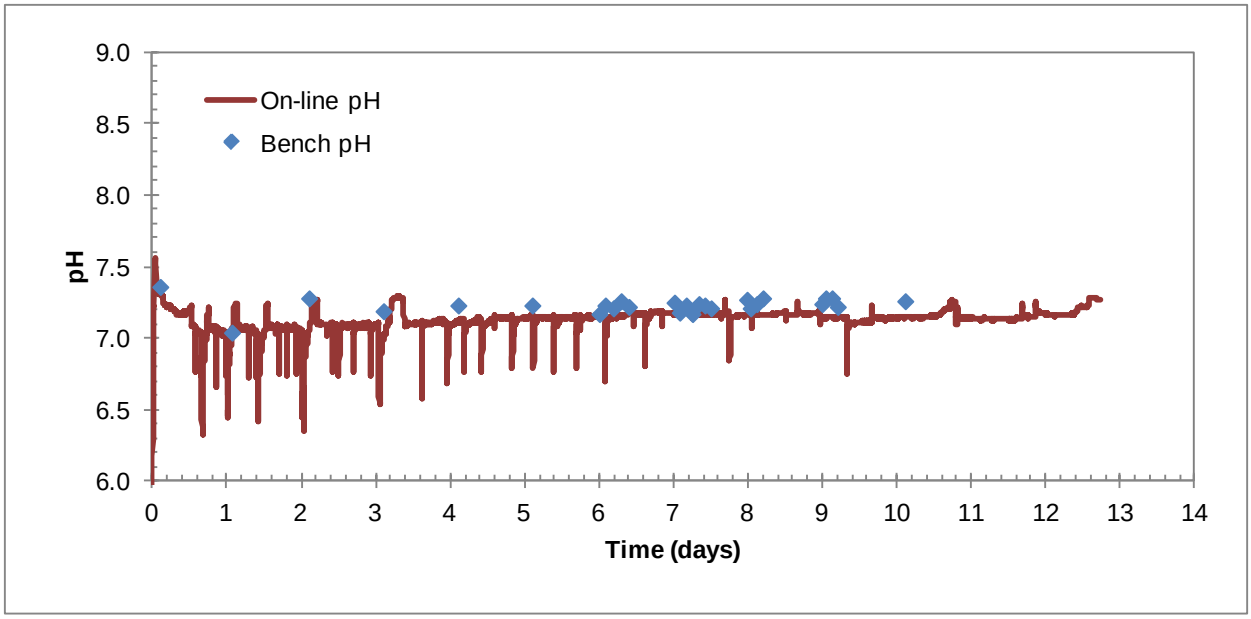

Figure 17: pH during the NEI fiber test.

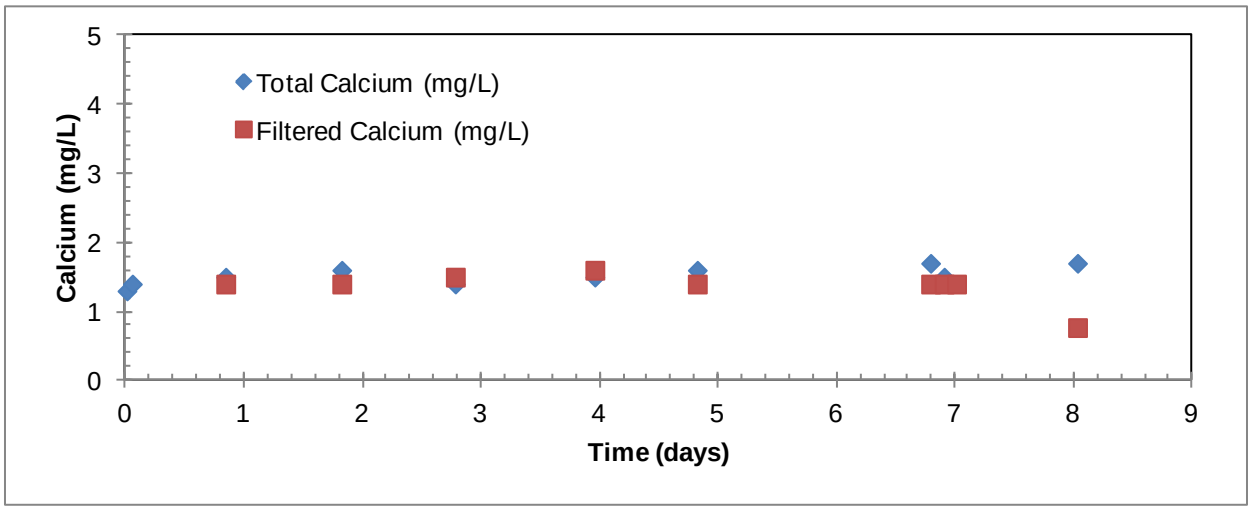

Figure 18: Measured calcium in the CHLE pool solution during the blended fiber test.

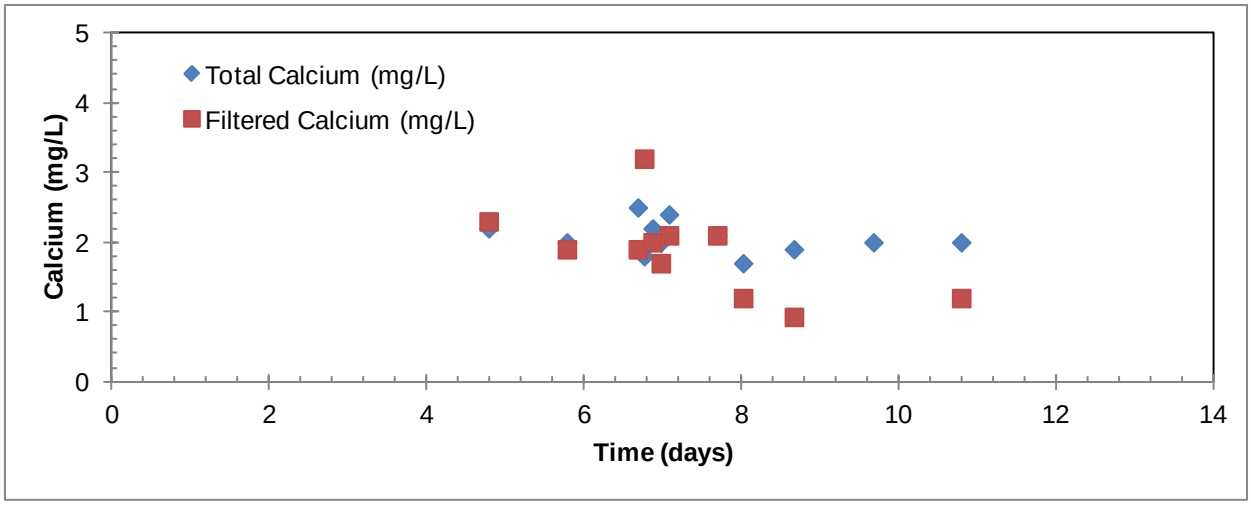

Figure 19: Measured calcium in the CHLE pool solution during the NEI fiber test.

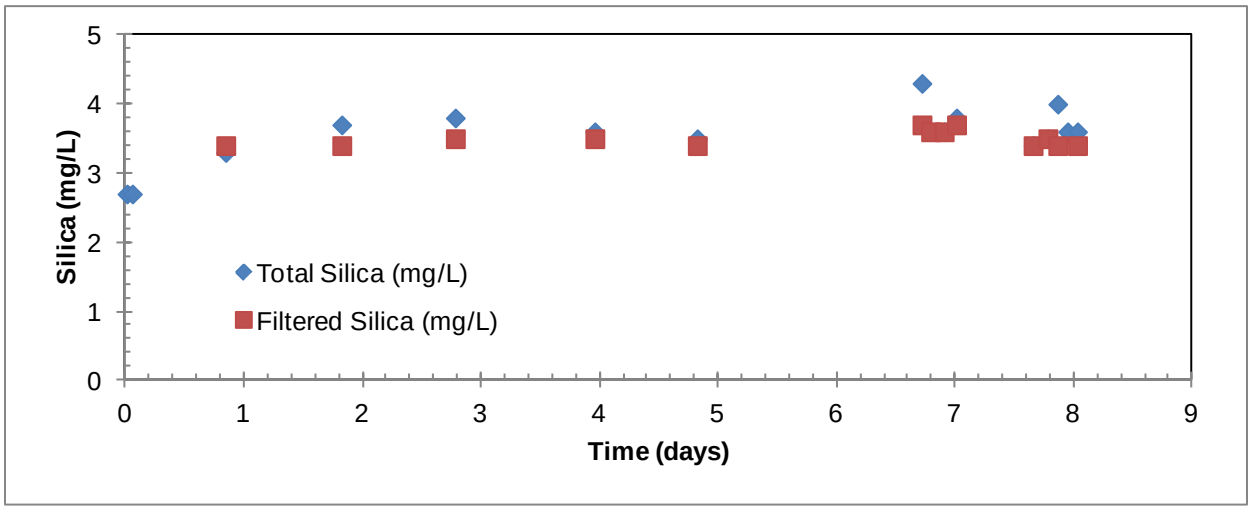

Figure 20: Measured silica in the CHLE pool solution during the blended fiber test.

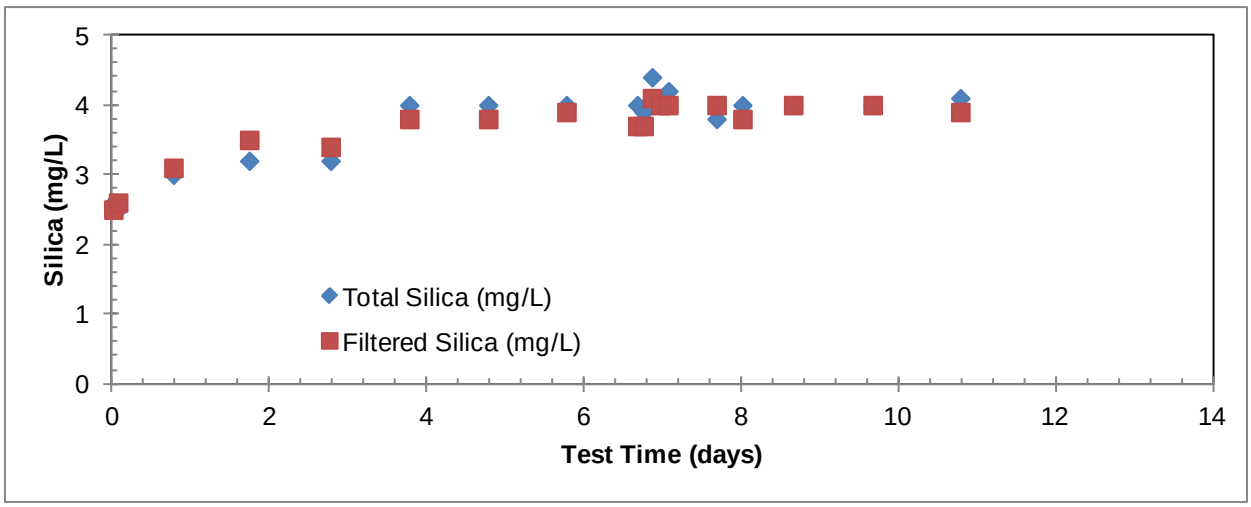

Figure 21: Measured silica in the CHLE pool solution during the NEI fiber test.

Effect of Aluminum Addition

After 6.7 days of operation with no materials in the tank, aluminum nitrate were added to the tank in each test. Aluminum nitrate was added at a slow rate (an increase of 0.02 mg/L per minute) to minimize the potential for precipitation to occur due to localized high concentration at the point of injection. For the blender preparation method, aluminum addition continued until a concentration of 6 mg/L as Al was reached in the solution with, and the test was terminated when the head loss in two of the three columns exceeded 80 inches of water. No significant change in head loss was observed in the test with the NEI pressure-washed preparation method; therefore, the aluminum addition was added in 7 periodic batches until 40 mg/L as Al was reached in the solution.

Turbidity

Several parameters were monitored as aluminum was added, including aluminum, calcium, and silicon concentrations in solution; total suspended solids; and turbidity. Determining the concentrations and suspended solids required sample analysis that took several days, but turbidity can be determined immediately. Turbidity correlated well with the formation of precipitates in the solution. In the test with the blended fiber, the turbidity started at about 0.81 NTU after the TSP was added and the CHLE tank was circulating through the head loss columns. Turbidity dropped slowly over several days, reaching 0.32 NTU on Day 6. After aluminum was added, the turbidity increased in direct proportion to the quantity of aluminum that was added, as shown in Figure 22. Turbidity is determined by measuring scattered light in a solution and is an indicator of particles in solution. Therefore, the turbidity is evidence that a precipitate was forming. Furthermore, the slight decrease in turbidity from 0.97 NTU after the first addition of aluminum was complete to 0.78 NTU before the second addition started (between days 7 and 8) may be an indication of removal of precipitates, possibly by being captured in the debris beds.

Similar results were observed for the test with the NEI fiber preparation. The turbidity started at about 0.63 NTU after the TSP was added and the CHLE tank was circulating through the head loss columns. The turbidity then dropped slowly, reaching 0.40 NTU on Day 6. After aluminum was added, the turbidity again increased in direct proportion to the quantity of aluminum that was added, as shown in Figure 23. The strength of this correlation indicates that essentially all of the aluminum that was being added was precipitating as particles in solution. The correlation between the amount of aluminum added and the turbidity in the solution for the NEI preparation method is shown in Figure 24.

Aluminum Concentration

Samples were taken for total and filtered aluminum and analyzed by a commercial laboratory. The results of the analysis are shown in Figure 25 for the blended fiber beds and Figure 26 for the NEI fiber beds. In both cases, the total aluminum in solution agrees well with the amount of aluminum that was added in solution. However, the concentration of aluminum in the filtered samples is significantly lower. These results indicate that a portion of the aluminum was removed during the filtration process, as would be expected when precipitates form. However, in both cases, several mg/L of aluminum were measured in the filtered samples, indicating that not all of the precipitates that were detected by the turbidity measurements were removed by the

laboratory filter. The standard filter for measuring filtered metals, however, has a nominal pore size of 0.45 µm. As will be shown later, evidence was found that the in-situ precipitates formed by the addition of aluminum nitrate were smaller than this size and a portion of the precipitates could have passed through the filter.

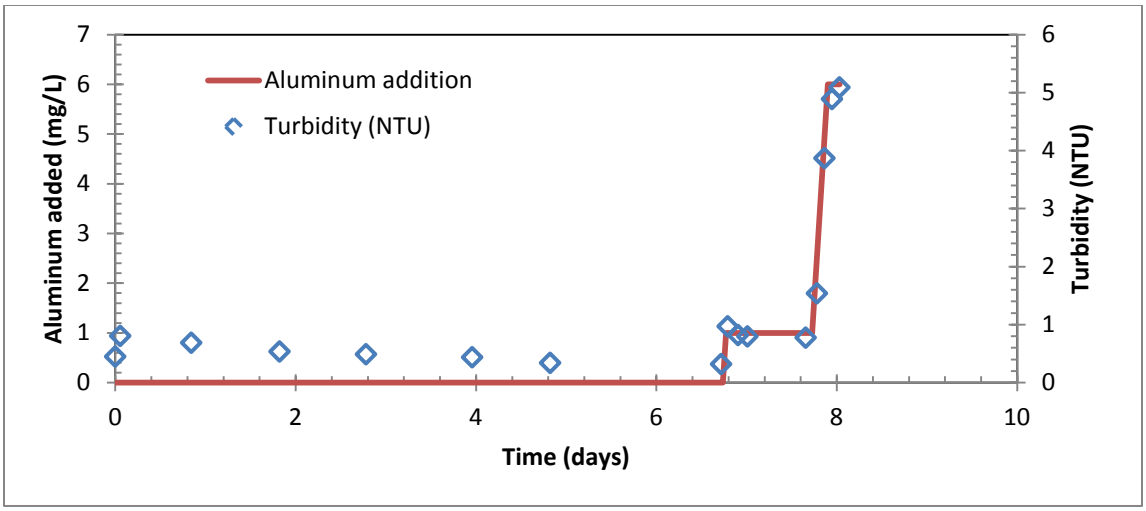

Figure 22: Measured turbidity in solution, and aluminum added to the CHLE tank over time during test with blended fiber preparation.

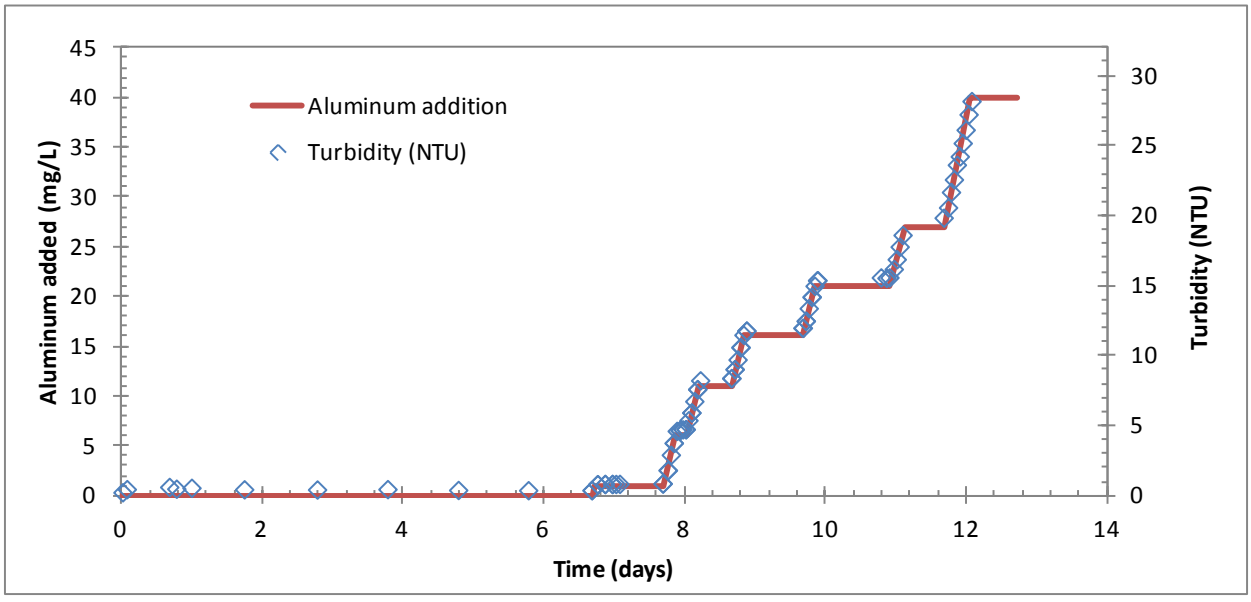

Figure 23: Measured turbidity in solution, and aluminum added to the CHLE tank over time during test with NEI pressure-washed fiber preparation.

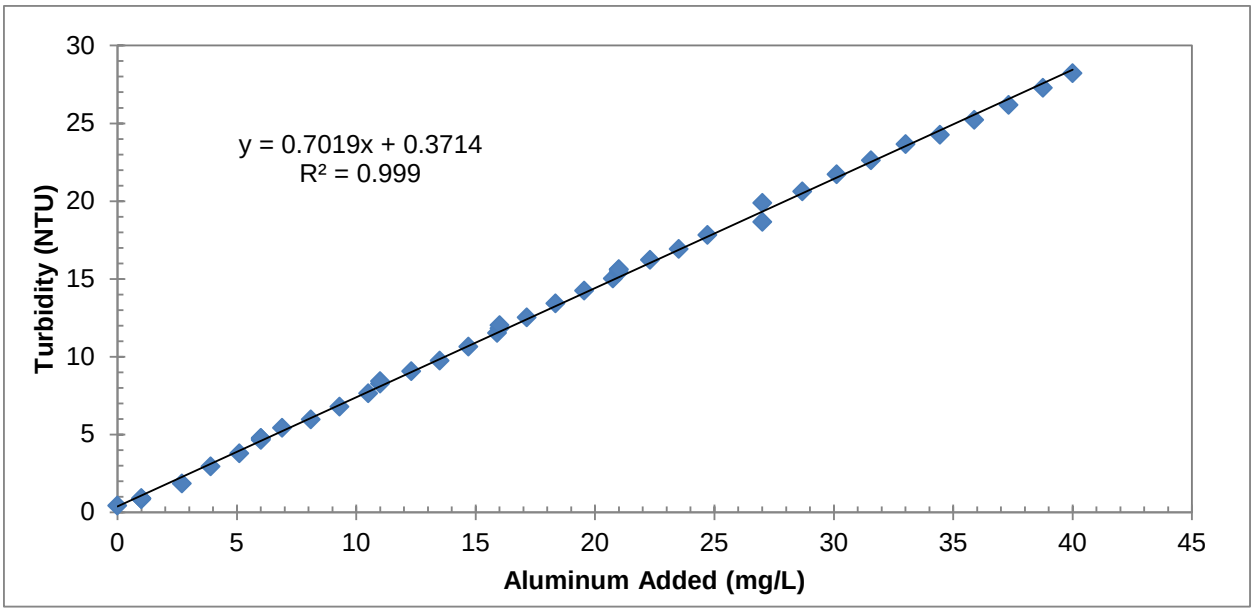

Figure 24: Correlation between measured turbidity in solution and amount of aluminum added to the CHLE tank in the form of aluminum nitrate.

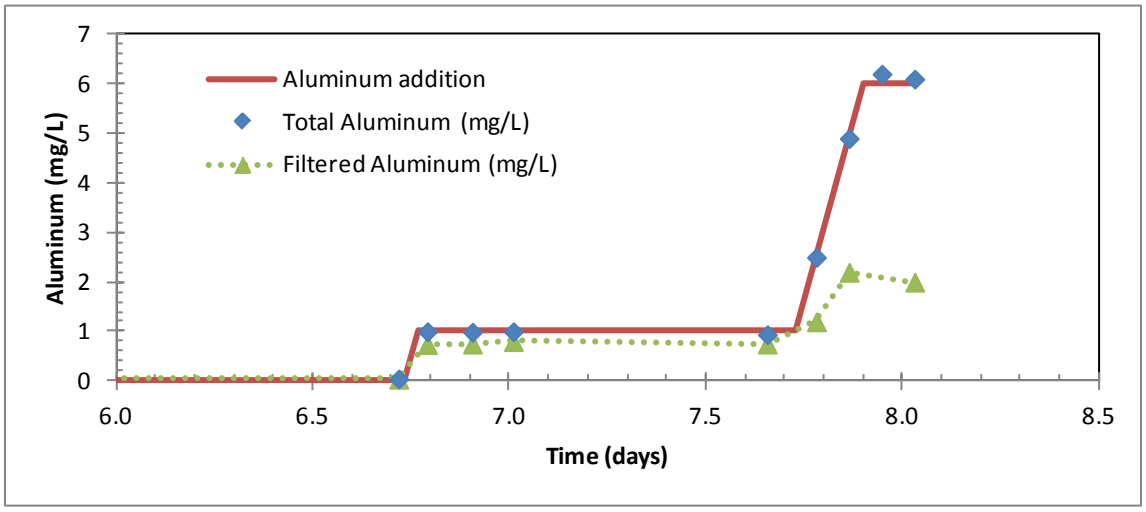

Figure 25: Measured total and filtered aluminum concentration in the CHLE pool solution during the blended fiber test, along with the aluminum that was added.

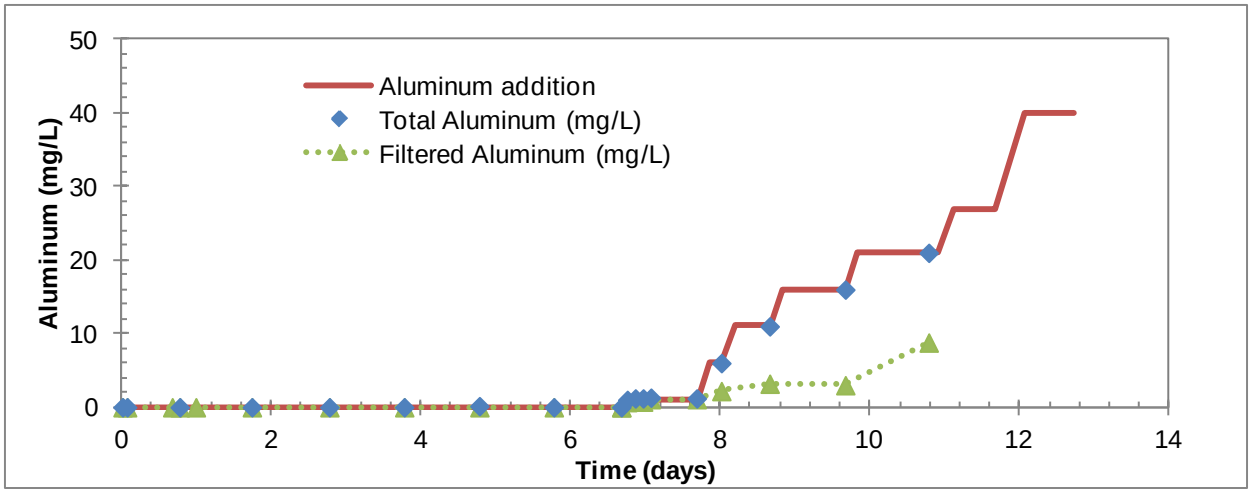

Figure 26: Measured total and filtered aluminum concentration in the CHLE pool solution during the NEI fiber test, along with the aluminum that was added.

Total Suspended Solids

Total suspended solids (TSS) was a less reliable indicator of the presence of precipitates than turbidity was. The TSS results are shown in Figure 27 for the blended fiber beds and Figure 28 for the NEI fiber beds. The factor most likely contributing to the poor correlation between TSS and precipitation formation was the particle size of the precipitates relative to the nominal pore size of the filter. The filter used for the TSS analysis is a glass-fiber filter with a nominal pore size of 1.2 µm (Whatman GF/C). As will be demonstrated later, the precipitates had an average size smaller than that, and many of the particles may have passed through the filter without having been measured as suspended solids. Prior to the addition of aluminum nitrate, the TSS of the solution was between 3 and 5 mg/L for both tests.

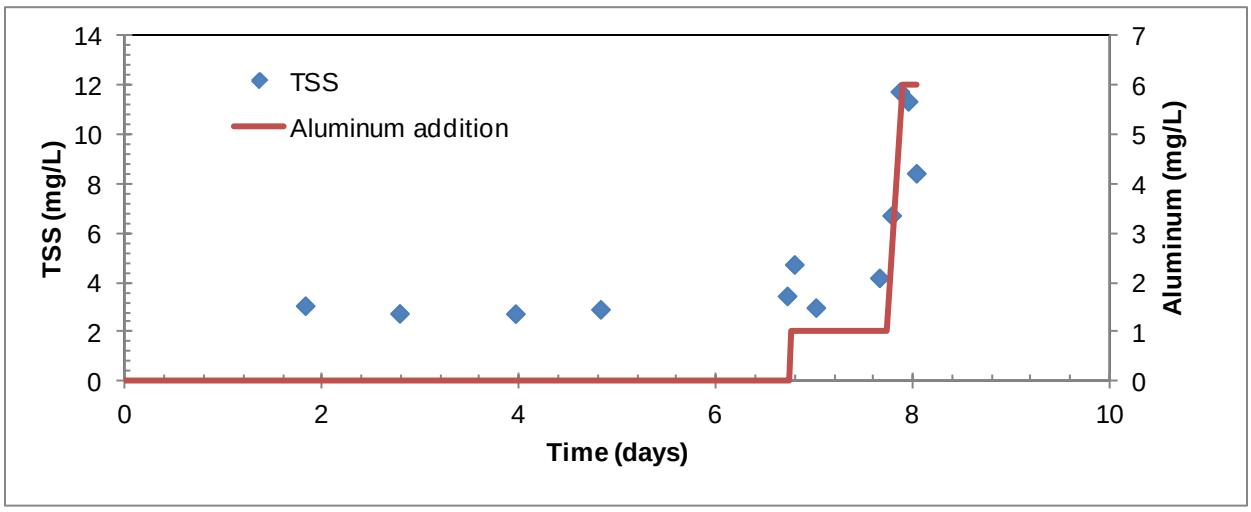

Figure 27: Measured total suspended solids (TSS) in the CHLE pool solution during the blended fiber test, along with the aluminum that was added.

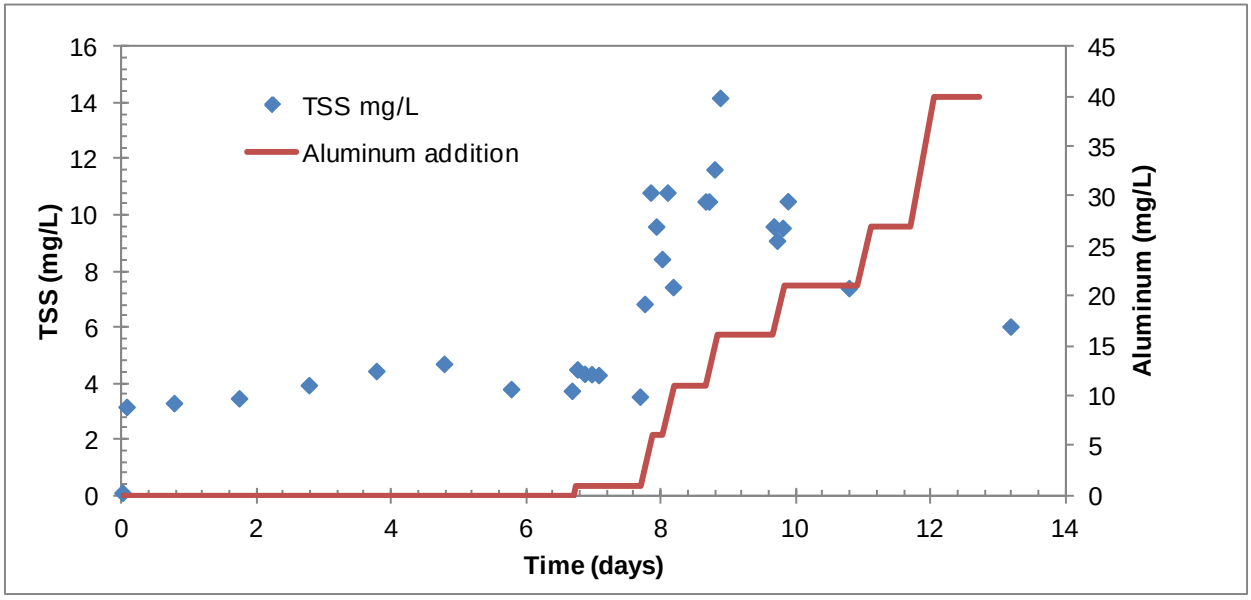

Figure 28: Measured total suspended solids (TSS) in the CHLE pool solution during the NEI fiber test, along with the aluminum that was added.

Debris Bed Head Loss

The head loss trends after the aluminum was added to the blended fiber beds are shown in Figure 29. After 1 mg/L of aluminum had been added, the head loss in all three columns started increasing. After 12 hours of operation, Column 3 reached its maximum head loss and its operation was terminated. The following day, 5 mg/L of aluminum was added (yielding a total of 6 mg/L). The head loss in Columns 1 and 2 started increasing rapidly, and the test was terminated after an additional 6 hours. Details of the statistical significance of the change in head loss after aluminum was added is described in Appendix 1.

Previous tests were conducted by adding pre-formed WCAP precipitate directly to the CHLE tank in batches. These tests were previously summarized in CHLE-008. The results of a test with WCAP precipitate and blended fiber beds are shown in Figure 30. The tests with in-situ precipitate formation and WCAP precipitate addition are difficult to compare because the latter had larger quantities of precipitate added over shorter periods of time. In addition, the tests in this series had been exposed to circulating solution for over 6 days, which may have led to sufficient local compaction to permit a more rapid response to the aluminum nitrate compared to the earlier tests. In the WCAP tests, five batches of WCAP precipitate, totaling 21.8 mg/L of aluminum, were added over a 4-hour period. Head loss started increasing rapidly about 4 hours after the first addition of WCAP precipitate, and the test was terminated an hour later. However, it is evident that in the case of blended fiber beds, both in-situ precipitate formation and the addition of pre-formed WCAP precipitates can cause significant head loss. It should be noted that the timing of head loss generation can be influenced by physical arrangement of debris in the bed and the degree of compaction that has been allowed to occur prior to the chemical arrival.

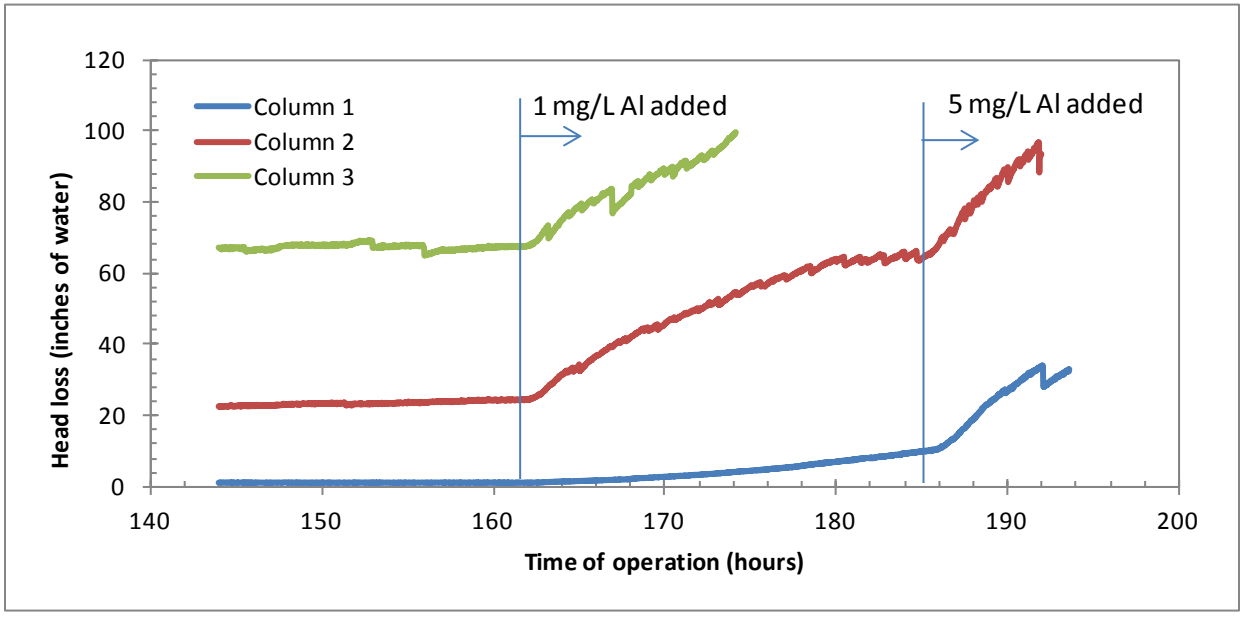

Figure 29: Head loss through debris beds with blended fiber preparation when in-situ precipitation occurred due to the addition of aluminum nitrate to the CHLE tank.

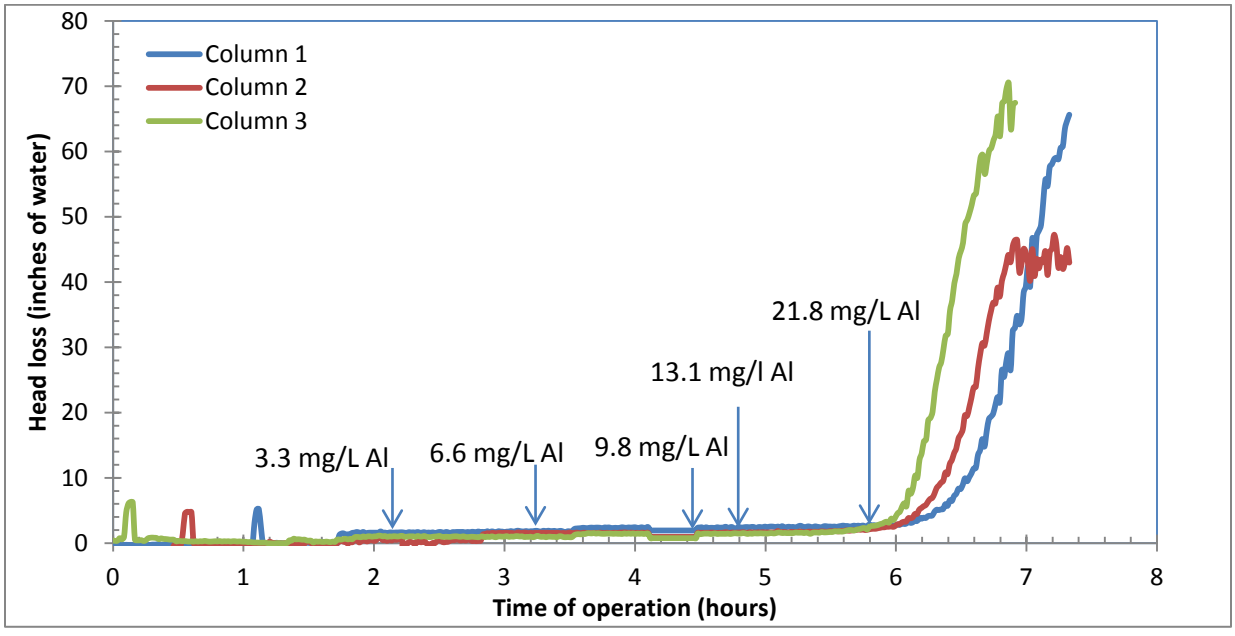

Figure 30: Head loss through debris beds with blended fiber preparation when pre-formed WCAP precipitates were added to the CHLE tank.

Significantly different results were obtained when in-situ precipitation was achieved in the tests with NEI pressure-washed fiber preparation. The initial 1 mg/L and 5 mg/L aluminum additions

did not cause any change in head loss. Thus, head loss additions continued daily for several additional days, until a total of 40 mg/L of aluminum had been added to the solution. The aluminum addition and head loss results are shown in Figure 31. Column 2 had a change in performance after 16 mg/L of aluminum had been added, and this change in performance was determined to be statistically significant, as described in Appendix 1. However, the change appears to be in the range of 0.1 inches of water, a change in head loss that would not be considered problematic during a LOCA. No statistically significant changes in head loss occurred in Columns 1 and 3 even after 40 mg/L of aluminum had been added.

Figure 32 shows that the NEI pressure-washed fiber beds behaved significantly differently when pre-formed WCAP precipitates were added to the CHLE tank. The same quantity of aluminum (40 mg/L) was added in the form of WCAP precipitates, except that it was added in a much shorter period of time (about 2 hours for WCAP versus about 5 days for the in-situ precipitate formation) and the WCAP was added in three batches versus seven addition cycles for the in-situ precipitate formation. However, when WCAP precipitates were added, the debris beds rapidly reached their maximum head loss values. When the same amount of aluminum was added to cause in-situ precipitation, no head loss occurred over a period of days, despite that the same type of debris beds (NEI pressure-washed) were present, and with the same quantity of fiber (18 g per bed). A comparison of Figures 31 and 32 is evidence that the slow formation of precipitates in-situ due to the addition of aluminum nitrate over a period of days into a buffered, borated solution typical of a LOCA at STP is not the same as the precipitates that are formed by the WCAP protocol. The same addition of aluminum caused over 80 inches of water of head loss when added as the WCAP precipitate, versus less than 1 inch of water of head loss when formed as an in-situ precipitate. It is important to understand the physical mechanisms that permit NEI fiber to pass in situ chemical products compared to the significant filtration of WCAP material.

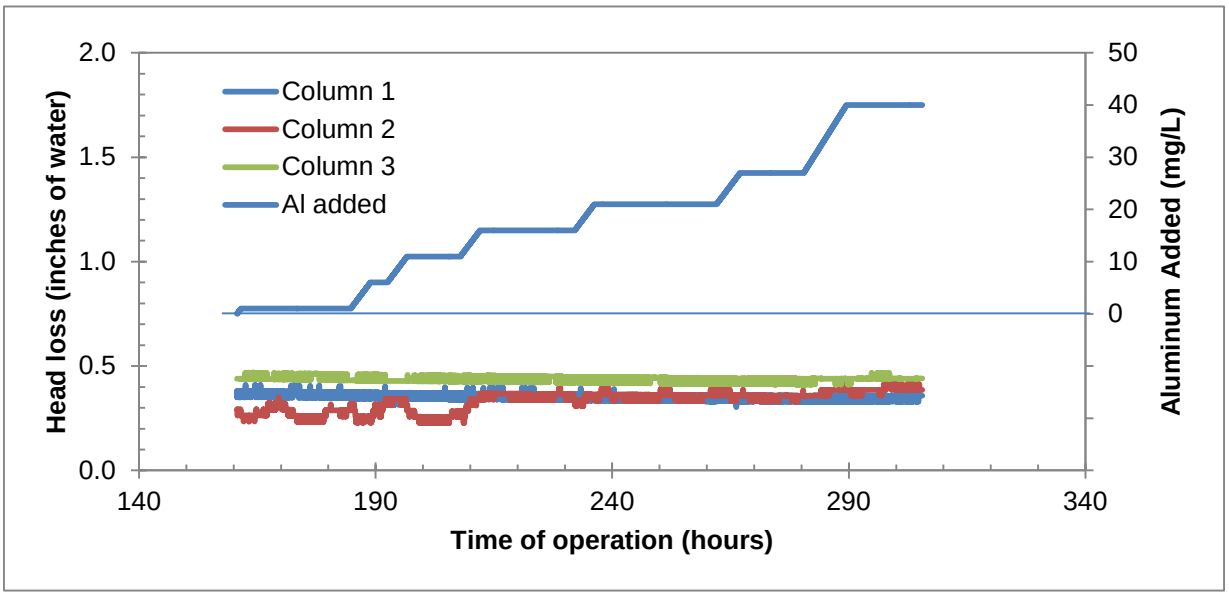

Figure 31: Head loss through debris beds with NEI pressure-washed fiber preparation when in-situ precipitation occurred due to the addition of aluminum nitrate to the CHLE tank.

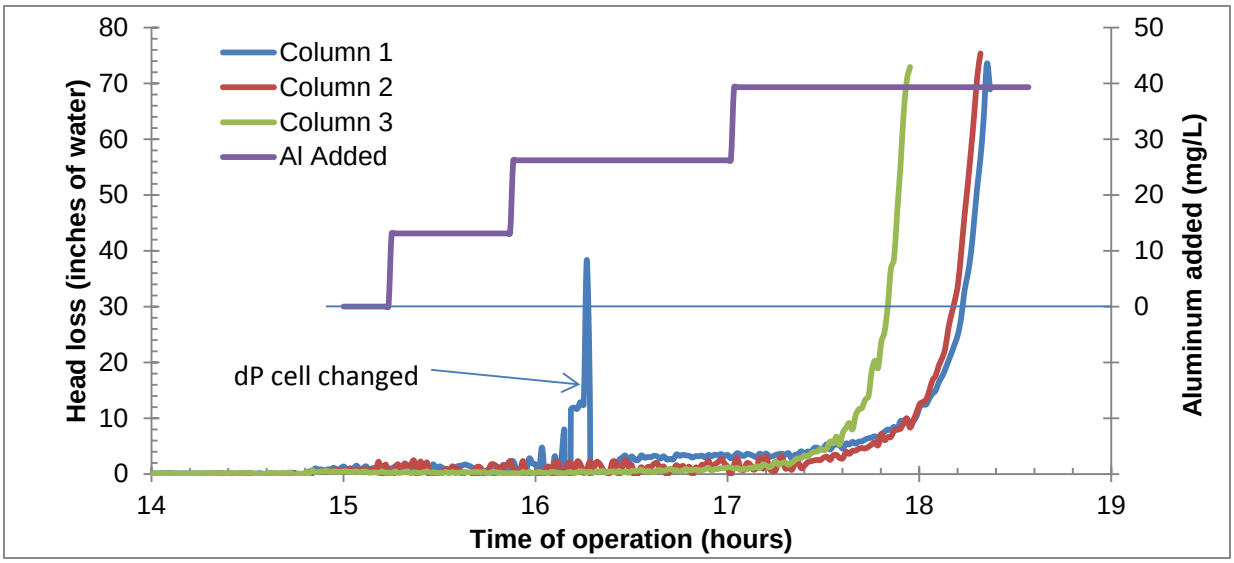

Figure 32: Head loss through debris beds with NEI pressure-washed fiber preparation when pre-formed WCAP precipitates were added to the CHLE tank.

Particle Size and Zeta Potential

To determine the cause of the difference in performance of the in-situ and pre-formed WCAP precipitates, the particle size and zeta potential of the precipitates were measured. The zeta potential is a measure of the surface charge of particles, which can affect their ability to aggregate into larger particles or to be retained in a filter. The analysis revealed distinct differences between the in-situ and pre-formed WCAP precipitates. The particle size and zeta potential measurements are summarized in Table 2. The preformed WCAP precipitates had a particle size of about 1.6 µm when they were in a solution containing boric acid and TSP at the concentrations used in the CHLE tests. This size was consistent over three samples of WCAP precipitates. When the WCAP precipitates were placed in a solution containing water that had been deionized by reverse osmosis, the particle size was slightly larger, ranging from 1.8 to 2.5 µm. This difference in size is unlikely to make a substantive difference in how the particles behave in solution or their ability to be retained in a debris bed. When the WCAP precipitates were placed in a solution containing tap water, the particle size was about the same size, 1.2 µm.

An important result in Table 2 is the size of the in-situ precipitates. These precipitates were measured at 0.17 µm on the day that the NEI test was completed. This size is one-tenth that of the pre-formed WCAP precipitates. The substantial difference in size may help explain why the pre-formed WCAP precipitates were retained by the NEI fiber beds but the precipitates formed in-situ were not. Samples of solution from the NEI test were stored in a laboratory oven at the final temperature of the test (40 °C) for two weeks, after which the particle size was measured again. The particle size was virtually identical in the second measurement, indicating that no aggregation had taken place over the storage period. In addition, visual observation indicated that no settling had occurred over the storage period, which is consistent with the small size of the particles.

Table 2: Particle size and zeta potential of aluminum hydroxide precipitates [1]

	Particle Size (μm)	Zeta Potential (mV)
Pre-formed WCAP Precipitates		
In boron/TSP water, 30 mg/L dilution	1.6	-28
In boron/TSP water, 40 mg/L dilution	1.6	-25
In boron/TSP water, 10 mg/L dilution	1.6	-27
In deionized water, 40 mg/L dilution	1.8	29
In deionized water, 10 mg/L dilution	2.5	30
In tap water	1.2	-3
In-situ Precipitates (in boron/TSP water)		
At end of test	0.17	-31
Two weeks later	0.18	-32

1. Each value given is the average of three measurements

When precipitates were placed in water containing boric acid and TSP, they had a zeta potential ranging from -25 to -32, regardless of whether they were pre-formed WCAP precipitates or in-situ precipitates. The in-situ precipitates were slightly more negative than the pre-formed WCAP precipitates. When particles are retained in a debris bed entirely by mechanical sieving, the charge on the particles is not important. However, when particles are smaller than the void dimensions in the debris bed, surface charge can have a significant impact on particle retention. Particles that have similar charge to the media in the debris bed will have electrostatic repulsion with the media and are less likely to be retained. Particles that are neutral or have opposite charge to the media can be retained by van der Waals forces or by electrostatic attractive forces.

Previous work by Duke Energy indicated that Nukon fibers are also negatively charged, although the magnitude of the charge depended on the solution in which the fibers were immersed. At a pH of about 7, that report found that Nukon fibers had a zeta potential of about -25 in water containing boric acid but about -12 in either deionized water or tap water. The report by Duke Energy noted that head loss through fiber beds could be a function of the type of water used, and attributed some of the difference in head loss performance to the zeta potential.

Because the in-situ particles and the Nukon fiber both have significant negative charge when immersed in water containing boric acid and TSP, they will have repulsive electrostatic forces and will not be retained unless the void dimensions in the debris bed are small enough to physically sieve the particles. These effects may explain the differences between the blended and NEI debris beds. The blended beds had hard nodules of fiber adjacent to the perforated screen, and these nodules had apparently retained some dirt or other material, leading to a difference in head loss among the three columns. The nodules apparently had small enough void dimensions that they were able to retain both pre-formed WCAP precipitates and in-situ precipitates. The NEI fiber bed, however, did not have the hard nodules of fiber and had void spaces small enough to retain the pre-formed WCAP precipitates but not small enough to retain the in-situ precipitates, which were one-tenth the size.

The results in Table 2 also indicate that the zeta potential of pre-formed WCAP precipitates was dependent on solution chemistry. In water containing boric acid and TSP, the precipitates were negatively charged with a zeta potential around -27. In tap water, the precipitates were nearly neutral with a zeta potential around -3. In deionized water, the precipitates were positively charged with a zeta potential around +30. These results could be significant for the use of pre-formed WCAP precipitates for some head loss tests. If debris beds are formed that are porous enough that they do not physically sieve precipitates, pre-formed WCAP precipitates that are used in tests containing deionized water or tap water are likely to be retained in the debris bed by electrostatic attraction or van der Waals attractive forces. In contrast, if the tests used water containing boric acid and TSP, the precipitates would be less likely to be retained because of the repulsive electrostatic forces, and less head loss would occur. Neither deionized nor tap water conditions exist within the post LOCA accident environment, so negative repulsive forces are likely to exist between fiberglass debris and aluminum based chemical products that may form in the sump environment.

Conclusions

The tests described in this report were developed to investigate (1) the suitability of debris beds for use in long-term corrosion/head loss experiments, which may be up to 30 days long, and (2) the response of the debris beds to the slow addition of aluminum nitrate, which can simulate the release of aluminum into solution by corrosion.

The fiber beds prepared with blending in a blender were not reproducible between columns. After 6 days of operation, the head loss varied from 1.2 inches of water to 61 inches of water through debris beds that were circulating the same water at the same rate. The lack of reproducibility would make it difficult to use this fiber bed preparation method in the CHLE program to assess the importance of chemical effects, because the difference in performance of due to variability may be greater than the difference in performance due to the addition of chemical effects. The lack of reproducibility of the fiber beds with the blended preparation appears to be due to localized regions of more dense fiber packing immediately adjacent to the perforated support plate.

In contrast, the fiber beds prepared with the NEI pressure-washing method were reproducible between columns and had steady performance over time. Testing by an outside laboratory demonstrated that the NEI pressure-washing method results in longer fibers. The shorter “shards” of fibers in the blended beds may be a key reason for the irreproducibility of those debris beds.

When aluminum nitrate was introduced into the solution, precipitates formed, as evidenced by turbidity measurements. There was a strong correlation between the turbidity measurements and the amount of aluminum that had been added. After aluminum nitrate was introduced into the solution, the head loss through the blended fiber beds increased. For the NEI pressure-washed debris beds, one of the three beds had a statistically significant response to the addition of aluminum nitrate, but the change in head loss was only about 0.1 inches of water in that column, which is enough to cause concern during a LOCA. The other two NEI pressure-washed debris

beds did not have a statistically significant response to the addition of aluminum nitrate, even though in earlier tests they did experience a significant increase in head loss after pre-formed WCAP precipitates were added to the system.

Particle size analyses indicate that the size of precipitates formed in-situ are up to 10 times smaller than the pre-formed WCAP precipitates with similar solution conditions (0.17 µm versus 1.6 µm in diameter). This significant difference in size appears to be sufficient to cause the pre-formed WCAP precipitates to be retained by the NEI fiber debris beds but allow the in-situ precipitates to pass through the NEI fiber debris beds. The results indicate that head loss may be less significant than indicated by the use of pre-formed WCAP precipitates, depending on the filtration characteristics of the debris bed.

Zeta potential analyses indicate that solution chemistry affects the surface charge of pre-formed WCAP precipitates. When tests were conducted in deionized water, pre-formed WCAP precipitates had a positive zeta potential. When tests were conducted in Albuquerque tap water, the pre-formed WCAP precipitates were nearly neutral. When tests were conducted in water containing boric acid and TSP, the precipitates had a significant negative charge. The reversal of charge depending on solution chemistry suggests that head loss testing using pre-formed WCAP precipitates may not adequately predict the extent of head loss through a strainer under conditions in which debris beds are not reliant on physical sieving for the retention of particles.

Despite the slow introduction of aluminum nitrate, corrosion conditions may not have been perfectly emulated in these tests. It is possible that conditions that minimize aluminum release, such as the passivation of aluminum surfaces or the formation of a low-solubility oxide layer, would result in an upper limit to the aluminum concentration measured in solution. In addition, saturation conditions relevant for direct nucleation of precipitation products within the fiber bed may have been artificially exceeded. If direct nucleation is a credible formation mechanism, then the tests reported here best describe the filtration behavior between the two preparation methods and not necessarily the in-situ head-loss sensitivity. Direct nucleation would avoid the complications of particle filtration, perhaps leading to different head loss response in the NEI pressure-washed debris beds. As a result, additional tests that investigate precipitate formation under prototypical corrosion conditions are needed.

It is important to note that a growing suite of routine diagnostics is available to detect and characterize the presence of chemical products. These tests include: optical turbidity, analytical measurements of solution chemistry, particle sizing, zeta potential, SEM fiber examination, chemical addition mass balance, online differential pressure, and visual estimation of debris beds. There is no exclusive dependency on differential pressure to detect the presence of chemical products. The use of several of these experimental methods can be used to detect the presence of chemical precipitates in an integrated corrosion/head loss test to evaluate whether precipitates that may form following a corrosion process are similar to the precipitates detected here after the addition of aluminum nitrate. In addition, the tests can be coupled with the use of NEI pressure-washed debris beds in the head loss columns to determine whether the head loss characteristics in response to direct nucleation of precipitates in the fiber bed are similar to the response of precipitates that form after the addition of aluminum nitrate.

APPENDIX A

CHLE Tank Test Results for Blended and NEI Fiber Beds with Aluminum Addition: Correlated Control Charts for Head Loss Response to Aluminum Addition

CHLE Tank Test Results for Blended and NEI Fiber Beds with Aluminum Addition: Correlated Control Charts for Head Loss Response to Aluminum Addition

by Jeremy Tejada and David Morton, The University of Texas at Austin

August 17, 2012

1. Summary of Analysis

We develop and analyze control charts for the head loss data in Report CHLE-010: CHLE Tank Test Results for Blended and NEI Fiber Beds with Aluminum Addition (Howe, 2012). Table 1 summarizes the results that we describe in detail in subsequent sections. The analysis consists of assessing the performance of control charts for head loss for three columns using, in turn, three CHLE head loss columns for the NEI fiber beds and three CHLE head loss columns for the blended fiber beds.

	NEI Fiber Bed	**Blended Fiber Bed**
Column 1	Lack of evidence suggesting change in head loss process after addition of aluminum.	Strong statistical evidence of change in head loss process after aluminum is added.
Column 2	Statistically significant change in head loss process after addition of aluminum. Conclusion based violations of upper control limit over multiple half-day time periods.	Strong statistical evidence of change in head loss process after aluminum is added.
Column 3	Lack of evidence suggesting change in head loss process after addition of aluminum.	Statistically significant change in head loss process after addition of aluminum. Conclusion based violations of upper control limit using half-day moving average.

Table 1. Summary of Results of Analyzing Control Charts for Temperature-corrected Head Loss Process in Three Columns using NEI Fiber Bed and Blended Fiber Bed.

2. Introduction

The objective of this analysis is to determine whether the addition of aluminum over time caused a statistically significant response in terms of head loss through the debris beds. The experiment was

designed to record data each minute, with each data point being the average of six measurements during that minute. Thus, the data from the experiment forms a time series where the (average) head loss through the debris bed is provided for each minute over several days of experimentation. The experiment used three identical physical, vertical columns, and data are provided for each column separately. Thus we perform the analysis we describe on each column separately. We report analysis for six data sets: Three CHLE head loss columns for the NEI fiber beds and three CHLE head loss columns for the blended fiber beds. In order to assess whether we observe a statistically significant response in head loss due to the addition of aluminum over time, we use control charts. Specifically, we use control charts designed to handle correlations and trends in time series data (Croux et al., 2010). We organize the remainder of this analysis as follows: Section 3 presents some of the details of the time series control charts that we use, and Sections 4 and 5 present the results for the NEI fiber beds and the blended fiber beds, respectively, along with a brief discussion of these results.

3. Control Charts for Time Series Data

In this section, we present some of the details for a control chart for a time series, $\{y_t\}$, and our description follows closely that of Croux et al. (2010). At each point in time we obtain a one-step-ahead forecast using the Holt-Winters forecasting algorithm, and we plot the errors from this one-step-ahead forecast on a control chart. We construct the control limits to monitor new observations from a training sample, and we use the one day (1440 minutes) before aluminum was added in the experiment as our training period, as we assume the error process has reached a steady state by this point (about 5.8 days into the experiment).

3.1. Holt-Winters Forecasting Algorithm

Assume we have observed a time series up to time period $t-1$. The Holt-Winters method predicts the series at time t, which we denote $\hat{y}_{t|t-1}$. After we observe the actual value, y_t, we compute the one-step-ahead forecast error e_t according to

$$e_t = y_t - \hat{y}_{t|t-1}. \tag{1}$$

We denote the level of the time series by α_t, and the trend in the series by β_t. The Holt-Winters method for estimating these values after each realization, y_t, is as follows

$$\hat{\alpha}_t = \lambda_1 y_t + (1-\lambda_1)(\hat{\alpha}_{t-1} - \hat{\beta}_{t-1}) \tag{2}$$

$$\hat{\beta}_t = \lambda_2(\hat{\alpha}_t - \hat{\alpha}_{t-1}) + (1-\lambda_2)\hat{\beta}_{t-1} \tag{3}$$

and this results in the forecast

$$\hat{y}_{t|t-1} = \hat{\alpha}_{t-1} + \hat{\beta}_{t-1}. \tag{4}$$

The parameters λ_1 and λ_2 in (2)-(3) are smoothing parameters that take on values between zero and one. Larger parameters values lead to less smoothing and more weight being placed on the current values opposed to the previous level and trend. The relations (2)-(3) begin after a warm up period, in our case about 5.8 days. A linear model is fitted to the warm-up data in order to determine estimates of the initial level α_0 and trend β_0. After the warm-up period, there is a training period, in our case 1 day or 1440 minutes. We determine the values for the smoothing parameters λ_1 and λ_2 by minimizing the sum of squared forecast errors over a training period as follows:

$$(\lambda_1^{\text{opt}}, \lambda_2^{\text{opt}}) \in \underset{(\lambda_1,\lambda_2)}{\arg\min} \sum (y_t - \hat{y}_{t|t-1})^2. \tag{5}$$

A simple two dimensional guess-and-check search over these parameter values can provide the optimal values to within two decimal places very quickly.

3.2. Control Chart

We monitor and plot the one-step ahead forecast errors on the control chart in order to determine if, and when, the process goes out of statistical control. As with most control charts, we assume the forecast errors (not the data itself) are normally distributed. The upper control limit (UCL) and lower control limit (LCL) are set using the forecast errors during the training period. We denote the mean of the squared prediction errors in the training period by

$$S^2 = \frac{\sum e_t^2}{n}, \tag{6}$$

where n is the number of data points in the training period. The target value for the forecast errors is zero, so the $(1-\alpha)$-level UCL and LCL are:

$$UCL = z_{\alpha/2} * S$$
$$LCL = -z_{\alpha/2} * S \tag{7}$$

where $z_{\alpha/2}$ is the $(1-\alpha/2)$-level quantile of the standard normal distribution.

For each new observation in the test period, the recursive relations (2)-(3) are updated, and the forecast error for that observation can be computed and plotted on the control chart. If it falls outside the limits, its value is statistically significantly different from the predicted value, indicating some unexpected changed in the process. Observations that are part of the test period influence future forecast errors via the Holt-Winters forecast formulas as these are continually updated. However, these observations do not alter the control limits.

In what follows, we build two-sided control charts as we describe above, using (7). That said, we have interest in increases in head loss, and so we pay particular attention to violations of the upper control limit in equation (7). Some violation of that control limit is expected, even if the system remains "in control" due to the statistical nature of the process. Such violations of the upper control limit would occur at rate $\alpha/2$. For this reason, when a more nuanced analysis is needed (Section 4 and Section 5.3), we track a moving average of the rate of violation to help assess whether the head loss process has indeed changed after the addition of aluminum.

4. Control Charts for NEI Fiber Bed Data and Discussion

For each of the three CHLE head loss columns with the NEI fiber bed, we present the control chart with α = 0.05, both with the initial training period included and only after aluminum addition. For the NEI fiber beds, based on a preliminary analysis, it appeared that there may be responses at two points in time after aluminum was added. Thus, we consider a second training period starting at day 10.5 and ending at day 11.5, and we set new control limits for the process after that point. We also give the estimated λ_1 and λ_2 values for both training periods and the observation periods. Finally, we discuss the meaning of the charts for each column.

4.1 Column 1

Period 1

Training Fraction Outside Control Limits (two-sided) = 0.0694
Training Fraction Outside Upper Control Limit = 0.0417
Observed Fraction Outside Control Limits (two-sided) = 0.0953

Observed Fraction Outside Upper Control Limit = 0.0126

$\lambda_1 = 0.12$

$\lambda_2 = 0.43$

Period 2

Training Fraction Outside Control Limits (two-sided) = 0.0063

Training Fraction Outside Upper Control Limit = 0.0000

Observed Fraction Outside Control Limits (two-sided) = 0.0028

Observed Fraction Outside Upper Control Limit = 0.0021

$\lambda_1 = 0.07$

$\lambda_2 = 0.10$

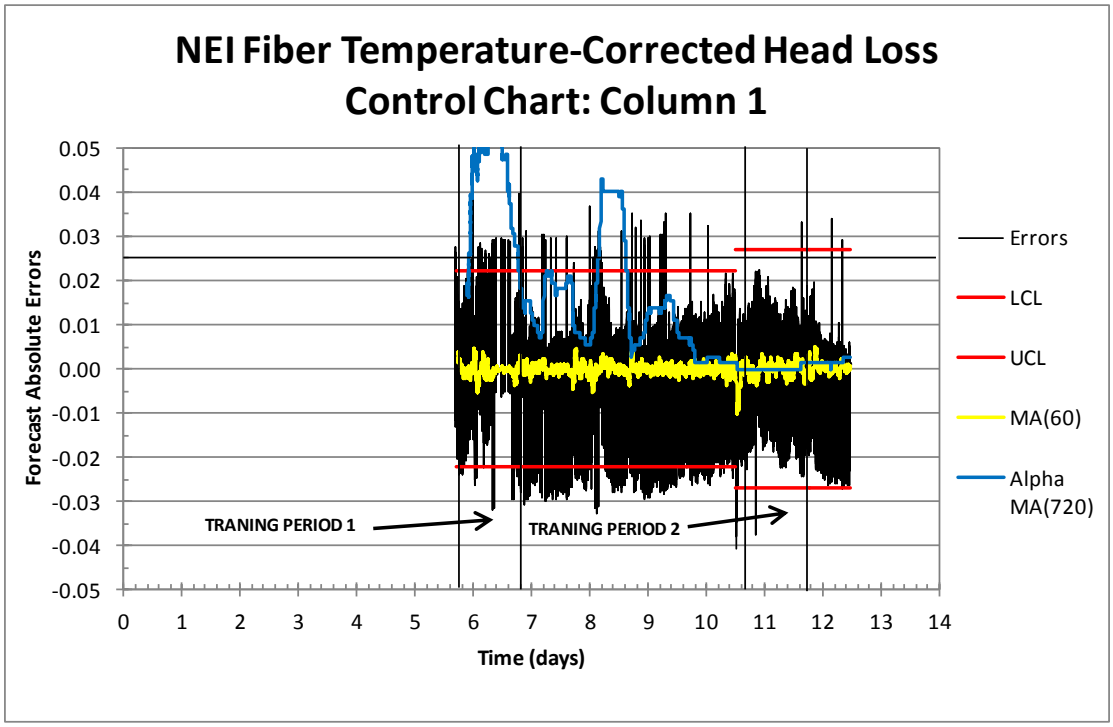

Figure 2. NEI Fiber Temperature-Corrected Head Loss Control Chart Column 1 - Initial Training Period Included. The figure depicts errors (see equation (1)), the lower control limit and the upper control limit (see equation (7)), a moving average of errors based on the last 60 one-minute periods, and a moving average of violations of the upper control limit for the last 720 one-minute periods. Subsequent figures have similar formatting.

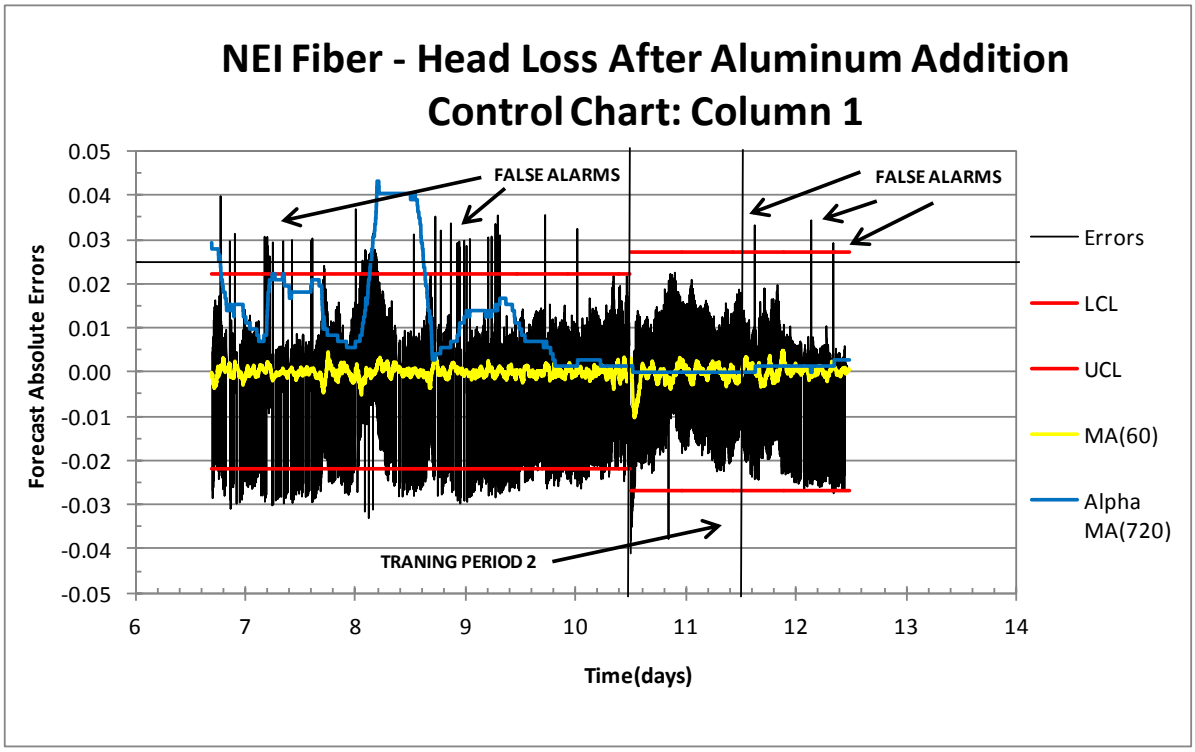

Figure 3. NEI Fiber Temperature-Corrected Head Loss Control Chart Column 1 - Initial Training Period Not Included

During the initial training period, the observed alpha value (i.e., the fraction of observations outside the two-sided control limits) of 0.0694 is slightly higher than the expected 0.05, but within reason, leading us to conclude the control limits are reasonable. During the initial observation period, the observed alpha value for two-sided violation rose to 0.0943. However, the fraction of violations of the upper control limit are only 0.0126, well within the expected value of 0.025. The only exception to this for a narrower time window is the denser mass of errors near the upper control limit depicted early in day 8; see Figure 2. The moving average of the rate of the upper control limit violation over half-a-day (720 minutes) grows to about 0.04, compared to an expected upper limit violation of 0.025, but we regard this as being at most a weak signal. An analogous analysis for the second period gives no indication of a signal. Based on this, we do not find compelling evidence that in column 1 there was a statistically significant increase in head loss as aluminum was added over time.

4.2 Column 2

Period 1

Training Fraction Outside Control Limits (two-sided) = 0.0958

Training Fraction Outside Upper Control Limit = 0.0243

Observed Fraction Outside Control Limits (two-sided) = 0.0892

Observed Fraction Outside Upper Control Limit = 0.0451

$\lambda_1 = 0.23$

$\lambda_2 = 0.00$

Period 2

Training Fraction Outside Control Limits (two-sided) = 0.0903

Training Fraction Outside Upper Control Limit = 0.0417

Observed Fraction Outside Control Limits (two-sided) = 0.1091

Observed Fraction Outside Upper Control Limit = 0.0539

$\lambda_1 = 0.15$

$\lambda_2 = 0.01$

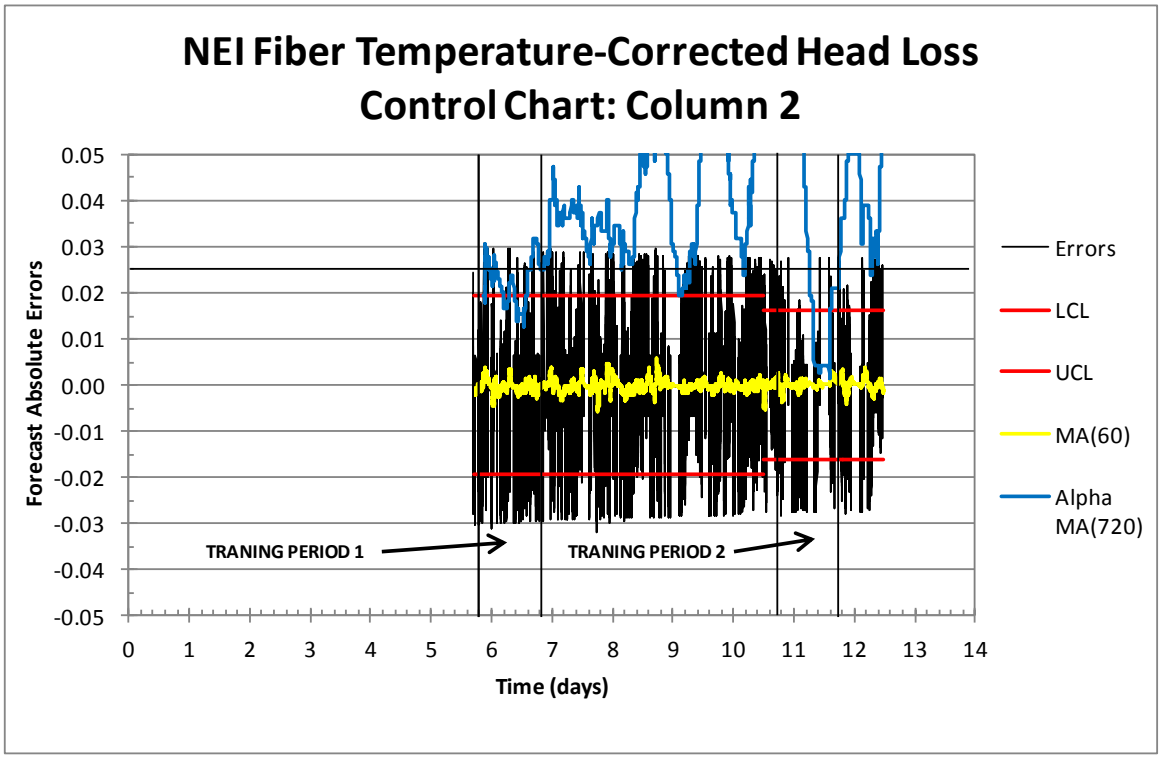

Figure 4. NEI Fiber Temperature-Corrected Head Loss Control Chart Column 2 - Initial Training Period Included

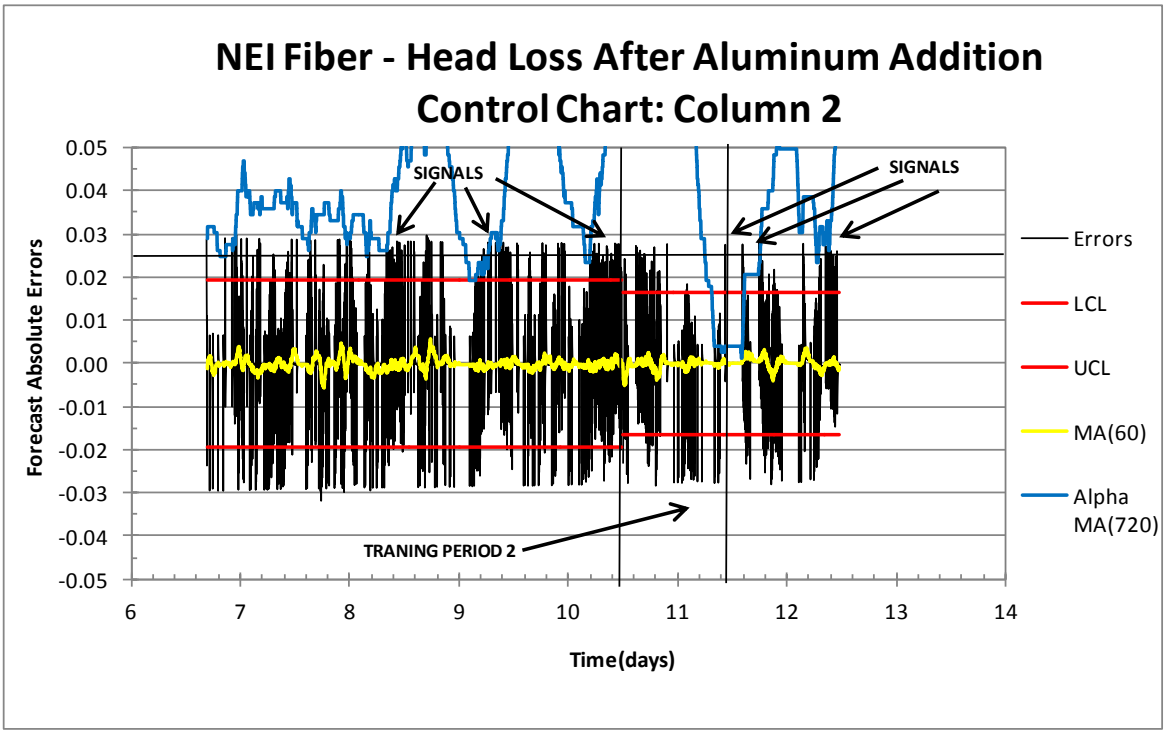

Figure 5. NEI Fiber Temperature-Corrected Head Loss Control Chart Column 2 - Initial Training Period Not Included

During the first training period, the observed alpha value of 0.0958 is again a bit higher than the expected 0.05, but perhaps close to within reason. The observed upper control limit violations of 0.0243 matches closely the expected 0.025 during the first training period. During the first observation period, the observed alpha value for upper control limit violations climbs to a modest value of 0.0451. However, as the moving-average values in Figure 4 depict, for substantial portions of day 8 and days 9-10.4, there are significant violations of the upper control limit. The associated "blue line" exceeds the chart's maximum, and peaks at 0.0625 during the first such interval (day 8) and 0.0722 during the second interval. There is similar behavior during the second period. So while the process is not consistently out of statistical control after the addition of aluminum, there are significant periods of more than one-half day in length where the process deviates well beyond the control limits. This suggests a statistically significant deviation of the process after the addition of aluminum. We further note that the timing of these deviations is consistent with visible jumps in the level of the head loss for column 2 in Figure 2 of Howe (2012).

4.3 Column 3

Period 1

Training Fraction Outside Control Limits (two-sided) = 0.0271

Training Fraction Outside Upper Control Limit = 0.0146

Observed Fraction Outside Control Limits (two-sided) = 0.0202

Observed Fraction Outside Upper Control Limit = 0.0130

$\lambda_1 = 0.11$

$\lambda_2 = 0.32$

Period 2

Training Fraction Outside Control Limits (two-sided) = 0.0125

Training Fraction Outside Upper Control Limit = 0.0097

Observed Fraction Outside Control Limits (two-sided) = 0.0135

Observed Fraction Outside Upper Control Limit = 0.0078

$\lambda_1 = 0.10$

$\lambda_2 = 0.13$

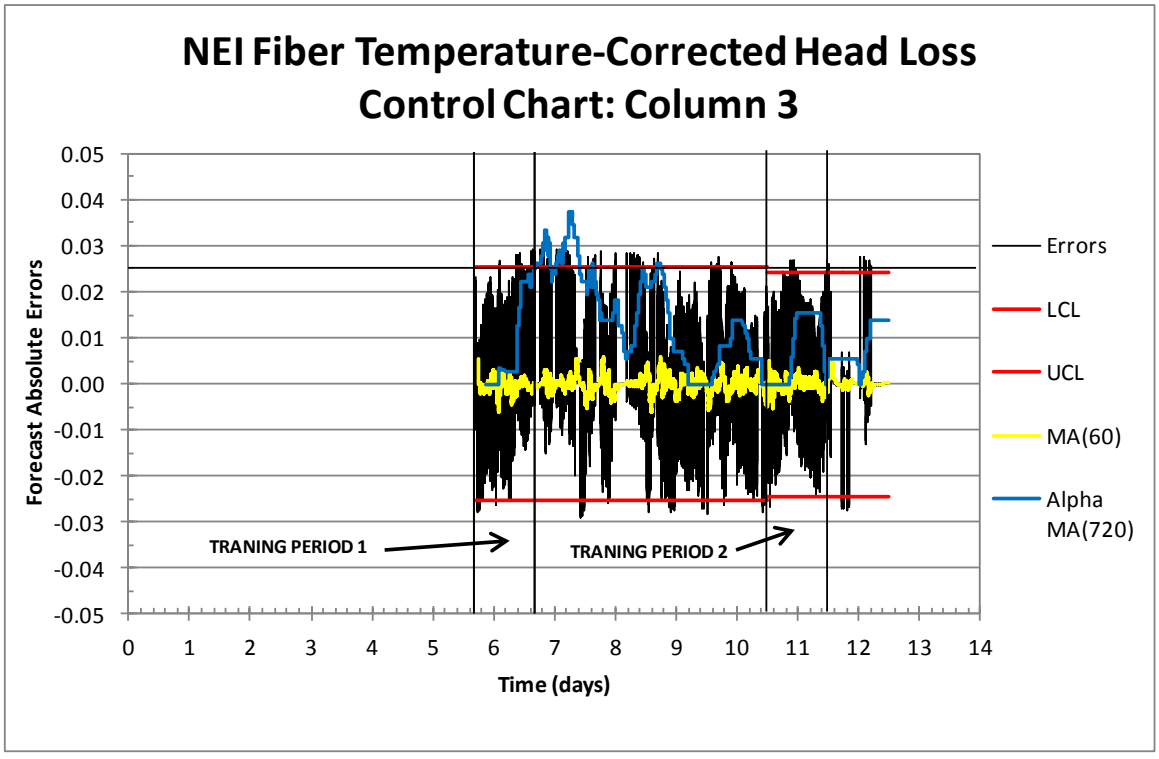

Figure 6. NEI Fiber Temperature-Corrected Head Loss Control Chart Column 3 - Initial Training Period Included

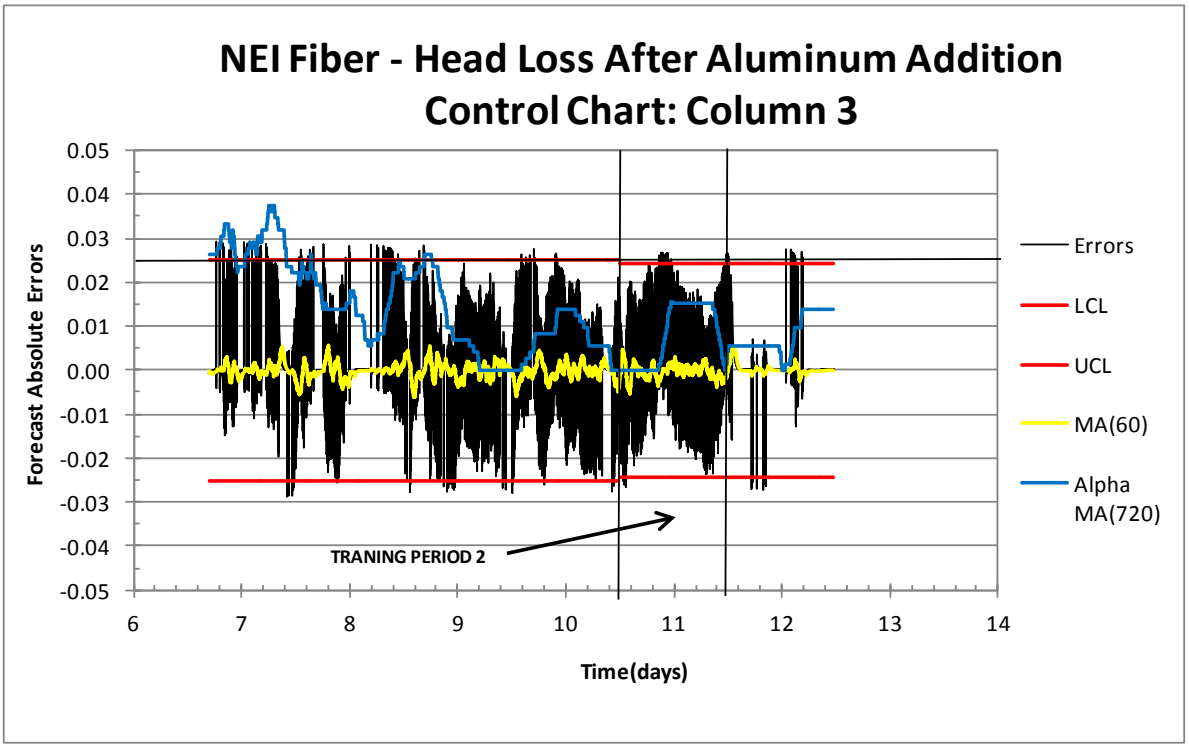

Figure 7. NEI Fiber Temperature-Corrected Head Loss Control Chart Column 3 - Initial Training Period Not Included

During both training periods and observation periods, the observed alpha values are less than 0.05 for violations of the two-sided control limits and less than 0.025 for violations of the upper control limit. Individual errors violate control limits only on rare occasions. The moving-average of violations of the upper control limit modestly exceeds 0.025 for part of day 7, but otherwise is almost exclusively below 0.025. It is reasonable to conclude that in column 3, there was not a statistically significant increase in head loss as aluminum was added over time.

5. Control Charts for Blended Fiber Bed Data and Discussion

Again for each of the three columns under the blended fiber bed data, we present control charts with α = 0.05 both with the initial training period included and only after the addition of aluminum. For the blended fiber beds, we only use one training period and one observation period. We again provide the observed alpha values and optimal smoothing parameters for both the training and observation period. The results here are not subtle for columns 1 and 2 and a formal statistical analysis is arguably overkill in these cases. (See Figure 1 of Howe, 2012.) We simplify the discussion slightly by not distinguishing two-

sided and upper-limit violations, and by suppressing presentation of the upper control limit violation, at least until the discussion in Section 5.3.

5.1 Column 1

Training Period Fraction Outside Control Limits = 0.0454

Observation Period Fraction Outside Control Limits = 0.3832

$\lambda_1 = 0.16$

$\lambda_2 = 0.48$

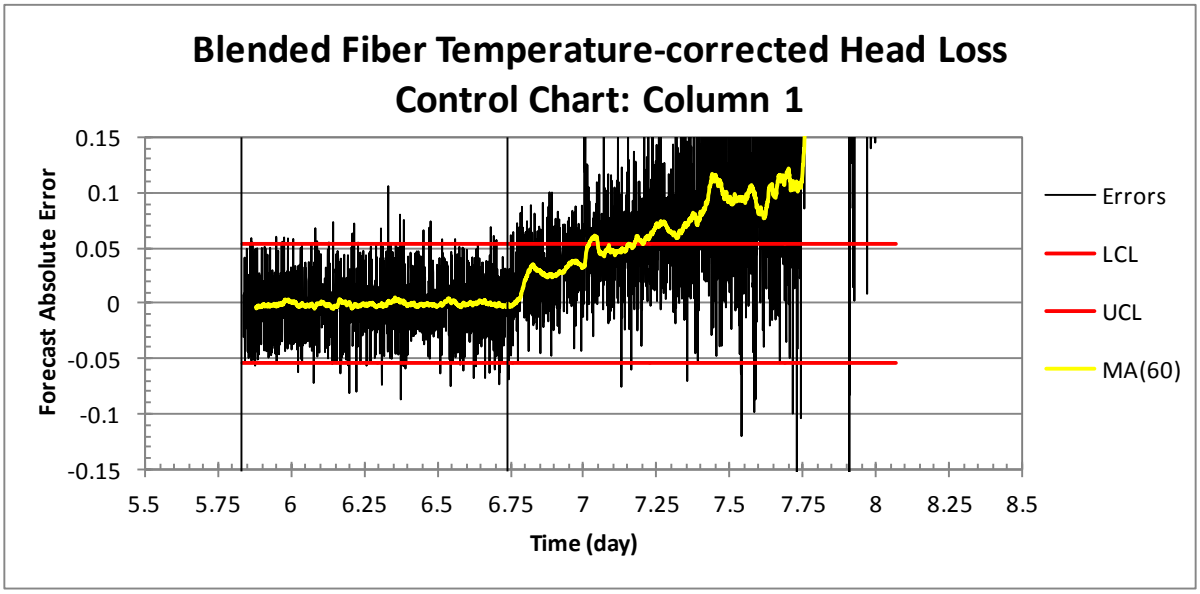

Figure 8. Blended Fiber Temperature-Corrected Head Loss Control Chart Column 1 - Initial Training Period Included

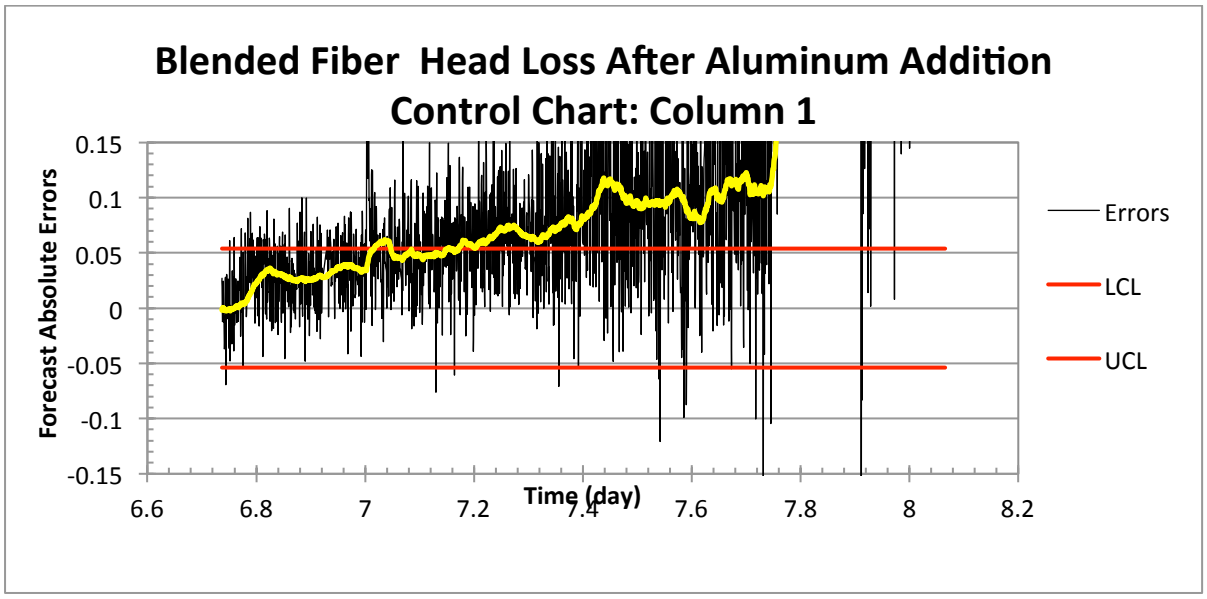

Figure 9. Blended Fiber Temperature-Corrected Head Loss Control Chart Column 1 - Initial Training Period Not Included

The observed alpha value during the training period of 0.045 is close to the expected 0.05, leading us to conclude the control limits set during training are sound. Examining Figure 7, the steady state assumption of the error process during the training period appears appropriate. From both Figures 7 and 8, we observe an almost immediate response after aluminum is added, with a delay of about 0.05 days. The one-hour moving average captures this change fairly well, and the errors quickly exceed the upper control limit. At about 7.3 days, the errors increase significantly and the process jumps to a further out-of-control state. In column 1, there is clearly a statistically significant response to the addition of aluminum, much more pronounced than with any of the NEI fiber beds.

5.2 Column 2

Training Period Fraction Outside Control Limits = 0.0477

Observation Period Fraction Outside Control Limits = 0.2462

$\lambda_1 = 0.40$

$\lambda_2 = 0.00$

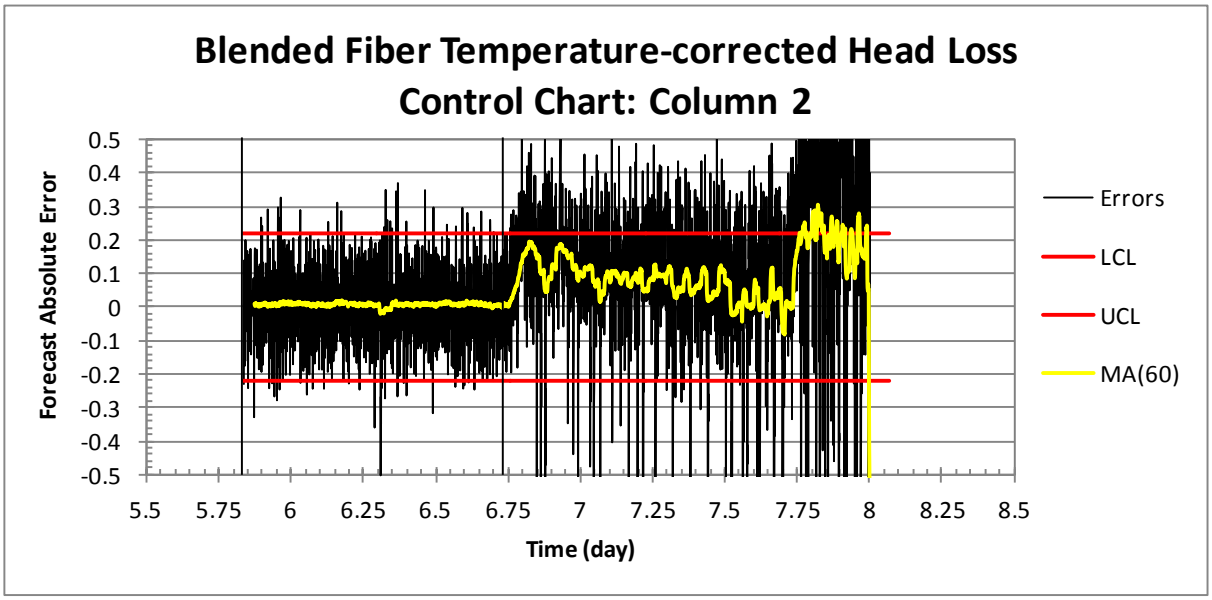

Figure 10. Blended Fiber Temperature-Corrected Head Loss Control Chart Column 2 - Initial Training Period Included

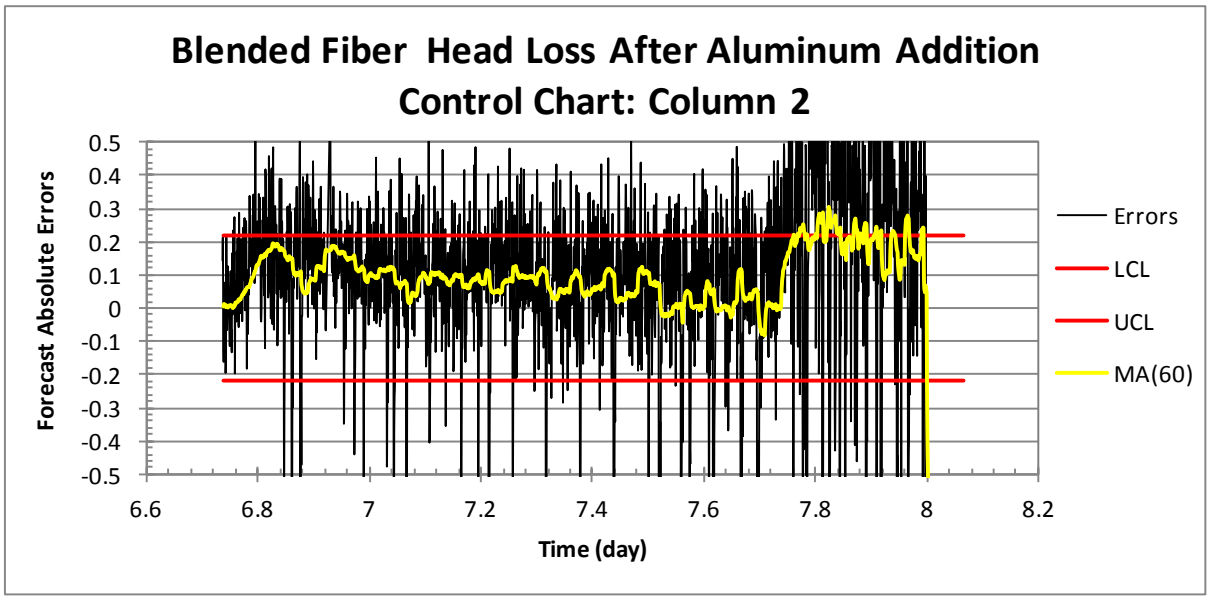

Figure 11. Blended Fiber Temperature-Corrected Head Loss Control Chart Column 2 - Initial Training Period Not Included

The observed forecast errors for column 2 are very similar to those of column 1. The observed alpha value during the training period is 0.045. From Figure 9, we see that the error process during the training

period is relatively stable, consistent with a steady state error process. Examining Figure 10, we see another immediate response after aluminum is added, with a delay of about 0.05 days. The one-hour moving average again captures this change fairly well and the errors quickly exceed the upper control limit. For this column, the error process appears to stabilize over the next day, and then at day 7.7 another large shift above the upper control limit occurs. In column 2, there is clearly a statistically significant response to the addition of aluminum.

5.3 Column 3

Training Period Fraction Outside Control Limits = 0.0293

Observation Period Fraction Outside Control Limits = 0.0525

$\lambda_1 = 0.60$

$\lambda_2 = 0.19$

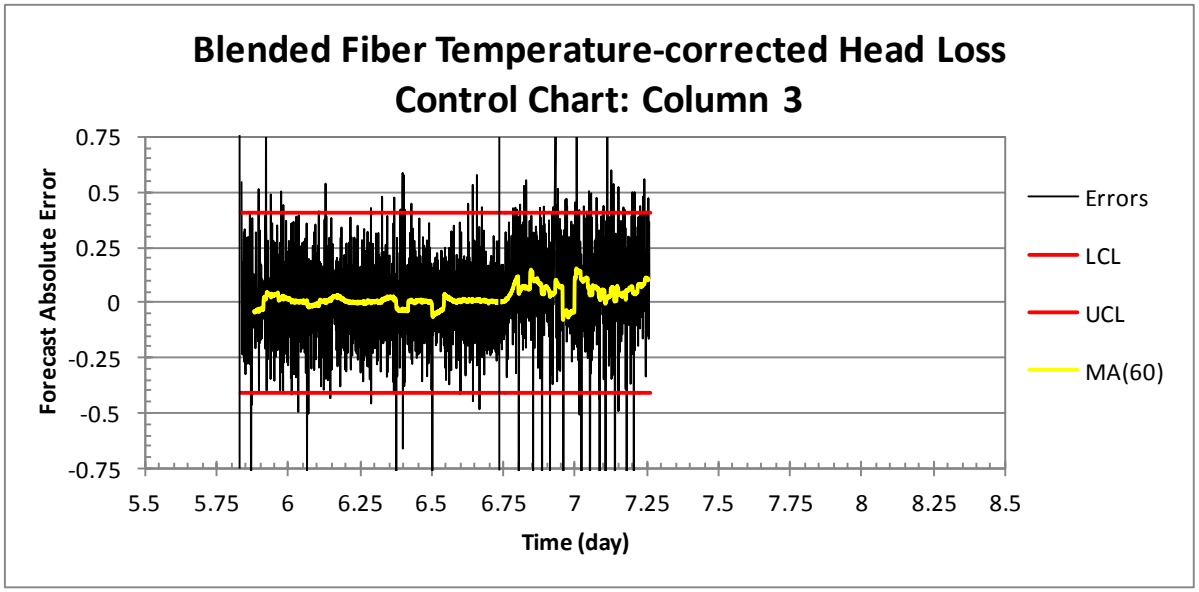

Figure 12. Blended Fiber Temperature-Corrected Head Loss Control Chart Column 3 - Initial Training Period Included

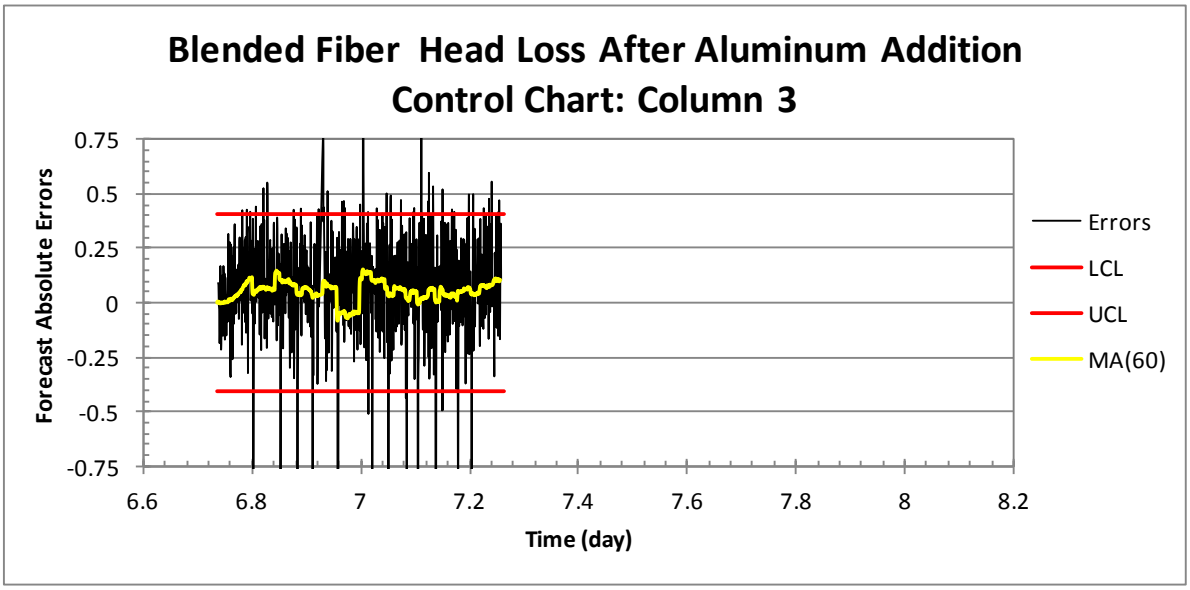

Figure 13. Blended Fiber Temperature-Corrected Head Loss Control Chart Column 3 - Initial Training Period Not Included

Examining Figure 1 in Howe (2012) for column 3, we see an apparent change in the process, i.e., an apparent change in slope. However, compared to columns 1 and 2 for the blended fiber beds, the volatility of column 3's process makes this more difficult to establish statistically. In contrast to columns 1 and 2, the observed violation of the two-sided control limits for column 3 is 0.0525. The fraction of violation of the upper control limit is 0.0324. However, when forming a moving average of the upper control limit violation of 720 minutes (not depicted in the figures) we find that the violation steadily climbs from around 0.014 at day 6.33 to 0.064 at day 7.25; i.e., the moving average climbs to a value substantially larger than the expected value of 0.025. While more subtle than columns 1 and 2, this suggests a change in the head loss process after the addition of aluminum. That said, the change is only statistically significant—according to the moving average measure—substantially later than for columns 1 and 2.

References

Croux, C., Gelper, S., & Mahieu, K. (2010 1-April). *Robust Control Charts for Time Series Data.* Retrieved 2012 5-August from http://dx.doi.org/10.2139/ssrn.1588646

Howe, K. (2012). *CHLE Tank Test Results for Blended and NEI Fiber Beds with Aluminum Addition.* University of New Mexico, Department of Civil Engineering, Albuquerque.